USING THE SOCIAL AMOEBA *Dictyostelium discoideum* AS A MODEL TO STUDY CLN5 DISEASE

A Thesis Dissertation Submitted to the Committee of Graduate Studies in Partial

Fulfillment of the Requirements for the

Degree of Philosophy

in the Faculty of Arts and Sciences

TRENT UNIVERSITY

Peterborough, Ontario, Canada

Environmental and Life Sciences – Ph.D. Graduate Program

January 2026

ABSTRACT

USING THE SOCIAL AMOEBA *Dictyostelium discoideum* AS A MODEL TO STUDY CLN5 DISEASE

William David Kim

The neuronal ceroid lipofuscinoses (NCLs), collectively referred to as Batten disease, are a group of neurodegenerative diseases that affect all ages, primarily children. Batten disease is caused by mutations in 1 of the 13 ceroid lipofuscinosis neuronal (CLN) genes (*CLN1*-*CLN8, CLN10*-*CLN14*), each of which causes an NCL subtype when mutated. One of the NCL subtypes, CLN5 disease, is caused by mutations in the *CLN5* gene. CLN5 is a soluble lysosomal protein that localizes to the endoplasmic reticulum (ER), the Golgi complex, the cytoplasm, and extracellularly. CLN5 has four putative molecular functions, including as a ceramide synthase, glycoside hydrolase, depalmitoylase, and bis(monoacylglycerol)phosphate synthase. CLN5 plays various roles within the cell, such as lipid metabolism, autophagy, and proteasome degradation. However, the function and the exact pathway in which CLN5 is involved are unclear. CLN5 is secreted and contains a signal peptide sequence via bioinformatics analysis. Furthermore, there are currently 70 CLN5 disease-causing mutations reported in the NCL mutation database. 12 CLN5 disease-causing mutations have been studied thus far in terms of their cellular impact, as well as the release of CLN5 to a certain extent. However, there is a lack of research into the functionality of the signal peptide in CLN5 and an in-depth analysis of the molecular impact of mutations in CLN5 disease. Consequently, this Ph.D. thesis focused on using comparative transcriptomics to reveal biological pathways affected by *cln5*-deficiency, revealing mechanisms that regulate the secretion of Cln5 and CtsD, and using *Dictyostelium* to gain insights into the molecular effects of mutations in CLN5 disease.

Comparative transcriptomics reveal many differentially expressed genes that are linked to phenotypes observed in *cln5*-deficient cells and identified pathways affected in other CLN5 disease models, such as autophagy. Furthermore, novel findings, like affected expression of lysosomal enzymes and pathways, including secretion, are identified within the comparative transcriptomics analysis. Subsequently, this research also shows the secretory role of the signal peptide in Cln5 and CtsD. Finally, this Ph.D. thesis revealed that mutations in CLN5 disease affect the lysosomal biology and secretion of Cln5 and other lysosomal enzymes.

KEYWORDS: Batten disease, CLN5 disease, CLN5, CTSD, *Dictyostelium discoideum,* enzymes, genes, lysosome, mutation, secretion, signal peptide.

ACKNOWLEDGEMENTS

I would like to acknowledge my committee members, including Dr. Michael Donaldson, Dr. Barry Saville, and Dr. Aaron Shafer, for their patience, guidance, and helpful feedback on my PhD thesis. I would like to further extend my appreciation to Dr. Donaldson for providing me with an engaging and safe environment to discuss science and for giving me advice in my PhD life. Moreover, I would like to thank many important figures at Trent University, including Smolly Coulson, Debbie Lietz, Dr. Sarah Piper, Kelly Boadway, Christopher Williams, Angela Sikma, Tracy Ross, Linda Sweeting, Ashley Maschke, Dr. Emily Slepkov, Dr. Aaron Slepkov, Dr. Stephen Hill, Dr. Elizabeth Russell, and Dr. Neil Emery. These individuals enhanced my experience at Trent University by helping me with things that I was uncertain of and/or giving time out of their schedule to help me navigate science. In addition to the Trent University family, I want to thank Shirley, the caretaker in the DNA building. She is like a second mother, always checking up on me and always on me when I work long hours. I appreciated your support and our conversations about Texas very much. I want to acknowledge Dr. Susan Cotman, her team (especially Drs. Seda Yasa and Uma Chandrachud), and other members at Massachusetts General Hospital during my international internship. I am exceptionally fortunate for that experience as I interacted with brilliant and the nicest scientists whom I can call friends. It would also be an injustice not to mention Dr. Robert Huber's lab members, in particular Samer Owiar, Sean Condie, Adam DiGicianto, Cassandra Pyne, Emma Jorge, Blythe Ferguson, Thomas Burnside, and Alison Sikma. Thank you for letting me be able to be a mentor in science for you. All of you provided great discussions on science, taught me how to effectively communicate as a mentor, and brought good energy into the lab. Moreover, I want to further acknowledge Samer and his family as they were, and still are, there when I needed help with science,

life, and with my car (it was not a good car). Samer's family treated me like I was part of theirs, and he is like a brother to me. He has supported me in my goals, been proud of my achievements, provided valuable advice, and shared many great moments in science. The other person whom I am thankful for being my mentor in both my undergraduate and in science is Saby Mathavarajah. Thank you for introducing me to research during my time as an undergraduate and showing me that hard work does pay off. I appreciated the talks we had regarding science and life. I enjoyed working together on papers that we co-authored, and I still hold the gifts that you gave me (e.g., Morty figure, the letters, and the book titled '*Tunnels*' by Roderick Gordon). I am grateful that we developed a meaningful friendship and that we remained in contact after you departed from Trent University. I am extremely grateful to have completed my PhD thesis under the supervision of Dr. Robert Huber. He has been pivotal in my PhD through his mentorship within the lab and in my professional development. I am thankful for his support in sending me to multiple conferences, giving me the opportunity in an exchange program at Massachusetts General Hospital under the guidance of Dr. Susan Cotman, and allowing me to explore novel research ideas with lots of flexibility. I also appreciated that Rob enabled me to co-supervise many of his students to gain essential skills in becoming a Principal Investigator. Rob was someone whom I could ask for advice on my career choice and in life. He pushed me to be my best while also having a great time. His kindness, work ethic, and leadership skills are traits I would like to emulate when I start my independent research laboratory. I hope that I stay in touch with Rob later in life. I am forever grateful to you. Furthermore, I would like to extend my gratitude to my family, including my brothers (Stephen, Michael, and Jimmy) and my mom (Myung-Hee), for also supporting my goals and helping me when things in the PhD life were rough. Finally, I also want to give my final gratitude to my dad

(Hyun-Sik). I am sorry that I was late in making you proud when I was young. I hope you can see what I have accomplished and what I will become soon. Thank you to everyone, as I wouldn't have completed this thesis without your support.

PREFACE

This Ph.D. dissertation is in manuscript presentation. Chapters 2-3 include published papers containing data acquired from this research thesis. Each chapter in this thesis contains a preface which outlines the contribution of each co-author.

Additional co-authored publications conceived in, but not part of, the thesis (# indicates equal authorship):

Kim W.D. & Huber R.J. Modelling Lysosomal Disease in *Dictyostelium discoideum*: Examining the Localization and Secretion of Lysosomal Proteins. In: Lysosomes – Models and Analyses. *Methods in Molecular Biology*, accepted.

Mathavarajah, S, Chipurupalli, S., Habib, E.B., **Kim, W.D.**, Aoki, M.M., Corkery, D.P., Whelan, K., Lukacs, J., Erkan, M., Martinez, V.D., Smith, K.S., Montgomery, S.B., Salsman, J., Huber, R.J. & Dellaire, G. (2025). The evolutionarily conserved PRP4K-*CHMP4B/vps32* splicing circuit regulates autophagy. *Cell Reports* 44, 115870. doi: 10.1016/j.celrep.2025.115870.

Condie S.V.#, **Kim W.D.#** & Huber R.J. (2025). Lysosomal enzyme processing and trafficking in the social amoeba *Dictyostelium discoideum*. Biochemistry and Cell Biology 103, 1-11. doi: 10.1139/bcb-2025-0062

Huber, R.J. & **Kim, W.D.** (2024). Trafficking of adhesion and aggregation-modulating proteins during the early stages of *Dictyostelium* development. *Cellular Signalling*. 121, 111292.

Kim, W.D., DiGicianto, A.F. & Huber, R.J. (2024). Assaying lysosomal enzyme activity in *Dictyostelium discoideum*. In: *Dictyostelium discoideum*. *Methods in Molecular Biology*, vol 2814, Kimmel AR (Editor), Humana, New York, NY. pp. 55-79. ISBN: 978-1-0716-3893-4.

Huber, R.J.#, Gray, J.# & **Kim, W.D.** (2023). Loss of mfsd8 alters the secretome during *Dictyostelium* aggregation. *European Journal of Cell Biology*. 102, 151361.

Yap, S.Q., **Kim, W.D.** & Huber, R.J. (2022). Mfsd8 modulates growth and the early stages of multicellular development in *Dictyostelium discoideum. Frontiers in Cell and Developmental Biology*. 10, 930235.

Kim, W.D.#, Mathavarajah, S.# & Huber, R.J.# (2022). The cellular and developmental roles of cullins, neddylation, and the COP9 signalosome in *Dictyostelium discoideum. Frontiers in Physiology*. 13, 827435.

Kim, W.D., Wilson-Smillie, M.L.D.M., Thanabalasingam, A., Lefrancois, S., Cotman, S.L. & Huber, R.J. (2022). Autophagy in the neuronal ceroid lipofuscinoses (Batten disease). Frontiers in Cell and Developmental Biology, 10, 812728.

McLaren M.D.#, Mathavarajah S.#, **Kim W.D.**, Yap S.Q. & Huber R.J. (2021). Aberrant autophagy impacts growth and multicellular development in a *Dictyostelium* knockout model of CLN5 disease. *Frontiers in Cell and Developmental Biology*, 9, 657406.

Huber, R.J., **Kim, W.D.** & Mathavarajah, S. (2021). Inhibiting neddylation with MLN4924 suppresses growth and delays multicellular development in *Dictyostelium discoideum*. *Biomolecules*, 11(3), 482.

Kim, W.D.#, Yap, S.Q.# & Huber, R.J.# (2021). A proteomics analysis of calmodulin-binding proteins in *Dictyostelium discoideum* during the transition from unicellular growth to multicellular development. *International Journal of Molecular Sciences*, 22(4), 1722.

TABLE OF CONTENTS

ABSTRACT……. **ii**

ACKNOWLEDGEMENTS……..……..……..…… **iv**

PREFACE……..….. **vii**

TABLE OF CONTENTS……...… **ix**

LIST OF FIGURES……..….. **xv**

LIST OF TABLES…….. **xviii**

LIST OF ABBREVIATIONS…… **xx**

1.0. GENERAL INTRODUCTION…….…….. **1**

1.1. THE NEURONAL CEROID LIPOFUSCINOSES……. **1**

1.2. CLN5 DISEASE…….. **2**

1.3. USING THE SOCIAL AMOEBA *Dictyostelium discoideum* AS A BIOMEDICAL MODEL TO STUDY BATTEN DISEASE ……..… **5**

1.4 FINDINGS REGARDING *Dictyostelium* Cln5……. **6**

1.5. RESEARCH OBJECTIVES…….. **7**

1.6. FIGURES AND TABLES…….. **10**

1.7. REFERENCES……... **12**

2.0. CHAPTER 2 – *AN ALTERED TRANSCRIPTOME UNDERLIES cln5-DEFICIENCY PHENOTYPES IN Dictyostelium discoideum*…….. **17**

2.1. PREFACE……... **17**

2.2. ABSTRACT……. **18**

2.3. INTRODUCTION…….…… **20**

2.4. METHODS AND MATERIALS……....……... **22**

2.4.1. CELL LINES, MEDIA, AND ANTIBODIES…….. **22**

2.4.2. RNA PREPARATION…… **23**

2.4.3. RNA SEQUENCING AND BIOINFORMATICS..... **23**

2.4.4. ENZYME ACTIVITY ASSAYS..... **25**

2.4.4.1. α-MANNOSIDASE and β-GLUCOSIDASE..... **25**

2.4.4.2. α-GLUCOSIDASE..... **25**

2.4.4.3. α- AND β-GALACTOSIDASE..... **26**

2.4.4.4. PALMITOYL-PROTEIN THIOESTERASE 1..... **26**

2.4.4.5. TRIPEPTIDYL PEPTIDASE 1..... **27**

2.4.4.6. CATHEPSIN D AND CATHEPSIN F..... **27**

2.4.4.7. CATHEPSIN B..... **28**

2.4.4.8. N-ACETYLGLUCOSAMINIDASE..... **28**

2.4.5. PROTEASOME ACTIVITY..... **29**

2.4.6. SDS-PAGE AND WESTERN BLOTTING..... **29**

2.5. RESULTS..... **30**

2.5.1. COMPARATIVE TRANSCRIPTOMICS REVEALS THE EFFECTS OF *cln5*-DEFICIENCY ON GENE EXPRESSION IN *D. discoideum*..... **30**

2.5.2. GO TERM ENRICHMENT ANALYSES OF DIFFERENTIALLY EXPRESSED GENES IN *cln5*$^-$ CELLS..... **31**

2.5.3. DIFFERENTIALLY EXPRESSED GENES ASSOCIATED WITH *cln5*-DEFICIENCY PHENOTYPES DURING GROWTH..... **33**

2.5.4. DIFFERENTIALLY EXPRESSED GENES ASSOCIATED WITH *cln5*-DEFICIENCY PHENOTYPES DURING STARVATION..... **35**

2.5.5. LOSS OF *cln5* AFFECTS THE EXPRESSION AND ACTIVITY OF SEVERAL CARBOHYDRATE ENZYMES..... **37**

2.5.6. LOSS OF *cln5* AFFECTS THE EXPRESSION AND ACTIVITY OF THE PROTEASOME..... **38**

2.5.7. LOSS OF *cln5* AFFECTS THE EXPRESSION AND ACTIVITY OF OTHER CLN-LIKE PROTEINS IN *D. discoideum*……... 40

2.6. DISCUSSION…….. 41

2.7. ACKNOWLEDGMENTS…….. 46

2.8. FIGURES AND TABLES…….. 47

2.9. REFERENCES……..... 55

3.0. CHAPTER 3 – *DETERMINING THE FUNCTIONAL ROLE OF THE SIGNAL PEPTIDE IN CLN5 AND CTSD*…… 66

3.1. PREFACE……... 66

3.2. ABSTRACT……. 67

3.3. INTRODUCTION…….……. 69

3.4. METHODS……...……... 71

3.4.1. CELL LINES, CULTURING, AND MATERIALS…… 71

3.4.2. Cln5 AND CtsD SP-NULL PLASMID CONSTRUCTION AND *Dictyostelium* TRANSFORMATION…….. 72

3.4.3. IMMUNOFLUORESCENCE ASSAY…….. 73

3.4.4. CELL PROLIFERATION ASSAY……... 74

3.4.5. STARVATION ASSAY…….. 74

3.4.6. LATE MULTICELLULAR DEVELOPMENT ASSAY…… 75

3.4.7. PROTEIN QUANTIFICATION AND WESTERN BLOTTING.. 75

3.5.0. RESULTS……. 76

3.5.1. DETERMINING THE INTRACELLULAR LOCALIZATION OF Cln5 AND CtsD LACKING THEIR PUTATIVE SP……. 76

3.5.2. EVALUATING THE PUTATIVE SP ON THE SECRETION OF Cln5 AND CtsD……..……. 77

3.5.3. EVALUATING THE EFFECT OF BLOCKING Cln5 SECRETION ON CELL PROLIFERATION, AGGREGATION, AND DEVELOPMENT……..... **78**

3.5.4. INVESTIGATION THE IMPACT OF BLOCKING Cln5 SECRETION IN ER STRESS RESPONSE……... **79**

3.6. DISCUSSION…….. **80**

3.7. ACKNOWLEDGMENTS…….. **83**

3.8. FIGURES AND TABLES…….. **84**

3.9. REFERENCES……..... **91**

4.0. CHAPTER 4 – ***CLN5 DISEASE-CAUSING MUTATIONS IMPACT INTRACELLULAR DEGRADATION AND PROTEIN SECRETION***……..... **96**

4.1. PREFACE……... **96**

4.2. ABSTRACT……. **97**

4.3. INTRODUCTION…….…… **98**

4.4 METHODS……... **100**

4.4.1. CELL LINES AND CULTURING…… **100**

4.4.2. ANTIBODIES…….…… **101**

4.4.3. PROTEIN STRUCTURAL ANALYSIS……..……. **101**

4.4.4. CONSTRUCTION OF EXPRESSION VECTORS……..…….. **102**

4.4.5. IMMUNOFLUORESCENCE MICROSCOPY…..…..... **103**

4.4.6. ENZYME ACTIVITY ASSAYS…….……..…. **104**

4.4.7. SDS-PAGE AND WESTERN BLOTTING……..…… **106**

4.4.8. CELL PROLIFERATION ASSAY…….…….. **107**

4.4.9. AGGREGATION ASSAY…….……. **107**

4.5. RESULTS…… **108**

4.5.1. CLN5 DISEASE-CAUSING MUTATIONS ARE CONSERVED IN *Dictyostelium* Cln5 AND AFFECT THE PREDICTED STRUCTURE OF *Dictyostelium* Cln5 AND HUMAN CLN5…….. **108**

4.5.2. CLN5 DISEASE-CAUSING MUTATIONS ALTER THE CELLULAR DISTRIBUTION OF Cln5…… **109**

4.5.3. CLN5 DISEASE-CAUSING MUTATIONS ALTER PROTEASOMAL-MEDIATED PROTEIN DEGRADATION……..…… **110**

4.5.4. CLN5 DISEASE-CAUSING MUTATIONS AFFECT COMPARTMENTS OF THE ENDO-LYSOSOMAL PATHWAY…… **111**

4.5.5. CLN5 DISEASE-CAUSING MUTATIONS AFFECT LYSOSOMAL ENZYME ACTIVITY…….. **113**

4.5.6. CLN5 DISEASE-CAUSING MUTATIONS ALTER THE INTRACELLULAR AMOUNTS OF CATHEPSIN B AND OTHER LYSOSOMAL ENZYMES LINKED TO NCL……. **114**

4.5.7. CLN5 DISEASE-CAUSING MUTATIONS REDUCE THE SECRETION OF Cln5 AND OTHER LYSOSOMAL ENZYMES……. **114**

4.5.8. CLN5 DISEASE-CAUSING MUTATIONS DO NOT AFFECT CELL PROLIFERATION AND AGGREGATION……. **116**

4.6. DISCUSSION…….. **116**

4.7. ACKNOWLEDGMENTS……..…. **124**

4.8. FIGURES AND TABLES ……. **125**

4.9. REFERENCES……. **141**

5.0. CHAPTER 5……. **150**

5.1. GENERAL DISCUSSION……. **150**

5.2. THE GENETICS BEHIND *cln5*-DEFICIENCY…….. **151**

5.3. THE BIOCHEMISTRY AND MOLECULAR BIOLOGY OF THE N-TERMINAL REGION OF CLN5 AND MUTATIONS IN CLN5 DISEASE……. **153**

5.4. FUTURE DIRECTIONS……..... **156**

5.5. FINAL CONCLUSIONS..... **158**

5.6. REFERENCES..... **159**

LIST OF FIGURES

CHAPTER 1 – GENERAL INTRODUCTION

Figure 1. The *Dictyostelium discoideum* lifecycle..... **10**

CHAPTER 2 – *AN ALTERED TRANSCRIPTOME UNDERLIES cln5-DEFICIENCY PHENOTYPES IN Dictyostelium discoideum*

Figure 2. A pictorial schematic of the methods used to determine the effects of *cln5* deletion on gene expression **47**

Figure 3. Loss of *cln5* affects the intracellular and extracellular levels of AprA and CfaD during growth **48**

Figure 4. Loss of *cln5* affects the abundance of proteins linked to cytokinesis during growth **49**

Figure 5. Loss of *cln5* affects the extracellular amount of CmfA during starvation **49**

Figure 6. Loss of *cln5* affects the intracellular and extracellular amounts of discoidin during starvation **50**

Figure 7. Loss of *cln5* affects the activity of carbohydrate enzymes during growth and starvation **51**

Figure 8. Loss of *cln5* increases the abundance of a proteasomal subunit during growth and starvation but decreases proteasome 20S activity **52**

Figure 9. Loss of *cln5* increases PPT1 activity during growth and starvation but has no effect on TPP1 activity **53**

Figure 10. Loss of *cln5* affects the activity of cathepsins during growth and starvation **53**

CHAPTER 3 – *DETERMINING THE FUNCTIONAL ROLE OF THE SIGNAL PEPTIDE IN CLN5 AND CTSD*

Figure 11. Loss of the SP disrupted the cellular distribution of Cln5, leading to more diffuse cytoplasmic localization..... **84**

Figure 12. Loss of the SP in CtsD did not impact its localization..... **84**

Figure 13. Loss of the SP prevented the secretion of Cln5 and CtsD..... **85**

Figure 14. Loss of extracellular release of CtsD elevated the secretion of Cln5……. **86**

Figure 15. Cell proliferation was unaffected by the loss of the SP in Cln5…….. **86**

Figure 16. N-terminus tagging of Cln5 with GFP causes reduced proliferation…..…… **86**

Figure 17. Loss of the SP in Cln5 did not impact *Dictyostelium* aggregation…….. **87**

Figure 18. Overexpression of Cln5 with N-terminal GFP delayed aggregation in WT cells…….. **87**

Figure 19. Late multicellular development was delayed in WT cells expressing GFP-Cln5, but unaffected in cells expressing Cln5 lacking its SP……. **88**

Figure 20. Expression of GFP-Cln5 in WT cells caused ER stress, while loss of the SP in Cln5 did not……. **89**

CHAPTER 4 – *CLN5 DISEASE-CAUSING MUTATIONS IMPACT INTRACELLULAR DEGRADATION AND PROTEIN SECRETION*

Figure 21. CLN5 disease-causing mutations are conserved in *Dictyostelium* Cln5 and generated in *Dictyostelium* Cln5……..... **125**

Figure 22. CLN5 disease-causing mutations affect the predicted structure of *Dictyostelium* Cln5 and human CLN5……... **126**

Figure 23. CLN5 disease-causing mutations alter the cellular distribution of Cln5…….. **127**

Figure 24. CLN5 disease-causing mutations alter proteasomal-mediated protein degradation and the intracellular amounts of proteasomal subunits and ubiquitin……...…… **128**

Figure 25. Mutations in CLN5 disease cause elevated 20S proteasome activity during growth…… **129**

Figure 26. CLN5 disease-causing mutations affect compartments of the endo-lysosomal system……..…….. **129**

Figure 27. CLN5 disease-causing mutations affect intracellular lysosomal enzyme activity……..…….. **130**

Figure 28. CLN5 disease-causing mutations alter the intracellular amount of cathepsin B and other lysosomal enzymes linked to NCL……..……. **131**

Figure 29. CLN5 disease-causing mutations reduce the secretion of Cln5 and other lysosomal enzymes……. **132**

Figure 30. Loss of *cln5* and CLN5 disease-causing mutations alter the activity of cathepsin B and other lysosomal enzymes linked to NCL……. **133**

Figure 31. CLN5 disease-causing mutations do not affect cell proliferation or aggregation……...…… **134**

Figure 32. Visual models displaying processes affected by mutations in CLN5 disease …….. **135**

Figure 33. A visual model summarizing all literature on the effects of CLN5 disease-causing mutations on its protein trafficking ……... **137**

LIST OF TABLES

CHAPTER 1 – GENERAL INTRODUCTION

Table 1. A table containing the *Dictyostelium* CLN-like and human CLN proteins, and the extracellular detection of *Dictyostelium* Cln proteins……. **11**

CHAPTER 2 – *AN ALTERED TRANSCRIPTOME UNDERLIES cln5-DEFICIENCY PHENOTYPES IN Dictyostelium discoideum*

Table 2. Quantitative summary of DEGs and annotated genes determined by LAGO in *cln5*$^{-}$ cells during growth and after 4 h of starvation ……. **54**

CHAPTER 3 – *DETERMINING THE FUNCTIONAL ROLE OF THE SIGNAL PEPTIDE IN CLN5 AND CTSD*

Table 3. List of primers used to generate the ΔSP-Cln5GFP, ΔSP-CtsDGFP, and full-length CtsDGFP plasmids ……... **90**

CHAPTER 4 – *CLN5 DISEASE-CAUSING MUTATIONS IMPACT INTRACELLULAR DEGRADATION AND PROTEIN SECRETION*

Table 4. CLN5 disease-causing mutations created in this study ……. **138**

Table 5. Summarized table of the effect of CLN5 disease-causing mutations on the cellular distribution of Cln5 …….. **138**

Table 6. Summarized table of impaired ubiquitin and 20S proteasome biology affected by mutations in CLN5 disease …….. **139**

Table 7. Summarized table of the endo-lysosomal compartments affected by mutated Cln5 …….. **139**

Table 8. Summarized table of CLN5 disease-causing mutations affecting intracellular lysosomal enzyme activity ……... **139**

Table 9. Summarized table of CLN5 disease-causing mutations affecting the amounts of intracellular cathepsin B and other lysosomal enzymes linked to NCL ……. **139**

Table 10. Summarized table of the impact of mutations in CLN5 disease on the secretion of Cln5, cathepsin B, and other lysosomal enzymes linked to NCL ……. **140**

Table 11. Summarized table of affected extracellular lysosomal enzyme activity caused by CLN5 disease-causing mutations …….. **140**

LIST OF ABBREVIATIONS

α-galactosidase	α-Gal
α-glucosidase	α-Glu
α-mannosidase	α-Man
β-galactosidase	β-Gal
β-glucosidase	β-Glu
2-(N-morpholino) ethanesulfonic acid	MES
3′,5′-cyclic-nucleotide phosphodiesterase	RegA
Autocrine proliferation repressor	AprA
Autophagy gene	*atg*
Bis(monoacylglycerol)phosphate	BMP
Beclin-1	BECN1
Benjamin-Hochberg	BH
Calreticulin	CalR
Cathepsin B	CTSB/CtsB
Cathepsin D	CTSD/CtsD
Cathepsin F	CTSF
Cation-independent mannose-6-phosphate receptor	CI-MPR
Ceroid lipofuscinosis neuronal	CLN/Cln
Combined overlap extension polymerase chain reaction	COE-PCR
Conditioned buffer	CB
Conditioned medium	CM
Conditioned medium factor A	CmfA
Conditioned medium factor B	CmfB
Cortexillin I	CtxA
Cortexillin II	CtxB
Countin A	CtnA
Counting factor-associated protein	CfaD
Cyclic adenosine monophosphate	cAMP
Cyclic adenosine monophosphate receptor A	*carA*
Differentially expressed genes	DEGs
Discoidin	Dsc
Endoplasmic reticulum	ER
Escherichia coli	*E. coli*
Gene ontology	GO
Glucose-regulated protein 78	Grp78
Hexosaminidase A	HEXA
Hierarchical indexing for spliced alignment of transcripts 2	HISAT2
N-acetylglucosaminidase	NagA
Myosin heavy chain type II	MhcA
Neuronal ceroid lipofuscinosis	NCL
p62/sequestosome 1	SQSTM1
Palmitoyl thioesterase 1	PPT1/Ppt1
Proteasomal subunit	PS
Proteasomal subunit 5	PS5
RNA sequencing	RNA-seq

Statistical analysis of RNA-seq data tools	SARTools
Signal peptide	SP
Subunit C of the mitochondrial ATP synthase	SCMAS
Tripeptidyl peptidase 1	TPP1
Tripeptidyl peptidase 1A	Tpp1A
Tripeptidyl peptidase 1B	Tpp1B
V-H-ATPase subunit C	VatC
Vinculin A	VinA
Whole cell	WC
Wild-type	WT

1.0. GENERAL INTRODUCTION

1.1. THE NEURONAL CEROID LIPOFUSCINOSES

The neuronal ceroid lipofuscinoses (NCLs), collectively referred to as Batten disease, are neurodegenerative diseases caused by genetic mutations in the ceroid lipofuscinosis neuronal (CLN) genes (*CLN1-CLN8, CLN10-CLN14*), each of which results in a subtype of NCL (e.g., mutations in *CLN1* lead to CLN1 disease) (Butz et al., 2020; Simonati & Mole, 2022). Recently, a new subtype of Batten disease, denoted as CLN15 disease, has been identified and is caused by mutations in the TBC1 domain-containing kinase gene (Liu et al., 2013; Chong et al., 2016; Beck-Wödl et al., 2018). Although distinct in genetic mutations, all NCL subtypes, except CLN14 disease, display a common feature of pathological intra-lysosomal accumulation of ceroid lipofuscin, a biological aggregate of lipids, metals, and proteins including subunit C of the mitochondrial ATP synthase (SCMAS) (Palmer et al., 1992; Tyynelä et al., 1993; Kousi et al., 2012; Staropoli et al., 2012; Haltia & Goebel, 2013; Metz et al., 2018). One of the focuses within the NCL field is revealing the underpinning mechanism of SCMAS accumulation (Jolly et al., 1993; Seehafer & Pearce, 2006). Many hypotheses have been proposed, one suggesting that ceroid lipofuscin accumulation occurs through a Schiff-base reaction, resulting in the SCMAS protein being glycated/lapidated (Jolly et al., 1993; Jolly et al., 2002). Other researchers postulated alternative mechanisms of intra-lysosomal ceroid lipofuscin accumulation including compromised mitochondrial function leading to increased reactive oxygen species that can crosslink lipids with SCMAS and impair its protein turnover, altered lysosomal function such as lysosomal enzymes, or perturbed intracellular trafficking pathways that direct vesicular compartments and biological compounds to the

lysosome such as autophagy (Seehafer & Pearce, 2006). Although the exact mechanism of ceroid lipofuscin accumulation in lysosomes remains uncertain, this accumulation has been detected within neurons and other cell types (Rietdorf et al. 2020). At a macroscale level, Batten disease affects all ages, predominantly children (Butz et al., 2020; Simonati & Mole, 2022). Individuals diagnosed with Batten disease manifest various clinical symptoms, including continual degenerative capability in their movement, vision, and cognition, as well as epileptic seizures and a reduced lifespan (Butz et al., 2020; Simonati & Mole, 2022). Unfortunately, there is no cure for this devastating disease due to a lack of knowledge in the biological processes and molecular functions associated with most of the CLN proteins. However, there is currently a temporary treatment for CLN2 disease with the administration of cerliponase alfa or Bineura, an enzyme replacement therapy, but it has only been shown to delay the progression of the disease (Lewis et al., 2019).

1.2. CLN5 DISEASE

CLN5 disease is an NCL subtype caused by mutations in the *CLN5* gene (Butz et al., 2020). CLN5 is translated into a 407 aa long type II transmembrane-bound protein within the endoplasmic reticulum (ER) and is found within the Golgi complex, lysosomes, and extracellularly (Isosomppi et al., 2002; Jules et al., 2017). The first 92 aa of the CLN5 peptide sequence, shown with bioinformatics tools, encodes a signal peptide (SP) sequence (Moharir et al., 2013; Jules et al., 2017; Huber & Mathavarajah, 2018a). This sequence is cleaved by the signal peptide peptidase/signal peptide peptidase-like intramembrane protease family within the ER, leading to a soluble enzyme that is directed to the lysosome (Isosomppi et al., 2002; Lyly et al., 2009; Schmiedt et al., 2010; Jules et al., 2017; Huber & Mathavarajah et al. 2018a). Consistent with that proteins containing a SP are secreted

proteins, many researchers found that CLN5 is secreted (Isosomppi et al., 2002; Moharir et al., 2013; Hughes et al., 2014; Huber & Mathavarajah, 2018a). However, there is a lack of knowledge about whether this SP plays a role in the secretion of CLN5.

CLN5 is further proteolytically processed via cysteine proteases within lysosomes to form the mature CLN5 protein (De Silva et al., 2015). In its mature form, CLN5 putatively functions as a depalmityolase, a glycoside hydrolase, a ceramide synthase, or a bis(monoacylglycerol)phosphate (BMP) synthase (Haddad et al., 2012; Huber & Mathavarajah, 2018a; Luebben et al., 2022; Medoh et al., 2023). Although the function of CLN5 is not well defined, many studies reveal interactions and processes in which CLN5 is involved. CLN5 interacts with proteins within the CLN protein family including protein palmitoyl thioesterase 1 (PPT1), tripeptidyl peptidase 1 (TPP1), CLN3, CLN6, and CLN8, which was postulated that the CLN protein family are involved at different stages within a single pathway (Vesa et al., 2002; Persaud-Sawin et al., 2007; Lyly et al., 2009; Huber, 2023). Outside of the CLN proteins, CLN5 also interacts with sortilin, a lysosomal sorting receptor (Mamo et al., 2012). Loss of *CLN5* prevents sortilin and another lysosomal sorting receptor, denoted as cation-independent mannose-6-phosphate receptor (CI-MPR), in endosomes from being recycled in the Golgi complex, but are rather degraded in the lysosome (Mamo et al., 2012). In addition to this process, CLN5 is involved in other biological processes within the eukaryotic cell, including but not limited to lipid metabolism, biometal regulation, and autophagy (Haddad et al., 2012; Grubman et al., 2014; Leinonen et al., 2017; Adams et al., 2019; McLaren et al., 2021). Although research on CLN5 has been extensive, the exact molecular function and the pathway in which CLN5 precisely plays a role remain unclear.

Many research studies show that autophagy is a process that is commonly affected in the NCLs, including CLN5 disease (Kim et al., 2022). Autophagy is an intracellular process that breaks down organelles and protein cargo linked with a ubiquitin tag (as reviewed in Kocaturk & Gozuacik, 2020). One of the main focuses in CLN5 disease research includes investigating the role of CLN5 in autophagy. Many studies show that the effect of loss of *CLN5* is complex on the autophagy pathway. For example, the process of regulating autophagy is affected as an increased amount of beclin-1 (BECN1) is observed in mice with *Cln5*-deficiency (Leinonen et al., 2017). Furthermore, the ratio of LC3-II-LC3-I and the amount of p62/sequestosome 1 (SQSTM1), a receptor for protein cargo delivery to autophagosomes for degradation, were elevated in CLN5-deficient mice. This indicates that fusion between autophagosomes-lysosomes and autophagic protein turnover are affected, respectively (Leinonen et al., 2017). Other CLN5 disease models also showed these dysregulated events, including sheep neuronal cells, *HeLa* cells, and patient-derived fibroblasts, along with both sheep and human neuronal cells deficient in CLN5 showing decreased lysosomal acidity (Best et al., 2017; Adams et al., 2019; Basak et al., 2021; Yasa et al., 2021). Finally, loss of *CLN5* impacted the activity of the lysosomal protein cathepsin B (CTSB) and slowed the movement of lysosomes within human neurons (Basak et al., 2021). Overall, autophagy is a process that is affected in CLN5 disease, but further research is required to pinpoint the exact mechanism that is affected within this pathway.

There are 70 distinct mutations linked to CLN5 disease reported as of January 2025 (https://www.ucl.ac.uk/ncl-disease/mutation-and-patient-database/mutation-and-patient-datasheets-human-ncl-genes/cln5). There is heterogeneity behind CLN5 disease, with different onsets and pathological classifications for each mutation in this disease. However, premature death ensues for all individuals who inherited mutations linked to CLN5 disease.

In CLN5 disease research, most of the research focuses on the p.Tyr343* mutation, which causes the common late-infantile form of CLN5 disease (Vesa et al., 2002; Schmiedt et al., 2010; Yasa et al., 2021). In addition to this mutation, there are other nonsense mutations caused by either a frameshift or missense mutation, along with duplication and missense mutations. Only a select few mutations in CLN5 disease are studied in terms of their impact on the intracellular localization of CLN5, its binding with protein partners, its function within lysosomes, and in biological processes including autophagy (Isosomppi et al., 2002; Vesa et al., 2002; Schmiedt et al., 2010; Moharir et al., 2013; Qureshi et al., 2018; Adams et al., 2019; Luo et al., 2020; Yasa et al., 2021). However, most of the CLN5 disease-causing mutations remain unknown regarding their overall impact on individuals, along with a lack of information on the biochemical and cellular impacts of most of the CLN5 disease-causing mutations.

1.3. USING THE SOCIAL AMOEBA *Dictyostelium discoideum* AS A BIOMEDICAL MODEL TO STUDY BATTEN DISEASE

Many organismal models have been used to study human diseases, such as large-scale models like mouse, sheep, and canine, and at a microscale, including but not limited to lower eukaryotic models of yeast, nematode, and fruit fly (Huber, 2016). In addition to this list, *Dictyostelium discoideum* is a powerful model in disease research (Mathavarajah et al., 2017). *Dictyostelium discoideum* is a social amoeba that contains a unicellular-multicellular life cycle and is dependent on nutrient availability (Figure 1) (Mathavarajah et al., 2017; Huber et al., 2022). When nutrients are present (e.g., liquid medium and bacteria), *Dictyostelium discoideum* cells are unicellular and divide via mitosis. Under nutrient deprivation, single cells release cyclic-adenosine monophosphate (cAMP) radial

signals and chemotax into multiple segregated aggregates denoted as mounds. Following mound formation, cells differentiate into various multicellular structures, including structures resembling a finger, a slug, and eventually a fruiting body. The fruiting body contains a sorus, a structure containing live spores, which is held on top of the stalk. Finally, the spores within the sorus germinate once introduced to a nutrient-rich environment.

Dictyostelium is a powerful model in studying diseases, in particular neurological diseases, as its genome encodes many homologs associated with neurodegeneration, such as Huntington's, Tay-Sachs disease, and Batten disease (Haver & Scaglione, 2021). The *Dictyostelium* genome encodes many CLN-like proteins (Table 1) (Huber, 2021). Moreover, *Dictyostelium* is the only early eukaryote that contains a CLN5-like protein, Cln5, and is 30% identical to the human CLN5 protein (Huber & Mathavarajah, 2018a). Finally, *Dictyostelium* has a rapid proliferation rate, and biological processes from humans are conserved within this model. Thus, novel discoveries can be quick and allow researchers to translate work done in *Dictyostelium* into mammalian and human cell models (Huber, 2016).

1.4 FINDINGS REGARDING *Dictyostelium* Cln5

Dictyostelium Cln5 localizes to the ER, the cytoplasm, and the cellular cortex (Huber & Mathavarajah, 2018a). Like human CLN5, *Dictyostelium* Cln5 is glycosylated, predicted to contain a SP, and is secreted (Huber & Mathavarajah, 2018ab). Furthermore, *Dictyostelium* Cln5 has been shown to interact with other Cln proteins, including tripeptidyl peptidase 1B (Tpp1B) (homolog of human tripeptidyl peptidase 1 (TPP1)), cathepsin D (CtsD), and a homolog of cathepsin F (CTSF), which is consistent with previous findings in other models (Huber & Mathavarajah, 2018a). Loss of *cln5* results in aberrant

phenotypes during growth, including reduced cellular proliferation, affected cytokinesis, and reduced folic acid-mediated chemotaxis (McLaren et al., 2021). During multicellular development, *cln5*-deficiency in *Dictyostelium* reduces many processes, including aggregation, cAMP-mediated chemotaxis, and cellular adhesion, and enhances multicellular development after mound formation (Huber & Mathavarajah, 2018b; McLaren et al., 2021). Considering these aberrant phenotypes, autophagy is impacted during growth (McLaren et al., 2021). During growth, elevated amounts of ubiquitin-positive proteins and increased numbers of autophagosomes are present, suggesting elevated basal autophagic activity. Furthermore, loss of two autophagy genes (*atg*), *atg1* and *atg9*, reduces the secretion of Cln5, indicating that these proteins and the process of autophagy regulate the secretory mechanism of Cln5 (McLaren et al., 2021). Along with this, *Dictyostelium* Cln5 interacts with the human hexosaminidase A (HEXA) homolog, N-acetylglucosaminidase (NagA), and is highly co-expressed with each other in human tissues (McLaren et al., 2021). This suggests that these two proteins participate in and regulate the same pathway, such as autophagy (McLaren et al., 2021). However, the secretory processes that modulate the release of Cln5 are not well understood.

1.5. RESEARCH OBJECTIVES

The main objective of this PhD thesis is using *Dictyostelium* as a model to study CLN5 disease. Since previous research in *Dictyostelium* revealed the function of Cln5 as a glycoside hydrolase, aberrant phenotypes associated with loss of *cln5*, and proteins that play a role in the secretion of Cln5 (Huber & Mathavarajah, 2018ab; McLaren et al., 2021), one of the aims of this thesis is to conduct comparative transcriptomics to reveal biological pathways affected by loss of *cln5*. In this data chapter, I hypothesize that Cln5 participates

in biological processes within the cell, and that there would be a selection of differentially expressed genes that encode proteins involved in *cln5*-deficient phenotypes. Not surprisingly, the hypothesis is supported through our RNA sequencing analysis as there are differentially expressed genes (DEGs) associated with cell proliferation, cytokinesis, aggregation, and autophagy, as well as genes associated with secretion being affected (Chapter 3) (Kim & Huber, 2022). Since affected secretion is present in many NCL subtypes, including CLN5 disease as shown in our previous work (Huber & Mathavarajah, 2018ab; Huber, 2021; Kim & Huber, 2022), we investigate the role of the SP in Cln5 and CtsD (Chapter 4). I hypothesize that the SP in Cln5 and CtsD modulates their secretion, and loss of the SP prevents the release of these proteins. In removing the SP from these proteins, we found that these proteins are trapped within the cell, indicating a functional role of secretion for this amino acid sequence in Cln5 and CtsD (Huber et al., 2024). We also found that loss of signal peptide motif in CtsD alters Cln5 secretion while the reverse is not true (Huber et al., 2024). Finally, we show that an ER stress response is induced when Cln5 is trapped in the ER via N-terminal GFP tagging in WT cells. As the SP is a segment of Cln5 affecting its trafficking, we use *Dictyostelium* to explore the molecular impact of CLN5 disease-causing mutations (Chapter 5). I hypothesize that mutations in CLN5 disease impact processes within the cell, suggesting dysregulation in biological and cellular processes in which Cln5 is involved. We show that mutations in CLN5 disease affect the lysosomal biology of the cell, including lysosome biogenesis and both the intracellular and extracellular activity of lysosomal enzymes. Furthermore, mutant forms of Cln5 alter the ubiquitin-proteasome system and the secretion of both Cln5 and other lysosomal proteins. Altogether, this section of the PhD thesis highlights the heterogeneity of CLN5 disease. Overall, these results collected from this PhD thesis reveal novel insights into a few

mechanisms which Cln5 plays a role in, the functional role of the SP in Cln5 and CtsD, and further our understanding of the molecular effects of mutations linked to CLN5 disease.

This Ph.D. thesis is presented in a manuscript style and includes a general introduction, preface, three thesis chapters, and concludes with a general discussion. The PhD thesis sections are broken down as follows: 1) General Introduction, 2) a data chapter on comparative transcriptomics in *cln5*-deficiency published in *Frontiers in Genetics* (Kim & Huber, 2022), 3) a data chapter on the processes modulating the secretion of Cln5 and CtsD - parts of the data published in *Traffic* (Huber et al., 2024), 3) a data chapter focusing on using *Dictyostelium* to reveal novel insights into the molecular impact in CLN5 disease-causing mutations - currently in submission for a publication (Kim et al., unpublished), and 5) a general discussion that summarizes all findings from the research with this PhD thesis along with shedding some light into future direction of this research.

1.6. FIGURES AND TABLES

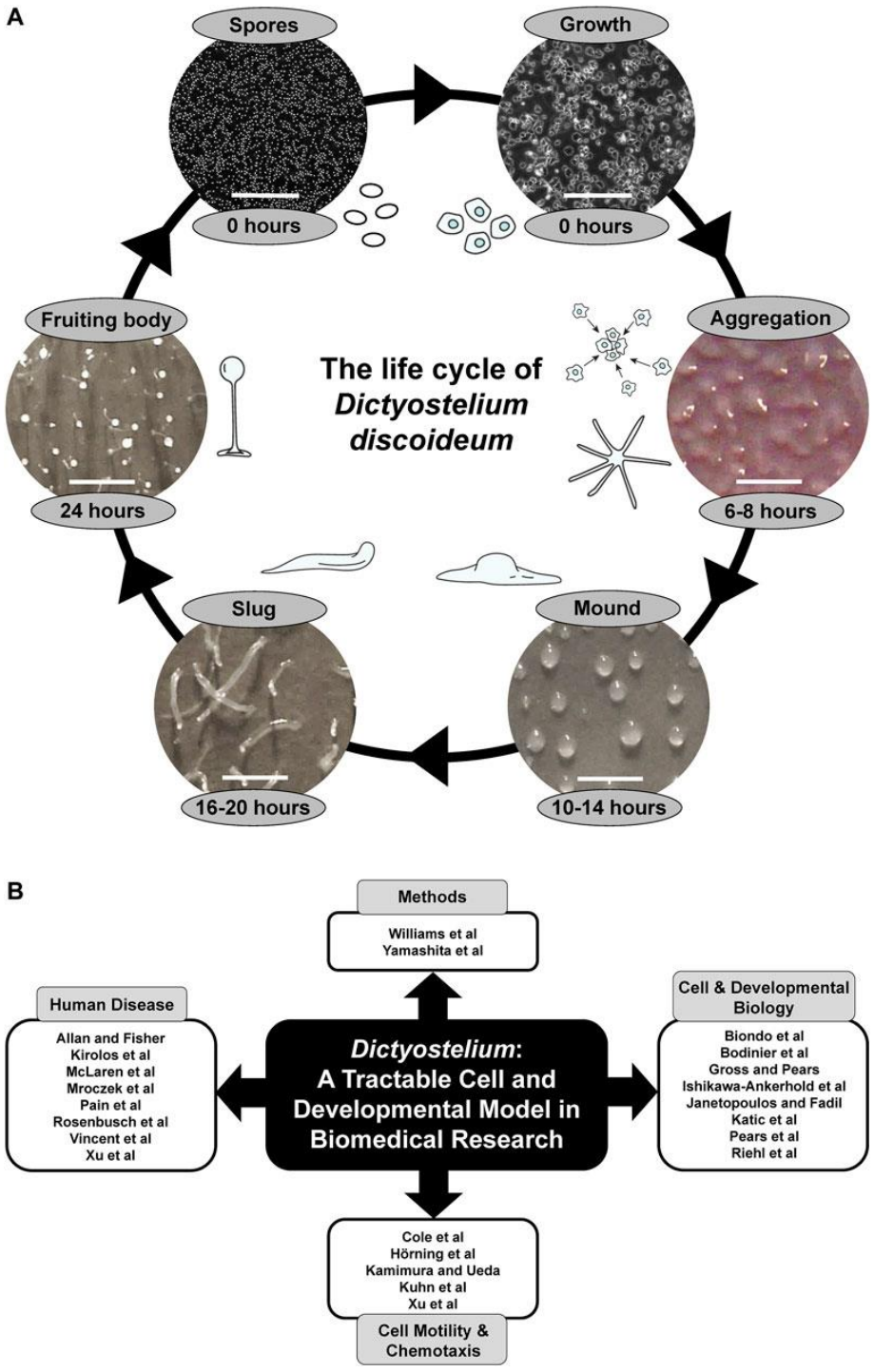

Figure 1. The *Dictyostelium discoideum* lifecycle. **(A)** *Dictyostelium* cells undergo mitosis and are unicellular during its growth phase. Single cells aggregate when nutrients are depleted, and cells undergo various morphological changes, which end in a fruiting body composed of a stalk holding a sorus on top. The sorus contains live spores, which germinate under nutrient-rich conditions and restart the lifecycle. **(B)** A visual representation of the use of *Dictyostelium* in research. Figure is from Huber et al. (2022).

Table 1. A table containing the *Dictyostelium* CLN-like and human CLN proteins, and the extracellular detection of *Dictyostelium* Cln proteins. Table is from Huber (2021).

Human				*D. discoideum*			
						Extracellular location	
NCL subtype	NCL-related protein	Molecular function of NCL-related protein	Accession number	Homolog	dictyBase ID	Bakthavatsalam and Gomer, 2010*	Huber, 2017*
CLN1	PPT1	Thioesterase that removes palmitate residues from proteins	NP_000301	Ppt1	DDB0233890	Yes	Yes
CLN2	TPP1	Serine protease that cleaves peptide bonds in proteins	NP_000382	Tpp1A	DDB0234303	No	No
				Tpp1B	DDB0306176	Yes	Yes
				Tpp1C	DDB0185020	Yes	Yes
				Tpp1D	DDB0309140	No	No
				Tpp1E	DDB0304592	No	No
				Tpp1F	DDB0214912	Yes	Yes
CLN3	CLN3	Transmembrane protein with unknown function	NP_000077	Cln3	DDB0233983	No	No
CLN4	DNAJC5	Co-chaperone involved in intracellular trafficking	NP_079495	DDB_G0290017	DDB0306688	No	No
				Ddj1	DDB0215016	No	No
CLN5	CLN5	Hydrolase that breaks glycosidic bonds in complex sugars	NP_006484	Cln5	DDB0234077	No	Yes
CLN6	CLN6	ER-resident protein with unknown function	NP_060352	No homolog			
CLN7	MFSD8	Transmembrane protein with unknown function	NP_689991	Mfsd8	DDB0307149	No	No
CLN8	CLN8	ER-resident protein with unknown function	NP_061764	No homolog			
CLN10	CTSD	Aspartyl protease that cleaves peptide bonds in proteins	NP_001900	CtsD	DDB0215012	Yes	Yes
CLN11	GRN	Secreted protein with unknown function	NP_002078	Grn	DDB0238428	No	No
CLN12	ATP13A2	Transmembrane protein with unknown function	NP_071372	Kil2	DDB0237611	No	No
CLN13	CTSF	Cysteine protease that cleaves peptide bonds in proteins	NP_003784	CprA	DDB0201647	No	Yes
				CprB	DDB0214998	No	Yes
				DDB_G0291191	DDB0252831	Yes	Yes
CLN14	KCTD7	Cytosolic protein with unknown function	NP_694578	Kctd9	DDB0231824	No	No
				DDB_G0269760	DDB0238663	No	No
				DDB_G0285861	DDB0346929	No	No
				DDB_G0269022	DDB0347398	No	No

*Bakthavatsalam and Gomer (2010), and Huber (2017) used LC–MS/MS to identify secreted proteins during *D. discoideum* development.

1.7. REFERENCES

Adams, J., Feuerborn, M., Molina, J. A., Wilden, A. R., Adhikari, B., Budden, T., & Lee, S. Y. (2019). Autophagy–lysosome pathway alterations and alpha-synuclein up-regulation in the subtype of neuronal ceroid lipofuscinosis, CLN5 disease. *Scientific Reports*, 9(1), 151. https://doi.org/10.1038/s41598-018-36379-z

Basak, I., Hansen, R. A., Ward, M. E., & Hughes, S. M. (2021). Deficiency of the Lysosomal Protein CLN5 Alters Lysosomal Function and Movement. *Biomolecules*, 11(10), 1412. https://doi.org/10.3390/biom11101412

Beck-Wödl, S., Harzer, K., Sturm, M., Buchert, R., Rieß, O., Mennel, H.-D., Latta, E., Pagenstecher, A., & Keber, U. (2018). Homozygous TBC1 domain-containing kinase (TBCK) mutation causes a novel lysosomal storage disease – a new type of neuronal ceroid lipofuscinosis (CLN15)? *Acta Neuropathologica Communications*, 6(1), 145. https://doi.org/10.1186/s40478-018-0646-6

Best, H. L., Neverman, N. J., Wicky, H. E., Mitchell, N. L., Leitch, B., & Hughes, S. M. (2017). Characterisation of early changes in ovine CLN5 and CLN6 Batten disease neural cultures for the rapid screening of therapeutics. *Neurobiology of Disease*, 100, 62–74. https://doi.org/10.1016/j.nbd.2017.01.001

Butz, E. S., Chandrachud, U., Mole, S. E., & Cotman, S. L. (2020). Moving towards a new era of genomics in the neuronal ceroid lipofuscinoses. *Biochimica et Biophysica Acta (BBA) - Molecular Basis of Disease*, 1866(9), 165571. https://doi.org/10.1016/j.bbadis.2019.165571

Chong, J. X., Caputo, V., Phelps, I. G., Stella, L., Worgan, L., Dempsey, J. C., Nguyen, A., Leuzzi, V., Webster, R., Pizzuti, A., Marvin, C. T., Ishak, G. E., Ardern-Holmes, S., Richmond, Z., Bamshad, M. J., Ortiz-Gonzalez, X. R., Tartaglia, M., Chopra, M., & Doherty, D. (2016). Recessive Inactivating Mutations in TBCK, Encoding a Rab GTPase-Activating Protein, Cause Severe Infantile Syndromic Encephalopathy. *The American Journal of Human Genetics*, 98(4), 772–781. https://doi.org/10.1016/j.ajhg.2016.01.016

De Silva, B., Adams, J., & Lee, S. Y. (2015). Proteolytic processing of the neuronal ceroid lipofuscinosis related lysosomal protein CLN5. *Experimental Cell Research*, 338(1), 45–53. https://doi.org/10.1016/j.yexcr.2015.08.021

Grubman, A., Pollari, E., Duncan, C., Caragounis, A., Blom, T., Volitakis, I., Wong, A., Cooper, J., Crouch, P. J., Koistinaho, J., Jalanko, A., White, A. R., & Kanninen, K. M. (2014). Deregulation of biometal homeostasis: The missing link for neuronal ceroid lipofuscinoses?†. *Metallomics*, 6(4), 932–943. https://doi.org/10.1039/c4mt00032c

Haddad, S. E., Khoury, M., Daoud, M., Kantar, R., Harati, H., Mousallem, T., Alzate, O., Meyer, B., & Boustany, R.-M. (2012). CLN5 and CLN8 protein association with

ceramide synthase: Biochemical and proteomic approaches. *ELECTROPHORESIS*, 33(24), 3798–3809. https://doi.org/10.1002/elps.201200472

Haltia, M., & Goebel, H. H. (2013). The neuronal ceroid-lipofuscinoses: A historical introduction. *Biochimica et Biophysica Acta (BBA) - Molecular Basis of Disease*, 1832(11), 1795–1800. https://doi.org/10.1016/j.bbadis.2012.08.012

Haver, H. N., & Scaglione, K. M. (2021). *Dictyostelium discoideum* as a Model for Investigating Neurodegenerative Diseases. *Frontiers in Cellular Neuroscience*, 15. https://doi.org/10.3389/fncel.2021.759532

Huber, R. J. (2016). Using the social amoeba *Dictyostelium* to study the functions of proteins linked to neuronal ceroid lipofuscinosis. *Journal of Biomedical Science*, 23(1), 83. https://doi.org/10.1186/s12929-016-0301-0

Huber, R. J. (2021). Altered protein secretion in Batten disease. *Disease Models & Mechanisms*, 14(12), dmm049152. https://doi.org/10.1242/dmm.049152

Huber, R. J., Williams, R. S., & Müller-Taubenberger, A. (2022). Editorial: Dictyostelium: A Tractable Cell and Developmental Model in Biomedical Research. *Frontiers in Cell and Developmental Biology*, *10*. https://doi.org/10.3389/fcell.2022.909619

Huber, R. J. (2023). Recent insights into the networking of CLN genes and proteins in mammalian cells. *Journal of Neurochemistry*, 165(5), 643–659. https://doi.org/10.1111/jnc.15822

Huber, R. J., Kim, W. D., & Wilson-Smillie, M. L. D. M. (2024). Mechanisms regulating the intracellular trafficking and release of CLN5 and CTSD. *Traffic*, 25(1), e12925. https://doi.org/10.1111/tra.12925

Huber, R. J., & Mathavarajah, S. (2018a). Cln5 is secreted and functions as a glycoside hydrolase in *Dictyostelium. Cellular Signalling*, 42, 236–248. https://doi.org/10.1016/j.cellsig.2017.11.001

Huber, R. J., & Mathavarajah, S. (2018b). Secretion and function of Cln5 during the early stages of *Dictyostelium* development. *Biochimica et Biophysica Acta (BBA) - Molecular Cell Research*, 1865(10), 1437–1450. https://doi.org/10.1016/j.bbamcr.2018.07.017

Hughes, S. M., Hope, K. M., Xu, J. B., Mitchell, N. L., & Palmer, D. N. (2014). Inhibition of storage pathology in prenatal CLN5-deficient sheep neural cultures by lentiviral gene therapy. *Neurobiology of Disease*, 62, 543–550. https://doi.org/10.1016/j.nbd.2013.11.011

Jolly, R. D., Dalefield, R. R., & Palmer, D. N. (1993). Ceroid, lipofuscin and the ceroid-lipofuscinoses (Batten Disease). *Journal of Inherited Metabolic Disease*, 16(2), 280–283. https://doi.org/10.1007/BF00710265

Jolly, R. D., Palmer, D. N., & Dalefield, R. R. (2002). The analytical approach to the nature of lipofuscin (age pigment). *Archives of Gerontology and Geriatrics*, 34(3), 205–217. https://doi.org/10.1016/S0167-4943(01)00219-9

Kim, W. D., & Huber, R. J. (2022). An altered transcriptome underlies cln5-deficiency phenotypes in *Dictyostelium discoideum*. *Frontiers in Genetics*, 13. https://doi.org/10.3389/fgene.2022.1045738

Kim, W. D., Wilson-Smillie, M. L. D. M., Thanabalasingam, A., Lefrancois, S., Cotman, S. L., & Huber, R. J. (2022). Autophagy in the Neuronal Ceroid Lipofuscinoses (Batten Disease). *Frontiers in Cell and Developmental Biology*, 10. https://doi.org/10.3389/fcell.2022.812728

Kocaturk, N. M., & Gozuacik, D. (2018). Crosstalk Between Mammalian Autophagy and the Ubiquitin-Proteasome System. *Frontiers in Cell and Developmental Biology*, 6. https://doi.org/10.3389/fcell.2018.00128

Kousi, M., Anttila, V., Schulz, A., Calafato, S., Jakkula, E., Riesch, E., Myllykangas, L., Kalimo, H., Topçu, M., Gökben, S., Alehan, F., Lemke, J. R., Alber, M., Palotie, A., Kopra, O., & Lehesjoki, A.-E. (2012). Novel mutations consolidate KCTD7 as a progressive myoclonus epilepsy gene. *Journal of Medical Genetics*, 49(6), 391–399. https://doi.org/10.1136/jmedgenet-2012-100859

Leinonen, H., Keksa-Goldsteine, V., Ragauskas, S., Kohlmann, P., Singh, Y., Savchenko, E., Puranen, J., Malm, T., Kalesnykas, G., Koistinaho, J., Tanila, H., & Kanninen, K. M. (2017). Retinal Degeneration In A Mouse Model Of CLN5 Disease Is Associated With Compromised Autophagy. *Scientific Reports*, 7(1), 1597. https://doi.org/10.1038/s41598-017-01716-1

Lewis, G., Morrill, A. M., Conway-Allen, S. L., & Kim, B. (2020). Review of Cerliponase Alfa: Recombinant Human Enzyme Replacement Therapy for Late-Infantile Neuronal Ceroid Lipofuscinosis Type 2. *Journal of Child Neurology*, 35(5), 348–353. https://doi.org/10.1177/0883073819895694

Liu, Y., Yan, X., & Zhou, T. (2013). TBCK Influences Cell Proliferation, Cell Size and mTOR Signaling Pathway. *PLOS ONE*, 8(8), e71349. https://doi.org/10.1371/journal.pone.0071349

Luebben, A. V., Bender, D., Becker, S., Crowther, L. M., Erven, I., Hofmann, K., Söding, J., Klemp, H., Bellotti, C., Stäuble, A., Qiu, T., Kathayat, R. S., Dickinson, B. C., Gärtner, J., Sheldrick, G. M., Krätzner, R., & Steinfeld, R. (2022). Cln5 represents a new type of cysteine-based S-depalmitoylase linked to neurodegeneration. *Science Advances*, 8(15), eabj8633. https://doi.org/10.1126/sciadv.abj8633

Luo, S., Bi, B., Zhu, B., Tan, L., Zhao, P., Huang, Y., Wu, G., Zhou, A., & He, X. (2020). Functional Analysis of a Novel CLN5 Mutation Identified in a Patient With Neuronal

Ceroid Lipofuscinosis. *Frontiers in Genetics*, 11. https://doi.org/10.3389/fgene.2020.536221

Lyly, A., von Schantz, C., Heine, C., Schmiedt, M.-L., Sipilä, T., Jalanko, A., & Kyttälä, A. (2009). Novel interactions of CLN5 support molecular networking between Neuronal Ceroid Lipofuscinosis proteins. *BMC Cell Biology*, 10(1), 83. https://doi.org/10.1186/1471-2121-10-83

Mamo, A., Jules, F., Dumaresq-Doiron, K., Costantino, S., & Lefrancois, S. (2012). The Role of Ceroid Lipofuscinosis Neuronal Protein 5 (CLN5) in Endosomal Sorting. *Molecular and Cellular Biology*, 32(10), 1855–1866. https://doi.org/10.1128/MCB.06726-11

Mathavarajah, S., Flores, A., & Huber, R. J. (2017). *Dictyostelium discoideum*: A Model System for Cell and Developmental Biology. *Current Protocols Essential Laboratory Techniques*, 15(1), 14.1.1-14.1.19. https://doi.org/10.1002/cpet.15

McLaren, M. D., Mathavarajah, S., Kim, W. D., Yap, S. Q., & Huber, R. J. (2021). Aberrant Autophagy Impacts Growth and Multicellular Development in a *Dictyostelium* Knockout Model of CLN5 Disease. *Frontiers in Cell and Developmental Biology*, 9. https://doi.org/10.3389/fcell.2021.657406

Medoh, U. N., Hims, A., Chen, J. Y., Ghoochani, A., Nyame, K., Dong, W., & Abu-Remaileh, M. (2023). The Batten disease gene product CLN5 is the lysosomal bis(monoacylglycero)phosphate synthase. *Science*, 381(6663), 1182–1189. https://doi.org/10.1126/science.adg9288

Metz, K. A., Teng, X., Coppens, I., Lamb, H. M., Wagner, B. E., Rosenfeld, J. A., Chen, X., Zhang, Y., Kim, H. J., Meadow, M. E., Wang, T. S., Haberlandt, E. D., Anderson, G. W., Leshinsky-Silver, E., Bi, W., Markello, T. C., Pratt, M., Makhseed, N., Garnica, A., … Hardwick, J. M. (2018). KCTD7 deficiency defines a distinct neurodegenerative disorder with a conserved autophagy-lysosome defect. *Annals of Neurology*, 84(5), 766–780. https://doi.org/10.1002/ana.25351

Moharir, A., Peck, S. H., Budden, T., & Lee, S. Y. (2013). The Role of N-Glycosylation in Folding, Trafficking, and Functionality of Lysosomal Protein CLN5. *PLOS ONE*, 8(9), e74299. https://doi.org/10.1371/journal.pone.0074299

Palmer, D. N., Fearnley, I. M., Walker, J. E., Hall, N. A., Lake, B. D., Wolfe, L. S., Haltia, M., Martinus, R. D., & Jolly, R. D. (1992). Mitochondrial ATP synthase subunit c storage in the ceroid-lipofuscinoses (Batten disease). *American Journal of Medical Genetics*, 42(4), 561–567. https://doi.org/10.1002/ajmg.1320420428

Persaud-Sawin, D.-A., Mousallem, T., Wang, C., Zucker, A., Kominami, E., & Boustany, R.-M. N. (2007). Neuronal Ceroid Lipofuscinosis: A Common Pathway? *Pediatric Research*, 61(2), 146–152. https://doi.org/10.1203/pdr.0b013e31802d8a4a

Qureshi, Y. H., Patel, V. M., Berman, D. E., Kothiya, M. J., Neufeld, J. L., Vardarajan, B., Tang, M., Reyes-Dumeyer, D., Lantigua, R., Medrano, M., Jiménez-Velázquez, I. J., Small, S. A., & Reitz, C. (2018). An Alzheimer's Disease-Linked Loss-of-Function CLN5 Variant Impairs Cathepsin D Maturation, Consistent with a Retromer Trafficking Defect. *Molecular and Cellular Biology*, 38(20), e00011-18. https://doi.org/10.1128/MCB.00011-18

Rietdorf, K., Coode, E. E., Schulz, A., Wibbeler, E., Bootman, M. D., & Ostergaard, J. R. (2020). Cardiac pathology in neuronal ceroid lipofuscinoses (NCL): More than a mere co-morbidity. *Biochimica et Biophysica Acta (BBA) - Molecular Basis of Disease*, 1866(9), 165643. https://doi.org/10.1016/j.bbadis.2019.165643

Schmiedt, M.-L., Bessa, C., Heine, C., Ribeiro, M. G., Jalanko, A., & Kyttälä, A. (2010). The neuronal ceroid lipofuscinosis protein CLN5: New insights into cellular maturation, transport, and consequences of mutations. *Human Mutation*, 31(3), 356–365. https://doi.org/10.1002/humu.21195

Seehafer, S. S., & Pearce, D. A. (2006). You say lipofuscin, we say ceroid: Defining autofluorescent storage material. *Neurobiology of Aging*, 27(4), 576–588. https://doi.org/10.1016/j.neurobiolaging.2005.12.006

Simonati, A., & Williams, R. E. (2022). Neuronal Ceroid Lipofuscinosis: The Multifaceted Approach to the Clinical Issues, an Overview. *Frontiers in Neurology*, 13. https://doi.org/10.3389/fneur.2022.811686

Staropoli, J. F., Karaa, A., Lim, E. T., Kirby, A., Elbalalesy, N., Romansky, S. G., Leydiker, K. B., Coppel, S. H., Barone, R., Xin, W., MacDonald, M. E., Abdenur, J. E., Daly, M. J., Sims, K. B., & Cotman, S. L. (2012). A Homozygous Mutation in KCTD7 Links Neuronal Ceroid Lipofuscinosis to the Ubiquitin-Proteasome System. *The American Journal of Human Genetics*, 91(1), 202–208. https://doi.org/10.1016/j.ajhg.2012.05.023

Tyynelä, J., Palmer, D. N., Baumann, M., & Haltia, M. (1993). Storage of saposins A and D in infantile neuronal ceroid-lipofuscinosis. *FEBS Letters*, 330(1), 8–12. https://doi.org/10.1016/0014-5793(93)80908-D

Vesa, J., Chin, M. H., Oelgeschläger, K., Isosomppi, J., DellAngelica, E. C., Jalanko, A., & Peltonen, L. (2002). Neuronal Ceroid Lipofuscinoses Are Connected at Molecular Level: Interaction of CLN5 Protein with CLN2 and CLN3. *Molecular Biology of the Cell*, 13(7), 2410–2420. https://doi.org/10.1091/mbc.E02-01-0031

Yasa, S., Sauvageau, E., Modica, G., & Lefrancois, S. (2021). CLN5 and CLN3 function as a complex to regulate endolysosome function. *Biochemical Journal*, 478(12), 2339–2357. https://doi.org/10.1042/BCJ20210171

2.0. CHAPTER 2

AN ALTERED TRANSCRIPTOME UNDERLIES *cln5*-DEFICIENCY PHENOTYPES IN *Dictyostelium discoideum*

2.1. PREFACE

This chapter is a primary journal article that was published in *Frontiers in Genetics*. This chapter contains content from this publication (see below), including written text and figures.

TITLE	An altered transcriptome underlies *cln5*-deficiency phenotypes in *Dictyostelium discoideum*
AUTHORS	William D. Kim & Robert J. Huber
REFERENCE	Kim W.D. & Huber R.J. (2022). An altered transcriptome underlies cln5-deficiency phenotypes in *Dictyostelium discoideum*. *Frontiers in Genetics*. 13, 1045738.
CONTRIBUTIONS	WDK and RJH wrote the first original draft. WDK collected and analyzed all data within this manuscript. All authors read and approved the final draft of the manuscript.
COPYRIGHT	

2.2. ABSTRACT

Mutations in CLN5 cause a subtype of neuronal ceroid lipofuscinosis (NCL) called CLN5 disease. The NCLs, commonly referred to as Batten disease, are a family of neurodegenerative lysosomal storage diseases that affect all ages and ethnicities globally. Previous research showed that CLN5 participates in a variety of cellular processes. However, the precise function of CLN5 in the cell and the pathway(s) regulating its function are not well understood. In the model organism *Dictyostelium discoideum*, loss of the CLN5 homolog, *cln5*, impacts various cellular and developmental processes including cell proliferation, cytokinesis, aggregation, cell adhesion, and terminal differentiation. In this study, we used comparative transcriptomics to identify differentially expressed genes underlying cln5-deficiency phenotypes during growth and the early stages of multicellular development. During growth, genes associated with protein ubiquitination/deubiquitination, cell cycle progression, and proteasomal degradation were affected, while genes linked to protein and carbohydrate catabolism were affected during early development. We followed up this analysis by showing that loss of cln5 alters the intracellular and extracellular amounts of proliferation repressors during growth and increases the extracellular amount of conditioned medium factor, which regulates cAMP signalling during the early stages of development. Additionally, *cln5*$^{-}$ cells displayed increased intracellular and extracellular amounts of discoidin, which is involved in cell-substrate adhesion and migration. Previous work in mammalian models reported altered lysosomal enzyme activity due to mutation or loss of CLN5. Here, we detected altered intracellular activities of various carbohydrate enzymes and cathepsins during *cln5*$^{-}$ growth and starvation. Notably, cln5- cells displayed reduced β-hexosaminidase activity, which aligns with previous work showing that *D. discoideum* Cln5 and human CLN5 can cleave

the substrate acted upon by β-hexosaminidase. Finally, consistent with the differential expression of genes associated with proteasomal degradation in cln5- cells, we also observed elevated amounts of a proteasome subunit and reduced proteasome 20S activity during *cln5*$^{-}$ growth and starvation. Overall, this study reveals the impact of *cln5*-deficiency on gene expression in D. discoideum, provides insight on the genes and proteins that play a role in regulating Cln5-dependent processes, and sheds light on the molecular mechanisms underlying CLN5 disease.

Keywords: Batten disease, CLN5, Dictyostelium discoideum, enzyme activity, neuronal ceroid lipofuscinosis, proteasome, RNA-seq

2.3. INTRODUCTION

The neuronal ceroid lipofuscinoses (NCLs), also known as Batten disease, are a family of neurodegenerative diseases linked to mutations in 13 ceroid lipofuscinosis neuronal (CLN) genes (CLN1-8, CLN10-14) (Schulz et al., 2013; Mole and Cotman, 2015). Each of the 13 different subtypes of NCL are characterized by the lysosomal accumulation of autoflourescent lipid-protein aggregates called ceroid lipofuscin in neurons, as well as other cell types outside the central nervous system (Palmer et al., 1992; Mole and Cotman, 2015). The accumulation of ceroid lipofuscin has been associated with numerous clinical symptoms, including seizures, reduced motor, visual, and cognitive function, as well as a reduced lifespan (Schulz et al., 2013; Mole and Cotman, 2015). While most of the *CLN* genes have been studied, the precise cellular mechanisms impacted by *CLN* gene mutations remain elusive.

Mutations in CLN5 cause the CLN5 disease subtype of NCL (Schulz et al., 2013; Mole and Cotman, 2015). CLN5 is a soluble lysosomal and extracellular protein that is predicted to function as either a glycoside hydrolase or depalmitoylase (Isosomppi et al., 2002; Hughes et al., 2014; Jules et al., 2017; Huber and Mathavarajah, 2018a; Basak et al., 2021b; Luebben et al., 2022). CLN5 has been linked to several cellular processes, including, but not limited to, endosomal sorting, biometal homeostasis, sphingolipid metabolism, and autophagy (El Haddad et al., 2012; Mamo et al., 2012; Grubman et al., 2014; Doccini et al., 2020; McLaren et al., 2021). However, like most CLN proteins, the association of CLN5 with a defined biological pathway is still under investigation.

Dictyostelium discoideum is a eukaryotic microbe that is used as a biomedical model system for studying a variety of human diseases, including the NCLs (Huber, 2016; Huber et al., 2022). The *D. discoideum* life cycle is comprised of single cell and

multicellular phases that allow for a diversity of fundamental cellular and developmental processes to be examined in great biochemical detail (Mathavarajah et al., 2017). During the growth phase of the life cycle, haploid amoebae feed on a food source (in nature: microorganisms in the soil; in the laboratory: bacteria and nutrient-rich liquid media) and divide mitotically. When starved, amoebae initiate a 24-h multicellular developmental programme that begins with the chemotactic aggregation of cells. The multicellular mounds that form then undergo a series of morphological changes to form motile slugs. During the later stages of multicellular development, cells within slugs terminally differentiate to form fruiting bodies composed of stalk cells and viable spores that can restart the life cycle when nutrients become available.

The *D. discoideum* genome encodes homologs for 11 of the 13 human CLN proteins (Huber, 2016; Huber et al., 2020). Our previous work showed that the homolog of human CLN5, Cln5, has glycoside hydrolase activity and is secreted (Huber and Mathavarajah, 2018a). Our work also linked the function of Cln5 in *D. discoideum* to cell proliferation, cytokinesis, folic acid-mediated chemotaxis, and autophagy during growth, and since cAMP-chemotaxis, aggregation, and developmental timing during multicellular development (Huber and Mathavarajah, 2018b; McLaren et al., 2021).

In this study, we used comparative transcriptomics to identify genes that are impacted by *cln5*-deficiency in *D. discoideum* during growth and after 4 h of starvation (when cln5 expression is maximal) (Stajdohar et al., 2017). During growth, genes associated with protein ubiquitination/deubiquitination, cell cycle progression, and proteasomal degradation were affected, while genes linked to protein and carbohydrate catabolism were affected in cells starved for 4 h. We then showed that loss of *cln5* affects the levels of proliferation repressors during growth and proteins required for cAMP-

mediated chemotaxis and adhesion during the early stages of multicellular development. Finally, we showed that deletion of *cln5* affects the activities of lysosomal enzymes and the proteasome. Together, this study examines the impact of *cln5*-deficiency on the *D. discoideum* transcriptome and provides further insight into the multifaceted role of CLN5 in the eukaryotic cell.

2.4. MATERIALS AND METHODS

2.4.1. CELL LINES, MEDIA, AND ANTIBODIES

AX3 (hereafter referred to as WT, parental cell line of *cln5*$^{-}$) and *cln5*$^{-}$ cells were maintained on SM/2 agar containing *Klebsiella aerogenes* (Fey et al., 2007). Cells used in experiments were cultured axenically in nutrient-rich medium (HL5) at 22°C and 150 RPM (Formedium, Hunstanton, Norfolk, United Kingdom). HL5 was supplemented with streptomycin sulfate (300 μg/ml) and ampicillin (100 μg/ml) to prevent bacterial growth. Blasticidin S hydrochloride (10 μg/ml) was used to select cln5- cells. For all experiments, cells were harvested during the mid-log phase of growth (1–5 x 106 cells/ml). KK2 buffer was formulated as follows: 0.7 g/L K2HPO4, 2.2 g/L KH2PO4, pH 6.5. Mouse monoclonal anti-cortexillin-I (CtxA) (241-438-1) (Faix et al., 2001), mouse monoclonal anti-cortexillin-II (CtxB) (232-238-10) (Faix et al., 2001), mouse monoclonal anti-discoidin (Dsc) (80-52-13) (Wetterauer et al., 1993), mouse monoclonal myosin heavy chain type II (MhcA) (56-396-5) (Pagh and Gerisch, 1986), mouse monoclonal anti-proteasomal subunit (PS) (159-183-10) (Schauer et al., 1993), and mouse monoclonal anti-proteasomal subunit 5 (PS5) (171-337) (Schauer et al., 1993) were purchased from the Developmental Studies Hybridoma Bank (University of Iowa, Iowa City, Iowa, United States). Mouse monoclonal anti-β-actin (SC-47778) was purchased from Santa Cruz Biotechnology Incorporated

(Dallas, Texas, United States). Rabbit polyclonal anti-autocrine proliferation repressor (AprA) (Brock and Gomer, 2005), rabbit polyclonal anti-counting factor-associated protein D (CfaD) (Bakthavatsalam et al., 2008), and rabbit polyclonal anti-conditioned medium factor (CmfA) (Jain et al., 1992) were generous gifts from Dr. Richard Gomer (Texas A&M University, Texas, United States). HRP-linked secondary antibodies were purchased from New England Biolabs Canada (Whitby, Ontario, Canada).

2.4.2. RNA PREPARATION

Cells grown in suspension were deposited onto Petri dishes containing HL5 medium and left to adhere to the dish for at least 1 h at 22°C (Figure 2A). The medium was replaced with fresh HL5 medium containing ampicillin (100 μg/ml) and streptomycin sulphate (300 μg/ml) and left overnight to allow for two mitotic doubling times. The following day, growth-phase cells and cells starved for 4 h in KK2 buffer were harvested and stored at −80°C for future use. A 4-h starvation timepoint was selected since this is when cln5 is maximally expressed in *D. discoideum* (http://dictyexpress.biolab.si/) (Stajdohar et al., 2017). Growth-phase and starved cells from −80°C storage were lysed and RNA was extracted using the Monarch Total RNA Miniprep Kit according to the manufacturer's instructions (New England Biolabs Canada, Whitby, Ontario, Canada). A total of three biological replicates each for growth and starvation were submitted for RNA sequencing (RNA-seq) analysis.

2.4.3. RNA SEQUENCING AND BIOINFORMATICS

RNA-seq was performed by The Centre for Applied Genomics at the Hospital for Sick Children (Toronto, Ontario, Canada). All RNA samples were prepared with a stranded

poly(A) mRNA library preparation kit (NEBNext, New England Biolabs Canada, Whitby, Ontario, Canada) and the quality of RNA was determined using a Bioanalyzer (Agilent Technologies, Santa Cruz, California, United States). The RNA-seq analysis for all mRNA libraries were done through an Illumina NovaSeq SP flowcell PE100 sequencer (San Diego, California, United States). Adaptor sequences attached to the raw paired reads were removed with Trimmomatic (Bolger et al., 2014). The quality of the raw paired reads from the sequencer was assessed with FastQc (https://www.bioinformatics.babraham.ac.uk/projects/fastqc/). The *D. discoideum* reference genome acquired from the Ensembl database was indexed with hierarchical indexing for spliced alignment of transcripts 2 (HISAT2) and the paired reads were mapped onto the indexed reference genome with HISAT2 (Kim et al., 2019). To obtain read counts, FeatureCounts was used on the mapped reads (Liao et al., 2014). The differential gene expression analysis was done using the DeSeq2 version of statistical analysis of RNA-seq data tools (SARTools) package (Love et al., 2014; Varet et al., 2016). In the SARTools parameters, an alpha value of 0.05 along with the Benjamin-Hochberg (BH) multiple-testing correction were used in the differential gene expression analysis. Furthermore, a log2 fold change threshold of 1.25 was applied on the list of differentially expressed genes (DEGs) (Kim & Huber, 2022). Logically accelerated gene ontology term finder (LAGO) was used for gene ontology (GO) term enrichment analyses of the DEGs (Boyle et al., 2004). A p-value of 0.05, combined with the Benjamin-Hochberg (BH) correction was applied. Within each GO term enrichment analysis (e.g., biological process, molecular function, and cellular component), only annotated genes that were identified by the LAGO database were used.

2.4.4. ENZYME ACTIVITY ASSAYS

Growth-phase cells and cells starved for 4 h were lysed with 0.1% NP40 in 0.05 M 2-(N-morpholino) ethanesulfonic acid (MES) (pH 6.5). All enzyme activity assays were performed using equal amounts of protein from whole cell (WC) lysates (100-200 µg). Proteins in WC lysates were quantified using a Qubit 2.0 Fluorometer (Fisher Scientific Company, Ottawa, Ontario, Canada). Each assay was performed in triplicate and measured using a Synergy HTX multi-mode plate reader (BioTek Instruments Incorporated, Winooski, Vermont, United States). All activity values were subtracted from values acquired from the blank solution. Enzyme activities in *cln5*$^{-}$ WC lysates were standardized against activities in WC lysates from WT cells. Data were statistically analyzed using the one-sample t-test and a p-value < 0.05 was considered significant.

2.4.4.1. α-MANNOSIDASE and β-GLUCOSIDASE

For α-mannosidase, methods were adapted from Loomis (1970). Briefly, WC lysates were added to 5 mM acetate buffer (pH 5.0) containing a final concentration of 5 mM para-nitrophenyl-α-D-mannopyranoside substrate (N2127, Sigma Aldrich Canada, Oakville, Ontario, Canada). For β-glucosidase, methods were adapted from Coston and Loomis (1969) using a final concentration of 10 mM para-nitrophenyl-β-D-glucopyranoside substrate (487507, Sigma Aldrich Canada, Oakville, Ontario, Canada) in 50 mM acetate buffer (pH 5.0). For both assays, reaction mixtures were incubated at 35°C for 45 min, quenched with an equal volume of 1 M Na_2CO_3, and activity was measured at 405 nm absorbance.

2.4.4.2. α-GLUCOSIDASE

Methods were adapted from Wimmer et al. (1997). Briefly, WC lysates were added to 0.1 M sodium succinate (pH 6.0) containing 2 mM p-nitrophenyl-α-D-glucopyranoside substrate (487506, Sigma Aldrich Canada, Oakville, Ontario, Canada). Reactions were incubated at 65°C for 1 h and then quenched with two equal volumes of 1 M Na_2CO_3. Activity was measured at 395 nm absorbance.

2.4.4.3. α- AND β-GALACTOSIDASE

Methods were adapted from Kilpatrick and Stirling (1976) and Maruhn (1976). The α-galactosidase activity assay was performed using 2 mM para-nitrophenyl α-D-galactopyranoside substrate (N0877, Sigma Aldrich Canada, Oakville, Ontario, Canada) in citrate/phosphate buffer (pH 4.5), while the β-galactosidase activity assay contained a reaction solution of 5 mM ortho-nitrophenyl-β-D-galactopyranoside substrate (48712-M, Sigma Aldrich Canada, Oakville, Ontario, Canada) in 100 mM citrate buffer (pH 4.0). In both assays, the reaction solutions were incubated at 37°C for 45 min. The α-galactosidase reactions were quenched with an equal volume of 1 M sodium glycinate (pH 10.4). β-galactosidase reactions were terminated using an equal volume of 2-amino-2-methyl-propanol/HCl buffer. Activity was measured at 405 nm absorbance.

2.4.4.4. PALMITOYL-PROTEIN THIOESTERASE 1

Methods were modified from van Diggelen et al. (1999). Briefly, WC lysates were added to 0.2 mM 4-methylumbelliferyl 6-thio-palmitate-β-D-glucopyranoside substrate (19524, Cedarlane Labs, Burlington, Ontario, Canada) in McIlvain's phosphate/citrate buffer containing 15 mM dithiothreitol and 0.375% (v/v) Triton X-100 (pH 4.0). Reactions were incubated for 1 h at 37°C and then stopped by heating the solution for 2 min at 95°C.

1 U of β-glucosidase enzyme (from almonds, dissolved in distilled water containing 0.2% (w/v) bovine serum albumin) (Sigma Aldrich Canada, Oakville, Ontario, Canada) was added to the cooled reaction mixture while adjusting the pH to 5 with NaOH. The samples were left at 37°C for 1 h and then an equal volume of 0.5 M Na_2CO_3/$NaHCO_3$ buffer containing 0.025% (v/v) Triton X-100 (pH 10.7) was added to terminate the reaction. Fluorescence was detected using the following filters: 360/40 nm excitation, 460/40 nm emission.

2.4.4.5. TRIPEPTIDYL PEPTIDASE 1

Methods were adapted from Stumpf et al. (2017). Briefly, WC lysates were combined with 120 µM Ala-Ala-Phe-7-amido-4-methylcoumarin tripeptidyl peptidase 1 (TPP1) substrate (A3401, Sigma Aldrich Canada, Oakville, Ontario, Canada) in buffer containing 100 mM sodium acetate/150 mM NaCl/0.1% (v/v) Triton X-100 (pH 4.5). Reactions were incubated at 37°C for 1 h in the dark, after which time an equal volume of quenching solution (100 mM sodium acetate, 150 mM NaCl, pH 4.3) was added to stop the reaction. Fluorescence was detected using the following filters: 360/40 nm excitation, 460/40 nm emission.

2.4.4.6. CATHEPSIN D AND CATHEPSIN F

Cathepsin D (CTSD) enzymatic activity was assessed using the CTSD Activity Assay Kit according to the manufacturer's instructions (10013-596, VWR International, Mississauga, Ontario, Canada) and fluorescence was detected using the following filters: 360/40 nm excitation, 460/40 nm emission. Cathepsin F (CTSF) activity was measured using a method adapted from Fonovič et al. (2004). Briefly, WC lysates were mixed with

5 µg/ml pepsin (10108057001, Sigma Aldrich Canada, Oakville, Ontario, Canada) (pH 4.5–5.0). Reactions were preincubated for 1 h at 37°C, after which time 1 µM Z-FR-AMC substrate (80350BP, Cedarlane Labs, Burlington, Ontario, Canada), as well as 0.1 M sodium phosphate buffer containing 1 mM EDTA and 0.1% (v/v) PEG 600 (pH 6.5) were added to the reaction mixture. The reaction was adjusted to a final DMSO content of 5% (v/v) and then incubated at 27°C for 1 h. Fluorescence was detected using the following filters: 360/40 nm excitation, 460/40 nm emission.

2.4.4.7. CATHEPSIN B

Methods were adapted from Barrett (1980). Briefly, samples were mixed with reaction buffer (352 mM KH2PO4, 48 mM Na2HPO4, 4 mM disodium EDTA) supplemented with fresh cysteine at a final concentration of 8 mM. Reactions were preincubated for 5 min at 40°C, after which time they were incubated for 1 h at 40°C in the presence of 1.5 mM of fluorogenic cathepsin B (CTSB) substrate (219392, Sigma Aldrich Canada, Oakville, Ontario, Canada). Reactions were stopped with two equal volumes of 100 mM sodium chloroacetate/30 mM sodium acetate/70 mM acetic acid buffer (pH 4.3) and fluorescence was detected using the following filters: 360/40 nm excitation, 460/40 nm emission.

2.4.4.8. N-ACETYLGLUCOSAMINIDASE

Methods were adapted from Loomis (1969) and Huber and Mathavarajah (2018a). Briefly, WC lysates were mixed with 4.2 mM para-nitrophenyl N-acetyl-β-D-glucosaminide substrate (N9376, Sigma Aldrich Canada, Oakville, Ontario, Canada) in 100 mM acetate buffer (pH 5.0). Reactions were incubated for 5 min at 35°C. An equal volume

of 1 M Na_2CO_3 was added to stop the reaction. Activity was measured at 405 nm absorbance.

2.4.5. PROTEASOME ACTIVITY

Proteasomal activity was assessed using the Proteasome 20S Activity Assay Kit according to the manufacturer's instructions (MAK172, Sigma Aldrich Canada, Oakville, Ontario, Canada). Briefly, growth-phase cells and cells starved for 4 h were lysed with 0.1% (v/v) NP40 in 0.05 M MES buffer (pH 6.5) and equal protein amounts (100-150 µg) from WC lysates were used in the assay. Proteins in WC lysates were quantified using a Qubit 2.0 Fluorometer. Samples were incubated for 1 h at 37°C and activity was measured using a Synergy HTX multi-mode plate reader and the following filters: 360/40 nm excitation, 460/40 nm emission. All activity values were subtracted from the blank solution and reads obtained from the *cln5*$^-$ line were normalized to WT activity values. Data were statistically analyzed using the one-sample t-test and a p-value of <0.05 was considered significant.

2.4.6. SDS-PAGE AND WESTERN BLOTTING

WC lysates were prepared from growth-phase cells and cells starved for 4 h. In addition, WT and *cln5*$^-$ conditioned media (CM) was collected during growth and conditioned buffer (CB) was collected after 4 h of starvation. CM and CB were clarified through centrifugation (4°C/1500 RPM/5 min). Protein concentrations were determined using a Qubit 2.0 Fluorometer. SDS-PAGE and western blotting were performed using standard methods (2-hour incubation at 22°C for primary and secondary antibodies in 5% (w/v) milk/TBST. The following antibody dilutions were used: anti-AprA (1:1,000), anti-

CfaD (1:1,000), anti-CtxA (1:2,000), anti-CtxB (1:2,000), anti-MhcA (1:1,000), anti-CmfA (1:1,000). anti-Dsc (1:1,000), anti-PS (1:1,000), anti-PS5 (1:1,000), and anti-β-Actin (1:1,000). All primary antibodies used for western blotting detected proteins at molecular weights that were consistent with previous studies (see Section 2.4.1 for citations). HRP-linked secondary antibodies were used at a dilution of 1:2,000. The ChemiDoc Imaging System (Bio-Rad Laboratories Canada, Mississauga, Ontario, Canada) was used to digitally scan the immunoblots. Protein bands were quantified using Fiji/ImageJ and values obtained from WC lysates were normalized to the corresponding levels of β-Actin (Schindelin et al., 2012). Values obtained from *cln5*$^{-}$ samples were standardized against WT values and the one-sample t-test was used to assess statistical significance. A p-value of <0.05 was considered significant.

2.5. RESULTS

2.5.1. COMPARATIVE TRANSCRIPTOMICS REVEALS THE EFFECTS OF *cln5*-DEFICIENCY ON GENE EXPRESSION IN *D. discoideum*

Previous work in *D. discoideum* linked the function of Cln5 to cell proliferation, cytokinesis, folic acid-mediated chemotaxis, and autophagy during growth, and cyclic adenosine monophosphate (cAMP)-mediated chemotaxis, adhesion, and aggregation during the early stages of multicellular development (Huber and Mathavarajah, 2018b; McLaren et al., 2021). To gain insight into the molecular mechanisms underlying *cln5*-deficiency phenotypes in *D. discoideum* and the biological pathways impacted by the loss of *cln5*, we performed RNA-seq analysis on growth-phase cells and cells starved for 4 h in KK2 buffer. We chose the 4-hour timepoint since this is when *cln5* expression is maximal (Stajdohar et al., 2017). The list of DEGs was filtered to include only those genes with a

log2 fold change of 1.25 (increase or decrease) and a p-value < 0.05. A volcano plot was generated to visualize the profile of DEGs (Figure 2B). RNA-seq revealed 2324 unique DEGs in cln5- cells during growth that included 1041 upregulated genes and 1283 downregulated genes (including *cln5*) (Table 2). After 4 h of starvation, 644 genes were upregulated in *cln5*$^{-}$ cells and 394 were downregulated (including *cln5*), totalling 1038 unique genes.

During growth, the most significantly downregulated genes were those encoding heat shock proteins (*hspE-1, hspG3, hspG4, hspG5, hspG6, hspG7, hspG8, hspG12, hspH, hspJ, hspM, dnaja1*) and genes involved in protein ubiquitination (*ubqG, ubqH, ubqI, ubqJ, DDB_G0285907*) (Kim & Huber, 2022). Conversely, the most significantly upregulated genes were those associated with cell cycle progression, including but not limited to, subunits of the anaphase-promoting complex (*anapc3, anapc5, anapc6, anapc7, anapc10*), and genes involved in mitosis, such as kinesin-related genes (*kif2, kif4, kif10, kif12, kif13*) (Castro et al., 2005; Nag et al., 2008; Tikhonenko et al., 2009; Koonce, 2020). During starvation, genes related to development (*cotC, cotD, cotE*) were significantly downregulated in *cln5*$^{-}$ cells. In contrast, genes encoding ADP-ribosylation factors (*arrJ, arrH, arrK*), which modulate the trafficking of endocytic and secretory vesicles, and ponticulin-like proteins (*ponC1, ponC2, ponC3, ponC4, ponC5*), which are involved in actin bundling and cell-cell adhesion, were the most significantly upregulated genes in *cln5*-deficient cells (Ingalls et al., 1989; Shariff and Luna, 1990; Chia et al., 1993; Li and Guo, 2022).

2.5.2. GO TERM ENRICHMENT ANALYSES OF DIFFERENTIALLY EXPRESSED GENES IN *cln5*$^{-}$ CELLS

As a first step towards analyzing DEGs during growth and starvation, we performed GO term enrichment analyses using LAGO; an online program that clusters genes based on common biological processes they have been associated with, molecular functions of the proteins encoded by the genes, and the subcellular localizations of the proteins (Boyle et al., 2004). For this analysis, we excluded those genes that were uncharacterized (e.g., annotated, but unknown function) (Table 2). Out of 2324 DEGs during growth, this resulted in a list of 1603 genes for biological process, 1586 genes for molecular function, and 1652 genes for cellular component. During growth, DEGs associated with *cln5*-deficiency are linked to a variety of biological processes including macroautophagy (20 genes), protein ubiquitination (60 genes) and deubiquitination (15 genes), proteasomal-mediated ubiquitin-dependent protein catabolism (56 genes), signal transduction (147 genes), and lipid metabolism (111 genes) (Kim & Huber, 2022). Proteins encoded by DEGs during growth have kinase activity (75 genes), hydrolase activity (330 genes), and bind to a variety of biological substrates (e.g., protein, 228 genes; carbohydrates, 296 genes; lipids, 44 genes; nucleotides, 323 genes; ions, 535 genes). In addition, the protein products of the DEGs primarily localize to the nucleus (446 genes), ubiquitin ligase complex (37 genes), cell periphery (171 genes), plasma membrane (139 genes), cytoplasm (672 genes), and cellular components associated with cell division (e.g., microtubule organizing centre, 29 genes; spindle pole, 11 genes; spindle, 20 genes; microtubule cytoskeleton, 39 genes; kinetochore, 10 genes; centromeric region of the chromosome, 15 genes; chromosome, 73 genes).

Like growth, only characterized genes (e.g., annotated with a known or predicted function) from the starvation DEG list were used in LAGO analyses, which included 657, 669, and 728 genes for biological process, molecular function, and cellular component, respectively (Table 2). DEGs during starvation are involved in several biological processes

including signal transduction (83 genes), protein phosphorylation (42 genes), and catabolic processes involving carbohydrates (8 genes) and proteins (51 genes) (Kim & Huber, 2022). Proteins encoded by the DEGs during starvation have a variety of molecular functions including kinase (37 genes) and hydrolase (125 genes) activity and bind to a variety of substrates (carbohydrates, 113 genes; ions, 221 genes; nucleotides, 123 genes; proteins, 100 genes). Additionally, some GO terms related to molecular function were only observed in DEGs during starvation including ubiquitin conjugation (8 genes), cysteine-type endopeptidase activity (14 genes), and actin binding (19 genes). Finally, proteins encoded by DEGs during starvation are associated with lysosomes (25 genes), secretory vesicles (8 genes), the cell periphery (118 genes), the cytoplasm (320 genes), the plasma membrane (78 genes), and extracellularly (20 genes). Overall, LAGO analyses revealed that loss of *cln5* influences the expression of hydrolases and genes involved in protein processing during growth and starvation. In addition, LAGO analyses revealed clusters of DEGs involved in lipid metabolism during growth and carbohydrate metabolism during starvation. Lastly, *cln5*-deficiency appears to impact the expression of genes that encode proteins within the secretory pathway during starvation.

2.5.3. DIFFERENTIALLY EXPRESSED GENES ASSOCIATED WITH *cln5*-DEFICIENCY PHENOTYPES DURING GROWTH

In *D. discoideum*, *cln5*-deficiency reduces cell proliferation and impairs cytokinesis during growth (McLaren et al., 2021). Here, RNA-seq revealed that loss of *cln5* affects the expression of several genes that encode proteins related to cell proliferation including, but not limited to, kinases (*aurK* and *cdk1*, increased; *qkgA-1*, LRRK family protein kinase, decreased), and proteins involved in cell division (*rblA*, *cdc45*, and *cycB*) (all increased)

(Kim & Huber, 2022) (Luo et al., 1995; Sharma et al., 1999; Li et al., 2008; Phillips and Gomer, 2010; Sanchez-Pulido and Ponting, 2011; Strasser et al., 2012). Loss of *cln5* also increased the expression of *aprA*, which encodes the secreted AprA (Brock and Gomer, 2005; Choe et al., 2009). At the protein level, we observed a decreased amount of intracellular AprA and an elevated amount extracellularly suggesting that loss of *cln5* increases the secretion of AprA (Figures 3A,B). AprA exerts its effect by interacting with CfaD (Bakthavatsalam et al., 2008; Choe et al., 2009). Although *cfaD* was not identified as a DEG during growth, loss of *cln5* increased the intracellular and extracellular amounts of CfaD (Figures 3A,C). Together, these data suggest that Cln5 regulates the levels of AprA and CfaD to modulate cellular proliferation.

Consistent with the effect of *cln5*-deficiency on cytokinesis, we detected several DEGs during growth that are associated with cytokinesis including vinculin A (*vinA*), *ctxA*, and *mhcA*, which were all decreased (Kim & Huber, 2022) (De Lozanne and Spudich, 1987; Faix et al., 1996; Stock et al., 1999; Weber et al., 1999; Nagasaki et al., 2009). In *D. discoideum*, cytokinesis can occur via two processes, one is dependent on myosin II and the other on cell adhesion (Zang et al., 1997). CtxA and MhcA participate in myosin II-dependent cytokinesis, while VinA localizes to focal adhesion regions and is thought, along with CtxB, to be involved in cell adhesion-dependent cytokinesis (Zang et al., 1997; Bukharova et al., 2005; Duran et al., 2009; Nagasaki et al., 2009). In addition, cortexillins function as actin-bundling proteins to help form the cleavage furrow during cytokinesis (Weber et al., 1999). To expand upon these findings, we assessed the amounts of CtxA, CtxB, and MhcA protein in *cln5*$^{-}$ cells. Loss of *cln5* had no effect on the amount of CtxA but did decrease and increase the intracellular amounts of CtxB and MhcA, respectively (Figures 4A,B). Overall, these results support the role of Cln5 in cell

proliferation and cytokinesis and provide insight into the genes and proteins affected by *cln5*-deficiency during growth.

2.5.4. DIFFERENTIALLY EXPRESSED GENES ASSOCIATED WITH *cln5*-DEFICIENCY PHENOTYPES DURING STARVATION

cln5-deficiency in *D. discoideum* delays aggregation, inhibits cAMP-mediated chemotaxis, and reduces adhesion during the early stages of development (Huber and Mathavarajah, 2018b; McLaren et al., 2021). Therefore, we surveyed our list of DEGs during starvation to identify dysregulated genes that may contribute to these phenotypes. When we scanned the starved DEG list for genes that have been linked to delayed aggregation, *myoK* (myosin-K heavy chain) and *rps4* (40S ribosomal protein S4) were increased in expression, while *qkgA-1* was reduced (Kim & Huber, 2022). RNA-seq also revealed genes that encode proteins involved in cAMP signalling (e.g., cAMP receptor D, *carD*, increased; cAMP-like receptor 4, *crlD*, decreased) and degradation (e.g., 3′,5′-cyclic-nucleotide phosphodiesterase, *regA*, increased) (Kim & Huber, 2022). The *D. discoideum* genome encodes four receptors that bind cAMP (CarA, CarB, CarC, and CarD) (Kim et al., 1996). *carD* is expressed the highest during the later stages of multicellular development, while cAMP receptor A (*carA*) is expressed the highest during aggregation. RNA-seq revealed that *carA* was not differentially expressed in *cln5*$^{-}$ cells. CarA elevates cAMP synthesis during aggregation by stimulating adenylyl cyclase activity and its expression *via* protein kinase A (Mann et al., 1997; Loomis, 1998; Loomis, 2014). RegA reduces intracellular cAMP levels and leads to reducing cAMP sensitivity in *D. discoideum* (Sun and Devreotes, 1991; Schulkes and Schaap, 1995; Loomis, 1998; Shaulsky et al., 1998; Loomis, 2014). Additionally, cAMP synthesis and binding, as

well as the activation of both CarA and early developmental genes, are modulated by CmfA, which binds to the conditioned media factor receptor (CmfB) (Gomer et al., 1991; Yuen et al., 1995; van Haastert et al., 1996; Deery and Gomer, 1999). In our RNA-seq analysis, *cmfA* was not differentially expressed, but *cmfB* was elevated. Furthermore, while loss of *cln5* had no effect on the amount of intracellular CmfA, *cln5*-deficiency elevated the amount of extracellular CmfA (Figures 5A,B). Together, these findings show that *cln5*-deficiency impacts the expression of genes associated with cAMP signalling during aggregation.

Cell-substrate and cell-cell adhesion also play roles in *D. discoideum* aggregation, which is delayed by the loss of *cln5* (Huber and Mathavarajah, 2018b). In addition to cAMP-mediated chemotaxis, CmfA also influences the expression of discoidin I, a lectin that is secreted and involved in cell-substrate adhesion and migration (Springer et al., 1984; Barondes et al., 1985; Gomer et al., 1991). In scanning the list of DEGs during starvation, genes encoding discoidin subunits (*dscB, dscC, dscD*) were elevated in expression (Kim & Huber, 2022). In support of the differential expression, elevated amounts of intracellular and extracellular discoidin were observed with the loss of *cln5* (Figures 6A,B). Similarly, *D. discoideum* contains a protein complex composed of counting factors (CF45-1, CF50-1, and CF60) and countin (CtnA), that collectively regulate cell adhesion and migration (Brock and Gomer, 1999; Roisin-Bouffay et al., 2000; Tang et al., 2002). Our RNA-seq analysis revealed elevated expression of *cf45-1* and *cf50-1* in *cln5*$^{-}$ cells during starvation. Furthermore, RNA-seq revealed no change in expression of *cf60* and *ctnA*, which is consistent with previous findings of unaltered CtnA protein levels in *cln5*$^{-}$ cells (McLaren et al., 2021). Finally, upregulation of *smlA* (small aggregate formation protein) was observed, which encodes a protein that influences protein

processing and secretion (Brock et al., 1996). Altogether, these observations support previous findings of Cln5 playing a role in aggregation and adhesion.

2.5.5. LOSS OF *cln5* AFFECTS THE EXPRESSION AND ACTIVITY OF SEVERAL CARBOHYDRATE ENZYMES

In previous studies, several lysosomal enzymes were identified as direct or indirect interactors of Cln5 including α-mannosidase, β-glucosidase, and NagA (Huber and Mathavarajah, 2018a). While the *D. discoideum* genome encodes several α-mannosidases, *manA* is the most highly expressed α-mannosidase gene during growth and aggregation (Stajdohar et al., 2017). The *D. discoideum* genome also encodes two β-galactosidases, *glb1* and *glb2*. Two α-galactosidases are encoded by the *D. discoideum* genome, *melA* and *DDB_G0291524*, with the latter being expressed more than *melA* during the *D. discoideum* life cycle. Two α-glucosidases (*gaa*, *modA*) are encoded by the *D. discoideum* genome with *modA* being expressed more than *gaa* during the life cycle (Stajdohar et al., 2017). Finally, the *D. discoideum* genome encodes one β-glucosidase (*gluA*). In our transcriptomics dataset, we observed many carbohydrate enzymes that were differentially expressed during *cln5*$^{-}$ growth and starvation. During growth, loss of *cln5* increased the expression of *glb1*, *manA*, *melA*, and *gaa* (Kim & Huber, 2022). When starved, *cln5*$^{-}$ cells increased the expression of *gluA* and decreased the expression of the putative α-galactosidase (*DDB_G0291524*) and α-mannosidase (*DDB_G0268754*) genes. Next, we assessed the intracellular activity of the aforementioned enzymes. During growth, loss of *cln5* decreased β-glucosidase and NagA activity and increased the activity of α-glucosidase (Figure 7A). During starvation, *cln5*-deficiency decreased α-mannosidase, β-glucosidase, and NagA activity (Figure 7B). We observed no

effect of *cln5*-deficiency on α-galactosidase and β-galactosidase activity during both growth and starvation. Collectively, these findings suggest that Cln5 regulates the activities of several carbohydrate enzymes.

2.5.6. LOSS OF *cln5* AFFECTS THE EXPRESSION AND ACTIVITY OF THE PROTEASOME

Ceroid lipofuscin accumulation is a common hallmark of the NCLs and has been postulated to occur due to alterations in the autophagy pathway (Cárcel-Trullols et al., 2015; Leinonen et al., 2017; Adams et al., 2019; Mukherjee et al., 2019; McLaren et al., 2021). Dysregulated autophagy has been observed in many CLN5 disease models including *D. discoideum* (Best et al., 2017; Leinonen et al., 2017; Adams et al., 2019; Doccini et al., 2020; McLaren et al., 2021). By scanning the list of DEGs, we identified genes involved in autophagy initiation (*atg1, atg13*) and autophagosome formation and turnover (*atg6A, atg8, atg18*) (all decreased) during growth, but no DEGs related to autophagy during starvation (Kim & Huber, 2022) (Tanida et al., 2005; Mizushima, 2010; Bento et al., 2016; Mesquita et al., 2017). Since our previous work in *D. discoideum* reported increased numbers of ubiquitin-positive proteins in *cln5*$^{-}$ cells during growth, we also examined our growth DEG list for genes associated with protein ubiquitination (Pickart, 2001; Jin et al., 2008; Williamson et al., 2009; Shao et al., 2013; McLaren et al., 2021). Not surprisingly, we identified DEGs that encode proteins involved in ubiquitin attachment, such as polyubiquitin proteins (*ubqA, ubqD, ubqF, ubqG, ubqH, ubqI, ubqJ*), all of which were downregulated during growth (Kim & Huber, 2022). In addition, DEGs encoding proteins involved in ubiquitin conjugation (E2 complex) were reduced, including ubiquitin-conjugating enzyme E2 (*ubcB*) and a gene similar to

human *UBE2J2* (*ube2j2*), and genes encoding Ube2C and Ube2S (*ube2c* and *ube2s*, respectively) were elevated. Ubiquitin ligase genes (*skp1B, rnf160*) were also reduced in expression. However, some genes associated with the ligase activity of the E3 complex were increased such as subunits of the anaphase-promoting complex (*anapc3, anapc4, anapc5, anapc6, anapc7, anapc10, cdc20, cdc26*) (Kim & Huber, 2022) (Matyskiela et al., 2009; Wang et al., 2009). Finally, genes involved in protein deubiquitination such as ubiquitin hydrolases and thioesterases were reduced in expression (e.g., *uch2, yod1*) (Deol et al., 2020). Overall, these findings revealed the genetic impact of *cln5*-deficiency on the autophagy and protein ubiquitination pathways, which further supports the role of Cln5 in autophagy.

Interestingly, the autophagy pathway and ubiquitin-proteasome system crosstalk with each other and both use ubiquitin as a tag to signal protein degradation (Kocaturk and Gozuacik, 2018). Our RNA-seq analysis showed that loss of *cln5* increased the expression of a gene predicted to be involved in proteasome assembly, *psmG4*, as well as reduced the expression of *psmE3*, which encodes a proteasome subunit that regulates the activity of the proteasome during *D. discoideum* growth (Kim & Huber, 2022) (Le Tallec et al., 2007; Masson et al., 2009). In addition, we observed elevated amounts of one proteasome subunit, PS5, during *cln5*$^{-}$ growth and starvation (Figures 8A,B), no effect on another proteasome subunit (Figure 8C), and decreased proteasome 20S activity during both growth and starvation (Figure 8D). These findings, coupled with previous work, suggest that Cln5 plays a role in proteasomal degradation and that the loss of *cln5* leads to dysfunctional protein turnover *via* both autophagy and through the proteasome.

2.5.7. LOSS OF *cln5* AFFECTS THE EXPRESSION AND ACTIVITY OF OTHER CLN-LIKE PROTEINS IN *D. discoideum*

It has been suggested that CLN proteins collectively participate in a shared biological pathway or pathways that converge to regulate a common cellular process (Persaud-Sawin et al., 2007; Huber, 2020). As a result, we scanned our list of DEGs and revealed several *CLN*-like genes that were differentially expressed in *cln5*$^-$ cells (Kim & Huber, 2022). During growth, *tpp1E* (similar to human *TPP1/CLN2*), *ddj1* (similar to human *DNAJC5/CLN4*), and *kctd9* (similar to human *KCTD7/CLN14*) were reduced in expression in *cln5*$^-$ cells relative to WT cells, while *tpp1F* (similar to human *TPP1/CLN2*) and *grn* (similar to human *GRN/CLN11*) were elevated. During starvation, the expression of *tpp1B* and *tpp1F* (similar to human *TPP1/CLN2*), *ctsD* (similar to human *CTSD/CLN10*), *DDB_G0291191* (similar to human *CTSF/CLN13*), and *DDB_G0269760* (similar to human *KCTD7/CLN14*) were increased, while *cprB* (similar to human *CTSF/CLN13*) was reduced. Based on these findings, we next assessed the intracellular activities of CLN proteins with demonstrated enzymatic activity in mammals including PPT1, TPP1, CTSD, and CTSF. While there was no effect of *cln5*-deficiency on *ppt1* expression, we detected increased PPT1 activity in both growth and starved cells (Figures 9A,B). Despite the effects of *cln5*-deficiency on *tpp1E* and *tpp1F* expression during growth, and *tpp1B* and *tpp1F* expression during starvation, there was no correlated impact on TPP1 activity in *cln5*$^-$ cells. There was elevated CTSD and CTSF activity observed in *cln5*$^-$ cells during growth but no changes were observed during starvation (Figures 10A,B). Finally, elevated *ctsB* expression was observed in *cln5*$^-$ cells during growth and cells starved for 4 h, but reduced CTSB activity was observed in *cln5*$^-$ cells during starvation. From these findings, it is evident that Cln5

influences the expression and activity of some CLN proteins, which further supports the molecular networking of *CLN* genes and proteins (Huber, 2020).

2.6. DISCUSSION

In *D. discoideum*, *cln5*-deficiency suppresses cell proliferation, reduces cytokinesis, increases the basal level of autophagy, delays aggregation, impairs cAMP-mediated chemotaxis, reduces cell-substrate and cell-cell adhesion, and causes precocious multicellular development after mound formation (Huber and Mathavarajah, 2018b; McLaren et al., 2021). In this study, we used comparative transcriptomics to gain insight into the molecular mechanisms underlying these phenotypes. We then used the expression data to inform follow up work that examined the effect of *cln5*-deficiency on protein levels and enzyme activity during growth and the early stages of development.

Loss of *cln5* increases the intracellular levels of ubiquitinated proteins during growth (McLaren et al., 2021). Here, comparative transcriptomics revealed that the most significantly downregulated genes during growth were those that encode heat shock proteins and proteins associated with protein ubiquitination, which could reflect an attempt by *cln5*$^-$ cells to limit the expression of genes linked to protein ubiquitination. The most significantly upregulated genes were associated with cell cycle progression and mitosis. Since loss of *cln5* inhibits cell proliferation (McLaren et al., 2021), these findings indicate that *cln5*$^-$ cells increase the expression of genes linked to cell proliferation to help restore the normal rate of proliferation. During starvation, the most significantly downregulated genes were linked to development. Conversely, the most significantly upregulated genes were involved in intracellular trafficking and cell-cell adhesion. These findings are

consistent with the defects in developmental timing and adhesion observed in *cln5*$^{-}$ cells (Huber and Mathavarajah, 2018b; McLaren et al., 2021).

GO term analysis revealed an enrichment of DEGs associated with autophagy, protein homeostasis, and lipid metabolism during growth. These findings are consistent with work in *D. discoideum* and mammalian models of CLN5 disease that have linked the function of CLN5 to these cellular processes (El Haddad et al., 2012; Schmiedt et al., 2012; Best et al., 2017; Leinonen et al., 2017; Adams et al., 2019; Doccini et al., 2020; McLaren et al., 2021; Yasa et al., 2021; Doccini et al., 2022). Previous work suggests that CLN5 functions as either a glycoside hydrolase or depalmitoylase (Huber and Mathavarajah, 2018a; Luebben et al., 2022). Here, comparative transcriptomics showed that loss of *cln5* during growth alters the expression of genes that encode enzymes. During starvation, GO term analysis identified an enrichment of DEGs that encode enzymes and proteins involved in catabolic processes. In addition, consistent with the extracellular localization of Cln5 in *D. discoideum* and CLN5 in mammals (Isosomppi et al., 2002; Moharir et al., 2013; Hughes et al., 2014; Huber and Mathavarajah, 2018a; Huber and Mathavarajah, 2018b; McLaren et al., 2021), GO term analyses identified an enrichment of DEGs that encode proteins that localize to secretory vesicles, the cell periphery, the plasma membrane, and extracellularly, which is consistent with previous work that indicated a role for CLN5 in protein secretion (Hersrud et al., 2016; Huber, 2021; Iwan et al., 2021). Notably, GO term enrichment analyses also showed that loss of *cln5* affects the expression of genes that encode lysosomal enzymes, which aligns with the lysosomal localization of CLN5 in mammalian cells (Isosomppi et al., 2002).

LAGO analysis revealed altered expression of genes linked to cell cycle progression and mitosis in *cln5*$^{-}$ cells, which is consistent with the reduced proliferation of *cln5*$^{-}$ cells

(McLaren et al., 2021). In addition, we showed that loss of *cln5* significantly increases the expression of *aprA*, which encodes the well-established proliferation repressor AprA (Brock and Gomer, 2005). Intriguingly, *cln5*-deficiency decreased the intracellular amount of AprA, but increased the extracellular amount, suggesting that loss of *cln5* increases AprA secretion. These findings support the reduced proliferation of *cln5*$^{-}$ cells since more AprA is present outside cells to repress proliferation. In addition, it appears that *cln5*$^{-}$ cells increase the expression of *aprA* to counteract the reduced intracellular amount of the protein. Finally, loss of *cln5* also increased the intracellular and extracellular levels of CfaD, which participates in AprA-dependent signalling. Combined, these observations indicate that *cln5*$^{-}$ cells cannot modulate AprA-dependent signalling and the increased secretion of AprA is exacerbated by the increased expression of *aprA* in *cln5*-deficient cells, which ultimately supresses cell proliferation.

Our previous work in *D. discoideum* reported reduced cytokinesis in *cln5*-deficient cells (McLaren et al., 2021). Here, RNA-seq revealed reduced expression of genes associated with cytokinesis including *ctxA*, *mhcA*, and *vinA*. We also observed significantly increased amounts of MhcA protein in *cln5*$^{-}$ cells, which could explain the reduced expression of *mhcA*, and reflect an attempt by *cln5*$^{-}$ cells to mitigate defects in MhcA-dependent cytokinesis. Interestingly, our RNA-seq analysis revealed a cluster of DEGs that encode proteins that bind to the cytoskeleton, which is consistent with a previous study that revealed DEGs in *Cln1*$^{-/-}$ mice related to cytoskeleton organization (von Schantz et al., 2008). Moreover, altered cytokinesis has also been reported in yeast and *D. discoideum* knockout models of CLN3 disease (Codlin et al., 2008; Mathavarajah et al., 2018) indicating that multiple *CLN* genes regulate cytokinesis.

Comparative transcriptomics identified DEGs associated with aggregation, cAMP-mediated chemotaxis, and cell adhesion in *cln5*$^{-}$ cells, which is consistent with the delayed aggregation, suppressed cAMP-mediated chemotaxis, and reduced adhesion observed in *cln5*-deficient cells (Huber and Mathavarajah, 2018b; McLaren et al., 2021). We also found that loss of *cln5* elevates the amount of secreted CmfA and expression of the gene encoding the CmfA receptor, *cmfB*, which together modulate cAMP-mediated chemotaxis and the expression of early developmental genes (Gomer et al., 1991; Yuen et al., 1995; van Haastert et al., 1996; Deery and Gomer, 1999). In addition, *cln5*-deficiency increased the expression of the gene encoding the cAMP phosphodiesterase RegA. These findings suggest that the delayed aggregation of *cln5*$^{-}$ cells can be at least partly due to altered CmfA-dependent signalling and increased degradation of cAMP due to elevated expression of *regA*. Finally, consistent with the role of Cln5 in cell adhesion (Huber and Mathavarajah, 2018b), loss of *cln5* increased the expression of genes that encode subunits of discoidin, which resulted in a correlated increase in the intracellular and extracellular amounts of discoidin protein in starved cells. Discoidins are secreted lectins that regulate cell migration and cell-substrate adhesion in *D. discoideum* (Springer et al., 1984; Barondes et al., 1985). Thus, the increased expression and amount of discoidin protein likely reflected an attempt by *cln5*-deficient cells to restore adhesion to WT levels.

RNA-seq identified DEGs in *cln5*$^{-}$ cells associated with protein tagging, protein degradation, and autophagy, which aligns with studies from *D. discoideum*, mice, and humans linking the function of CLN5 to autophagy (Best et al., 2017; Leinonen et al., 2017; Huber and Mathavarajah, 2018b; Adams et al., 2019; Doccini et al., 2020; Basak et al., 2021b; McLaren et al., 2021). Intriguingly, autophagy is dysregulated in many NCL subtypes (Kim et al., 2022). Accumulated evidence suggests that autophagy and the

ubiquitin-proteasome system work together to regulate protein degradation and operate in a compensatory manner when one of the pathways is inhibited (Kocaturk and Gozuacik, 2018). Our previous work showed that loss of *cln5* increases the basal level of autophagy during growth (McLaren et al., 2021). Here, we reported an accumulation of one of the proteasomal subunits in *cln5*$^{-}$ cells, but a reduction in proteasome 20S activity during both growth and starvation, which is consistent with the increased abundance of ubiquitin-positive proteins in *cln5*$^{-}$ cells (McLaren et al., 2021). Together, these results indicate that Cln5 influences protein degradation *via* autophagy and the ubiquitin-proteasome system.

Autophagy is dependent on lysosomal function. Not surprisingly, our RNA-seq dataset contained several DEGs in *cln5*$^{-}$ cells that encode carbohydrate enzymes including β-glucosidase and α-mannosidase, which both interact with Cln5 (Huber and Mathavarajah, 2018a). We followed up this analysis by showing that *cln5*-deficiency affects the activity of various carbohydrate enzymes. Notably, *cln5*$^{-}$ cells displayed reduced NagA activity during growth and starvation, which is consistent with previous work that reported that *D. discoideum* Cln5 and human CLN5 can also cleave the NagA substrate and that Cln5 and NagA may participate in a common pathway in *D. discoideum* that regulates autophagy (Huber and Mathavarajah, 2018a; McLaren et al., 2021). We also showed that loss of *cln5* alters the expression and activities of other CLN-like proteins in *D. discoideum*. This aligns with previous work that reported an interaction between CLN5 and PPT1 in COS-1 cells (Lyly et al., 2009). In addition, *D. discoideum* Cln5 interacts with CtsD, various homologs of human CTSF (CprA, CprD, CprE, and CprG), NagA, α-mannosidase, and β-glucosidase, all of which may have displayed altered enzymatic activity due to the absence, and hence, lack of interaction with Cln5, in *cln5*$^{-}$ cells (Huber and Mathavarajah, 2018a). While our previous work showed that loss of *cln5* decreases the intracellular

amount of CtsD during starvation (McLaren et al., 2021), in this study, comparative transcriptomics revealed increased expression of *ctsD* in starved *cln5*$^{-}$ cells. These findings indicate that *cln5*$^{-}$ cells upregulate the expression of *ctsD* to restore the intracellular amount of the protein. Also, our work showed that loss of *cln5* elevates *ctsB* expression but reduces CTSB activity. Previous work also reported reduced CTSB activity in *CLN5*-deficient cells and it was suggested that the loss of *CLN5* impairs intracellular trafficking and the movement of lysosomes (Mamo et al., 2012; Basak et al., 2021a; Yasa et al., 2021). Consistent with these findings, LAGO analyses revealed an enrichment of GO terms associated with intracellular vesicles including lysosomes, endocytic vesicles, and phagocytic vesicles. In CLN5-depleted HeLa cells, endosomal sorting is perturbed due to abolished retromer interaction and recruitment to the endosome, as well as poor fusion between the lysosome and autophagosome (Mamo et al., 2012; Yasa et al., 2021). Combined, these findings indicate that loss or mutation of *CLN5* affects the expression, synthesis, and/or delivery of enzymes to lysosomes.

In conclusion, this study sheds light on the pathways perturbed in *cln5*$^{-}$ cells, highlights the multifaceted role of CLN5 in eukaryotic cells, and contributes knowledge to the mechanisms that may be disrupted in CLN5 disease patients.

2.7. ACKNOWLEDGMENTS

The authors would like to thank Richard Gomer (Texas A&M University) for providing antibodies against AprA, CfaD, and CmfA, Compute Canada for allowing the authors to use the SHARCNET cluster for the bioinformatics pipeline, and Aaron Shafer and Michael Donaldson (both from Trent University, Peterborough, Ontario, Canada) for their advice in the bioinformatics analysis.

2.8. FIGURES AND TABLES

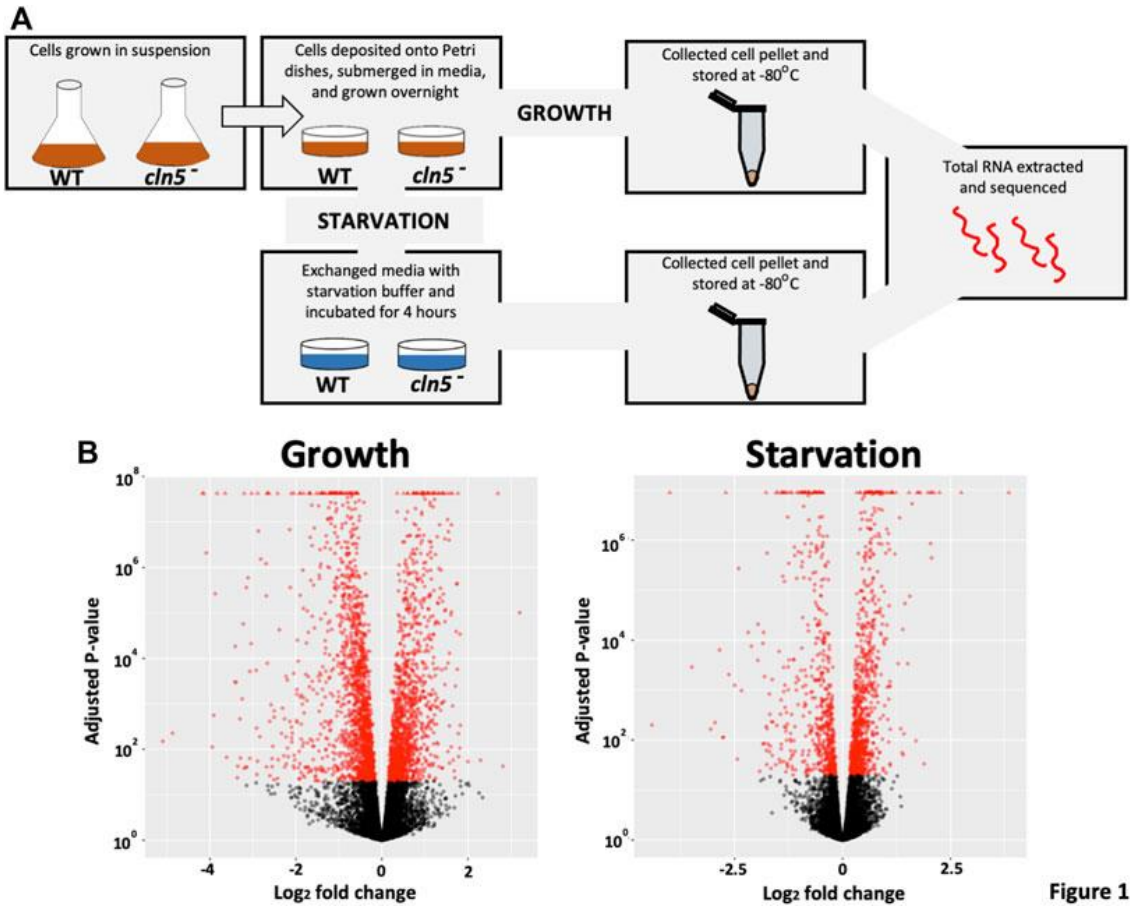

FIGURE 2. A pictorial schematic of the methods used to determine the effects of *cln5* deletion on gene expression. (A) WT and *cln5*⁻ cells grown in suspension and in the mid-log phase of growth were deposited onto Petri dishes and grown overnight in HL5. Growth-phase cells were harvested after the overnight incubation, while starved cells were collected after a 4-hour incubation in KK2 buffer. All cell pellets were stored at −80°C until RNA extraction was done. Extracted RNA samples were sequenced at The Hospital for Sick Children (Toronto, Ontario, Canada). **(B)** Following differential expression analysis via SARTools, volcano plots were generated to visualize the profile of DEGs during growth and after 4 h of starvation.

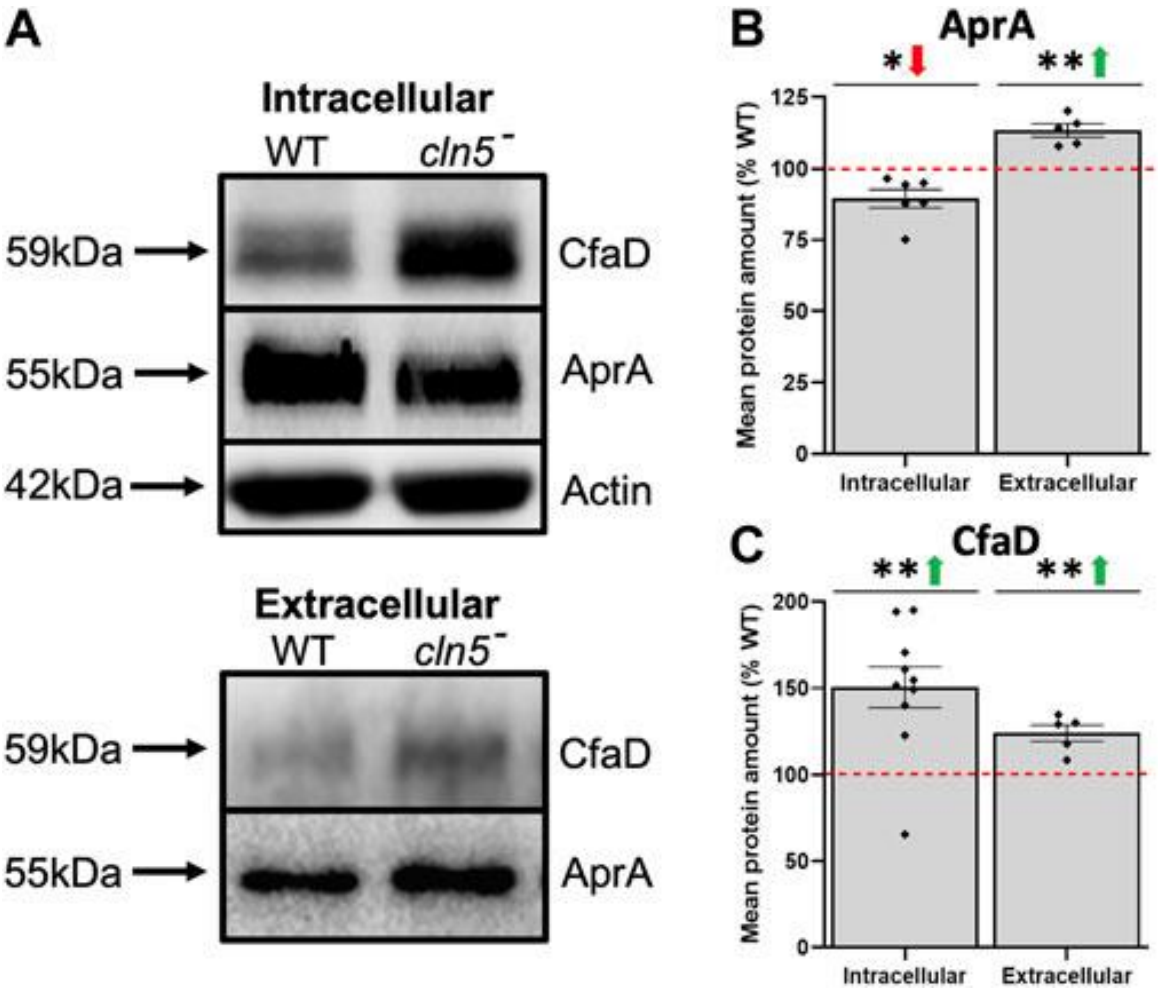

FIGURE 3. Loss of *cln5* affects the intracellular and extracellular levels of AprA and CfaD during growth. Whole cell (WC) lysates (20-30 µg) and samples of conditioned media (CM) (0.1–0.375 µg) from growth-phase WT and *cln5*$^{-}$ cells were separated by SDS-PAGE and analyzed by western blotting. **(A)** Membranes were probed with anti-AprA, anti-CfaD, and anti-β-actin (loading control). Intracellular and extracellular amounts of **(B)** AprA and **(C)** CfaD were quantified using Fiji/ImageJ and intracellular values were standardized against the levels of β-actin. Data presented as mean protein amount (% WT) ± SEM ($n \geq 5$). *$p < 0.05$ (one sample *t*-test).

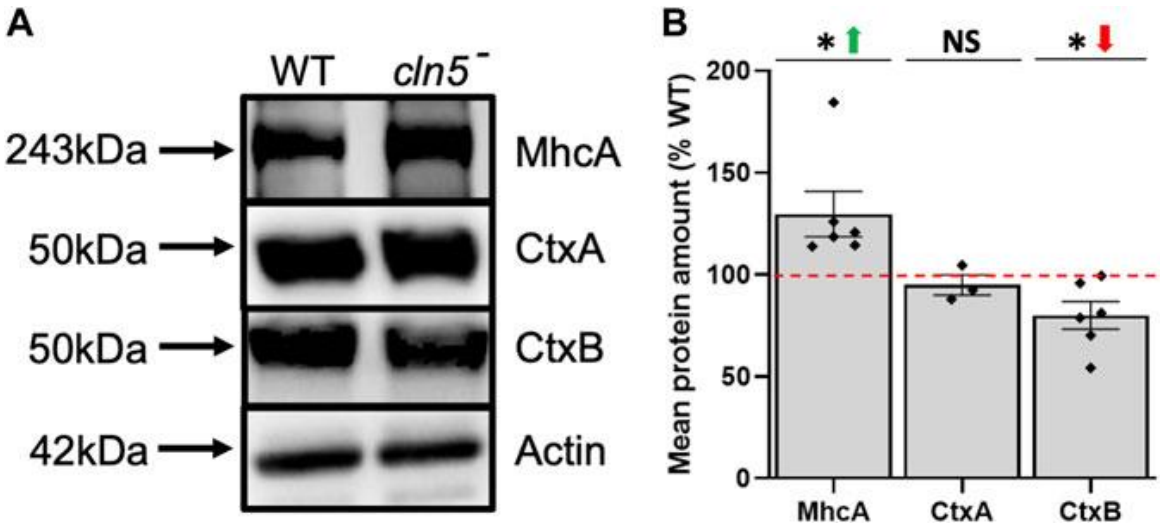

FIGURE 4. Loss of *cln5* affects the abundance of proteins linked to cytokinesis during growth. (A) Whole cell (WC) lysates (20-30 µg) from growth-phase WT and *cln5*-deficient cells were separated by SDS-PAGE and analyzed by western blotting. Membranes were probed with anti-CtxA, anti-CtxB, anti-MhcA, and anti-β-actin (loading control). **(B)** Intracellular amounts of CtxA, CtxB, and MhcA were quantified using Fiji/ImageJ and standardized against the levels of β-actin. Data presented as mean protein amount (% WT) ± SEM ($n \geq 3$). *$p < 0.05$ (one sample *t*-test). NS – not significant.

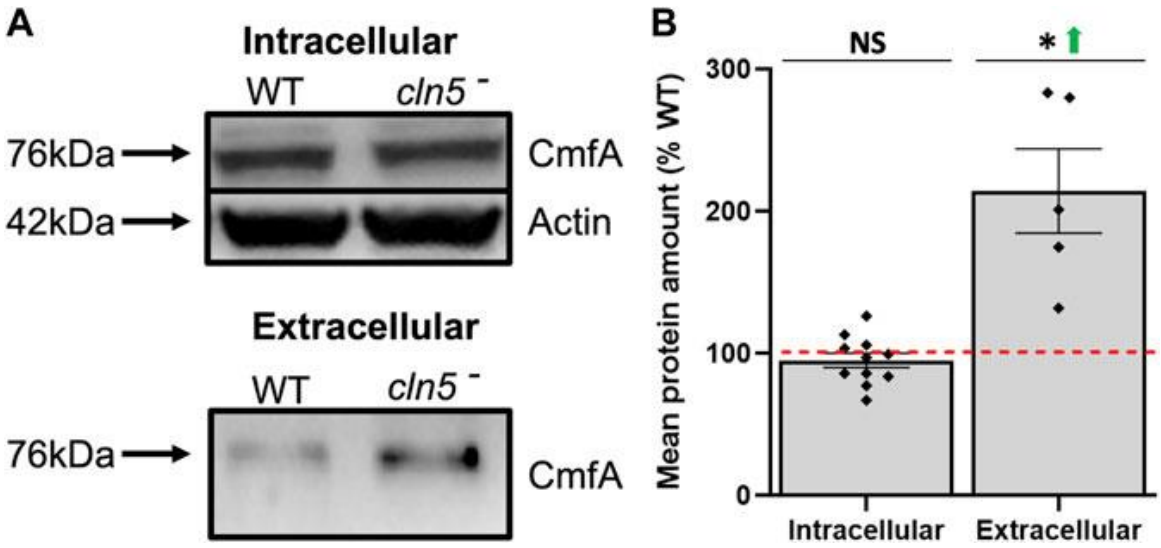

FIGURE 5. Loss of *cln5* affects the extracellular amount of CmfA during starvation. (A) WT and *cln5*-deficient cells starved for 4 h were lysed and standard SDS-PAGE/western blotting was performed on equal protein amounts from whole cell (WC) lysates (20-40 µg) and clarified conditioned buffer (CB) (0.15–0.375 µg). Membranes were probed with anti-CmfA and anti-β-actin (loading control). **(B)** Intracellular and extracellular amounts of CmfA were quantified with Fiji/ImageJ and intracellular amounts of CmfA were standardized against the levels of β-actin. Data presented as mean

protein amount (% WT) ± SEM ($n \geq 5$). *$p < 0.05$ (one sample *t*-test). NS – not significant.

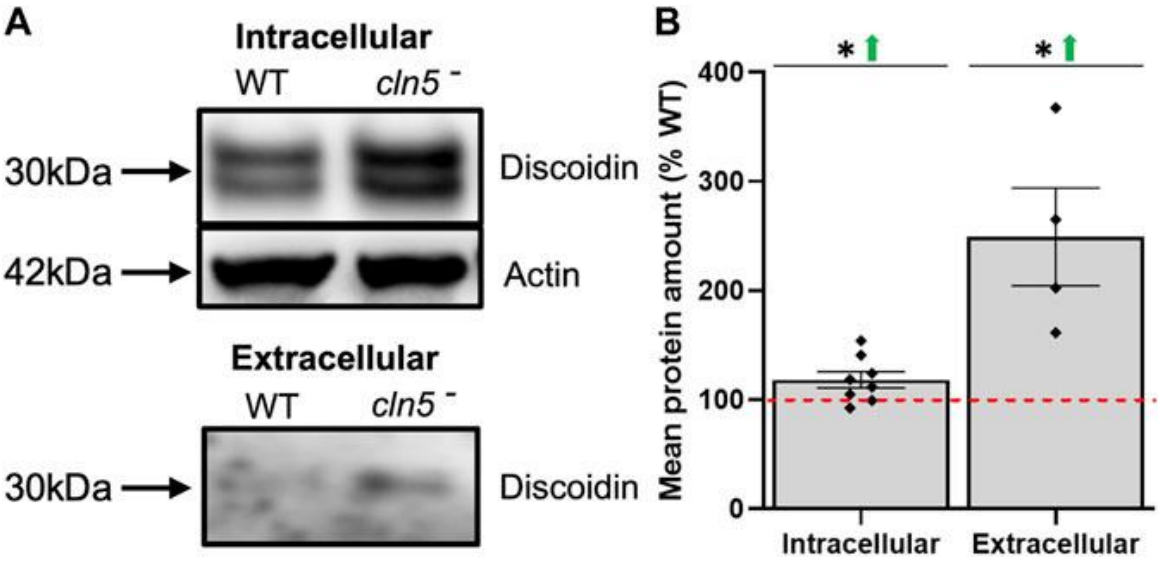

FIGURE 6. Loss of *cln5* affects the intracellular and extracellular amounts of discoidin during starvation. (A) Whole cell (WC) lysates (30-50 µg) and clarified conditioned buffer (CB) (0.15–0.375 µg) were collected from WT and *cln5*-cells starved for 4 h. Equal protein amounts were subjected to SDS-PAGE/western blotting, and membranes were probed with anti-Dsc and anti-β-actin (loading control). **(B)** Protein bands were quantified using Fiji/ImageJ and the intracellular values for discoidin were standardized against the levels of β-actin. Data presented as mean protein amount (% WT) ± SEM ($n \geq 4$). *$p < 0.05$ (one sample *t*-test). NS – not significant.

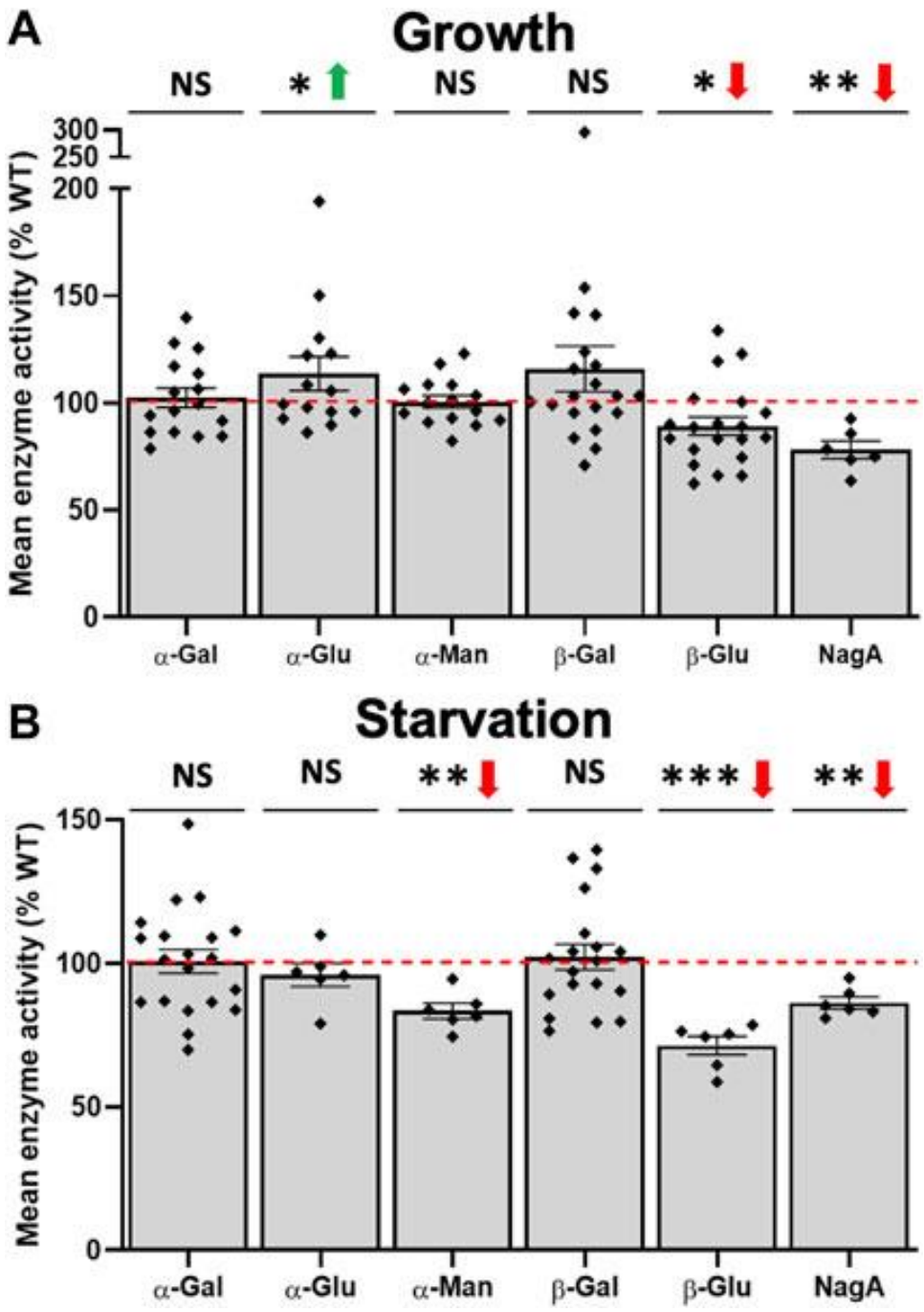

FIGURE 7. Loss of *cln5* affects the activity of carbohydrate enzymes during growth and starvation. WT and *cln5*-deficient cells during **(A)** growth and **(B)** 4-hour starvation were lysed and the activities of various carbohydrate enzymes were assessed including α-galactosidase (α-Gal), β-galactosidase (β-Gal), α-glucosidase (α-Glu), β-glucosidase (β-Glu), α-mannosidase (α-Man), and N-acetylglucosaminidase (NagA). Raw enzymatic values were subtracted from the blank solution and activities in *cln5*-deficient lysates were standardized against the activities in WT samples. Data presented as mean enzyme activity (% WT) ± SEM ($n \geq 6$). *$p < 0.05$, **$p < 0.01$, ***$p < 0.001$ (one sample *t*-test). NS – not significant.

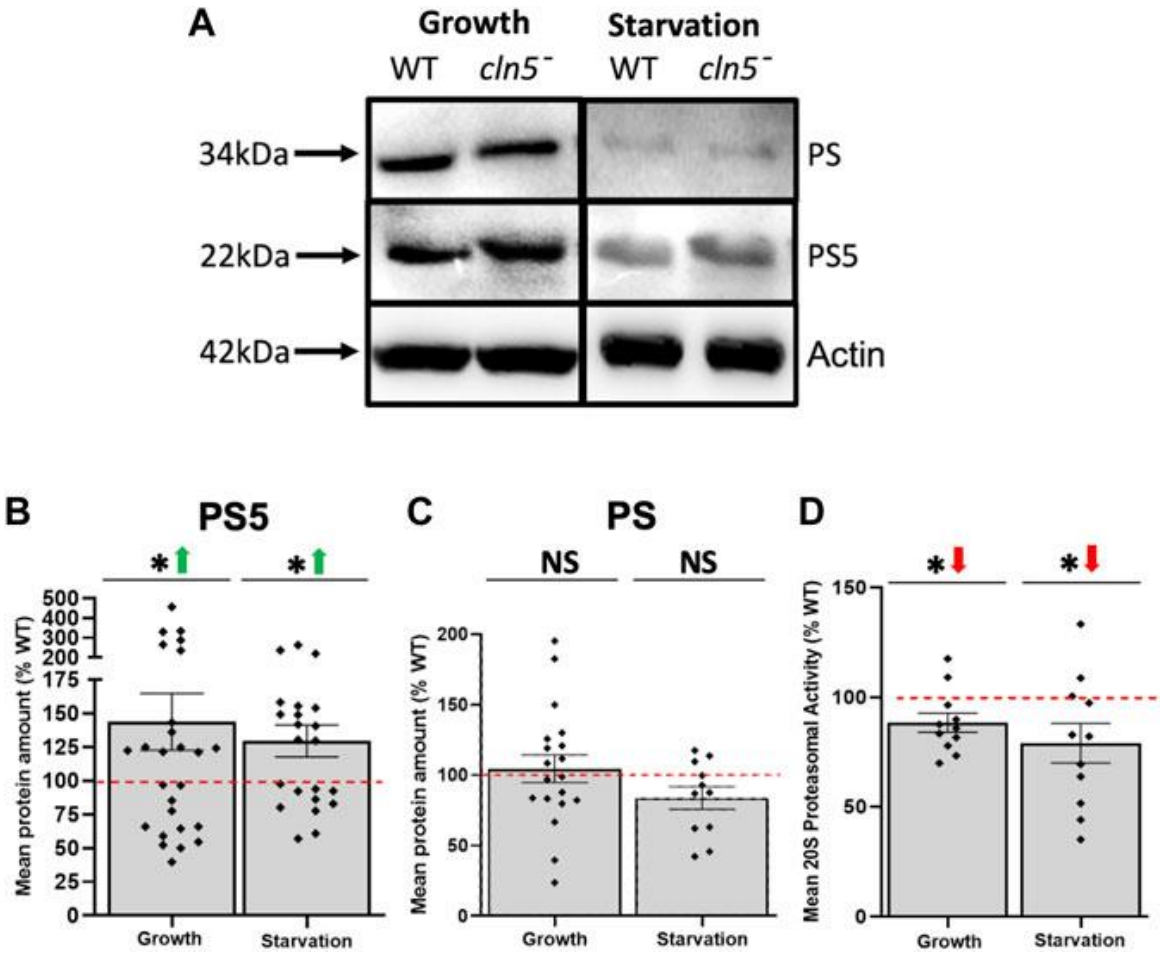

FIGURE 8. Loss of *cln5* increases the abundance of a proteasomal subunit during growth and starvation but decreases proteasome 20S activity. (A) Whole cell (WC) lysates from growth-phase and 4 h starved WT and *cln5*⁻- cells were separated by SDS-PAGE and analyzed by western blotting. Membranes were probed with anti-PS, anti-PS5, and anti-β-actin (loading control). Fiji/ImageJ was used to quantify **(B)** PS5 and **(C)** PS protein bands, which were then standardized against the levels of β-actin. Data presented as mean protein amount (% WT) ± SEM ($n \geq 11$). *$p < 0.05$ (one sample *t*-test). NS – not significant. **(D)** Proteasome 20S activity was assessed by collecting WT and *cln5*⁻ cells during growth and after 4 h of starvation. Cells were then lysed and proteasome 20S activity was measured using a commercially available kit. Raw activity values were subtracted from the blank solution and activities in *cln5*-deficient lysates were standardized against the activities in WT samples. Data presented as mean proteasome 20S activity (% WT) ± SEM (n = 11). *$p < 0.05$ (one sample *t*-test).

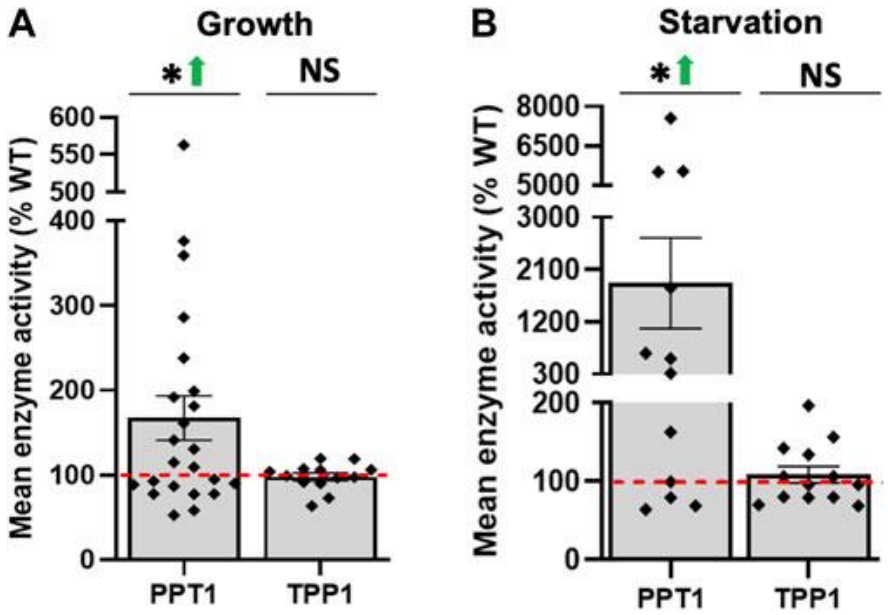

FIGURE 9. Loss of *cln5* increases PPT1 activity during growth and starvation but has no effect on TPP1 activity. (A) Growth-phase and **(B)** 4-hour starved WT and *cln5*$^{-}$ cells were lysed PPT1 and TPP1 activity in whole cell (WC) lysates were subtracted from the blank solution and activities in *cln5*-deficient lysates were standardized against the activities in WT samples. Data presented as mean enzyme activity (% WT) ± SEM (n ≥ 12). *$p < 0.05$ (one sample *t*-test). NS – not significant.

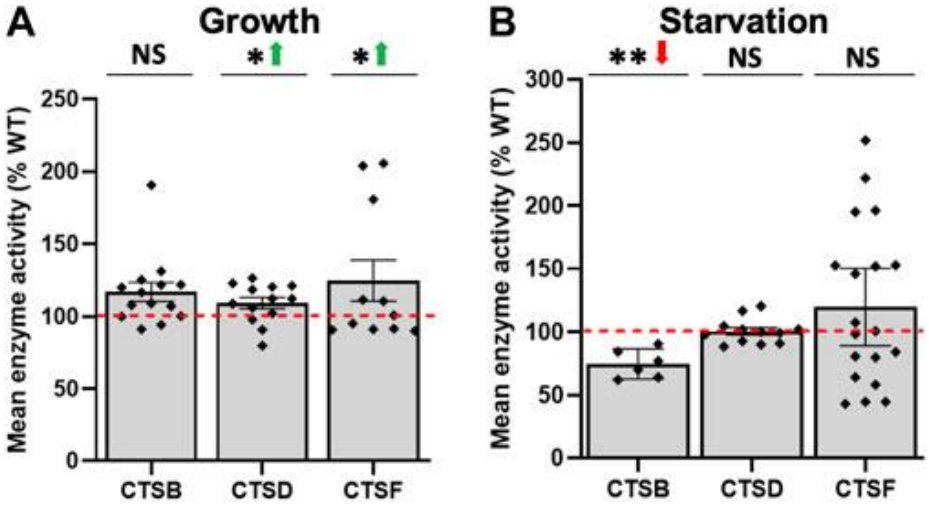

FIGURE 10. Loss of *cln5* affects the activity of cathepsins during growth and starvation. The activity of cathepsins were assessed during **(A)** growth and **(B)** 4-hour starvation in WT and *cln5*$^{-}$ cells as described in the Materials and methods. Activities in whole cell (WC) lysates were subtracted from the blank solution and activities in *cln5*$^{-}$ lysates were standardized against the activities in WT samples. Data presented as mean enzyme activity (% WT) ± SEM (n ≥ 6). *$p < 0.05$, **$p < 0.01$ (one sample *t*-test). NS – not significant.

TABLE 2. Quantitative summary of DEGs and annotated genes determined by LAGO in *cln5*$^{-}$ cells during growth and after 4 h of starvation. A log2 fold threshold of 1.25 was applied.

				LAGO annotated genes		
Condition	Number of up-regulated genes	Number of down-regulated genes	Total DEGs	Biological process	Cellular component	Molecular function
Growth	1,041	1,283	2,324	1,603	1,652	1,586
Starvation	644	394	1,038	657	728	669

The Supplementary Material for this article can be found online at: https://www.frontiersin.org/articles/10.3389/fgene.2022.1045738/full#supplementary-material

2.9. REFERENCES

Adams, J., Feuerborn, M., Molina, J. A., Wilden, A. R., Adhikari, B., Budden, T., et al. (2019). Autophagy–lysosome pathway alterations and alpha-synuclein up-regulation in the subtype of neuronal ceroid lipofuscinosis, CLN5 disease. *Sci. Rep*. 9, 151. doi:10.1038/s41598-018-36379-z

Bakthavatsalam, D., Brock, D. A., Nikravan, N. N., Houston, K. D., Hatton, R. D., and Gomer, R. H. (2008). The secreted *Dictyostelium* protein CfaD is a chalone. *J. Cell Sci*. 121, 2473–2480. doi:10.1242/jcs.026682

Barondes, S. H., Haywood-Reid, P. L., and Cooper, D. N. W. (1985). Discoidin I, an endogenous lectin, is externalized from *Dictyostelium discoideum* in multilamellar bodies. *J. Cell Biol*. 100, 1825–1833. doi:10.1083/jcb.100.6.1825

Barrett, A. (1980). Fluorimetric assays for cathepsin B and cathepsin H with methylcoumarylamide substrates. Biochem. J. 187, 909–912. doi:10.1042/bj1870909

Basak, I., Hansen, R. A., Ward, M. E., and Hughes, S. M. (2021a). Deficiency of the lysosomal protein cln5 alters lysosomal function and movement. *Biomolecules* 11, 1412. doi:10.3390/biom11101412

Basak, I., Wicky, H. E., McDonald, K. O., Xu, J. B., Palmer, J. E., Best, H. L., et al. (2021b). A lysosomal enigma CLN5 and its significance in understanding neuronal ceroid lipofuscinosis. *Cell. Mol. Life Sci*. 78, 4735–4763. doi:10.1007/s00018-021-03813-x

Bento, C. F., Renna, M., Ghislat, G., Puri, C., Ashkenazi, A., Vicinanza, M., et al. (2016). Mammalian autophagy: How does it work? *Annu. Rev. Biochem*. 85, 685–713529. doi:10.1146/annurev-biochem-060815-014556

Best, H. L., Neverman, N. J., Wicky, H. E., Mitchell, N. L., Leitch, B., and Hughes, S. M. (2017). Characterisation of early changes in ovine CLN5 and CLN6 Batten disease neural cultures for the rapid screening of therapeutics. *Neurobiol. Dis*. 100, 62–74. doi:10.1016/j.nbd.2017.01.001

Bolger, A. M., Lohse, M., and Usadel, B. (2014). Trimmomatic: A flexible trimmer for Illumina sequence data. *Bioinformatics* 30, 2114–2120. doi:10.1093/ bioinformatics/btu170

Boyle, E. I., Weng, S., Gollub, J., Jin, H., Botstein, D., Cherry, J. M., et al. (2004). GO::TermFinder – open source software for accessing Gene Ontology information and finding significantly enriched Gene Ontology terms associated with a list of genes. *Bioinformatics* 20, 3710–3715. doi:10.1093/bioinformatics/bth456

Brock, D. A., and Gomer, R. H. (1999). A cell-counting factor regulating structure size in *Dictyostelium*. *Genes Dev*. 13, 1960–1969. doi:10.1101/gad.13.15.1960

Brock, D. A., and Gomer, R. H. (2005). A secreted factor represses cell proliferation in *Dictyostelium*. *Development* 132, 4553–4562. doi:10.1242/dev.02032

Brock, D. A., Buczynski, G., Spann, T. P., Wood, S. A., Cardelli, J., and Gomer, R. H. (1996). A *Dictyostelium* mutant with defective aggregate size determination. *Development* 122, 2569–2578. doi:10.1242/dev.122.9.2569

Bukharova, T., Weijer, G., Bosgraaf, L., Dormann, D., van Haastert, P. J., Weijer, C. J., et al. (2005). Paxillin is required for cell-substrate adhesion, cell sorting and slug migration during *Dictyostelium* development. J. Cell Sci. 118, 4295–4310. doi:10.1242/jcs.02557

Cárcel-Trullols, J., Kovács, A. D., and Pearce, D. A. (2015). Cell biology of the NCL proteins: What they do and don't do. *Biochim. Biophys. Acta* 1852, 2242–2255. doi:10.1016/j.bbadis.2015.04.027

Castro, A., Bernis, C., Vigneron, S., Labbé, J. C., and Lorca, T. (2005). The anaphase-promoting complex: A key factor in the regulation of cell cycle. Oncogene 24, 314–325. doi:10.1038/sj.onc.1207973

Chia, C. P., Shariff, A., Savage, S. A., and Luna, E. J. (1993). The integral membrane protein, ponticulin, acts as a monomer in nucleating actin assembly. *J. Cell Biol*. 120, 909–922. doi:10.1083/jcb.120.4.909

Choe, J. M., Bakthavatsalam, D., Phillips, J. E., and Gomer, R. H. (2009). *Dictyostelium* cells bind a secreted autocrine factor that represses cell proliferation. *BMC Biochem*. 10, 4. doi:10.1186/1471-2091-10-4

Codlin, S., Haines, R. L., Burden, J. J. E., and Mole, S. E. (2008). Btn1 affects cytokinesis and cell-wall deposition by independent mechanisms, one of which is linked to dysregulation of vacuole pH. *J. Cell Sci*. 121, 2860–2870. doi:10.1242/jcs.030122

Coston, M. B., and Loomis, W. F. (1969). Isozymes of beta-glucosidase in *Dictyostelium discoideum. J. Bacteriol.* 100, 1208–1217. doi:10.1128/jb.100.3. 1208-1217.1969

De Lozanne, A., and Spudich, J. A. (1987). Disruption of the *Dictyostelium* myosin heavy chain gene by homologous recombination. *Science* 236, 1086–1091. doi:10.1126/science.3576222

Deery, W. J., and Gomer, R. H. (1999). A putative receptor mediating cell-density sensing in *Dictyostelium. J. Biol. Chem*. 274, 34476–34482. doi:10.1074/jbc.274.48. 34476

Deol, K. K., Crowe, S. O., Du, J., Bisbee, H. A., Guenette, R. G., and Strieter, E. R. (2020). Proteasome-bound UCH37/UCHL5 debranches ubiquitin chains to promote degradation. *Mol. Cell* 80, 796–809. doi:10.1016/j.molcel.2020.10.017

Doccini, S., Morani, F., Nesti, C., Pezzini, F., Calza, G., Soliymani, R., et al. (2020). Proteomic and functional analyses in disease models reveal CLN5 protein involvement in mitochondrial dysfunction. *Cell Death Discov*. 6, 18. doi:10. 1038/s41420-020-0250-y

Doccini, S., Marchese, M., Morani, F., Gammaldi, N., Mero, S., Pezzini, F., et al. (2022). Lysosomal proteomics links disturbances in lipid homeostasis and sphingolipid metabolism to CLN5 disease. *Cells* 11, 1840. doi:10.3390/ cells11111840

Duran, M. B., Rahman, A., Colten, M., and Brazill, D. (2009). *Dictyostelium discoideum* paxillin regulates actin-based processes. *Protist* 160, 221–232. doi:10. 1016/j.protis.2008.09.005

El Haddad, S., Khoury, M., Daoud, M., Kantar, R., Harati, H., Mousallem, T., et al. (2012). CLN5 and CLN8 protein association with ceramide synthase: Biochemical and proteomic approaches. *Electrophoresis* 33, 3798–3809. doi:10.1002/elps. 201200472

Faix, J., Steinmetz, M., Boves, H., Kammerer, R. A., Lottspeich, F., Mintert, U., et al. (1996). Cortexillins, major determinants of cell shape and size, are actin- bundling proteins with a parallel coiled-coil tail. *Cell* 86, 631–642. doi:10.1016/ S0092-8674(00)80136-1

Faix, J., Weber, I., Mintert, U., Köhler, J., Lottspeich, F., and Marriott, G. (2001). Recruitment of cortexillin into the cleavage furrow is controlled by Rac1 and IQGAP-related proteins. *EMBO J*. 20, 3705–3715. doi:10.1093/emboj/20.14.3705

Fey, P., Kowal, A. S., Gaudet, P., Pilcher, K. E., and Chisholm, R. L. (2007). Protocols for growth and development of Dictyostelium discoideum. *Nat. Protoc*. 2, 1307–1316. doi:10.1038/nprot.2007.178

Fonovič, M., Brömme, D., Turk, V., and Turk, B. (2004). Human cathepsin F: Expression in baculovirus system, characterization and inhibition by protein inhibitors. *Biol. Chem.* 385, 505–509. doi:10.1515/BC.2004.059

Gomer, R. H., Yuen, I. S., and Firtel, R. A. (1991). A secreted 80 x 103 Mr protein mediates sensing of cell density and the onset of development of *Dictyostelium. Development* 112, 269–278. doi:10.1242/dev.112.1.269

Grubman, A., Pollari, E., Duncan, C., Caragounis, A., Blom, T., Volitakis, I., et al. (2014). Deregulation of biometal homeostasis: The missing link for neuronal ceroid lipofuscinoses? *Metallomics* 6, 932–943. doi:10.1039/c4mt00032c

Hersrud, S. L., Geraets, R. D., Weber, K. L., Chan, C. H., and Pearce, D. A. (2016). Plasma biomarkers for neuronal ceroid lipofuscinosis. *FEBS J.* 283, 459–471. doi:10. 1111/febs.13593

Huber, R. J., and Mathavarajah, S. (2018a). Cln5 is secreted and functions as a glycoside hydrolase in *Dictyostelium*. *Cell. Signal*. 42, 236–248. doi:10.1016/j.cellsig.2017.11.001

Huber, R. J., and Mathavarajah, S. (2018b). Secretion and function of Cln5 during the early stages of *Dictyostelium* development. *Biochim. Biophys. Acta. Mol. Cell Res*. 1865, 1437–1450. doi:10.1016/j.bbamcr.2018.07.017

Huber, R. J., Hughes, S. M., Liu, W., Morgan, A., Tuxworth, R. I., and Russell, C. (2020). The contribution of multicellular model organisms to neuronal ceroid lipofuscinosis research. *Biochim. Biophys. Acta. Mol. Basis Dis*. 1866, 165614. doi:10.1016/j.bbadis.2019.165614

Huber, R. J., Williams, R. S. B., and Müller-Taubenberger, A. (2022). Editorial: *Dictyostelium*: A tractable cell and developmental model in biomedical research. *Front. Cell Dev. Biol.* 10, 909619. doi:10.3389/fcell.2022.909619

Huber, R. J. (2016). Using the social amoeba *Dictyostelium* to study the functions of proteins linked to neuronal ceroid lipofuscinosis. *J. Biomed. Sci*. 23, 83. doi:10.1186/s12929-016-0301-0

Huber, R. J. (2020). Molecular networking in the neuronal ceroid lipofuscinoses: Insights from mammalian models and the social amoeba *Dictyostelium discoideum. J. Biomed. Sci*. 27, 64. doi:10.1186/s12929-020-00653-y

Huber, R. J. (2021). Altered protein secretion in Batten disease. *Dis. Model. Mech*. 14, dmm049152. doi:10.1242/dmm.049152

Hughes, S. M., Hope, K. M., Xu, J. B., Mitchell, N. L., and Palmer, D. N. (2014). Inhibition of storage pathology in prenatal CLN5-deficient sheep neural cultures by lentiviral gene therapy. *Neurobiol. Dis.* 62, 543–550. doi:10.1016/j.nbd.2013.11.011

Ingalls, H. M., Barcelo, G., Wuestehube, L. J., and Luna, E. J. (1989). Developmental changes in protein composition and the actin-binding protein ponticulin in *Dictyostelium discoideum* plasma membranes purified by an improved method. *Differentiation*. 41, 87–98. doi:10.1111/j.1432-0436.1989.tb00736.x

Isosomppi, J., Vesa, J., Jalanko, A., and Peltonen, L. (2002). Lysosomal localization of the neuronal ceroid lipofuscinosis CLN5 protein. *Hum. Mol. Genet.* 11, 885–891. doi:10.1093/hmg/11.8.885

Iwan, K., Clayton, R., Mills, P., Csanyi, B., Gissen, P., Mole, S. E., et al. (2021). Urine proteomics analysis of patients with neuronal ceroid lipofuscinoses. *iScience* 24, 102020. doi:10.1016/j.isci.2020.102020

Jain, R., Yuen, I. S., Taphouse, C. R., and Gomer, R. H. (1992). A density-sensing factor controls development in *Dictyostelium. Genes Dev*. 6, 390–400. doi:10.1101/ gad.6.3.390

Jin, L., Williamson, A., Banerjee, S., Philipp, I., and Rape, M. (2008). Mechanism of ubiquitin-chain formation by the human anaphase-promoting complex. *Cell* 133, 653–665. doi:10.1016/j.cell.2008.04.012

Jules, F., Sauvageau, E., Dumaresq-Doiron, K., Mazzaferri, J., Haug-Kröper, M., Fluhrer, R., et al. (2017). CLN5 is cleaved by members of the SPP/SPPL family to produce a mature soluble protein. *Exp. Cell Res.* 357, 40–50. doi:10.1016/j.yexcr. 2017.04.024

Kilpatrick, D. C., and Stirling, J. L. (1976). Properties and developmental regulation of an alpha-d-galactosidase from *Dictyostelium discoideum. Biochem. J.* 158, 409–417. doi:10.1042/bj1580409

Kim, J. Y., Van Haastert, P., and Devreotes, P. N. (1996). Social senses: G-protein-coupled receptor signaling pathways in *Dictyostelium discoideum. Chem. Biol.* 3, 239–243. doi:10.1016/S1074-5521(96)90103-9

Kim, D., Paggi, J. M., Park, C., Bennett, C., and Salzberg, S. L. (2019). Graph-based genome alignment and genotyping with HISAT2 and HISAT-genotype. Nat. *Biotechnol*. 37, 907–915. doi:10.1038/s41587-019-0201-4

Kim, W. D., Wilson-Smillie, M. L. D. M., Thanabalasingam, A., Lefrancois, S., Cotman, S. L., and Huber, R. J. (2022). Autophagy in the neuronal ceroid lipofuscinoses (Batten disease). *Front. Cell Dev. Biol*. 10, 812728. doi:10.3389/fcell.2022.812728

Kocaturk, N. M., and Gozuacik, D. (2018). Crosstalk between mammalian autophagy and the ubiquitin-proteasome system. *Front. Cell Dev. Biol*. 6, 128. doi:10.3389/fcell.2018.00128

Koonce, M. P. (2020). 13 plus 1: A 30-year perspective on microtubule-based motility in *Dictyostelium. Cells* 9, 528. doi:10.3390/cells9030528

Le Tallec, B., Barrault, M. B., Courbeyrette, R., Guérois, R., Marsolier-Kergoat, M.-C., and Peyroche, A. (2007). 20S proteasome assembly is orchestrated by two distinct pairs of chaperones in yeast and in mammals. *Mol. Cell* 27, 660–674. doi:10. 1016/j.molcel.2007.06.025

Leinonen, H., Keksa-Goldsteine, V., Ragauskas, S., Kohlmann, P., Sing, Y., Savchenko, E., et al. (2017). Retinal degeneration in A mouse model of CLN5 disease is associated with compromised autophagy. *Sci. Rep*. 7, 1597. doi:10.1038/s41598-017-01716-1

Li, T., and Guo, Y. (2022). ADP-ribosylation factor family of small GTP-binding proteins: Their membrane recruitment, activation, crosstalk and functions. *Front. Cell Dev. Biol*. 10, 813353–813359. doi:10.3389/fcell.2022.813353

Li, H., Chen, Q., Kaller, M., Nellen, W., Gräf, R., and De Lozanne, A. (2008). *Dictyostelium* Aurora kinase has properties of both Aurora A and Aurora B kinases. *Eukaryot. Cell* 7, 894–905. doi:10.1128/EC.00422-07

Liao, Y., Smyth, G. K., and Shi, W. (2014). FeatureCounts: an efficient general purpose program for assigning sequence reads to genomic features. *Bioinformatics* 30, 923–930. doi:10.1093/bioinformatics/btt656

Loomis, W. F. (1969). Acetylglucosaminidase, an early enzyme in the development of *Dictyostelium discoideum. J. Bacteriol*. 97, 1149–1154. doi:10. 1128/JB.97.3.1149-1154.1969

Loomis, W. F. (1970). Developmental regulation of alpha-mannosidase in *Dictyostelium discoideum. J. Bacteriol.* 103, 375–381. doi:10.1128/JB.103.2.375-381.1970

Loomis, W. F. (1998). Role of PKA in the timing of developmental events in *Dictyostelium* cells. *Microbiol. Mol. Biol. Rev.* 62, 684–694. doi:10.1128/mmbr.62.3. 684-694.1998

Loomis, W. F. (2014). Cell signalling during development of *Dictyostelium. Dev. Biol.* 391, 1–16. doi:10.1016/j.ydbio.2014.04.001

Love, M. I., Huber, W., and Anders, S. (2014). Moderated estimation of fold change and dispersion for RNA-seq data with DESeq2. *Genome Biol*. 15, 550. doi:10. 1186/s13059-014-0550-8

Luebben, A. V., Bender, D., Becker, S., Crowther, L. M., Erven, I., Hofmann, K., et al. (2022). Cln5 represents a new type of cysteine-based S-depalmitoylase linked to neurodegeneration. *Sci. Adv.* 8, eabj8633–10. doi:10.1126/sciadv.abj8633

Luo, Q., Michaelis, C., and Weeks, G. (1995). Cyclin B and Cdc2 expression and Cd2 kinase activity during *Dictyostelium* differentiation. *DNA Cell Biol*. 14, 901–908. doi:10.1089/dna.1995.14.901

Lyly, A., Von Schantz, C., Heine, C., Schmiedt, M., Sipilä, T., Jalanko, A., et al. (2009). Novel interactions of CLN5 support molecular networking between Neuronal Ceroid Lipofuscinosis proteins. *BMC Cell Biol*. 10, 83. doi:10.1186/ 1471-2121-10-83

Mamo, A., Jules, F., Dumaresq-Doiron, K., Costantino, S., and Lefrancois, S. (2012). The role of ceroid lipofuscinosis neuronal protein 5 (CLN5) in endosomal sorting. *Mol. Cell. Biol.* 32, 1855–1866. doi:10.1128/mcb.06726-11

Mann, S. K. O., Brown, J. M., Briscoe, C., Parent, C., Pitt, G., Devreotes, P. N., et al. (1997). Role of cAMP-dependent protein kinase in controlling aggregation and postaggregative development in *Dictyostelium. Dev. Biol*. 183, 208–221. doi:10. 1006/dbio.1996.8499

Maruhn, D. (1976). Rapid colorimetric assay of β-galactosidase and N-acetyl-β-glucosaminidase in human urine. *Clin. Chim. Acta*. 73, 453–461. doi:10.1016/0009-8981(76)90147-9

Masson, P., Lundin, D., Söderbom, F., and Young, P. (2009). Characterization of a REG/PA28 proteasome activator homolog in Dictyostelium discoideum indicates that the ubiquitin- and ATP-independent REGγ proteasome is an ancient nuclear protease. *Eukaryot*. Cell 8, 844–851. doi:10.1128/EC.00165-08

Mathavarajah, S., Flores, A., and Huber, R. J. (2017). *Dictyostelium discoideum*: A model system for cell and developmental biology. *Curr. Protoc. Essent. Lab. Tech*. 14, 1.1–14.1.19. doi:10.1002/cpet.15

Mathavarajah, S., McLaren, M. D., and Huber, R. J. (2018). Cln3 function is linked to osmoregulation in a *Dictyostelium* model of Batten disease. *Biochim. Biophys. Acta. Mol. Basis Dis.* 1864, 3559–3573. doi:10.1016/j.bbadis.2018.08.013

Matyskiela, M. E., Rodrigo-Brenni, M. C., and Morgan, D. O. (2009). Mechanisms of ubiquitin transfer by the anaphase-promoting complex. *J. Biol.* 8, 92. doi:10.1186/ jbiol184

McLaren, M. D., Mathavarajah, S., Kim, W. D., Yap, S. Q., and Huber, R. J. (2021). Aberrant autophagy impacts growth and multicellular development in a *Dictyostelium* knockout model of CLN5 disease. *Front. Cell Dev. Biol*. 9, 657406. doi:10.3389/fcell.2021.657406

Mesquita, A., Cardenal-Muñoz, E., Dominguez, E., Muñoz-Braceras, S., Nuñez- Corcuera, B., Phillips, B. A., et al. (2017). Autophagy in *Dictyostelium*: Mechanisms, regulation and disease in a simple biomedical model. *Autophagy* 13, 24–40. doi:10. 1080/15548627.2016.1226737

Mizushima, N. (2010). The role of the Atg1/ULK1 complex in autophagy regulation. *Curr. Opin. Cell Biol*. 22, 132–139. doi:10.1016/j.ceb.2009.12.004

Moharir, A., Peck, S. H., Budden, T., and Lee, S. Y. (2013). The role of N-glycosylation in folding, trafficking, and functionality of lysosomal protein CLN5. *PloS One* 8, e74299. doi:10.1371/journal.pone.0074299

Mole, S. E., and Cotman, S. L. (2015). Genetics of the neuronal ceroid lipofuscinoses (Batten disease). *Biochim. Biophys. Acta* 1852, 2237–2241. doi:10. 1016/j.bbadis.2015.05.011

Mukherjee, A. B., Appu, A. P., Sadhukhan, T., Casey, S., Mondal, A., Zhang, Z., et al. (2019). Emerging new roles of the lysosome and neuronal ceroid lipofuscinoses. *Mol. Neurodegener.* 14, 4. doi:10.1186/s13024-018-0300-6

Nag, D. K., Tikhonenko, I., Soga, I., and Koonce, M. P. (2008). Disruption of four kinesin genes in *Dictyostelium. BMC Cell Biol.* 9, 21. doi:10.1186/1471-2121-9-21

Nagasaki, A., Kanada, M., and Uyeda, T. Q. (2009). Cell adhesion molecules regulate contractile ring-independent cytokinesis in *Dictyostelium discoideum. Cell Res*. 19, 236–246. doi:10.1038/cr.2008.318

Pagh, K., and Gerisch, G. (1986). Monoclonal antibodies binding to the tail of *Dictyostelium discoideum* myosin: Their effects on antiparallel and parallel assembly and actin-activated ATPase activity. *J. Cell Biol*. 103, 1527–1538. doi:10.1083/jcb. 103.4.1527

Palmer, D. N., Fearnley, I. M., Walker, J. E., Hall, N. A., Lake, B. D., Wolfe, L. S., et al. (1992). Mitochondrial ATP synthase subunit c storage in the ceroid-lipofuscinoses (Batten disease). *Am. J. Med. Genet*. 42, 561–567. doi:10.1002/ajmg.1320420428

Persaud-Sawin, D.-A., Mousallem, T., Wang, C., Zucker, A., Kominami, E., and Boustany, R.-M. N. (2007). Neuronal ceroid lipofuscinosis: A common pathway? *Pediatr. Res*. 61, 146–152. doi:10.1203/pdr.0b013e31802d8a4a

Phillips, J. E., and Gomer, R. H. (2010). The ROCO kinase QkgA is necessary for proliferation inhibition by autocrine signals in *Dictyostelium discoideum. Eukaryot. Cell* 9, 1557–1565. doi:10.1128/EC.00121-10

Pickart, C. M. (2001). Mechanisms underlying ubiquitination. *Annu. Rev. Biochem*. 70, 503–533. doi:10.1146/annurev.biochem.70.1.503

Roisin-Bouffay, C., Jang, W., Caprette, D. R., and Gomer, R. H. (2000). A precise group size in *Dictyostelium* is generated by a cell-counting factor modulating cell-cell adhesion. *Mol. Cell* 6, 953–959. doi:10.1016/S1097-2765(05)00082-1

Sanchez-Pulido, L., and Ponting, C. P. (2011). Cdc45: The missing recj ortholog in eukaryotes? *Bioinformatics* 27, 1885–1888. doi:10.1093/bioinformatics/btr332

Schauer, T. M., Nesper, M., Kehl, M., Lottspeich, F., Müller-Taubenberger, A., Gerisch, G., et al. (1993). Proteasomes from *Dictyostelium discoideum*: Characterization of structure and function. *J. Struct. Biol*. 111, 135–147. doi:10. 1006/jsbi.1993.1044

Schindelin, J., Arganda-Carreras, I., Frise, E., Kaynig, V., Longair, M., Pietzsch, T., et al. (2012). Fiji: An open-source platform for biological-image analysis. *Nat. Methods* 9, 676–682. doi:10.1038/nmeth.2019

Schmiedt, M. L., Blom, T., Blom, T., Kopra, O., Wong, A., von Schantz-Fant, C., et al. (2012). Cln5-deficiency in mice leads to microglial activation, defective myelination and changes in lipid metabolism. *Neurobiol.* Dis. 46, 19–29. doi:10. 1016/j.nbd.2011.12.009

Schulkes, C., and Schaap, P. (1995). cAMP-dependent protein kinase activity is essential for preaggregative gene expression in *Dictyostelium. FEBS Lett*. 368, 381–384. doi:10.1016/0014-5793(95)00676-Z

Schulz, A., Kohlschütter, A., Mink, J., Simonati, A., and Williams, R. (2013). NCL diseases — Clinical perspectives. *Biochim. Biophys. Acta* 1832, 1801–1806. doi:10. 1016/j.bbadis.2013.04.008

Shao, S., Von der Malsburg, K., and Hegde, R. S. (2013). Listerin-dependent nascent protein ubiquitination relies on ribosome subunit dissociation. *Mol. Cell* 50, 637–648. doi:10.1016/j.molcel.2013.04.015

Shariff, A., and Luna, E. J. (1990). *Dictyostelium discoideum* plasma membranes contain an actin-nucleating activity that requires ponticulin, an integral membrane glycoprotein. *J. Cell Biol*. 110, 681–692. doi:10.1083/jcb.110.3.681

Sharma, S. K., Michaelis, C., Lee, K. Y., Wang, J. H., and Weeks, G. (1999). Binding and catalytic properties of the Cdc2 and Crp proteins of *Dictyostelium. Eur. J. Biochem.* 260, 603–608. doi:10.1046/j.1432-1327.1999.00236.x

Shaulsky, G., Fuller, D., and Loomis, W. F. (1998). A cAMP-phosphodiesterase controls PKA-dependent differentiation. *Development* 125, 691–699. doi:10.1242/ dev.125.4.691

Springer, W. R., Cooper, D. N. W., and Barondes, S. H. (1984). Discoidin I is implicated in cell-substratum attachment and ordered cell migration of *Dictyostelium discoideum* and resembles fibronectin. *Cell* 39, 557–564. doi:10. 1016/0092-8674(84)90462-8

Stajdohar, M., Rosengarten, R. D., Kokosar, J., Jeran, L., Blenkus, D., Shaulsky, G., et al. (2017). dictyExpress: A web-based platform for sequence data management and analytics in *Dictyostelium* and beyond. *BMC Bioinforma*. 18, 291. doi:10.1186/ s12859-017-1706-9

Stock, A., Steinmetz, M. O., Janmey, P. A., Aebi, U., Gerisch, G., Kammerer, R. A., et al. (1999). Domain analysis of cortexillin I: Actin-bundling, PIP2-binding and the rescue of cytokinesis. *EMBO J*. 18, 5274–5284. doi:10.1093/emboj/18.19.5274

Strasser, K., Bloomfield, G., MacWilliams, A., Ceccarelli, A., MacWilliams, H., and Tsang, A. (2012). A retinoblastoma orthologue is a major regulator of S-phase, mitotic, and developmental gene expression in *Dictyostelium. PloS One* 7, e39914. doi:10.1371/journal.pone.0039914

Stumpf, M., Müller, R., Gaßen, B., Wehrstedt, R., Fey, P., Karow, M. A., et al. (2017). A tripeptidyl peptidase 1 is a binding partner of the Golgi pH regulator (GPHR) in *Dictyostelium. Dis. Model. Mech*. 10, 897–907. doi:10.1242/dmm.029280

Sun, T. J., and Devreotes, P. N. (1991). Gene targeting of the aggregation stage cAMP receptor cAR1 in *Dictyostelium. Genes Dev*. 5, 572–582. doi:10.1101/gad.5.4.572

Tang, L., Gao, T., McCollum, C., Jang, W., Vicker, M. G., Ammann, R. R., et al. (2002). A cell number-counting factor regulates the cytoskeleton and cell motility in *Dictyostelium. Proc. Natl. Acad. Sci. U. S. A.* 99, 1371–1376. doi:10.1073/pnas. 022516099

Tanida, I., Minematsu-Ikeguchi, N., Ueno, T., and Kominami, E. (2005). Lysosomal turnover, but not a cellular level, of endogenous LC3 is a marker for autophagy. *Autophagy* 1, 84–91. doi:10.4161/auto.1.2.1697

Tikhonenko, I., Nag, D. K., Robinson, D. N., and Koonce, M. P. (2009). Microtubule-nucleus interactions in *Dictyostelium discoideum* mediated by central motor kinesins. *Eukaryot. Cell* 8, 723–731. doi:10.1128/EC.00018-09

Van Diggelen, O. P., Keulemans, J. L. M., Winchester, B., Hofman, I. L., Vanhanen, S. L., Santavuori, P., et al. (1999). A rapid fluorogenic palmitoyl- protein thioesterase assay: Pre- and postnatal diagnosis of INCL. *Mol. Genet. Metab*. 66, 240–244. doi:10.1006/mgme.1999.2809

Van Haastert, P. J. M., Bishop, J. D., and Gomer, R. H. (1996). The cell density factor CMF regulates the chemoattractant receptor cAR1 in *Dictyostelium. J. Cell Biol.* 134, 1543–1549. doi:10.1083/jcb.134.6.1543

Varet, H., Brillet-Guéguen, L., Coppée, J. Y., and Dillies, M. A. (2016). SARTools: A DESeq2- and edgeR-based R pipeline for comprehensive differential analysis of RNA-seq data. *PloS One* 11, e0157022. doi:10.1371/journal.pone.0157022

von Schantz, C., Saharinen, J., Kopra, O., Cooper, J. D., Gentile, M., Hovatta, I., et al. (2008). Brain gene expression profiles of Cln1 and Cln5 deficient mice unravels common molecular pathways underlying neuronal degeneration in NCL diseases. *BMC Genomic*s 9, 146. doi:10.1186/1471-2164-9-146

Wang, J., Dye, B. T., Rajashankar, K. R., Kurinov, I., and Schulman, B. A. (2009). Insights into anaphase promoting complex TPR subdomain assembly from a CDC26-APC6 structure. *Nat. Struct. Mol. Biol.* 16, 987–989. doi:10.1038/nsmb. 1645

Weber, I., Gerisch, G., Heizer, C., Murphy, J., Badelt, K., Stock, A., et al. (1999). Cytokinesis mediated through the recruitment of cortexillins into the cleavage furrow. *EMBO J.* 18, 586–594. doi:10.1093/emboj/18.3.586

Wetterauer, B., Jacobsen, G., Morandini, P., and MacWilliams, H. (1993). Mutants of *Dictyostelium discoideum* with defects in the regulation of discoidin I expression. *Dev. Biol.* 159, 184–195. doi:10.1006/dbio.1993.1232

Williamson, A., Wickliffe, K. E., Mellone, B. G., Song, L., Karpen, G. H., and Rape, M. (2009). Identification of a physiological E2 module for the human anaphase-promoting complex. *Proc. Natl. Acad. Sci. U. S. A.* 106, 18213–18218. doi:10.1073/pnas.0907887106

Wimmer, B., Lottspeich, F., Ritter, J., and Bronnenmeier, K. (1997). A novel type of thermostable alpha-D-glucosidase from *Thermoanaerobacter thermohydrosulfuricus* exhibiting maltodextrinohydrolase activity. *Biochem. J.* 328, 581–586. doi:10.1042/bj3280581

Yasa, S., Sauvageau, E., Modica, G., and Lefrancois, S. (2021). CLN5 and CLN3 function as a complex to regulate endolysosome function. *Biochem. J.* 478, 2339–2357. doi:10.1042/BCJ20210171

Yuen, I. S., Jain, R., Bishop, J. D., Lindsey, D. F., Deery, W. J., Van Haastert, P. J. M., et al. (1995). A density-sensing factor regulates signal transduction in *Dictyostelium. J. Cell Biol.* 129, 1251–1262. doi:10.1083/jcb.129.5.1251

Zang, J.-H., Cavet, G., Sabry, J. H., Wagner, P., Moores, S. L., and Spudich, J. A. (1997). On the role of myosin-II in cytokinesis: Division of *Dictyostelium* cells under adhesive and nonadhesive conditions. *Mol. Biol. Cell* 8, 2617–2629. doi:10.1091/mbc.8.12.2617

3.0. CHAPTER 3

DETERMINING THE FUNCTIONAL ROLE OF THE SIGNAL PEPTIDE IN CLN5 AND CTSD

3.1. PREFACE

This chapter is a collection of data that was a part of a published primary paper in the journal of *Traffic* (see below), including written text and figures. In addition, this chapter includes raw data that have not been published.

TITLE	Mechanisms regulating the intracellular trafficking and release of CLN5 and CTSD
AUTHORS	Robert J. Huber, William D. Kim & Morgan M.L.D.M. Wilson-Smilie
REFERENCE	Huber, R.J., **Kim, W.D.** & Wilson-Smillie, M.L.D.M. (2024). Mechanisms regulating the intracellular trafficking and release of proteins associated with Batten disease. *Traffic*. 25, e12925.
CONTRIBUTIONS	WDK and RJH wrote the first original and final draft. WDK and RJH reviewed and edited the manuscript. WDK, RJH, and MLDMW-S collected data. WDK and RJH analyzed all data within this manuscript. All authors read and approved the final draft of the manuscript.
COPYRIGHT	The copyright policy can be found within the published manuscript online.

3.2. ABSTRACT

The neuronal ceroid lipofuscinoses, collectively known as Batten disease, are a group of neurodegenerative diseases that affect all ages, mainly children. Mutations in 1 of the 13 ceroid lipofuscinosis neuronal (*CLN*) genes (*CLN1-CLN8, CLN10-CLN14*) result in Batten disease, each of which causes a Batten disease subtype. Mutations in *CLN5* and cathepsin D (*CTSD*) cause CLN5 and CLN10 disease, respectively. CTSD functions as an aspartic endopeptidase, while the exact function of CLN5, like many CLN proteins, is still under investigation. As of now, CLN5 putatively functions as either a ceramide synthase, depalmitoylase, glycoside hydrolase, or bis(monoacylglycerol)synthase. Both proteins localize to lysosomes and are secreted into the extracellular space. However, there is limited information on the processes which cells use to secrete CLN5 and CTSD. In this chapter, we use the social amoeba *Dictyostelium discoideum* as a model to study the secretion of CLN5 and CTSD. Through SignalP 6.0, we detected a signal peptide (SP) sequence in both Cln5 and CtsD, and we generated cell lines expressing both proteins lacking their SP. Loss of SP in Cln5 and CtsD did not alter their intracellular localization, but did cause more cytoplasmic localization in Cln5. In addition, the deletion of the SP inhibits the release of Cln5 and CtsD, suggesting the SP region is essential in the secretion of these proteins. The secretion of Cln5 is also modulated by the secretion of CtsD, as loss of SP in CtsD caused an increase in extracellular Cln5 amounts. Finally, loss of SP in Cln5 resulted in delayed aggregation. WT cells expressing GFP-Cln5, an alternative to blocking the function of the SP but also traps Cln5 in the ER, display *cln5*-deficient phenotypes such as delayed cell proliferation and aggregation, along with delayed late multicellular development, which suggests that ER stress plays a role in CLN5 disease. Altogether, this chapter furthered our

understanding of the secretion of CLN5 and CTSD, and how ER entrapment contributes to CLN5 disease pathology.

KEYWORDS: Batten disease, CLN5, CTSD, *Dictyostelium*, ER, neuronal ceroid lipofuscinosis, secretion, signal peptide.

3.3. INTRODUCTION

CLN5 disease is one of the NCL subtypes and is caused by mutations in the *CLN5* gene (Butz et al., 2020; Simonati & Mole, 2022). CLN5 is a soluble protein that putatively functions as either a glycoside hydrolase, a bis(monoacylglycerol)phosphate synthase, or a depalmitoylase (Huber & Mathavarajah, 2018a; Luebben et al., 2022; Medoh et al., 2023). Like with its function, the process that CLN5 is directly involved in is uncertain; however, CLN5 plays a role in various biological processes within cells, including lipid processing, intracellular trafficking, and autophagy (Haddad et al., 2012; Mamo et al., 2012; Leinonen et al., 2017; Adams et al., 2019; Luo et al., 2020; McLaren et al., 2021; Yasa et al., 2021; Doccini et al., 2022). Human CLN5 localizes to the endoplasmic reticulum (ER) and the lysosome (Isosomppi et al., 2002; Jules et al., 2017). In addition to its intracellular localization, many organismal models, including mammalian models, human cell models, and human excrement samples, show that CLN5 is in the extracellular space (Moharir et al., 2013; Hughes et al., 2017; Iwan et al., 2021). Previous research showed that CLN5 has a signal peptide (SP) in its amino acid sequence, a N-terminal amino acid sequence that directs proteins for secretion (Jules et al., 2017; Huber & Mathavarajah, 2018a). However, experiments showcasing the role in the secretion of the SP in CLN5, as well as other CLN proteins including cathepsin D (CTSD), have yet to be determined.

In addition to these models, *Dictyostelium discoideum* contains a CLN5 homolog, Cln5, and is also present in the extracellular space (Huber & Mathavarajah, 2018ab). *Dictyostelium* is a social amoeba that exists unicellular under nutrient-rich conditions, feeding on bacteria or liquid media and dividing mitotically (Mathavarajah et al., 2017). When nutrients are depleted, *Dictyostelium* enters its multicellular phase, where single cells

aggregate into mounds and, through a series of developmental processes, form a fruiting body. Fruiting bodies are composed of a stalk holding a sorus containing spores that germinate under nutrient-rich conditions, restarting the *Dictyostelium* lifecycle. *Dictyostelium* serves as a powerful model in studying various neurological diseases as its genome contains many homologs linked to neurodegeneration and has conserved processes from humans (Haver & Scaglione, 2021; Huber et al., 2022). In the context of Batten disease, *Dictyostelium* is an early eukaryote that contains many homologs of CLN-like proteins and a CLN5-like protein, a feature that is not present in other eukaryotic models (Huber, 2016).

The molecular function of *Dictyostelium* Cln5 is a glycoside hydrolase and localizes within the ER, cytoplasmic punctate, and to the cellular periphery (Huber & Mathavarajah, 2018a). Loss of *cln5* causes phenotypic defects within the *Dictyostelium* lifecycle. During growth, *cln5*-deficiency reduces cell proliferation, cytokinesis, and affects basal activity in autophagy (McLaren et al., 2021). Cln5 also plays various roles within the early multicellular development, such as cell migration, cell-substrate and cell-cell adhesion (Huber & Mathavarajah, 2018b). Under both conditions, cells deficient in Cln5 display defective activity of many lysosomal enzymes and alter the intracellular and extracellular distribution of many proteins regulating these processes during growth and multicellular development (Kim & Huber, 2022). In *Dictyostelium*, Cln5 is secreted via an unconventional secretory pathway, an intracellular pathway that traffics proteins from the ER towards the cellular periphery but bypasses the Golgi complex (as reviewed in Néel et al., 2024). Previous research showed that both *Dictyostelium* Cln5 and human CLN5 amino acid sequences contain a putative SP (Jules et al., 2017; Huber & Mathavarajah, 2018a). In this study, we reveal that the SP plays a role in protein secretion in the Cln protein family,

including Cln5 and CtsD. We also show that removal of the SP does not alter the intracellular trafficking of Cln5 and CtsD. Finally, loss of SP in Cln5 only delays aggregation, while blocking ER exiting of Cln5 via N-terminal GFP tagging severely impacts the *Dictyostelium* lifecycle.

3.4. METHODS

3.4.1. CELL LINES, CULTURING, AND MATERIALS

AX3 cells, as well as both pDM323 and pTXGFP plasmids, were purchased from the Dicty Stock Center (Fey et al., 2019). The *cln5*$^-$ cell line (parental line: AX3) and AX3 cells overexpressing GFPCln5 in the pTXGFP plasmid used in this study were previously validated (Huber & Mathavarajah, 2018a). In this paper, parental lines are referred to as wild type (WT) in this chapter. All cell lines were kept on SM/2 agar containing *Klebsiella aerogenes* (Fey et al., 2007). Cells were cultured in HL5 medium (Formedium, Hunstanton, Norfolk, UK) containing 100µg/ml ampicillin and 300µg/ml streptomycin sulfate. *cln5*$^-$ cells were selected with 10µg/ml of blasticidin-S-chloride in HL5 medium, while cells with extrachromosomal DNA were selected with 10µg/ml G418 sulfate. For experiments, all cell cultures were grown at mid-log phase of growth (1–5 × 10^6 cells/ml) at 21^{o}C/150RPM. KK2 buffer was formulated as follows: 2.2 g/L KH_2PO_4 and 0.7 g/L K_2HPO_4, pH 6.5. The polyclonal rabbit anti-Cln5 and polyclonal rabbit anti-CtsD antibodies used in this study were validated in previous studies (Huber & Mathavarajah, 2018b; Huber et al., 2020). Mouse monoclonal anti-beta-actin (Cat #: SC-47 778) and mouse monoclonal anti-GFP (Cat #: SC-9996) were purchased from Santa Cruz Biotechnology Incorporated (Dallas, Texas, United States). The monoclonal mouse anti-GFP antibody (Cat #: 2555), as well as

the goat anti-rabbit (Cat #: 7074) and horse anti-mouse (Cat #: 7076) IgG linked to HRP, were purchased from New England Biolabs Canada (Whitby, Ontario, Canada). Mouse monoclonal anti-alpha-actinin (Cat #: 47-62-17) and mouse monoclonal anti-alpha-tubulin (Cat #: 12G10) were purchased from the Developmental Studies Hybridoma Bank (University of Iowa, Iowa City, Iowa, United States). Alexa Fluor-conjugated secondary antibodies were purchased from Fisher Scientific Company (Ottawa, Ontario, Canada). Protease cocktail inhibitor tablets were purchased from Fisher Scientific Company.

3.4.2. Cln5 AND CtsD SP-NULL PLASMID CONSTRUCTION AND *Dictyostelium* TRANSFORMATION

To determine the region where the putative SP is cleaved, we input the amino acid sequences of Cln5 and CtsD into SignalP 6.0 (Teufel et al., 2022). SignalP 6.0 has identified SP sequences from amino acid positions 1-20 and 1-18 in Cln5 and CtsD, respectively. Considering this, we designed primers that amplified after the SP sequence in Cln5 and CtsD (Table 3). Expression of C-terminal GFP of full-length CtsD (CtsD-GFP), as well as Cln5 and CtsD lacking their signal peptides (ΔSP-Cln5-GFP and ΔSP-CtsD-GFP), were created via amplifying PCR products with OneTaq 2X Master Mix with Standard Buffer Kit (Cat #: M0482). *Escherichia coli* containing the pDM323 plasmid were grown overnight (30^{o}C/250RPM), and the pDM323 plasmid was extracted using the Monarch Plasmid Miniprep Kit (Cat #: T1010). PCR amplicons and pDM323 vector were digested with *Bgl*II (Cat #: R0144) and *Spe*I (Cat #: R3133). Digested PCR amplicons were purified with the Monarch PCR & DNA Cleanup Kit (Cat #: T1030), while purification of the digested pDM323 vector was done via the Monarch Gel Extraction Kit (Cat #: T1020).

Digested PCR amplicons were ligated into the digested pDM323 vector with T4 DNA ligase (Cat #: M0202) and heat-shocked into competent *E. coli* bacteria (Cat #: C3040H). Heat-shocked *E. coli* cells were grown overnight, and plasmids in *E.coli* cells were extracted with Monarch Plasmid Miniprep Kit. All reagents used above in this protocol were purchased from New England Biolabs (Whitby, Ontario, Canada). Extracted plasmids were sequenced at The Hospital for Sick Children (Toronto, Ontario, Canada) to ensure no mutations were present. Methods of transforming AX3 and *cln5*$^{-}$ cells with the validated plasmids were adapted from a previous study (Gaudet et al., 2017) and done using the Bio-Rad MicroPulser Electroporator (Bio-Rad Laboratories Canada Limited, Mississauga, Ontario, Canada).

3.4.3. IMMUNOFLUORESCENCE ASSAY

An immunofluorescence (IF) assay was performed using a method previously described (Hagedorn et al., 2006). Briefly, cells (1.5×10^5 cells) in the mid-log phase of growth were deposited onto coverslips placed inside separate wells of a 12-well dish and then submerged overnight in low-fluorescence HL5 at room temperature. The next day, cells were starved for 2 hr in KK2 buffer and then fixed by submerging coverslips in −80°C methanol for 45 min. The primary anti-GFP (1:50) and secondary anti-rabbit Alexa Fluor 488 (1:100) were used. Coverslips were mounted onto slides using Prolong Gold Anti-Fade Reagent with DAPI (Fisher Scientific Company) and sealed with nail polish. Fixed cells were imaged using a Nikon Ts2R-FL inverted microscope equipped with a Nikon Digital Sight Qi2 monochrome camera (Nikon Canada Incorporated Instruments Division). Images were then merged with Fiji/ImageJ.

3.4.4. CELL PROLIFERATION ASSAY

Methods in conducting a cell proliferation assay were adapted from previous studies (McLaren et al., 2021; Yap et al., 2022). Briefly, cells in mid-log phase of growth were washed twice with HL5 medium. Cells were suspended at a cell density of 2.0 x 10^5 cells/mL with HL5 medium in 50 mL Erlenmeyer flasks. However, cells expressing GFP-Cln5 were unable to grow below the mid-log phase of growth (data not shown). Because of this, cells expressing GFP-Cln5 or the empty pTXGFP plasmid were set at an initial cell concentration of 1.0 x 10^6 cells/ml. All cell cultures in flasks used for the cell proliferation assay were incubated at 21^{o}C/150RPM. A $p<0.05$ under a two-way ANOVA coupled with Bonferroni's multiple comparison test was used to determine significance.

3.4.5. STARVATION ASSAY

Cells (5 x 10^6 cells) were left to adhere on 100 x 150mm Petri dishes containing HL5 medium for at least an hour, whereafter the medium was refreshed and left overnight. Confluent cells were rinsed twice with KK2 buffer and submerged in KK2 buffer for 12 hours. Cells were imaged every 2 hours using a Nikon Ts2R-FL inverted microscope equipped with a Nikon Digital Sight Qi2 monochrome camera (Nikon Canada Incorporated Instruments Division, Mississauga, Ontario, Canada). Along with the starvation assay, a subset of confluent cells was starved for 4 hours, and the starved cells and the conditioned buffer (CB) were harvested. The 4-hour starvation time point was chosen as this is when the expression of *cln5* and the process of enzyme secretion are at their maximum in *Dictyostelium* (Dimond et al., 1981; Rossomando et al., 1987; Stajdohar et al., 2017). The CB was collected and clarified via centrifugation (4°C/2000RPM/5mins) to remove any

free-floating cells. Clarified CB was concentrated through centrifugation (4°C/4200RPM) with the Amicon Ultra-4 centrifugal filter unit (Cat #: UFC801024; Fisher Scientific Company, Ottawa, Ontario, Canada). Starved cells on Petri dishes were lysed with 0.5% (v/v) NP-40 lysis buffer (50mM Tris, 150mM NaCl, pH 8.3) containing a protease inhibitor tablet.

3.4.6. LATE MULTICELLULAR DEVELOPMENT ASSAY

The protocol for performing a late multicellular development assay was modified from a previous study (McLaren et al., 2021). Cells in the mid-log phase of growth (5.0 x 10^6 cells) were deposited in 100 x 150mm Petri dishes and left overnight in HL5 medium. Confluent cells were harvested and washed twice with KK2 buffer. Cells were resuspended at a cell concentration of 3.0 x 10^7 cells/mL, and 35μL droplets of the cell solution were formed onto 0.1% (w/v) KK2 agar. Cells on KK2 agar were incubated in a moist chamber and wrapped with aluminum foil to avoid light exposure. Images were taken every 2 hours after the 12-hour timepoint using the internal 5MP CMOS camera attached to a Leica EZ4W stereomicroscope (Leica Microsystems Canada Incorporated, Richmond Hill, ON, Canada).

3.4.7. PROTEIN QUANTIFICATION AND WESTERN BLOTTING

The protein concentration of whole cell (WC) lysates and CB samples was quantified using the Qubit 2.0 Fluorometer (Fisher Scientific Company, Ottawa, Ontario, Canada). Samples were mixed 1:1 (v/v) with sample buffer and digested for 5 minutes at 95°C. Standard methods of SDS-PAGE and western blotting were used. In brief, equal amounts of protein (WC: 10-25μg; CB: 0.1-0.5μg) within samples were separated via SDS-

PAGE and transferred onto nitrocellulose membranes via wet transfer. Membranes were incubated in 5% (w/v) milk-TBST for 45 minutes, rinsed thrice with TBST, and incubated with the following antibodies: anti-Cln5 (1:500), anti-CtsD (1:500), anti-GFP (1:1000), anti-glucose-regulated protein 78 (Grp78) (1:1000); anti-alpha-actinin (1:1000), anti-alpha-tubulin (1:1000), anti-beta-actin (1:1000), and secondary anti-rabbit and anti-mouse IgG linked to HRP (1:5000).

3.5.0. RESULTS

3.5.1. DETERMINING THE INTRACELLULAR LOCALIZATION OF Cln5 AND CtsD LACKING THEIR PUTATIVE SP

The secretion of SP-bearing proteins follows the conventional secretory pathway, involving trafficking these proteins in the ER to the Golgi complex and ultimately to the plasma membrane for excretion (as reviewed in Néel et al., 2024). The amino acid sequences of human CLN5 and *Dictyostelium* Cln5 contain a potential N-terminal SP sequence, and blocking the N-terminus with GFP expression traps Cln5 in the ER (Jules et al., 2017; Huber & Mathavarajah, 2018a). In this study, we showed that removing the SP allows ER release of Cln5 (Figure 11). Additionally, a cytoplasmic distribution of Cln5 increases when the SP is deleted (Figure 11). Having established the impact of SP loss on Cln5 localization, we extended our analysis to CtsD, another protein with an SP that is linked to CLN10 Batten disease subtype when mutated (Butz et al., 2020). SignalP 6.0 predicted a putative SP from positions 1-18 within the CtsD amino acid sequence. We deleted the SP from CtsD and evaluated the localization of this SP-lacking protein. Our results showed that CtsD localizes to intracellular vesicles, cytoplasmic punctate structures,

and the plasma membrane (Figure 12). Deletion of the SP did not appear to alter the overall localization of CtsD. Overall, our findings indicate that loss of the SP affects the localization of Cln5, but not the localization for CtsD.

3.5.2. EVALUATING THE PUTATIVE SP ON THE SECRETION OF Cln5 AND CtsD

Since SP-bearing proteins are destined to be secreted, but our IF data show altered localization for the ΔSP-Cln5-GFP fusion protein, but not for the ΔSP-CtsD-GFP fusion protein, with loss of the SP, we followed up on these findings by determining if the secretion of these fusion proteins would be affected. We used western blotting to assess the presence of the deletion mutants intracellularly (in whole cell lysates) and extracellularly (in conditioned buffer). All four fusion proteins (Cln5-GFP, ΔSP-Cln5-GFP, CtsD-GFP, ΔSP-CtsD-GFP) were detected in whole cell lysates, and the molecular weights of the deletion mutants were reduced compared to the full-length proteins (Figure 13). When focusing on the extracellular space, the Cln5-GFP and CtsD-GFP fusion proteins were detected, while there was a lack of signal of their SP-lacking protein counterparts. This suggests that both Cln5 and CtsD contain a functional SP that regulates their release from cells.

Dictyostelium Cln5 interacts with CtsD (Huber & Mathavarajah, 2018a). Since we showed that the SP is essential for Cln5 and CtsD secretion, we investigated how loss of the SP affects the secretion of their protein partners. Intracellular and extracellular amounts of CtsD were not affected in cells expressing ΔSP-Cln5-GFP (Figure 14A). Although unaffected intracellular Cln5 amounts were observed in cells expressing ΔSP-CtsD-GFP,

elevated extracellular amounts of Cln5 were present (Figure 14B). This suggests that loss of the SP in Cln5 does not modulate CtsD secretion, while extracellular release of CtsD regulates Cln5 secretion.

3.5.3. EVALUATING THE EFFECT BLOCKING Cln5 SECRETION ON CELL PROLIFERATION, AGGREGATION, AND DEVELOPMENT

Loss of *cln5* reduces cell proliferation, reduces aggregation, and enhances late multicellular development (McLaren et al., 2021). Since previous research showed that blocking the N-terminus of Cln5 via GFP alters its intracellular localization and prevents its secretion (Huber & Mathavarajah, 2018a), we assessed the effect of inhibiting the secretion of Cln5 (e.g., N-terminal GFP tagging of Cln5, SP-lacking Cln5) on cell proliferation and multicellular development. Loss of the SP in Cln5 did not affect cell proliferation (Figure 15). Reduced cell proliferation in WT and *cln5*$^{-}$ cells expressing GFP-Cln5 within 48 hours of growth was observed, while cell proliferation was reduced at 72 hours of growth in *cln5*$^{-}$ cells (Figure 16). In line with this finding, cells expressing GFP-Cln5 displayed arrested proliferation in HL5 medium when below mid-log phase of growth (data not shown), suggesting cellular stress in these cell lines. This suggests that trapping Cln5 in the ER is more deleterious than the loss of *cln5* and the loss of the SP in Cln5 on cell proliferation.

Since N-terminal GFP tagging of Cln5 led to cellular defects during growth, we explored the effect of Cln5 lacking its SP and N-terminal GFP tagging on Cln5 in the multicellular phase of *Dictyostelium*. When cells were starved in KK2 buffer, Cln5 lacking its SP did not affect *Dictyostelium* aggregation (Figure 17), but the expression of GFP-Cln5 delayed aggregation in WT cells similar to *cln5*$^{-}$ cells (Figure 18). Interestingly, recovery

was observed in *cln5*$^{-}$ cells expressing GFP-Cln5. Like growth, we observed stress within cells expressing GFP-Cln5 as indicated by poor cell-substrate adhesion (data not shown). From this, we extended our analysis towards the latter part of the *Dictyostelium* multicellular development. Like aggregation, overexpressing GFP-Cln5 in *cln5*$^{-}$ cells showed recovery in late multicellular development (Figure 19A). WT cells expressing GFP-Cln5 started to enter late multicellular development at the 24-hour timepoint, as indicated by the formation of slugs. We also assessed late multicellular development in *cln5*$^{-}$ cells expressing ΔSP-Cln5-GFP and found that loss of the SP did not affect this part of the lifecycle (Figure 19B). Altogether, these data reveal that a lack of Cln5 or an overabundance of intracellular Cln5 impacts the *Dictyostelium* multicellular development.

3.5.4. INVESTIGATION THE IMPACT OF BLOCKING Cln5 SECRETION IN ER STRESS RESPONSE

Our previous work with *Dictyostelium* showed GFP-Cln5 is trapped in the ER (Huber & Mathavarajah, 2018a), and we observed severe phenotypes in WT cells expressing GFP-Cln5. Because of this and previous work suggesting ER stress in Batten disease (as reviewed in Marotta et al., 2017), we determined the amounts of Grp78, an ER protein that is activated when cells experience ER stress (Harding et al., 2002; Schröder & Kaufman, 2005), during growth and starvation. During growth, increased Grp78 amounts were observed only in WT cells expressing GFP-Cln5 (Figure 20A). When assessing Grp78 amounts during starvation, WT cells expressing GFP-Cln5 and *cln5*-deficient cells expressing the empty pTXGFP plasmid showed reduced Grp78 amounts (Figure 20B). These data suggest that WT cells containing GFP-Cln5 experience basal levels of ER stress and experience similar ER stress to *cln5*$^{-}$ cells during starvation.

3.6. DISCUSSION

This study shows that Cln5 and CtsD contain a functional SP in their amino acid sequence and are essential for their secretion. We showed that loss of SP in Cln5 does not affect the release of CtsD, but Cln5 release to the extracellular space is modulated by extracellular CtsD. Furthermore, loss of SP does not trap Cln5 and CtsD in the ER but rather causes more cytoplasmic localization and does not affect its localization, respectively. In addition, blocking the N-terminus of Cln5 via GFP tagging resulted in a significant reduction in cell proliferation in both WT and *cln5*$^-$ cells. Finally, overexpression of GFP-Cln5 drastically reduced the rate of aggregation and late development in WT cells, while recovery was observed in *cln5*$^-$ cells.

CLN5 is a lysosomal protein that is released into the extracellular space as demonstrated in various cellular models, including baby hamster kidney cells, ovine neurons, *Dictyostelium*, and human cell models (Isosomppi et al., 2002; Hughes et al., 2014; Huber & Mathavarajah, 2018ab; Minnis et al., 2020). Along with this study, previous research revealed a putative SP inside the *Dictyostelium* Cln5, human CLN5, and *Dictyostelium* CtsD amino acid sequences via informatics tools (Jules et al., 2017; Huber & Mathavarajah, 2018a). SP-bearing proteins are known to be secreted via the conventional secretory pathway, where proteins within the ER pass through the Golgi complex and are eventually secreted through plasma membrane fusion (Tacini et al., 2020; Néel et al., 2024). In this study, loss of the SP prevented the release of Cln5 and CtsD. Blocking the function of the SP via N-terminal GFP tagging also trapped Cln5 within cells (Huber & Mathavarajah, 2018a), which is consistent with our data. Proteins can also be secreted through the unconventional secretory pathway, a process that does not follow the ER-Golgi

route to release proteins in the extracellular space, such as lysosomes (Tacini et al., 2020; Néel et al., 2024). Several unconventional secretory pathways modulate the release of Cln5, including lysosomal exocytosis and autophagy (Huber et al., 2024). Additionally, *Dictyostelium* Cln5 follows another unconventional secretory process that utilizes autophagy for its secretion (Huber & Mathavarajah, 2018b), revealing the complexity behind the unconventional protein secretion and the secretion of this protein. Finally, we showed that loss of SP in CtsD elevated Cln5 secretion. Since Cln5 interacts with CtsD (Huber & Mathavarajah, 2018a), this indicates that this interaction could modulate the secretion of Cln5. Altogether, the secretion of Cln5 and CtsD is modulated via its SP, and the Cln5 secretion is regulated by the extracellular release of CtsD.

Loss of SP in CtsD led to no change to its localization in this study. Consistent with our work, the CTSD p.A58V mutation occurs within the SP region and expressing this mutation in SH-SY5Y cells does not impact the localization of the protein (Bunk et al., 2021). Furthermore, SH-SY5Y cells expressing the CTSD p.A58V mutation show no effect on the maturation and function of CTSD. It was suggested to be expected since the SP region is removed when maturation occurs in CTSD (Bunk et al., 2021). As for Cln5, N-terminal GFP tagging trapped Cln5 in the ER while SP deletion allowed Cln5 to be released from the ER (Huber & Mathavarajah, 2018a). Human CLN5 is a 407 aa-long protein whose SP is cleaved by the signal peptide peptidase/signal peptide peptidase-like (SPP/SPPL) protein family (Jules et al., 2017). This suggests that N-terminal GFP attachment caused the SP to become unrecognized by SP-cleaving proteases, which led to ER entrapment of Cln5. Additionally, introducing N-mutations at glycosylation sites, including N179, N252, N304, and N320, prevents ER release of CLN5 due to protein misfolding in *HeLa* cells (Moharir et al., 2013). The SP-lacking Cln5 localized to the cytoplasm; however, it is quite

dispersed. Considering this and the secretion data, this aligned with no Cln5 being secreted due to loss of SP, indicating that excess Cln5 is trapped within the cytoplasm.

Finally, GFP-Cln5 expression in WT and *cln5*$^{-}$ cells caused reduced cell proliferation, and cells did not proliferate when below the mid-log phase of growth. However, *cln5*$^{-}$ cells expressing ΔSP-Cln5-GFP show normal cell proliferation. GFP-Cln5 is trapped in the ER while ΔSP-Cln5-GFP is not. Therefore, the affected cell proliferation observed in cells expressing GFP-Cln5 was not a consequence of the lack of extracellular Cln5 but rather the overabundance of Cln5 in the ER. In line with this, we observed dysregulated Grp78 amounts in the WT cells expressing GFP-Cln5, suggesting cellular stress at the ER level. Consistent with this, expressing GFP-Cln5 delayed aggregation and late multicellular development in WT cells, while GFP-Cln5 expression or expression of Cln5 lacking its SP did not in *cln5*$^{-}$ cells. This suggests that trapping GFP-Cln5 in the ER with native Cln5 present in the cell dysregulates more intracellular processes than Cln5 ER entrapment alone. Although not directly shown, evidence of ER stress is present within NCL pathology (as reviewed in Marotta et al., 2017). Like our data, CLN1 disease patient-derived lymphoblasts, an NCL subtype caused by mutations in the protein palmitoyl thioesterase 1 gene (*PPT1*), show elevated GRP78 amounts (Kim et al., 2006). ER stress can induce the activation of autophagy and possibly regulate mitochondria via mitochondria-associated ER membranes (as reviewed in Morotta et al., 2017). Since mitochondrial dysregulation and aberrant autophagy are features observed in CLN5 disease pathology (Leinonen et al., 2017; Adams et al., 2019; McLaren et al., 2021; Doccini et al., 2020; Kim et al., 2022), further investigation is required to determine if ER stress is the uprising to these issues.

In conclusion, this study provides insights into the role of the SP in Cln5 and CtsD. Our data show that the SP plays a role in the localization and protein stability of Cln5 and CtsD, respectively. Furthermore, this study is the first to demonstrate that the SP is essential for the secretion of Cln5 and CtsD. Interestingly, extracellular Cln5 only plays a role in aggregation. Along with this datum, preventing ER release of Cln5 via GFP-Cln5 worsens the cell proliferation, aggregation, and late multicellular development in WT cells, suggesting that overabundance of Cln5 in the ER leads to cellular stress. Altogether, this study sheds light on the secretory processes that regulate Cln5 and CtsD, in addition to ER stress within the NCLs.

3.7. ACKNOWLEDGMENTS

None.

3.8. FIGURES AND TABLES

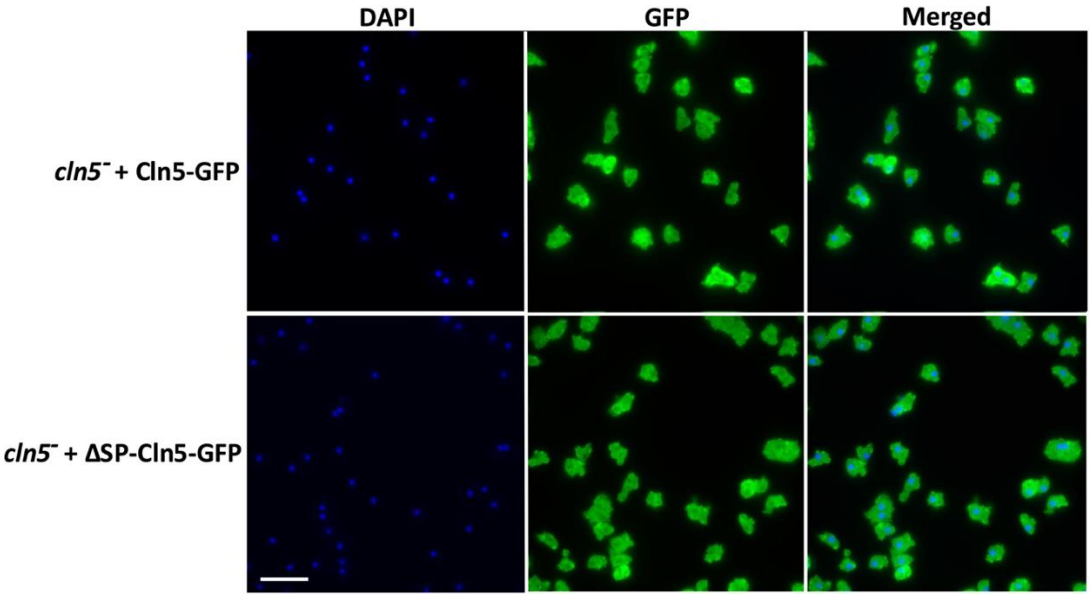

Figure 11. Loss of the SP disrupted the cellular distribution of Cln5, leading to more diffuse cytoplasmic localization. *cln5*$^-$ cells expressing Cln5-GFP or ΔSP-Cln5-GFP were fixed onto coverslips and incubated with anti-GFP and mounting solution containing DAPI. Images are representative of 8 independent experiments. Scale bar: Scale bar: 20μm.

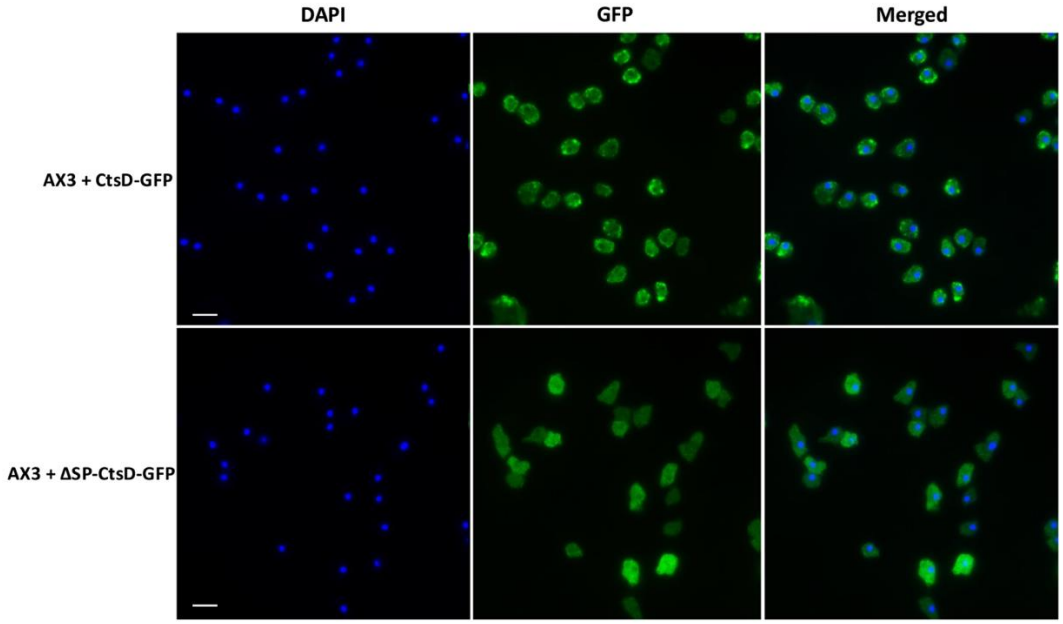

Figure 12. Loss of the SP in CtsD did not impact its localization. AX3 cells (2 x 10^5 cells) expressing either CtsDGFP or ΔSP-CtsDGFP were fixed in methanol, blocked with IF blocking buffer, and coverslips were incubated with the following antibody solutions for at least 45 minutes: 1:50 rabbit anti-GFP (CST 2555s) and 1:100 anti-rabbit Alexa 488

(green). Coverslips were mounted onto microscope slides with Prolong Gold Anti-Fade Reagent with DAPI (blue) (Fisher Scientific Company, Ottawa, Ontario, Canada) and sealed with nail polish. Images were captured using a Nikon Ts2R-FL inverted microscope with a Nikon Digital Sight Qi2 monochrome camera. The NIS Elements Basic Research software was used to view the images. Fiji/ImageJ was used to colour the images to their respective colour and overlaid to develop the merged image. Images are representative of 6 independent replicates. Scale bar: 10μm.

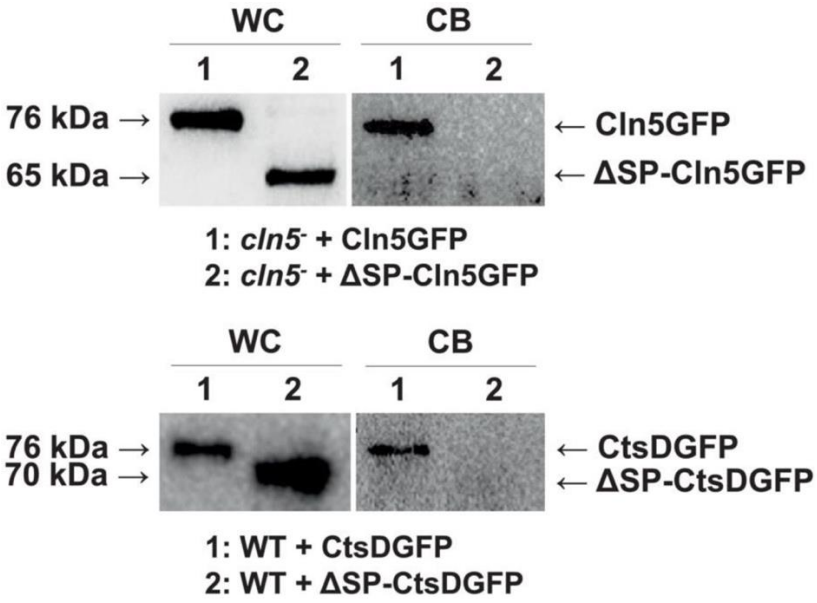

Figure 13. Loss of the SP prevented the secretion of Cln5 and CtsD. *cln5*$^{-}$ cells expressing either Cln5GFP or ΔSP-Cln5GFP and WT cells expressing either CtsDGFP or ΔSP-CtsDGFP were starved in KK2 buffer for 4 h. WC lysates (5 μg from *cln5*$^{-}$ + Cln5GFP and WT + CtsDGFP cells; 40 μg from *cln5*$^{-}$ + ΔSP-Cln5GFP and WT + ΔSP-CtsDGFP cells) and CB (0.0625 μg from *cln5*$^{-}$ + Cln5GFP and WT + CtsDGFP cells; 0.5 μg from *cln5*$^{-}$ + ΔSP-Cln5GFP and WT + ΔSP-CtsDGFP cells) were separated by SDS-PAGE and analyzed by western blotting using anti-GFP. Blots shown are representative of three independent experiments.

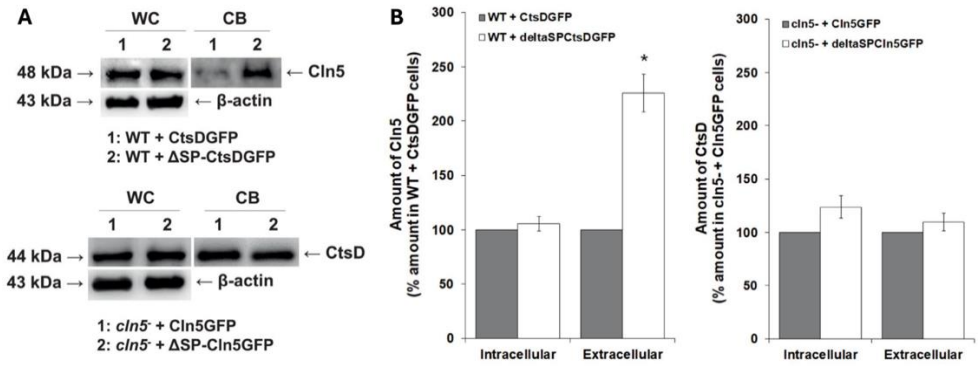

Figure 14. Loss of extracellular release of CtsD elevated the secretion of Cln5. (A) WT cells expressing either CtsDGFP or ΔSP-CtsDGFP and *cln5*⁻ cells expressing either Cln5GFP or ΔSP-Cln5GFP were starved in KK2 buffer for 4 h. WC lysates (40 µg) and CB (0.5 µg) were separated by SDS-PAGE and analyzed by western blotting using anti-GFP, anti-Cln5, and anti-CtsD. **(B)** Protein bands were quantified using Fiji/ImageJ, and bands in WC were standardized to the amounts of beta-actin to control for equal loading. Data presented as mean amount of Cln5 or CtsD (% amount in WT + CtsDGFP or *cln5*⁻ + Cln5GFP cells) ± SEM ($n = 3$). Statistical significance was determined using the one-sample *t*-test. *$p < 0.05$.

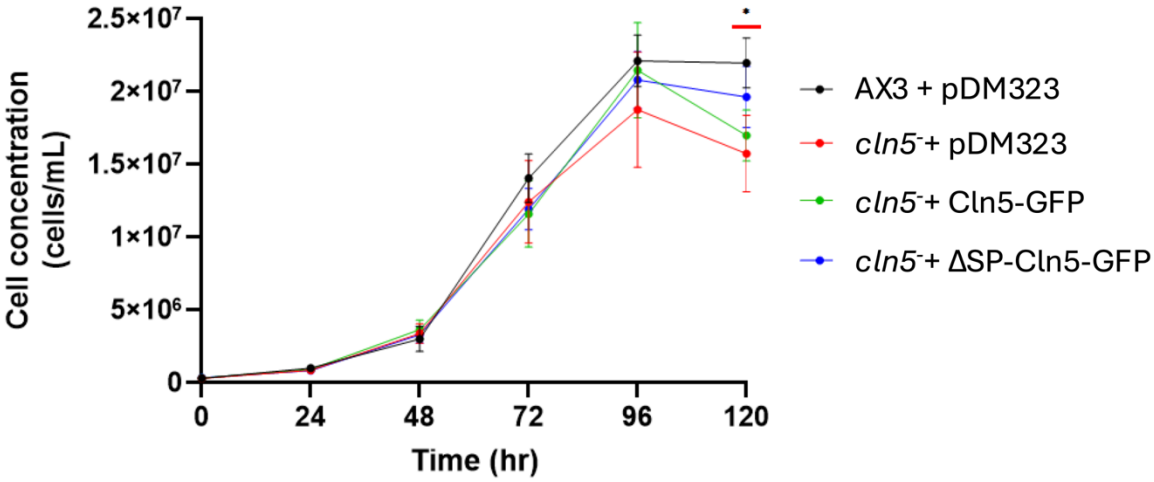

Figure 15. Cell proliferation was unaffected by the loss of the SP in Cln5. Cells were deposited at a cell concentration of $2x10^5$ cells/ml, and cell density was measured every 24 hours (n=8).

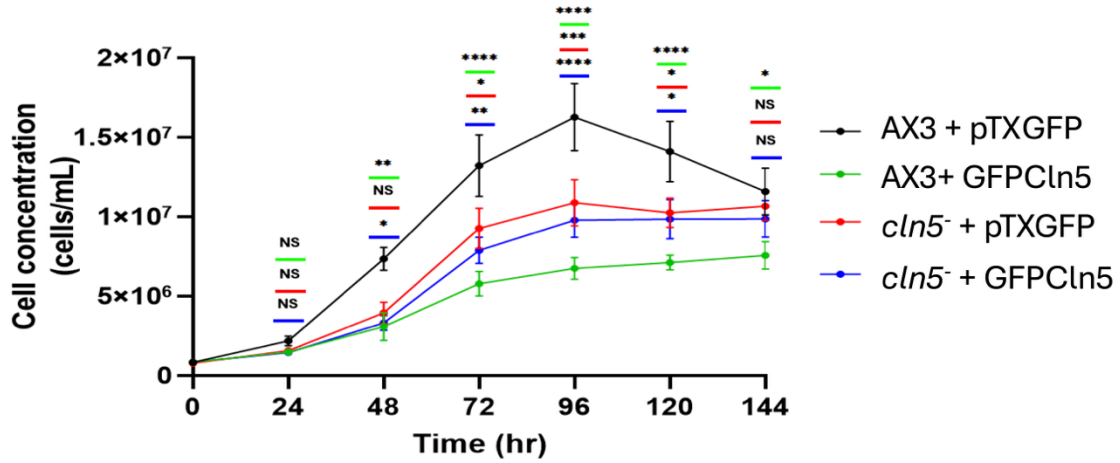

Figure 16. N-terminus tagging of Cln5 with GFP causes reduced proliferation. WT and *cln5*⁻ cells expressing either pTXGFP or GFP-Cln5 were incubated in HL5 medium at a cell concentration of 1.0 x 10^6 cells/ml and counted every 24 hours. Data is shown as mean cell concentration ± SEM (n = 5). Data at each time point were compared to WT cells expressing pTXGFP, and statistical significance was determined via a two-way ANOVA paired with a Bonferroni post-hoc analysis. NS: Not significant, *$p < 0.05$, **$p < 0.01$, ***$p < 0.001$, and ****$p < 0.0001$.

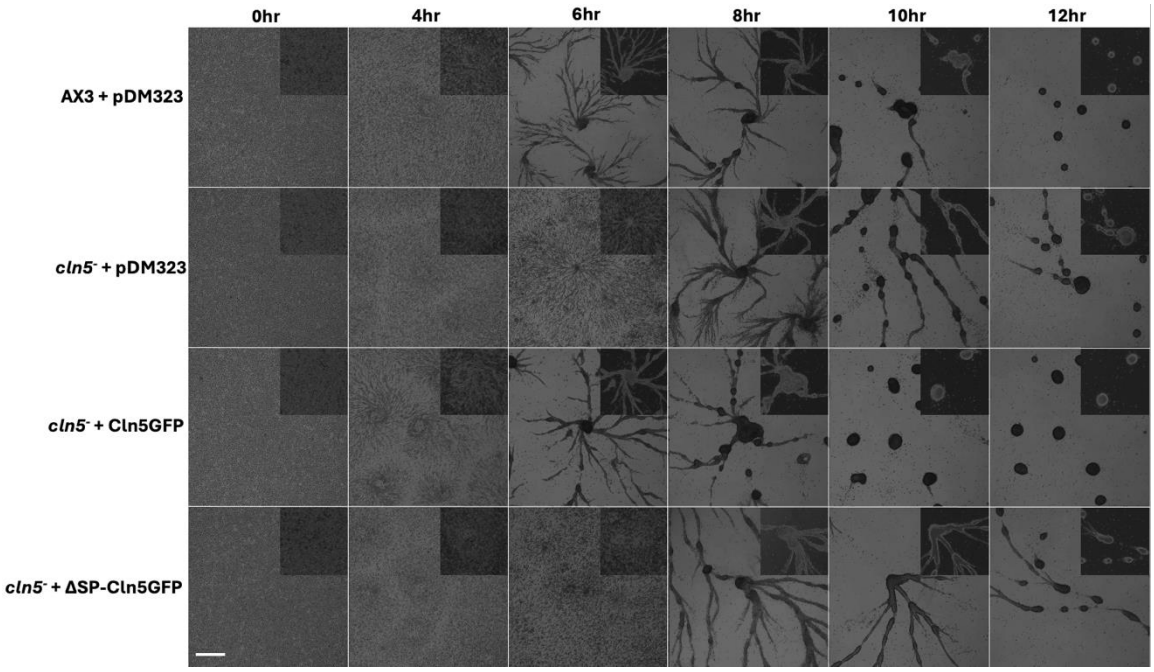

Figure 17. Loss of the SP in Cln5 did not impact *Dictyostelium* aggregation. Cells adhered to Petri dishes were submerged in KK2 buffer and were imaged every 2 hours after the 4-hour time interval until 12 hours of starvation. Images are representative of 7 independent experiments. Scale bar: 500μm.

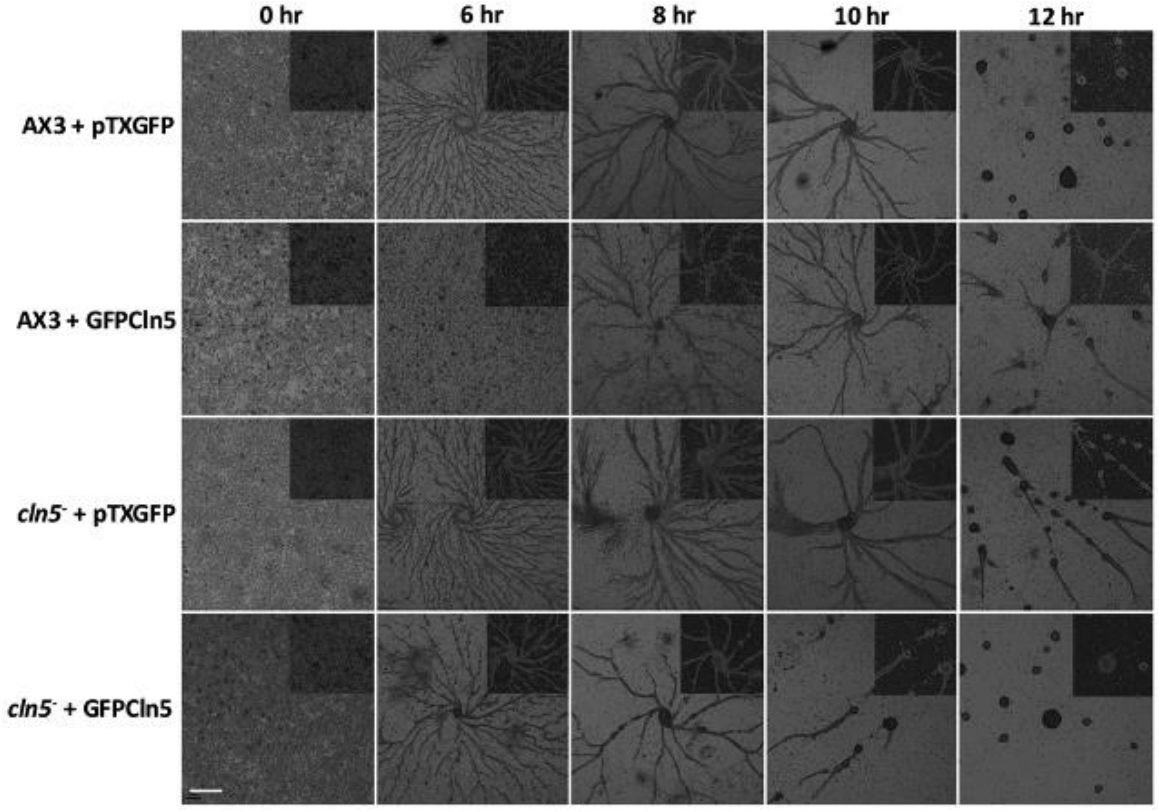

Figure 18. Overexpression of Cln5 with N-terminal GFP delayed aggregation in WT cells. Confluent cells were washed twice with KK2 buffer and submerged in KK2 buffer.

Images were taken at set timepoints with a Nikon Ts2R-FL inverted microscope equipped with a Nikon 10 Digital Sight Qi2 monochrome camera (Nikon Canada Incorporated Instruments Division, Mississauga, Ontario, Canada). Images are representative of 4 independent experiments. Scale bar: 500μm.

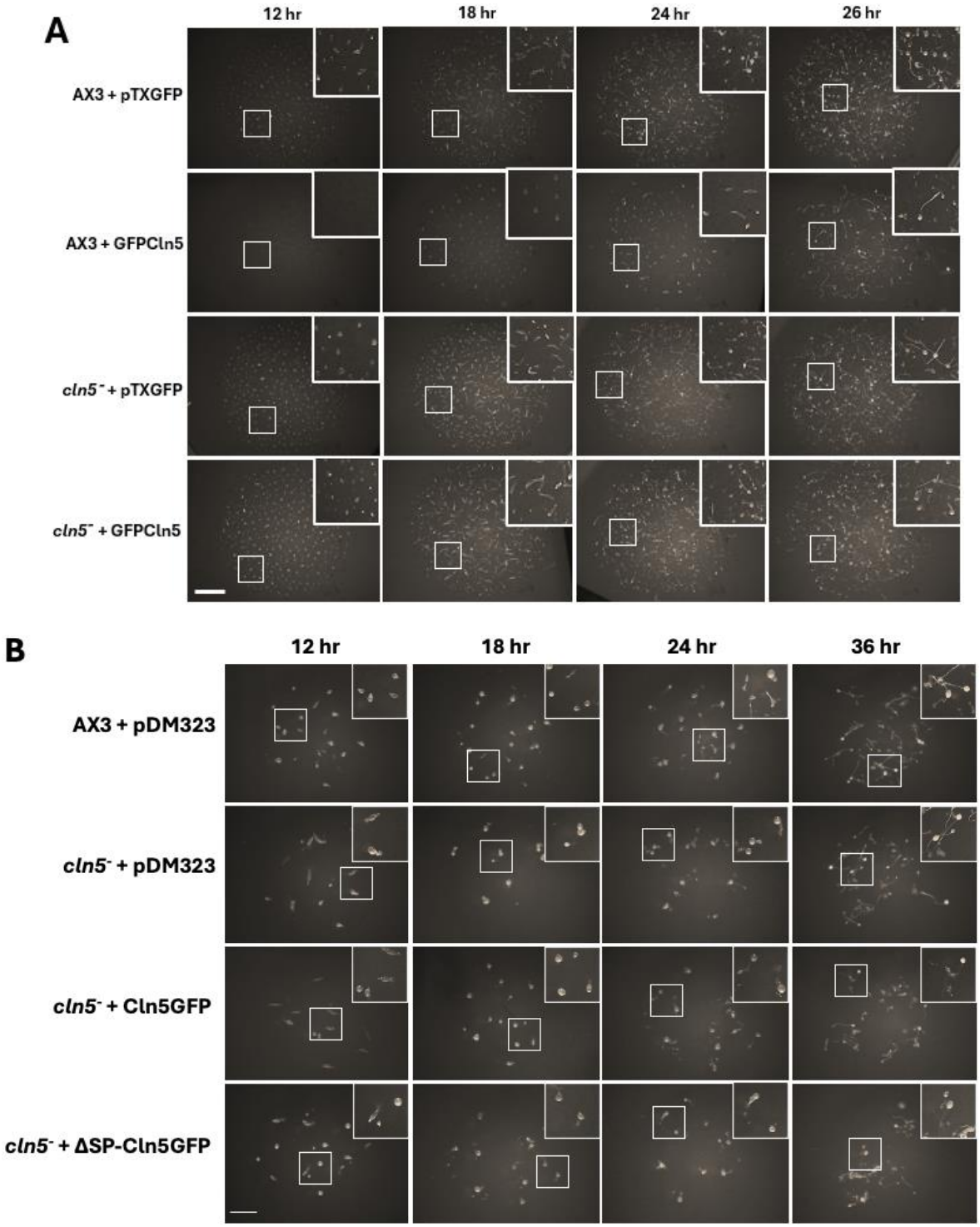

Figure 19. Late multicellular development was delayed in WT cells expressing GFP-Cln5, but unaffected in cells expressing Cln5 lacking its SP. Cells, including **(A)** WT

and *cln5*- cells expressing either pTXGFP or GFP-Cln5, as well as **(B)** WT cells expressing pDM323 or *cln5*- cells expressing pDM323, Cln5-GFP, or ΔSP-Cln5-GFP, were washed twice with KK2 buffer and concentrated down to a cell solution of 3.0 x 10^7 cells/mL in KK2 buffer. 35µL droplets were deposited onto 0.1% (w/v) KK2 agar. Images were taken every 12 hours between the 12-hour to the 24-hour time points. Images were taken with a Leica EZ4W stereomicroscope that was equipped with an internal 5MP CMOS camera. Images are representative of 4 independent replicates. Scale bar: 20mm.

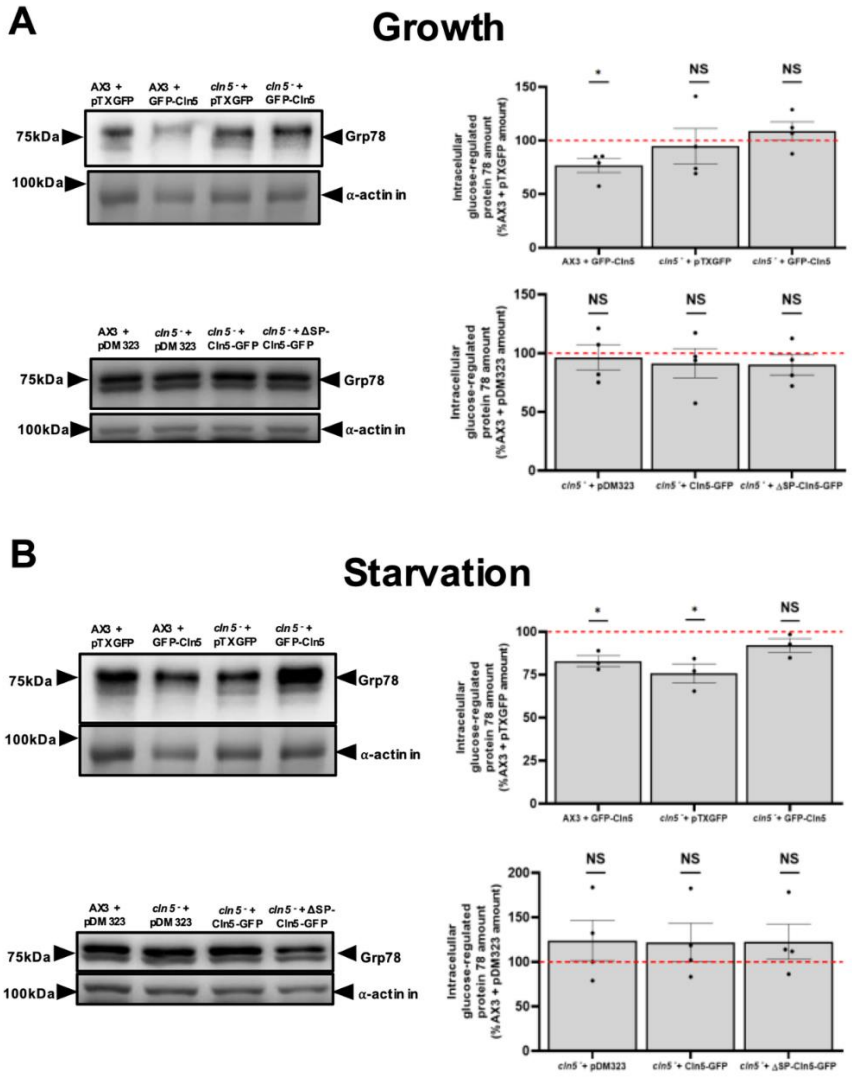

Figure 20. Expression of GFP-Cln5 in WT cells caused ER stress, while loss of the SP in Cln5 did not. Equal protein amounts (10-25µg) from WC lysates from **(A)** growth-phased and **(B)** starved cells were separated and analyzed via SDS-PAGE and western blotting, respectively. Blots were incubated in anti-Grp78, anti-α-actinin, α-tubulin, and β-actin. Protein bands were quantified via Fiji/ImageJ, and Grp78 amounts were normalized to anti-α-actinin. All Grp78 amounts were standardized against AX3 + pTXGFP amounts. Data were presented as mean protein amounts ± SEM ($n \leq 4$). NS: Not significant, *$p < 0.05$.

Table 3. List of primers used to generate the ΔSP-Cln5GFP, ΔSP-CtsDGFP, and full-length CtsDGFP plasmids.

Primer sequence	Target region
AGATCTAAAATGCAAATACCAG ATAATGATCCAGAATTATG	Forward primer used to generate the ΔSP-*cln5* insert containing a 5' BglII cut site, Kozak sequence, and a start codon
CCAACTAGTATTGAGATGAATA AAATTGCCATTTTC	Reverse primer used to amplify the ΔSP-*cln5* insert containing a SpeI cut site
CCAAGATCTAAAATGAAATTAC TTATTTTAACTTTATTTTTAGC	Forward primer used to amplify the full length *ctsD* insert containing a 5' BglII cut site, Kozak sequence, and a start codon
CCAAGATCTAAAATGTTAACAG TACCATTAAACTTCC	Forward primer used to generate the *ctsD* insert without the SP
CCAACTAGTACCTTGAATGGCA GT	Reverse primer to amplify both the full length and the ΔSP-*ctsD* insert containing a SpeI cut site

3.9. REFERENCES

Adams, J., Feuerborn, M., Molina, J. A., Wilden, A. R., Adhikari, B., Budden, T., & Lee, S. Y. (2019). Autophagy–lysosome pathway alterations and alpha-synuclein up-regulation in the subtype of neuronal ceroid lipofuscinosis, CLN5 disease. *Scientific Reports*, 9(1), 151. https://doi.org/10.1038/s41598-018-36379-z

Bunk, J., Prieto Huarcaya, S., Drobny, A., Dobert, J. P., Walther, L., Rose-John, S., Arnold, P., & Zunke, F. (2021). Cathepsin D Variants Associated With Neurodegenerative Diseases Show Dysregulated Functionality and Modified α-Synuclein Degradation Properties. *Frontiers in Cell and Developmental Biology*, 9, 581805. https://doi.org/10.3389/fcell.2021.581805

Butz, E. S., Chandrachud, U., Mole, S. E., & Cotman, S. L. (2020). Moving towards a new era of genomics in the neuronal ceroid lipofuscinoses. *Biochimica et Biophysica Acta (BBA) - Molecular Basis of Disease*, 1866(9), 165571. https://doi.org/10.1016/j.bbadis.2019.165571

Dimond, R. L., Burns, R. A., & Jordan, K. B. (1981). Secretion of Lysosomal enzymes in the cellular slime mold, *Dictyostelium discoideum. Journal of Biological Chemistry*, 256(13), 6565–6572. https://doi.org/10.1016/S0021-9258(19)69026-5

Doccini, S., Morani, F., Nesti, C., Pezzini, F., Calza, G., Soliymani, R., Signore, G., Rocchiccioli, S., Kanninen, K. M., Huuskonen, M. T., Baumann, M. H., Simonati, A., Lalowski, M. M., & Santorelli, F. M. (2020). Proteomic and functional analyses in disease models reveal CLN5 protein involvement in mitochondrial dysfunction. *Cell Death Discovery*, 6(1), 1–14. https://doi.org/10.1038/s41420-020-0250-y

Doccini, S., Marchese, M., Morani, F., Gammaldi, N., Mero, S., Pezzini, F., et al. (2022). Lysosomal proteomics links disturbances in lipid homeostasis and sphingolipid metabolism to CLN5 disease. *Cells* 11, 1840. doi:10.3390/ cells11111840

Fey, P., Dodson, R. J., Basu, S., Hartline, E. C., & Chisholm, R. L. (2019). dictyBase and the Dicty Stock Center (version 2.0)—A progress report. *The International Journal of Developmental Biology*, 63(8-9–10), Article 8-9–10. https://doi.org/10.1387/ijdb.190226pf

Fey, P., Kowal, A. S., Gaudet, P., Pilcher, K. E., & Chisholm, R. L. (2007). Protocols for growth and development of *Dictyostelium discoideum. Nature Protocols*, 2(6), 1307–1316. https://doi.org/10.1038/nprot.2007.178

Gaudet, P., Pilcher, K. E., Fey, P., & Chisholm, R. L. (2007). Transformation of *Dictyostelium discoideum* with plasmid DNA. *Nature Protocols*, 2(6), 1317–1324. https://doi.org/10.1038/nprot.2007.179

Haddad, S. E., Khoury, M., Daoud, M., Kantar, R., Harati, H., Mousallem, T., Alzate, O., Meyer, B., & Boustany, R.-M. (2012). CLN5 and CLN8 protein association with

ceramide synthase: Biochemical and proteomic approaches. *ELECTROPHORESIS*, 33(24), 3798–3809. https://doi.org/10.1002/elps.201200472

Hagedorn, M., Neuhaus, E. M., & Soldati, T. (2006). Optimized fixation and immunofluorescence staining methods for *Dictyostelium* cells. *Methods in Molecular Biology* (Clifton, N.J.), 346, 327–338. https://doi.org/10.1385/1-59745-144-4:327

Harding, H. P., Calfon, M., Urano, F., Novoa, I., & Ron, D. (2002). Transcriptional and Translational Control in the Mammalian Unfolded Protein Response. *Annual Review of Cell and Developmental Biology*, 18(Volume 18, 2002), 575–599. https://doi.org/10.1146/annurev.cellbio.18.011402.160624

Haver, H. N., & Scaglione, K. M. (2021). Dictyostelium discoideum as a Model for Investigating Neurodegenerative Diseases. *Frontiers in Cellular Neuroscience*, 15. https://doi.org/10.3389/fncel.2021.759532

Huber, R. J. (2016). Using the social amoeba *Dictyostelium* to study the functions of proteins linked to neuronal ceroid lipofuscinosis. *Journal of Biomedical Science*, 23(1), 83. https://doi.org/10.1186/s12929-016-0301-0

Huber, R. J., Kim, W. D., & Wilson-Smillie, M. L. D. M. (2024). Mechanisms regulating the intracellular trafficking and release of CLN5 and CTSD. *Traffic*, 25(1), e12925. https://doi.org/10.1111/tra.12925

Huber, R. J., & Mathavarajah, S. (2018a). Cln5 is secreted and functions as a glycoside hydrolase in *Dictyostelium. Cellular Signalling*, 42, 236–248. https://doi.org/10.1016/j.cellsig.2017.11.001

Huber, R. J., & Mathavarajah, S. (2018b). Secretion and function of Cln5 during the early stages of *Dictyostelium* development. *Biochimica et Biophysica Acta (BBA) - Molecular Cell Research*, 1865(10), 1437–1450. https://doi.org/10.1016/j.bbamcr.2018.07.017

Huber, R. J., Mathavarajah, S., & Yap, S. Q. (2020). Mfsd8 localizes to endocytic compartments and influences the secretion of Cln5 and cathepsin D in *Dictyostelium. Cellular Signalling*, 70, 109572. https://doi.org/10.1016/j.cellsig.2020.109572

Huber, R. J., Williams, R. S., & Müller-Taubenberger, A. (2022). Editorial: *Dictyostelium*: A Tractable Cell and Developmental Model in Biomedical Research. *Frontiers in Cell and Developmental Biology*, 10. https://doi.org/10.3389/fcell.2022.909619

Hughes, S. M., Hope, K. M., Xu, J. B., Mitchell, N. L., & Palmer, D. N. (2014). Inhibition of storage pathology in prenatal CLN5-deficient sheep neural cultures by lentiviral gene therapy. *Neurobiology of Disease*, 62, 543–550. https://doi.org/10.1016/j.nbd.2013.11.011

Isosomppi, J., Vesa, J., Jalanko, A., & Peltonen, L. (2002). Lysosomal localization of the neuronal ceroid lipofuscinosis CLN5 protein. *Human Molecular Genetics*, 11(8), 885–891. https://doi.org/10.1093/hmg/11.8.885

Iwan, K., Clayton, R., Mills, P., Csanyi, B., Gissen, P., Mole, S. E., Palmer, D. N., Mills, K., & Heywood, W. E. (2021). Urine proteomics analysis of patients with neuronal ceroid lipofuscinoses. *iScience*, 24(2), 102020. https://doi.org/10.1016/j.isci.2020.102020

Jules, F., Sauvageau, E., Dumaresq-Doiron, K., Mazzaferri, J., Haug-Kröper, M., Fluhrer, R., Costantino, S., & Lefrancois, S. (2017). CLN5 is cleaved by members of the SPP/SPPL family to produce a mature soluble protein. *Experimental Cell Research*, 357(1), 40–50. https://doi.org/10.1016/j.yexcr.2017.04.024

Kim, S.-J., Zhang, Z., Hitomi, E., Lee, Y.-C., & Mukherjee, A. B. (2006). Endoplasmic reticulum stress-induced caspase-4 activation mediates apoptosis and neurodegeneration in INCL. *Human Molecular Genetics*, 15(11), 1826–1834. https://doi.org/10.1093/hmg/ddl105

Kim, W. D., & Huber, R. J. (2022). An altered transcriptome underlies cln5-deficiency phenotypes in Dictyostelium discoideum. *Frontiers in Genetics*, 13. https://doi.org/10.3389/fgene.2022.1045738

Leinonen, H., Keksa-Goldsteine, V., Ragauskas, S., Kohlmann, P., Singh, Y., Savchenko, E., Puranen, J., Malm, T., Kalesnykas, G., Koistinaho, J., Tanila, H., & Kanninen, K. M. (2017). Retinal Degeneration In A Mouse Model Of CLN5 Disease Is Associated With Compromised Autophagy. *Scientific Reports*, 7(1), 1597. https://doi.org/10.1038/s41598-017-01716-1

Luebben, A. V., Bender, D., Becker, S., Crowther, L. M., Erven, I., Hofmann, K., Söding, J., Klemp, H., Bellotti, C., Stäuble, A., Qiu, T., Kathayat, R. S., Dickinson, B. C., Gärtner, J., Sheldrick, G. M., Krätzner, R., & Steinfeld, R. (2022). Cln5 represents a new type of cysteine-based S-depalmitoylase linked to neurodegeneration. *Science Advances*, 8(15), eabj8633. https://doi.org/10.1126/sciadv.abj8633

Luo, S., Bi, B., Zhu, B., Tan, L., Zhao, P., Huang, Y., Wu, G., Zhou, A., & He, X. (2020). Functional Analysis of a Novel CLN5 Mutation Identified in a Patient With Neuronal Ceroid Lipofuscinosis. *Frontiers in Genetics*, 11. https://doi.org/10.3389/fgene.2020.536221

Mamo, A., Jules, F., Dumaresq-Doiron, K., Costantino, S., & Lefrancois, S. (2012). The Role of Ceroid Lipofuscinosis Neuronal Protein 5 (CLN5) in Endosomal Sorting. *Molecular and Cellular Biology*, 32(10), 1855–1866. https://doi.org/10.1128/MCB.06726-11

Marotta, D., Tinelli, E., & Mole, S. E. (2017). NCLs and ER: A stressful relationship. *Biochimica et Biophysica Acta*, 1863(6), 1273–1281. https://doi.org/10.1016/j.bbadis.2017.04.003

Mathavarajah, S., Flores, A., & Huber, R. J. (2017). Dictyostelium discoideum: A Model System for Cell and Developmental Biology. *Current Protocols Essential Laboratory Techniques*, 15(1), 14.1.1-14.1.19. https://doi.org/10.1002/cpet.15

McLaren, M. D., Mathavarajah, S., Kim, W. D., Yap, S. Q., & Huber, R. J. (2021). Aberrant Autophagy Impacts Growth and Multicellular Development in a Dictyostelium Knockout Model of CLN5 Disease. *Frontiers in Cell and Developmental Biology*, 9. https://doi.org/10.3389/fcell.2021.657406

Medoh, U. N., Hims, A., Chen, J. Y., Ghoochani, A., Nyame, K., Dong, W., & Abu-Remaileh, M. (2023). The Batten disease gene product CLN5 is the lysosomal bis(monoacylglycero)phosphate synthase. *Science*, 381(6663), 1182–1189. https://doi.org/10.1126/science.adg9288

Minnis, C. J., Thornton, C. D., FitzPatrick, L. M., & McKay, T. R. (2020). Cellular models of Batten disease. *Biochimica et Biophysica Acta (BBA) - Molecular Basis of Disease*, 1866(9), 165559. https://doi.org/10.1016/j.bbadis.2019.165559

Moharir, A., Peck, S. H., Budden, T., & Lee, S. Y. (2013). The Role of N-Glycosylation in Folding, Trafficking, and Functionality of Lysosomal Protein CLN5. *PLOS ONE*, 8(9), e74299. https://doi.org/10.1371/journal.pone.0074299

Néel, E., Chiritoiu-Butnaru, M., Fargues, W., Denus, M., Colladant, M., Filaquier, A., Stewart, S. E., Lehmann, S., Zurzolo, C., Rubinsztein, D. C., Marin, P., Parmentier, M.-L., & Villeneuve, J. (2024). The endolysosomal system in conventional and unconventional protein secretion. *Journal of Cell Biology*, 223(9), e202404152. https://doi.org/10.1083/jcb.202404152

Rossomando, E. F., Maldonado, B., Crean, E. V., & Kollar, E. J. (1978). Protease secretion during onset of development in *Dictyostelium discoideum. Journal of Cell Science*, 30(1), 305–318. https://doi.org/10.1242/jcs.30.1.305

Schröder, M., & Kaufman, R. J. (2005). THE MAMMALIAN UNFOLDED PROTEIN RESPONSE. *Annual Review of Biochemistry*, 74(Volume 74, 2005), 739–789. https://doi.org/10.1146/annurev.biochem.73.011303.074134

Simonati, A., & Williams, R. E. (2022). Neuronal Ceroid Lipofuscinosis: The Multifaceted Approach to the Clinical Issues, an Overview. *Frontiers in Neurology*, 13. https://doi.org/10.3389/fneur.2022.811686

Stajdohar, M., Rosengarten, R. D., Kokosar, J., Jeran, L., Blenkus, D., Shaulsky, G., & Zupan, B. (2017). dictyExpress: A web-based platform for sequence data management

and analytics in Dictyostelium and beyond. *BMC Bioinformatics*, 18(1), 291. https://doi.org/10.1186/s12859-017-1706-9

Tancini, B., Buratta, S., Delo, F., Sagini, K., Chiaradia, E., Pellegrino, R. M., Emiliani, C., & Urbanelli, L. (2020). Lysosomal Exocytosis: The Extracellular Role of an Intracellular Organelle. *Membranes*, 10(12), Article 12. https://doi.org/10.3390/membranes10120406

Teufel, F., Almagro Armenteros, J. J., Johansen, A. R., Gíslason, M. H., Pihl, S. I., Tsirigos, K. D., Winther, O., Brunak, S., von Heijne, G., & Nielsen, H. (2022). SignalP 6.0 predicts all five types of signal peptides using protein language models. *Nature Biotechnology*, 40(7), 1023–1025. https://doi.org/10.1038/s41587-021-01156-3

Yap, S. Q., Kim, W. D., & Huber, R. J. (2022). Mfsd8 Modulates Growth and the Early Stages of Multicellular Development in *Dictyostelium discoideum. Frontiers in Cell and Developmental Biology*, 10. https://doi.org/10.3389/fcell.2022.930235

Yasa, S., Sauvageau, E., Modica, G., & Lefrancois, S. (2021). CLN5 and CLN3 function as a complex to regulate endolysosome function. *Biochemical Journal*, 478(12), 2339–2357. https://doi.org/10.1042/BCJ20210171

4.0. CHAPTER 4

CLN5 DISEASE-CAUSING MUTATIONS IMPACT INTRACELLULAR DEGRADATION AND PROTEIN SECRETION

4.1. PREFACE

This chapter is currently submitted to a primary journal and under peer review. The content between this Chapter and the published may appear different.

TITLE	CLN5 disease-causing mutations impact intracellular degradation and protein secretion
AUTHORS	William D. Kim, Samer A. Owiar, Cassandra H. Pyne, Stéphane Lefrançois, & Robert J. Huber
REFERENCE	**Kim, W.D.**, Owiar, S.A., Pyne, C.H., Lefrançois, S., & Huber, R.J. CLN5 disease-causing mutations impact intracellular degradation and protein secretion. *Submitted.*
CONTRIBUTIONS	WDK and RJH wrote the first original and final draft. WDK and RJH reviewed and edited the manuscript. WDK, SAO, CHP, and RJH collected data. WDK and RJH analyzed all data within this manuscript. All authors read and approved the final draft of the manuscript.
COPYRIGHT	None to report due to being under 'Submission' status in a primary journal.

4.2. ABSTRACT

CLN5 disease is a subtype of Batten disease (neuronal ceroid lipofuscinosis, NCL) that is caused by mutations in the CLN5 gene. While 70 distinct CLN5 disease-causing mutations have been documented, the pathological effects of these mutations are largely unknown. In this study, we used the model eukaryote Dictyostelium discoideum to study the molecular and cellular effects of five conserved mutations in CLN5. *Dictyostelium* is a well-established model for studying the localization and functions of proteins associated with neurological disease. The genome encodes many homologs of proteins linked to neurodegeneration, including CLN5 (Cln5 in *Dictyostelium*), and the *Dictyostelium* life cycle enables a thorough examination of the effects of gene knockout or mutation on conserved unicellular and multicellular processes. Here, we observed that mutations in Cln5 alter the structure of the protein and the cellular distribution of Cln5. Mutated Cln5 also impacts intracellular catabolic mechanisms, including 20S proteasome-mediated protein degradation and lysosomal enzyme-mediated breakdown. Finally, mutations in Cln5 affect vesicles within the endo-lysosome pathway and the release of Cln5 and other lysosomal enzymes, which impacts extracellular enzyme activity. Overall, this study provides insight into the effects of mutations in CLN5 on endo-lysosomal trafficking and lysosomal biology.

4.3. INTRODUCTION

Ceroid lipofuscinosis neuronal 5 (CLN5) is a soluble protein that localizes to organelles within the endomembrane system including the endoplasmic reticulum (ER), Golgi complex, and lysosome (Isosomppi et al., 2002; Moharir et al., 2013; Hughes et al., 2014). CLN5 has also been detected extracellularly in many experimental models (Isosomppi et al., 2002; Hughes et al., 2014; Huber & Mathavarajah, 2018a; Huber et al., 2024). Previous work suggested that CLN5 plays an important role in autophagy, protein degradation mediated by the proteasome, lipid metabolism, and retromer sorting and function (Haddad et al., 2012; Mamo et al., 2012; Cárcel-Trullols et al., 2015; Leinonen et al., 2017; Adams et al., 2019; Yasa et al., 2021; Kim & Huber, 2022). In addition, CLN5 has been proposed to function as either a glycoside hydrolase, depalmitoylase, or bis(monoacylglycerol)phosphate synthase (Huber & Mathavarajah, 2018a; Luebben et al., 2022; Medoh et al., 2023).

Mutations in *CLN5* cause a subtype of neuronal ceroid lipofuscinosis (NCL) called CLN5 disease (Butz et al., 2020; Simonati & Williams, 2022). The NCLs are severe forms of neurodegeneration caused by mutations in *CLN* genes (Butz et al., 2020; Simonati & Williams, 2022). To date, 13 different *CLN* genes have been identified (*CLN1-CLN8, CLN10-CLN14*), and mutations in these genes lead to the pathological accumulation of ceroid lipofuscin - an aggregate composed of lipids and proteins, including subunit C of the mitochondrial ATP synthase - within lysosomes (Palmer et al., 1986; Palmer et al., 1992; Tyynelä et al., 1993; Haltia & Goebel, 2013; Butz et al., 2020; Simonati & Williams, 2022). As of January 2025, the NCL Mutation Database lists 70 distinct NCL-causing mutations in *CLN5* (https://www.ucl.ac.uk/ncl-disease/mutation-and-patient-

database/mutation-and-patient-datasheets-human-ncl-genes/cln5). Previous work that examined a subset of these mutations revealed that they impact the localization of CLN5, its role in autophagy, and its interactions with proteins directly and indirectly such as CLN3 and CLN3 with retromer and RAB7, respectively (Isosomppi et al., 2002; Vesa et al., 2002; Schmiedt et al., 2010; Moharir et al., 2013; Qureshi et al., 2018; Adams et al., 2019; Luo et al., 2020; Yasa et al., 2021). However, the molecular and cellular impacts for most of the CLN5 disease-causing mutations are not known.

Many organismal models have been used to study the NCLs (Huber et al., 2020; Minnis et al., 2020; Nittari et al., 2022). One of these organisms is the social amoeba *Dictyostelium discoideum*, which has a unique life cycle composed of distinct unicellular and multicellular phases (Mathavarajah et al., 2017; Remtulla and Huber, 2023). During the unicellular growth phase, *Dictyostelium* exists as single cells that feed on bacteria or liquid growth medium. When deprived of nutrients, *Dictyostelium* enters its multicellular developmental phase that begins with the chemotactic aggregation of cells to form multicellular slugs. Cells within slugs then terminally differentiate to form fruiting bodies, each of which is composed of a stalk that supports a mass of viable spores. When spores are placed in a nutrient-rich environment, they germinate and release cells, which restarts the life cycle.

Dictyostelium is a powerful biomedical model that contains many homologs of proteins associated with neurological disease, including the NCLs (Haver & Scaglione, 2021; Huber et al., 2022). Intriguingly, *Dictyostelium* is the only early eukaryote that contains a homolog of human CLN5 (Huber, 2016). In *Dictyostelium*, loss of *cln5* impacts cell proliferation, cytokinesis, and autophagy during the growth phase of its life cycle

(McLaren et al., 2021). During the early stages of multicellular development, *cln5*-deficiency affects aggregation, adhesion (cell-cell and cell-substrate), and protein secretion (Huber & Mathavarajah, 2018b; Kim & Huber, 2022). Deletion of *cln5* also impacts the activity of various lysosomal enzymes (Kim & Huber, 2022). Here, we used *Dictyostelium* as a model system to study the molecular and cellular impacts of previously unstudied CLN5 disease-causing mutations. We introduced conserved mutations into *Dictyostelium* Cln5 and then assessed their effects on the endo-lysosomal system in this model organism. Altogether, our study provides new insight in the cellular pathology underlying CLN5 disease.

4.4. METHODS

4.4.1. CELL LINES AND CULTURING

AX3 cells and the pDM323 vector were purchased from the Dicty Stock Center (Fey et al., 2019). *cln5*$^{-}$ cells were generated in previous studies (Huber & Mathavarajah, 2018ab). All cell lines were maintained on SM/2 agar containing *Klebsiella aerogenes* (Fey et al., 2007). Cells used in experiments were cultured in HL5 medium (Formedium, Hunstanton, Norfolk, UK) with ampicillin (100 μg/ml) and streptomycin sulfate (300 μg/ml). Blasticidin S hydrochloride (10 μg/ml) was added to HL5 medium for selection of the *cln5*$^{-}$ cell line. Cell lines containing expression constructs were selected with G418 sulfate (10 μg/ml). All cells used in experiments were harvested from cultures grown in suspension in the mid-log phase of growth ($1–5 \times 10^6$ cells/ml). Low-fluorescence HL5 medium was purchased from Formedium (Hunstanton, Norfolk, UK). KK2 buffer contained 0.7g/L K_2HPO_4 and 2.2g/L KH_2PO_4 and was set at pH 6.5.

4.4.2. ANTIBODIES

Rabbit polyclonal anti-GFP (Cat #: CST-2555s) and mouse monoclonal anti-ubiquitin (Cat #: 3936S) were purchased from New England Biolabs Canada (Whitby, Ontario, Canada). Mouse monoclonal anti-V-H-ATPase subunit C (VatC) (Cat: 224-256-2) (Journet et al., 1999), mouse monoclonal anti-calreticulin (CalR) (Cat #: 252-234-2) (Müller-Taubenberger et al., 2001), mouse monoclonal anti-p80 (Cat #: H161) (Charette & Cosson, 2006; Charette & Cosson, 2008), mouse monoclonal anti-proteasomal subunit 4 (Cat #: 159-183-10) (Schauer et al., 1993), mouse monoclonal anti-proteasomal subunit 5 (Cat #: 171-337) (Schauer et al., 1993), and mouse monoclonal anti-α-actinin (Cat #: 47-18-9) (Schleicher et al., 1988) were purchased from the Developmental Studies Hybridoma Bank (University of Iowa, Iowa City, Iowa, United States). Rabbit polyclonal anti-palmitoyl protein thioesterase 1 (Ppt1) and rabbit polyclonal anti-cathepsin B (CtsB) were generated by GenScript Biotech Corporation (Piscataway, New Jersey, USA). The production and validation of rabbit polyclonal anti-cathepsin D (CtsD) was described in a previous study (Huber et al., 2020). Horse anti-mouse IgG linked to HRP (Cat #: 7076S) and goat anti-rabbit IgG linked to HRP (Cat #: 7074S) were purchased from New England Biolabs (Whitby, Ontario, Canada). Goat anti-rabbit IgG Alexa Fluor 488 (Cat #: A11034) and donkey anti-mouse IgG Alexa Fluor 555 (Cat #: A31570) were purchased from Fisher Scientific Company (Ottawa, Ontario, Canada).

4.4.3. PROTEIN STRUCTURAL ANALYSIS

The amino acid sequences of human CLN5 (NP_006484.2) and *Dictyostelium* Cln5 (XP_643842.1) were obtained from NCBI. Non-mutated and mutated sequences were

inputted into ColabFold (v.1.5.5) to generate predicted protein structures (Mirdita et al., 2022). To identify protein structural changes caused by CLN5 disease-causing mutations, protein structures from mutated human CLN5 and *Dictyostelium* Cln5 were aligned to their non-mutated counterpart using PyMol (The PyMOL Molecular Graphics System, Version 2.5.0 Schrödinger, LLC).

4.4.4. CONSTRUCTION OF EXPRESSION VECTORS

RNA was extracted from AX3 cells using the Monarch Total RNA Miniprep Kit and cDNA was synthesized using the LunaScript RT SuperMix Kit (Cat #: T2010 and Cat #: E3010, respectively; New England Biolabs Canada, Whitby, Ontario, Canada). Combined overlap extension polymerase chain reaction (COE-PCR) was used to generate different amplicons, each one containing a distinct CLN5 disease-causing mutation (Hussian & Chong, 2016). The following mutations were introduced: p.Tyr343* (*Dictyostelium*: p.Tyr298*), p.Tyr209Asp (*Dictyostelium*: p.Tyr178Asp), p.Glu303* (*Dictyostelium*: p.Glu258*), p.Cys77Tyr (*Dictyostelium*: p.Cys39Tyr), and p.Trp158Ser (*Dictyostelium*: p.Trp123Ser). All PCRs were performed using the OneTaq 2X Master Mix with Standard Buffer Kit (Cat #: M0482; New England Biolabs Canada, Whitby, Ontario, Canada) and primers synthesized by Integrated DNA Technologies (Coralville, Iowa, USA) (Table 4). Amplicons were extracted and purified using the Monarch DNA Gel Extraction Kit (Cat #: T1020; New England Biolabs Canada, Whitby, Ontario, Canada). pDM323 vector in *Escherichia coli* (*E. coli*) was extracted using the Monarch Plasmid Miniprep Kit (Cat #: T1010; New England Biolabs Canada, Whitby, Ontario, Canada). Amplicons and the pDM323 vector were digested with *Bgl*II and *Spe*I (Cat #: R0144 and Cat #: R3133, respectively; New England Biolabs Canada, Whitby, Ontario, Canada).

Digested amplicons were purified using the Monarch DNA Gel Extraction Kit and digested pDM323 vector was purified using the Monarch PCR and DNA Cleanup Kit (Cat #: T1030; New England Biolabs Canada, Whitby, Ontario, Canada). Digested amplicons and vector were ligated together using the T4 DNA Ligase Kit (Cat #: M0202; New England Biolabs Canada, Whitby, Ontario, Canada). Ligated vectors were then transformed into competent *E. coli* through heat shock (Cat #: C3040H; New England Biolabs Canada, Whitby, Ontario, Canada). Transformed bacteria were cultured overnight at 30°C and 250RPM. The following day, vectors were extracted from bacteria using the Monarch Plasmid Miniprep Kit and sent to The Hospital for Sick Children (Toronto, Ontario, Canada) for Sanger Sequencing. The manufacturer's instructions were followed for all kits used in the cloning process. Vectors validated by sequencing were then transformed into *Dictyostelium* cells using a Bio-Rad MicroPulser Electroporator (Bio-Rad Laboratories Canada Limited, Mississauga, Ontario, Canada) and a method that is described elsewhere (Gaudet et al., 2007). Transformed cells were selected with G418 sulfate (10 μg/ml).

4.4.5. IMMUNOFLUORESCENCE MICROSCOPY

Methods for immunofluorescence (IF) microscopy were adapted from a previous study (Hagedorn et al., 2006). Briefly, cells (2.0×10^5 total) in mid-log phase of growth were deposited into separate wells of a 12-well dish, with each well containing a sterile coverslip and HL5 medium. Cells were left to adhere to the coverslip for at least 45 minutes at 21°C, after which time the medium was replaced with low-fluorescence HL5. Cells were then left overnight at 21°C. The following day, growth-phase cells and cells starved for 2 hours in KK2 buffer were fixed in -80°C methanol for 45 minutes and then blocked with

IF blocking buffer (0.2% (v/v) triton-X100, 5% (w/v) gelatin, in KK2 buffer) for 30 minutes at 21°C. Coverslips were rinsed in KK2 buffer and then incubated with the following primary antibodies for 1 hour at 21°C (dilutions in parentheses): rabbit polyclonal anti-GFP (1:100), mouse monoclonal anti-p80 (1:50), mouse monoclonal anti-CalR (1:50), and mouse monoclonal anti-VatC (1:50). Following primary antibody incubations, cells were incubated with Alexa Fluoro-conjugated secondary antibodies (1:100) for 1 hour at 21°C. Each coverslip was rinsed in KK2 buffer and then placed onto a drop of Prolong Gold Anti-Fade Reagent with DAPI (Cat #: P36931; Fisher Scientific Company, Ottawa, Ontario, Canada) that was deposited on a microscope slide. Nail polish was used to seal coverslips to the slides. Images of fixed cells were captured using a Nikon Digital Sight Qi2 monochrome camera attached to a Nikon Ts2R-FL inverted microscope (Nikon Canada Incorporated Instruments Division, Mississauga, Ontario, Canada). Images were viewed and analyzed using Fiji/ImageJ (Schindelin et al., 2012). For co-localization analysis, a colocalization-colormap Fiji/imageJ plugin (version 12_11_2019) was used and an unpaired t-test was performed to determine statistical significance ($p<0.05$).

4.4.6. ENZYME ACTIVITY ASSAYS

Cells (1.5×10^6 total) in the mid-log phase of growth were deposited into separate wells of a 6-well dish containing HL5 medium. Cells were left to adhere to the dish for at least 45 minutes at 21°C, after which time the medium was replaced with low-fluorescence HL5 medium. Cells were then left overnight at 21°C. The following day, confluent cells and the corresponding conditioned medium (CM) during growth and conditioned buffer (CB) during 4 hours of starvation were harvested. Cells were lysed with ice-chilled 0.05M

2-(N-Morpholino)ethanesulfonic acid (MES) solution containing 0.1% (w/v) NP-40 (pH 6.5). MES (Cat #: MES503) was purchased from BioShop Canada Incorporated (Burlington, Ontario, Canada). Whole cell (WC) lysates were clarified through a brief centrifugation (10,000RPM for 1 minute) and then used to assess intracellular enzyme activity. CM and CB were clarified through centrifugation (10,000 RPM for 1 minute) and aliquoted into 1.5 ml tubes. A 4-hour starvation timepoint was selected since enzymes are maximally secreted during this stage of the life cycle and it is the peak expression for *cln5* (Dimond et al., 1981; Rossomando et al., 1987; Stajdohar et al., 2017). All enzyme assays used equal protein amounts (WC lysates: 30-75 μg; CM: 1 μg; CB: 0.1 μg) and were performed using protocols described elsewhere (Kim et al., 2024). Protein concentrations were determined using the Qubit Protein Assay Kit (Cat #: Q33211) and a Qubit 2.0 Fluorometer (Fisher Scientific Company, Ottawa, Ontario, Canada). Enzyme activities were measured using a BioTek Synergy HTX microplate reader (BioTek Instruments Incorporated, Winooski, Vermont, United States). Values obtained for the blank solution were subtracted from the sample activity values. Activity values from *cln5*$^{-}$ cells were normalized against AX3. Activity values from cells expressing mutated Cln5 were normalized against the *cln5*$^{-}$ line expressing Cln5-GFP. Statistical significance was determined using a one sample t-test ($p<0.05$ was considered significant). para-nitrophenyl α-D-galactopyranoside substrate (α-galactosidase substrate, Cat #: N0877), ortho-nitrophenyl-β-D-galactopyranoside substrate (β-galactosidase substrate, Cat #: 48712-M), para-nitrophenyl-α-D-mannopyranoside substrate (α-mannosidase substrate, Cat #: N2127), para-nitrophenyl-β-D-glucopyranoside substrate (β-glucosidase substrate, Cat #: 487507), para-nitrophenyl N-acetyl-β-D-glucosaminide substrate (N-

acetylglucosaminidase substrate, Cat #: N9376), cathepsin B (CTSB) fluorogenic substrate (Cat #: 219392), Ala-Ala-Phe-7-amido-4-methylcoumarin substrate (TPP1 substrate, Cat #: A3401), β-glucosidase enzyme from almonds (Cat#: 49290), and pepsin (Cat #: 10108057001) were purchased from Sigma Aldrich Canada (Oakville, Ontario, Canada). 4-methylumbelliferyl 6-thio-palmitate-β-D-glucopyranoside (PPT1 substrate, Cat #: 19524) and Z-FR-AMC substrate (CTSF substrate, Cat #: 80350BP) were purchased from Cedarlane Labs (Burlington, Ontario, Canada). The CTSD Activity Assay Kit (Cat #: 10013-596) was purchased from VWR International (Mississauga, Ontario, Canada). The Proteasome 20S Activity Assay Kit (Cat #: MAK172) was purchased from Sigma Aldrich Canada (Oakville, Ontario, Canada) and used according to a protocol described elsewhere (Kim & Huber, 2022).

4.4.7. SDS-PAGE AND WESTERN BLOTTING

Cells were harvested and lysed with 0.5% (v/v) NP-40 lysis buffer (50mM Tris, 150mM NaCl, pH 8.3) containing a protease inhibitor cocktail tablet (Cat #: A32963; Fisher Scientific Company, Ottawa, Ontario, Canada). Protein concentrations were determined using the Qubit Protein Assay Kit and a Qubit 2.0 Fluorometer. Standard methods of SDS-PAGE and western blotting were used, which included 1-2 hours of membrane incubations with primary and secondary antibodies in 5% (w/v) milk-TBST solution. The following antibody dilutions were used: anti-GFP (1:2000), anti-α-actinin (1:4000), anti-ubiquitin (1:3000), anti-proteasomal subunit 4 (1:1000), anti-proteasomal subunit 5 (1:1000), anti-VatC (1:1000), anti-p80 (1:1000), anti-Ppt1 (1:1000), anti-CtsD (1:1000), anti-CtsB (1:1000), anti-rabbit IgG linked to HRP (1:2000), and anti-mouse IgG linked to HRP

(1:2000). Protein bands were illuminated using the Clarity and Clarity Max enhanced Chemiluminescence substrates and viewed using the ChemiDoc Imagining System (Bio-Rad Laboratories Limited, Mississauga, Ontario, Canada). Protein bands were quantified using Fiji/ImageJ (Schindelin et al., 2012). Intracellular protein amounts were standardized to α-actinin, and normalized amounts from cells expressing mutated Cln5 were compared relative to cells expressing unmutated Cln5. Statistical significance was assessed using the one-sample t-test ($p<0.05$), unless stated otherwise.

4.4.8. CELL PROLIFERATION ASSAY

Methods for assessing cell proliferation were adapted from previous studies (McLaren et al., 2021; Yap et al., 2022). Briefly, cells in the mid-log phase of growth were washed twice with HL5 medium. Cells were resuspended at a final concentration of 2.0 x 10^5 cells/ml in 50ml Erlenmeyer flasks at 21^{o}C and 150RPM. Cell densities were counted every 24 hours. A two-way ANOVA along with a Bonferroni correction was done, and a $p<0.05$ was determined as significant.

4.4.9. AGGREGATION ASSAY

Cells (1.5 x 10^6 total) in the mid-log phase of growth were deposited into 6-well dishes containing HL5 medium. Cells were left to adhere for at least 45 minutes and then replaced with fresh HL5 medium. Cells were left overnight and 21^{o}C. Confluent cells were washed twice with KK2 buffer and then submerged in KK2 buffer for 12 hours. Images were taken every 2 hours with a Nikon Digital Sight Qi2 monochrome camera attached to

a Nikon Ts2R-FL inverted microscope (Nikon Canada Incorporated Instruments Division, Mississauga, Ontario, Canada).

4.5. RESULTS

4.5.1. CLN5 DISEASE-CAUSING MUTATIONS ARE CONSERVED IN *Dictyostelium* Cln5 AND AFFECT THE PREDICTED STRUCTURE OF *Dictyostelium* Cln5 AND HUMAN CLN5

Previous work reported that *Dictyostelium* Cln5 is 30% identical and 47% similar to human CLN5 (Huber and Mathavarajah, 2018a). To identify conserved CLN5 disease-causing mutations in *Dictyostelium* CLN5, we performed another alignment between human CLN5 (UniProt ID: O75503) and *Dictyostelium* Cln5 (UniProt ID: Q553W9) (Figure 21A). Within the 301 amino acid region of similarity, there were 19 amino acids documented as mutation sites in individuals with CLN5 disease conserved in *Dictyostelium* Cln5. While the cellular effects of some CLN5 disease-causing mutations have been previously studied (p.Arg63His, p.Arg63Pro, p.Asn143Ser, p.Arg96Pro, p.Trp175fs*30, p.Gln183*, p.Asp230Asn, p.Tyr293Ter, p.Tyr343*) (Isosomppi et al., 2002; Vesa et al., 2002; Schmiedt et al., 2010; Moharir et al., 2013; Adams et al., 2019; Luo et al., 2020; Yasa et al., 2021), it is still unclear how mutated CLN5 causes NCL. This prompted us to introduce a subset of CLN5 disease-causing mutations into *Dictyostelium* Cln5 and then express the mutated proteins in *cln5*$^{-}$ cells. Through our efforts, we successfully introduced five CLN5 disease-causing mutations into *Dictyostelium* Cln5 including p.Tyr343* (*Dictyostelium*: p.Tyr298*), p.Tyr209Asp (*Dictyostelium*: p.Tyr178Asp), p.Glu303* (*Dictyostelium*: p.Glu258*), p.Cys77Tyr (*Dictyostelium*: p.Cys39Tyr), and p.Trp158Ser (*Dictyostelium*: p.Trp123Ser) (Fig 1A). We then generated five distinct cell lines, each one

expressing one of the five mutated Cln5 proteins (Figure 21B). In addition to these five mutant proteins, we also successfully introduced the following CLN5 disease-causing mutations into *Dictyostelium* Cln5: p.Trp175fs (*Dictyostelium*: p.Trp140fs), p.Gly128Trpfs*10 (*Dictyostelium*: p.Gly91Trpfs*10), and p.Arg258fs* (*Dictyostelium*: p.Arg220fs*). However, while the transformed *cln5*$^{-}$ cells are viable during selection, we were unable to detect the mutant proteins via western blotting, suggesting that the proteins were degraded by cells (Figure 21C).

ColabFold and PyMol were used to examine the predicted structures of the five mutated Cln5 proteins that we were able to express in *cln5*$^{-}$ cells. Based on the structural alignments, the three missense mutations (p.Cys39Tyr, p.Trp123Ser, p.Tyr178Asp) affected the linker regions and alpha helices in Cln5 (Figure 22). The p.Trp123Ser mutation also shifted a few beta sheets within the Cln5 structure. Both nonsense mutations (p.Glu258*, p.Tyr298*), which occur close to the C-terminal end of the protein, impacted the directionality of the linker regions and the alpha helical and beta sheet alignments. Notably, all structural changes that occur in mutated Cln5 were also observed in mutated human CLN5, except for the p.Trp158Ser mutation (p.Trp123Ser in *Dictyostelium*), which did not cause structural changes in beta sheets as it did in *Dictyostelium* Cln5. Overall, these findings highlighted the sequence similarity between *Dictyostelium* Cln5 and human CLN5 and the effects of CLN5 disease-causing mutations on protein structure.

4.5.2. CLN5 DISEASE-CAUSING MUTATIONS ALTER THE CELLULAR DISTRIBUTION OF Cln5

In mammalian cells, CLN5 localizes to the ER, Golgi complex, and lysosome (Isosomppi et al., 2002; Moharir et al., 2013; Hughes et al., 2014). Previous work showed

that mutations in CLN5 cause the protein to be either retained in the ER (p.Tyr343*, p.Asp230Asn, p.Trp175fs*30, p.Arg63Pro, p.Arg63His, p.Glu253*), trapped within the Golgi complex (p.Tyr293Ter), trafficked to non-lysosomal vesicles (p.Tyr343*, p.Trp175fs*30, p.Arg63Pro, p.Glu253*), or prevented from entering lysosomes (p.Tyr293Ter, p.Arg96Pro) (Isosomppi et al., 2002; Schmiedt et al., 2010; Moharir et al., 2013; Luo et al., 2020). Importantly, the mutations we introduced into *Dictyostelium* Cln5, except p.Tyr343*, had not been previously studied. Thus, we investigated the effects of these mutations on the intracellular trafficking of Cln5. Like human CLN5, *Dictyostelium* Cln5 localize to the ER, cytoplasmic punctate, and cell periphery (Huber & Mathavrajah, 2018a). In this study, the Cln5 p.Cys39Tyr mutation increased the localization of Cln5 to the ER during starvation, suggesting that this mutation prevents Cln5 from exiting the ER (Figures 23AB; Table 5). The p.Tyr178Asp and p.Glu258* mutations caused more co-localization of Cln5 with the catalytic subunit of V-H-ATPase (VatC), indicating more Cln5 inside acidic compartments relative to unmutated Cln5. Finally, nonsense mutations in Cln5 (p.Tyr298* and p.Glu258*) increased its co-localization with the secretory lysosome marker-p80, suggesting that these mutations enhance the trafficking of Cln5 towards secretory lysosomes. Collectively, this data highlighted that mutations in Cln5 alter the localization of the protein in *Dictyostelium*.

4.5.3. CLN5 DISEASE-CAUSING MUTATIONS ALTER PROTEASOMAL-MEDIATED PROTEIN DEGRADATION

In mammalian models, mutation or loss of CLN5 dysregulates autophagy (Leinonen et al., 2017; Adams et al., 2019; Basak et al., 2021; Yasa et al., 2021). Similarly, loss of *cln5* in *Dictyostelium* affects basal autophagy, 20S proteasome activity, and the

expression of genes associated with ubiquitination (McLaren et al., 2021; Kim & Huber, 2022). In cells, protein cargo turnover can occur via the ubiquitin-proteasome system and autophagy, pathways that crosstalk with each other that degrade ubiquitin-tagged substrates (Kocaturk & Gozuacik, 2018). Based on these findings, we assessed 20S proteasome activity in cells expressing mutated Cln5. In this study, unless otherwise stated, we performed all our experiments using cells starved for 4 hours in KK2 buffer, since this is the time in the *Dictyostelium* life cycle when *cln5* is maximally expressed and autophagy is induced to provide cells with resources and energy for multicellular development (Otto et al., 2003; Stajdohar et al., 2017). All five mutated Cln5 proteins affected 20S proteasome activity in *cln5*$^{-}$ cells (p.Tyr298* and p.Cys39Tyr, decreased; p.Tyr178Asp, p.Glu258*, and p.Trp123Ser, increased) (Figure 24A; Table 6). An effect was also observed during the growth stage of the life cycle, where each mutant cell line showed elevated 20S proteasome activity (Figure 25). To extend our analysis, we quantified the amounts of free ubiquitin, ubiquitin-positive proteins, and two distinct subunits of the 20S proteasome (subunits 4 and 5). The amounts of ubiquitin-positive proteins were not affected in cells expressing mutated Cln5 (Figures 24BC). However, all mutations elevated the amounts of free ubiquitin and proteasomal subunit 5 in affected cells (Figures 24BC). The Cln5 p.Cys39Tyr and p.Trp123Ser mutants also increased the amounts of proteasomal subunit 4. Altogether, these experiments indicated that CLN5 disease-causing mutations impact ubiquitin homeostasis and protein degradation mediated by the 20S proteasome.

4.5.4. CLN5 DISEASE-CAUSING MUTATIONS AFFECT COMPARTMENTS OF THE ENDO-LYSOSOMAL PATHWAY

The findings described above, coupled with prior work that reported an effect of *cln5* loss on autophagy (McLaren et al., 2021), suggested that mutations in Cln5 affect lysosomal function, which is further supported by work in mammalian models (Seehafer & Pearce, 2006; Leinonen et al., 2017; Adams et al., 2019; Basak et al., 2021; Yasa et al., 2021). When *cln5*$^{-}$ cells expressing mutated Cln5 were stained for VatC (catalytic subunit of the V-ATPase), a marker for acidic vesicles within the endomembrane system (e.g., late endosomes, lysosomes) (Fok et al., 1993; Journet et al., 1999), we observed an increased number of vesicles compared to *cln5*$^{-}$ cells expressing unmutated Cln5 (Figures 26AB; Table 7). However, there were no significant effects on the size of VatC-positive vesicles or the intracellular amount of VatC (Figures 26BC). In *Dictyostelium*, once material within the lysosome is degraded, the lysosome is neutralized and a putative copper transporter called p80 is recruited to regulate its fusion with the plasma membrane and the subsequent release of its contents outside cells (Charette & Cosson, 2006; Charette & Cosson, 2008). In *cln5*$^{-}$ cells expressing mutated Cln5, we observed a significant decrease in the size of p80-positive vesicles, but no effect on their total numbers or the intracellular amount of p80 (Figures 26ABC). Collectively, these results indicated that mutations in Cln5 induce a block in the endo-lysosomal pathway. Acidic vesicles can form in *cln5*$^{-}$ cells expressing mutated Cln5, but they accumulate, which causes the size of p80-positive vesicles to decrease because there is less digested material for the cell to release extracellularly. In addition, since the number of VatC-positive vesicles was increased while the amount of VatC protein was unaltered, these findings suggested that VatC-positive vesicles are less acidic in cells expressing mutated Cln5.

4.5.5. CLN5 DISEASE-CAUSING MUTATIONS AFFECT LYSOSOMAL ENZYME ACTIVITY

In human neurons, loss of *CLN5* affects the intracellular activity of CTSB (Basak et al., 2021). The effects of mutated Cln5 on VatC and p80-positive compartments prompted us to examine the impacts of these mutations on intracellular lysosomal enzyme activity. All mutated forms of Cln5 reduced the activity of α-galactosidase, β-glucosidase, α-mannosidase, and N-acetylglucosiminidase (Figure 27A; Table 8). β-galactosidase activity was also impacted, however, the effect is not consistent across all mutations (p.Tyr298*, p.Glu258*, and p.Cys39Tyr, decreased; p.Trp123Ser, increased; p.Tyr178Asp, no effect). Based on these findings, we then examined the activity of other lysosomal enzymes in *cln5*$^{-}$ cells expressing mutated Cln5 using substrates designed to measure PPT1, TPP1, CTSB, CTSD, and CTSF activity in mammalian cells. TPP1 and CTSB activity were reduced across all mutant cell lines (Figure 27B). PPT1 activity in cells was also impacted by mutations in Cln5, but the effect is not consistent among the different mutants (p.Tyr178Asp and p.Glu258*, decreased; p.Cys39Tyr and p.Trp123Ser, increased; p.Tyr298*, no effect). This was also true when measuring CTSF activity (p.Glu258*, p.Cys39Tyr, and p.Trp123Ser, reduced; p.Try298*, increased; p.Try178Asp, no change). Interestingly, *cln5*$^{-}$ cells expressing mutations in Cln5 did not display affected CTSD activity, despite previous work showing that the *Dictyostelium* homolog of human CTSD (CtsD) interacts with Cln5 and may regulate its trafficking (Huber and Mathavarajah, 2018; Huber et al., 2024). Altogether, these findings showed that mutations in Cln5 affect lysosomal enzyme activity.

4.5.6. CLN5 DISEASE-CAUSING MUTATIONS ALTER THE INTRACELLULAR AMOUNTS OF CATHEPSIN B AND OTHER LYSOSOMAL ENZYMES LINKED TO NCL

As described above, we observed that CLN5 disease-causing mutations perturb the intracellular activity of several lysosomal enzymes. This led us to ask whether the aberrant activity could be explained by alterations in the amounts of enzymes within lysosomes, specifically those linked to NCL (Huber, 2023). To examine this, we performed western blotting using antibodies directed against the *Dictyostelium* homologs of human PPT1 (Ppt1), CTSD (CtsD), and CTSB (CtsB). The amount of Ppt1 was increased in cells expressing Cln5 containing the Cln5 p.Cys39Tyr or p.Trp123Ser mutation, but was unaffected in cells expressing the Cln5 p.Tyr298*, p.Tyr178Asp, or p.Glu258* mutation (Figure 28; Table 9). All mutations, except for p.Glu258*, increased the intracellular amount of CtsB in affected cells. Finally, the amount of CtsD was unaffected in cells affected by mutations in Cln5. Collectively, these findings showed that CLN5 disease-causing mutations affect the amount of some lysosomal proteins within cells.

4.5.7. CLN5 DISEASE-CAUSING MUTATIONS REDUCE THE SECRETION OF Cln5 AND OTHER LYSOSOMAL ENZYMES

Altered protein secretion has emerged as an important feature of NCL pathology (Huber, 2021). In *Dictyostelium*, Cln5 is actively released from cells via its SP and pathways linked to autophagy and lysosomal exocytosis (Huber et al., 2024). Based on these findings, we assessed the effects of CLN5 disease-causing mutations on the release of Cln5 from cells. We observed that all mutations significantly reduce the amount of extracellular Cln5 (Figure 29A; Table 10). In addition to Cln5, we also examined the effects

of CLN5 disease-causing mutations on the extracellular amount of CtsB and CtsD, as well as the activity associated with these enzymes. Notably, CTSD and CTSB have all been detected extracellularly in mammalian models (Poole et al., 1973; Kohan et al., 2005; Best et al., 2021; Iwan et al., 2021), and the *Dictyostelium* homologs CtsD and CtsB also localize outside cells (Bakthavatsalam & Gomer, 2010; Huber, 2017; Huber et al., 2023; Huber et al., 2024). In this study, *Dictyostelium* cells expressing each Cln5 mutation, except the Cln5 p.Trp123Ser mutation, reduced the extracellular amount of CtsB and CtsD (Figures 29BC).

Since mounting evidence supports a role for altered secretion in NCL pathology (Huber, 2021) and the ability to potentially use this information for biomarker development (Gammaldi et al., 2023), we assessed the extracellular activity of secreted lysosomal enzymes. We attempted to measure the activity of all enzymes mentioned in previous sections of this paper, but could only robustly measure α-mannosidase, β-glucosidase, N-acetylglucosaminidase, and CTSB activity in conditioned buffer. We first assessed the extracellular activity of these enzymes in *cln5*$^{-}$ cells. Loss of *cln5* increased the extracellular activity of α-mannosidase, N-acetylglucosaminidase, and CTSB, but did not affect β-glucosidase activity (Figure 30A). Expression of the Cln5 p.Tyr298* mutation in *cln5*$^{-}$ cells increased the extracellular activity of α-mannosidase, decreased the activity of β-glucosidase and N-acetylglucosaminidase, and did not affect CTSB activity (Figure 30B; Table 11). Extracellular β-glucosidase and N-acetylglucosaminidase activity were also decreased in *cln5*$^{-}$ cells expressing the Cln5 p.Tyr178Asp mutation. However, unlike the Cln5 p.Tyr298* mutant, the extracellular activity of CTSB was increased, while α-mannosidase activity was unaffected. As for expressing the Cln5 p.Cys39Tyr mutation in cells, it did not affect the extracellular activity of α-mannosidase, but did increase β-glucosidase activity and reduce the activity of N-acetylglucosaminidase and CTSB. Finally,

cells expressing the Cln5 p.Glu258* mutation increased the extracellular activity of all four enzymes, while expressing the Cln5 p.Tyr178Asp mutation decreased their activity. Overall, these data showed that mutations in Cln5 affect its secretion as well as the amount and activity of extracellular lysosomal enzymes.

4.5.8. CLN5 DISEASE-CAUSING MUTATIONS DO NOT AFFECT CELL PROLIFERATION AND AGGREGATION

At a cellular and biochemical level, our findings highlighted the impact of CLN5 disease-causing mutations on protein degradation, lysosomal biology, and the amount, activity, and secretion of lysosomal enzymes. Based on these findings, we needed to determine the impact of CLN5 disease-causing mutations on the growth and multicellular development of *Dictyostelium*. Intriguingly, we observed that mutations in Cln5 did not affect cell proliferation during growth, or aggregation during the early stages of multicellular development, suggesting that *Dictyostelium* cells can compensate for the cellular defects imparted by mutated Cln5 (Figures 31AB).

4.6. DISCUSSION

This study reveals the cellular impacts of CLN5 disease-causing mutations in the model organism *Dictyostelium* (Figure 32). We showed that CLN5 disease-causing mutations impact the intracellular localization of *Dictyostelium* Cln5 and proteasomal-mediated degradation within affected cells. We also observed that mutated Cln5 dysregulates the amount and activity of various lysosomal enzymes, both intracellularly and extracellularly. Collectively, our data highlight the impact of CLN5 disease-causing

mutations on cellular function and provide insight into the pathological mechanisms underlying CLN5 disease.

We developed five *Dictyostelium* models of CLN5 disease, each one expressing a different mutated version of Cln5. Using ColabFold and PyMol, we showed that CLN5 disease-causing mutations alter the predicted structure of both human CLN5 and *Dictyostelium* Cln5. One outcome of the altered structure could be reduced interactions with target proteins. This is supported by previous work showing that mutations in CLN5 prevent the protein from binding to TPP1 (p.Glu253*, p.Asp230Asn, p.Tyr343*) and weaken other CLN5-protein interactions, such as those between CLN3, RAB7, and retromer (p.Tyr343*) (Vesa et al., 2002; Yasa et al., 2021). In addition, structural alterations in CLN5 could impact its catalytic triad that has been reported to be required for depalmitoylase activity (Cys^{280}-His^{166}-Glu^{183}) (Luebben et al., 2022; Dangat et al., 2024).

As part of this study, we also introduced the p.Trp175fs (*Dictyostelium*: p.Trp140fs), p.Gly128Trpfs*10 (*Dictyostelium*: p.Gly91Trpfs*10), and p.Arg258fs* (*Dictyostelium*: p.Arg220fs*) mutations into *Dictyostelium* Cln5. While transformed cells were viable after selection, we could not detect the mutated proteins via western blotting, suggesting these proteins were degraded by cells. Therefore, these data indicate that some forms of CLN5 disease are caused by expression of mutated CLN5, while others are the result of a complete loss of the CLN5 protein. Moreover, the cellular pathology imparted by the p.Trp175fs, p.Gly128Trpfs*10, and p.Arg258fs* mutations in humans is likely due to the complete absence of the CLN5 protein in patient cells.

Introducing the p.Cys39Tyr mutation into *Dictyostelium* Cln5 (p.Cys77Tyr in human CLN5) inhibited the release of Cln5 from the ER, suggesting that CLN5 disease-causing mutations affect the localization of the protein (Figure 33). In support of our

findings, expression of CLN5 p.Arg63Pro, p.Arg63His, p.Asp230Asn, and p.Tyr343* in *HeLa* cells prevents CLN5 from exiting the ER (Schmiedt et al., 2010; Moharir et al., 2013). In addition, expressing the CLN5 p.Tyr343* mutant in baby hamster kidney (BHK) cells causes the mutated protein to mis-localize to the Golgi complex, as well as non-lysosomal vesicles (Isosomppi et al., 2002; Schmiedt et al., 2010). Here, we show that the p.Tyr298* and p.Glu258* mutations (p.Tyr343* and p.Glu303* in human CLN5, respectively) increase the localization of Cln5 to secretory lysosomes. The different effects of the Cln5 p.Tyr298* mutation and the equivalent mutation in mammalian cells (p.Tyr343*) on Cln5/CLN5 localization (mis-localization to secretory lysosomes in *Dictyostelium*, mis-localization to the Golgi complex and non-lysosomal vesicles in BHK cells, and ER retention in *HeLa* cells) could be attributed to differences in the experimental models. We also revealed increased localization of the Cln5 p.Tyr178Asp and p.Glu258* mutants (p.Tyr209Asp and p.Glu303* in human CLN5, respectively) to acidic compartments. Similarly, the CLN5 p.Asp230Asn and p.Asn271Ser mutations trap a large portion of the intracellular CLN5 pool in the ER, but low amounts of the mutated protein can still be directed to endo-lysosomal vesicles in *HeLa* cells, supporting our findings of altered Cln5 localization within the endo-lysosomal system (Schmiedt et al., 2010). Finally, while CLN5 can still traffic to lysosomes in *HeLa* cells expressing the CLN5 p.Asn143Ser mutant, the protein is functionally defective (Moharir et al., 2013). Overall, these data highlight that CLN5 disease-causing mutations alter the localization of Cln5 in *Dictyostelium* and CLN5 in human cells.

The 20S proteasome is a barrel structure that consists of multiple subunits (Kunjappu & Hochstrasser, 2014; Abi Habib et al., 2022). Previous work in *Dictyostelium* showed that *cln5*-deficiency affects the expression of genes encoding proteasomal proteins,

increases the amount of one proteasomal subunit, and impairs 20S proteasome activity (Kim & Huber, 2022). In this study, we found that mutations in Cln5 also affect 20S proteasomal activity and increase the amounts of two proteasomal subunits. In support of these observations, altered 20S proteasome activity and subunit amounts have been reported in Parkinson's disease and aging (St. P. McNaught et al., 2003; Husom et al., 2004). For the Cln5 p.Cys39Tyr mutant (p.Cys77Tyr in human CLN5), the amounts of both subunits are increased along with reduced 20S proteasomal activity, indicating poor formation of the proteasome. The 20S proteasome can facilitate the degradation of ubiquitinated and non-ubiquitinated biological substrates (Ben-Nissan & Sharon, 2014; Kumar Deshmukh et al., 2019; Sahu et al., 2021). While previous work showed that *cln5*-deficiency elevates the amounts of ubiquitin-positive proteins and affects the expression of genes encoding proteins in the ubiquitination pathway (McLaren et al., 2021; Kim & Huber, 2022), here, we observed that mutated Cln5 elevated the amount of free ubiquitin but did not alter the amounts of ubiquitin-positive proteins. This finding suggests that cells expressing mutated Cln5 increase ubiquitin production to clear out accumulated proteins within the cell. Altogether, these data indicate that CLN5 disease-causing mutations affect protein degradation mediated by the ubiquitin-proteasome system.

The ubiquitin-proteasome system cross-talks with autophagy, and both systems degrade ubiquitin-tagged substrates (Kocaturk & Gozuacik, 2018). The autophagic degradation of cargo relies on lysosomal function. Here, we showed that cells expressing mutated Cln5 contained an increased number of acidic compartments, suggesting the formation of more late endosomes/lysosomes, possibly due to poor retrograde transport of endosomes to the Golgi complex. CLN5 interacts with CLN3, and expression of the CLN5 p.Tyr343* mutant in *HeLa* cells weakens the interaction between CLN3-Rab7A and CLN3-

retromer, which plays an important role in endosome-trans-Golgi complex lysosomal sorting receptor retrieval (Vesa et al., 2002; Yasa et al., 2021). Since mutated Cln5 did not affect the amount of VatC but did increase the number of acidic compartments, this suggests reduced acidity in these acidic vesicles as there are less VatC protein per acidic vesicle. This feature of reduced acidity has also been documented in lysosomes within ovine neurons lacking CLN5 and CLN5-deficient human induced pluripotent stem cell (IPSC)-derived neurons (Best et al., 2017; Basak et al., 2021). In addition, the intracellular trafficking of lysosomes is dysregulated in human IPSC-derived neurons lacking CLN5 (Basak et al., 2021). Loss of *CLN5* in *HeLa* cells and IPSC-derived neurons impairs the trafficking of lysosomes towards the cell periphery, which has been suggested to reduce autophagosome-lysosome fusion (Basak et al., 2021; Yasa et al., 2021). However, another effect could be reduced lysosomal exocytosis, which would impact the secretion of lysosomal enzymes (Buratta et al.,2020; Tacini et al., 2020). In line with these previous studies, mutations in Cln5 reduce the size of secretory vesicles in *Dictyostelium*. Altogether, these findings indicate that CLN5 disease-causing mutations affect the size and movement of endo-lysosomal compartments.

We showed that expressing mutated Cln5 in *Dictyostelium* reduced the activity of glycoside hydrolases and some proteases, including TPP1 and CTSB. Human CLN5 interacts with TPP1 in COS-1 cells and *Dictyostelium* Cln5 interacts with alpha-mannosidase, beta-glucosidase, N-acetylglucosiminidase, and the TPP1-like protein, Tpp1B (Vesa et al., 2002; Lyly et al., 2009; Huber & Mathavarajah, 2018a). Since our data show that CLN5 disease-causing mutations alter the predicted structures of CLN5/Cln5, we can infer that this altered structure affects the ability of CLN5/Cln5 to interact with other lysosomal enzymes. Although an interaction between CLN5/Cln5 and CTSB/CtsB

has not been reported, loss of *CLN5*/*cln5* reduces CTSB/CtsB activity in humans and *Dictyostelium* (Basak et al., 2021; Kim & Huber, 2022). In addition, loss of *cln5* in *Dictyostelium* elevates *ctsB* expression, suggesting that cells upregulate the production of CtsB to compensate for impaired intracellular activity (Kim & Huber, 2022). In addition to CtsB, loss of *cln5* affects the expression and activity of various lysosomal enzymes (Kim & Huber, 2022). When all data are considered, we observed cases where both the amount and activity of a particular enzyme were increased due to mutations in Cln5 (e.g., PPT1), indicating that more of that enzyme was present within the cell. We also observed decreased activity with unaltered or increased protein amounts (e.g., CTSB), suggesting that the enzyme is not being fully matured, which would impair its activity. Finally, we observed situations where both the amount and activity of an enzyme are unaffected by mutated Cln5 (e.g., CTSD) Like CTSB, an interaction between human CLN5 and CTSD has not been reported. However, loss of *CLN5* in *HeLa* cells reduces the processing of CTSD to its mature form (Yasa et al., 2021; Huber, 2023). A previous study suggested that impaired retromer-mediated trafficking reduces CTSD processing in *HeLa* cells expressing the CLN5 p.Asn271Ser mutant (Qureshi et al., 2018). However, based on our work, an alternative explanation is that reduced acidity within lysosomes prevents the maturation of CTSD, which is also supported by previous studies that reported less acidic lysosomes/acidic compartments in other CLN5 disease models (Best et al., 2017; Basak et al., 2021). Although we observed no changes in CtsD protein amounts in our CLN5 disease models, *Dictyostelium* CtsD is processed differently compared to mammalian cells, where a single CtsD band is observed via western blotting in *Dictyostelium* (Journet et al., 1999). Thus, we cannot be certain whether there were differential amounts of the precursor and mature forms of CtsD in our CLN5 disease models. Altogether, these findings highlight

that CLN5 disease-causing mutations have different biochemical effects on cells, specifically with regards to lysosomal protein amounts and activity.

In *Dictyostelium*, Cln5 secretion is regulated by its SP, autophagy genes, and proteins associated with lysosomal exocytosis (Huber et al., 2024). In addition to breaking down intracellular material, the autophagy pathway can also secrete material through an unconventional mechanism known as secretory autophagy (Néel et al., 2024). Our work shows that mutations in Cln5 reduce its secretion (Fig. 13). In addition, we observed that the Cln5 p.Cys39Tyr mutation (p.Cys77Tyr in human CLN5) reduces the release of Cln5 from the ER. In *HeLa* cells, the CLN5 p.Asp230Asn and p.Asn271Ser mutations reduce or completely inhibit the release of CLN5 from the ER, leading to the mutated protein not being secreted or secreted in reduced amounts, respectively (Moharir et al., 2013; Qureshi et al., 2018). Also, the CLN5 Tyr343* mutation reduces the intracellular and extracellular amounts of CLN5, which has been speculated to be due to intracellular degradation of the protein (Moharir et al., 2013). Finally, the CLN5 p.Asn143Ser mutation increases the release of CLN5 from cells but does allow some of the intracellular pool of protein to localize to lysosomes (Moharir et al., 2013). Collectively, these data show that CLN5 disease-causing mutations impact the secretion of CLN5/Cln5.

Mutations in Cln5 affect not only its secretion but also the extracellular amount and activity of other lysosomal enzymes, which could provide valuable insight for biomarker identification for the NCLs (Gammaldi et al., 2023; Marchese et al., 2025). All mutations we studied, except the Cln5 p.Trp123Ser mutation (p.Trp158Ser in human CLN5), elevated CtsB secretion, which aligned with the reduced intracellular activity of CTSB in cells that expressed mutated Cln5. In cells that expressed the Cln5 p.Tyr298* mutant (p.Tyr343* in human CLN5), intracellular amounts of CtsB were elevated, but extracellular activity was

unaffected. Combined, these findings suggest that CtsB was not fully matured in cells that expressed the Cln5 p.Tyr298* mutant (p.Tyr343* in human CLN5), however, the increased extracellular amounts of CtsB compensate for the lack of extracellular activity. Furthermore, cells that expressed the Cln5 p.Tyr178Asp and p.Glu258* mutants (p.Tyr209Asp and p.Glu303* in human CLN5, respectively) displayed elevated extracellular CTSB activity, supporting the increased extracellular amount of CtsB. Finally, the Cln5 p.Trp123Ser and p.Cys39Tyr mutants (p.Trp158Ser and p.Cys77Tyr in human CLN5, respectively) increased the intracellular amount of CtsB and reduced extracellular CTSB activity. Altogether, these observations provide strong evidence that CLN5/Cln5 regulates the amount and activity of CTSB/CtsB and further support the involvement of CTSB in NCL pathology (Huber, 2023).

Interestingly, the CLN5 disease-causing mutations we studied did not affect cell proliferation in *Dictyostelium* despite our previous work showing that loss of *cln5* decreases cell proliferation (McLaren et al., 2021). Since there was no effect of mutant Cln5 or Cln5 lacking its SP on cell proliferation, these findings suggest that secreted Cln5 is not required for growth. In zebrafish, loss of *cln5* reduces axonal growth, while in mouse neural progenitor cells, *CLN5*-deficiency increases cell proliferation (Savchenko et al., 2017; Marchese et al., 2025). These different effects caused by *CLN5*-deficiency could be attributed to differences between experimental models. Mutated Cln5 also did not affect *Dictyostelium* aggregation. In contrast, Cln5 lacking its SP delayed aggregation, which was also observed for *cln5*$^{-}$ cells (McLaren et al., 2021). These findings align with the expression profile of *cln5* and its peak expression after 4 hours of multicellular development (Stajdohar et al., 2017; McLaren et al., 2021; Huber et al., 2024). The SP-lacking Cln5 protein localizes to the cell periphery and cytoplasm, but is not detected

extracellularly (Huber et al., 2024). Therefore, the low amount of mutated Cln5 that is present in the extracellular space may be enough for *Dictyostelium* cells to aggregate normally, while the complete lack of extracellular Cln5 leads to aggregation defects. Alternatively, *Dictyostelium* may have compensatory pathways to account for impairments of mutated Cln5 inside the cell and/or the reduced extracellular amounts of Cln5.

Overall, this study provides new insight into the range of cellular effects imparted by mutations in *CLN5*. Our data indicate that mutations in CLN5/Cln5 disease perturb lysosomal biology, with each mutation affecting the cell in different ways. Moreover, they provide insight for future work that examines the molecular and cellular pathology underlying CLN5 disease.

4.7. ACKNOWLEDGMENTS

The authors would like to thank Drs. Michael E. Donaldson and Barry J. Saville for their intellectual support in this study.

4.8. FIGURES AND TABLES

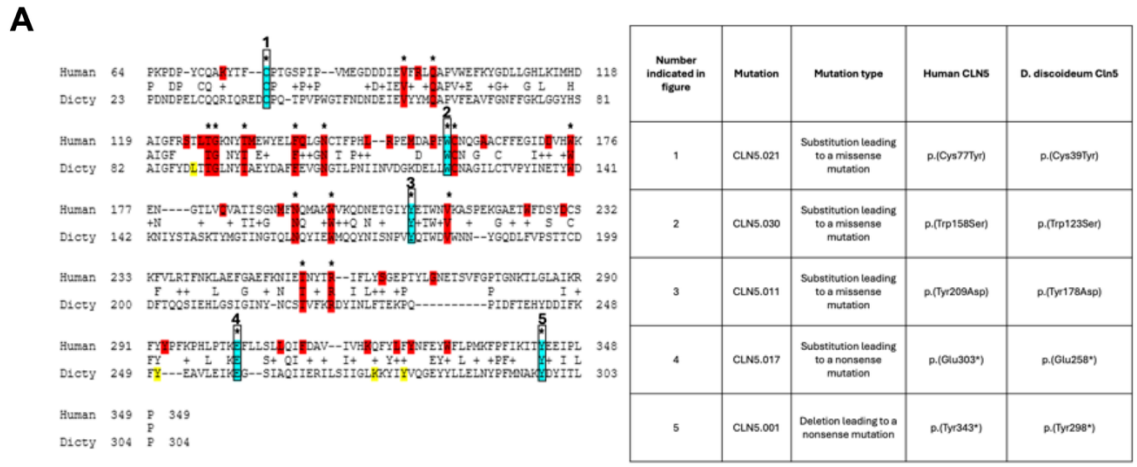

Number indicated in figure	Mutation	Mutation type	Human CLN5	D. discoideum Cln5
1	CLN5.021	Substitution leading to a missense mutation	p.(Cys77Tyr)	p.(Cys39Tyr)
2	CLN5.030	Substitution leading to a missense mutation	p.(Trp158Ser)	p.(Trp123Ser)
3	CLN5.011	Substitution leading to a missense mutation	p.(Tyr209Asp)	p.(Tyr178Asp)
4	CLN5.017	Substitution leading to a nonsense mutation	p.(Glu303*)	p.(Glu258*)
5	CLN5.001	Deletion leading to a nonsense mutation	p.(Tyr343*)	p.(Tyr298*)

Figure 21. CLN5 disease-causing mutations are conserved in *Dictyostelium* Cln5 and generated in *Dictyostelium* Cln5. (A) A BLAST alignment between *Dictyostelium* Cln5

(322aa, UniProt ID: Q553W9) and human CLN5 (358aa, UniProt ID: O75503). Red highlight indicates CLN5 disease-causing mutations reported in the NCL database. Blue highlight indicates CLN5 disease-causing mutations that are explored in this study. A table is provided with information for each mutation studied in this report. Yellow highlight indicates nucleotides within the *Dictyostelium* Cln5 amino acid sequence that would have aligned with mutations in CLN5 disease but were shifted by a single amino acid position. **(B)** A western blot image displaying equal protein amounts between non-mutated and mutated forms of Cln5 in *cln5*$^{-}$ cells. **(C)** Viable transformed *cln5*$^{-}$ cells that did not express the CLN5 disease-causing mutation. Three CLN5 disease-causing mutations that were introduced in *cln5*$^{-}$ cells include p.Trp140fs (human: p.Trp175fs), p.Gly91Trpfs*10 (human: p.Gly128Trpfs*10), and p.Arg220fs* (human: p.Arg258fs*).

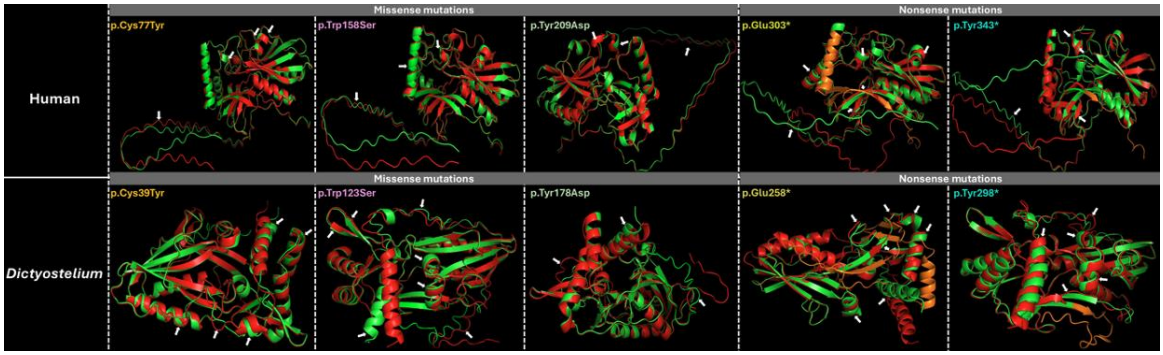

Figure 22. CLN5 disease-causing mutations affect the predicted structure of *Dictyostelium* Cln5 and human CLN5. Protein structural alignment analyses of predicted non-mutated and various mutant forms of *Dictyostelium* Cln5 and human CLN5 are done via Pymol. Mutated human CLN5 and *Dictyostelium* Cln5 are superimposed onto the non-mutated human CLN5 and *Dictyostelium* Cln5 counterpart respectively. White arrows indicate structural changes caused by CLN5 disease-causing mutations.

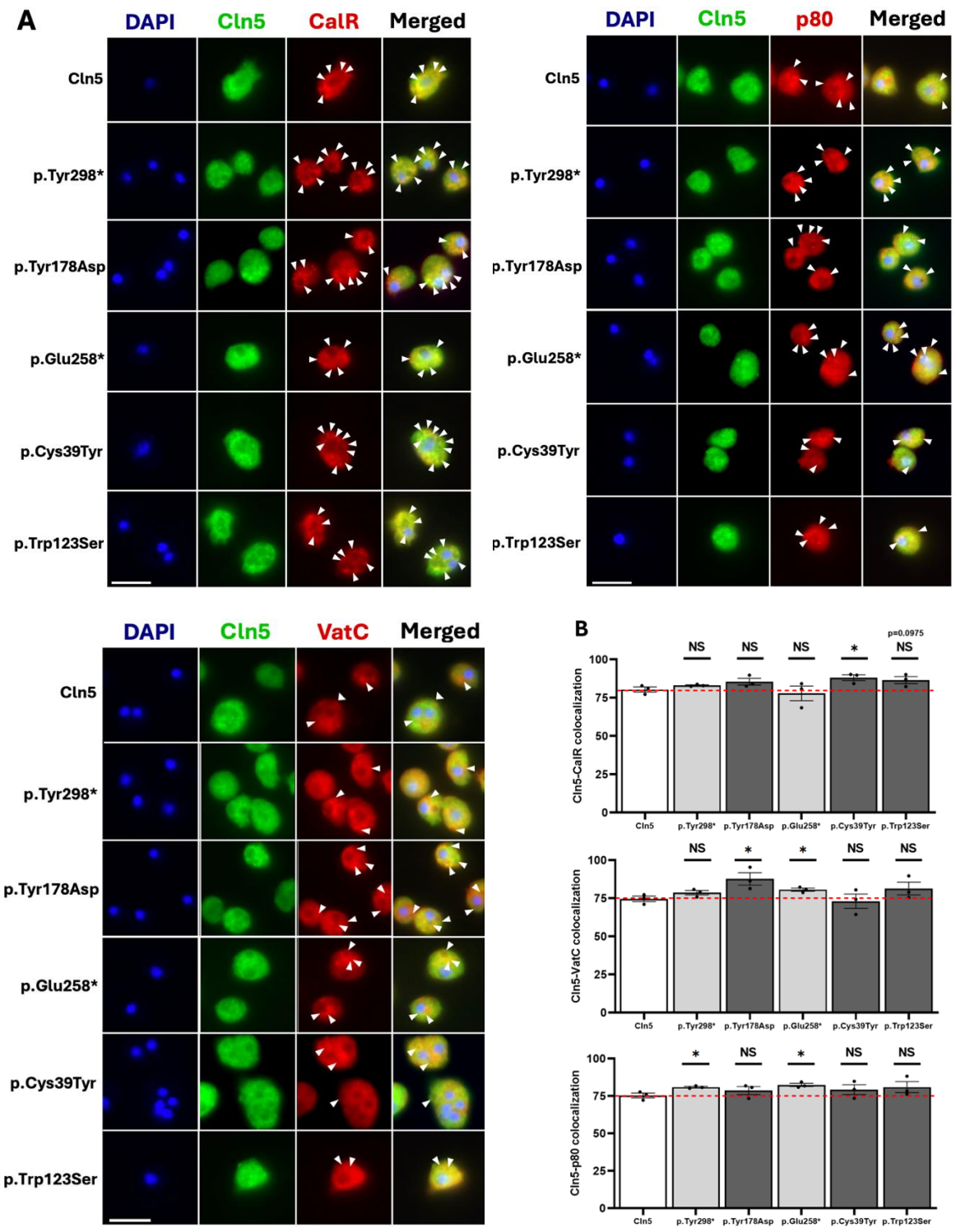

Figure 23. CLN5 disease-causing mutations alter the cellular distribution of Cln5. (A) Fixed cells were incubated with anti-GFP, anti-CalR, anti-VatC, and anti-p80 to target the Cln5-GFP fusion protein, the ER, acidic compartments, and secretory lysosomes respectively. Scale bar: 20μm. **(B)** Co-localization analysis of mutated Cln5 to these selected intracellular compartments was done via an ImageJ plugin and a one-way ANOVA

was done with a $p<0.05$ to determine significance. Data is presented as mean %co-localization (%Cln5) ± SEM (n=3). NS=not significant, *$p<0.05$.

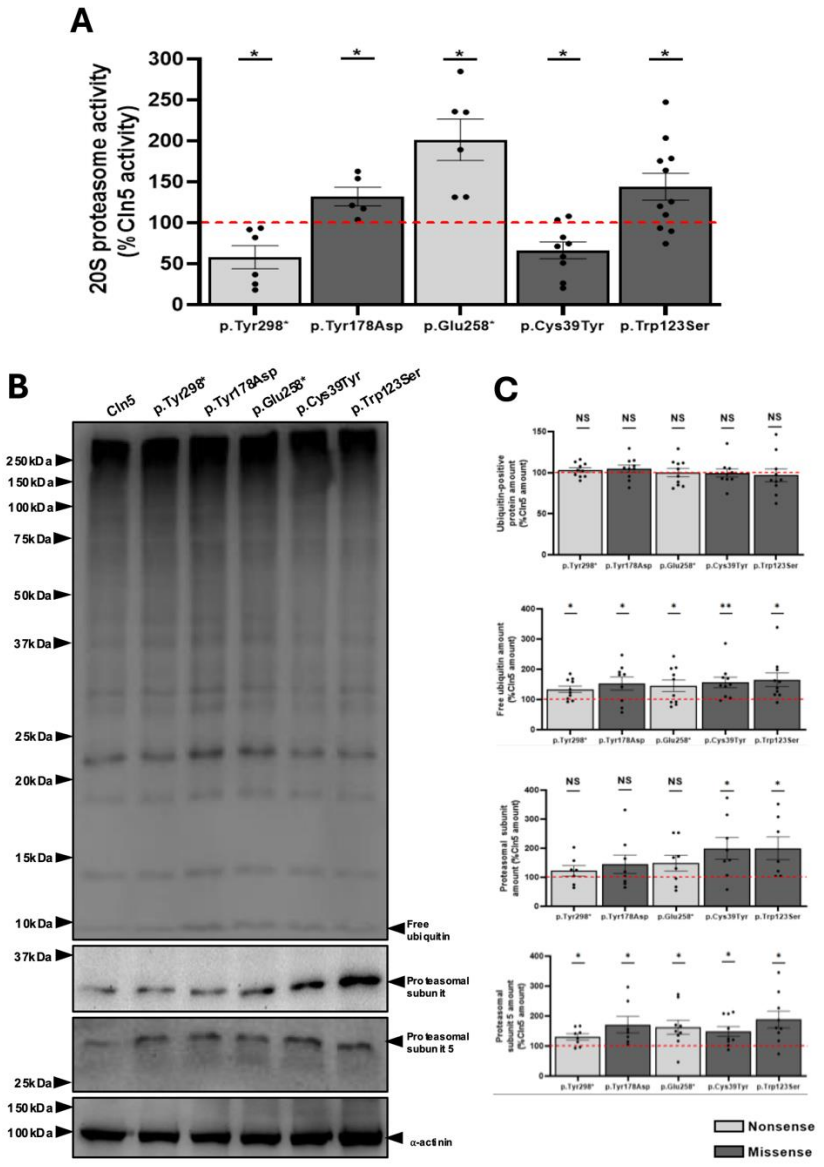

Figure 24. CLN5 disease-causing mutations alter proteasomal-mediated protein degradation and the intracellular amounts of proteasomal subunits and ubiquitin. (A) 20S proteasome activity is assessed in *cln5*$^{-}$ cells expressing either non-mutated or mutated Cln5. 20S proteasome activity data is presented as mean protein activity ± SEM (n≥5). **(B)** Western blot and **(C)** quantification of intracellular amounts of free ubiquitin, ubiquitin-positive proteins, proteasomal subunit 4, proteasomal subunit 5, and α-actinin in *cln5*$^{-}$ cells expressing either non-mutated or mutated Cln5. Western blot quantification data is presented as mean protein amount (%Cln5) ± SEM (n≥7). NS=not significant, *$p<0.05$.

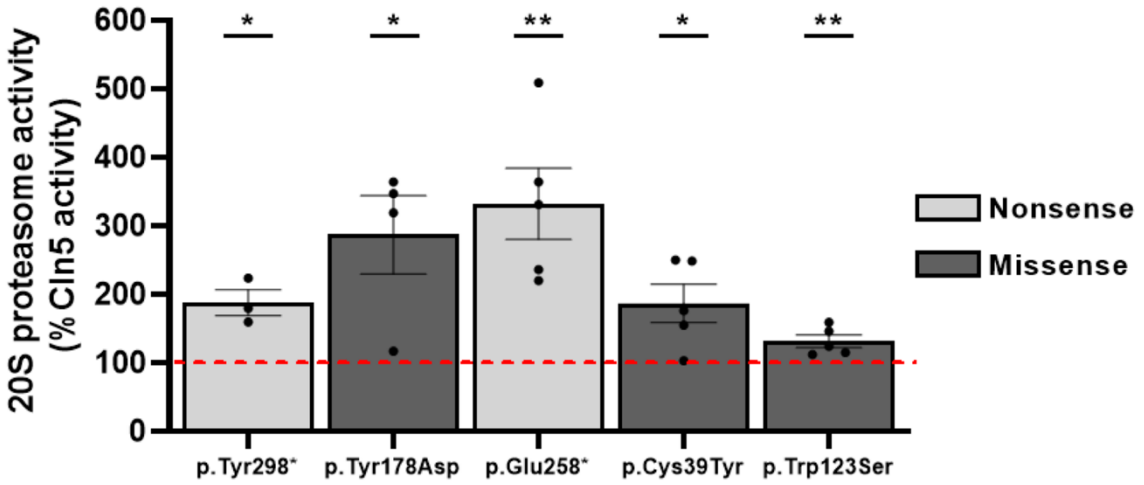

Figure 25. Mutations in CLN5 disease cause elevated 20S proteasome activity during growth. Intracellular 20S proteasome activity was measured in growth-phased *cln5*$^{-}$ cells expressing either non-mutated Cln5 or mutated Cln5. Activity values obtained from Cln5 mutants were compared to non-mutated Cln5 values. A one-sample t-test with a $p<0.05$ was determined to be significant. Data is presented as mean 20S proteasome activity (%Cln5) ± SEM (n≥3). *p<0.05, **p<0.01.

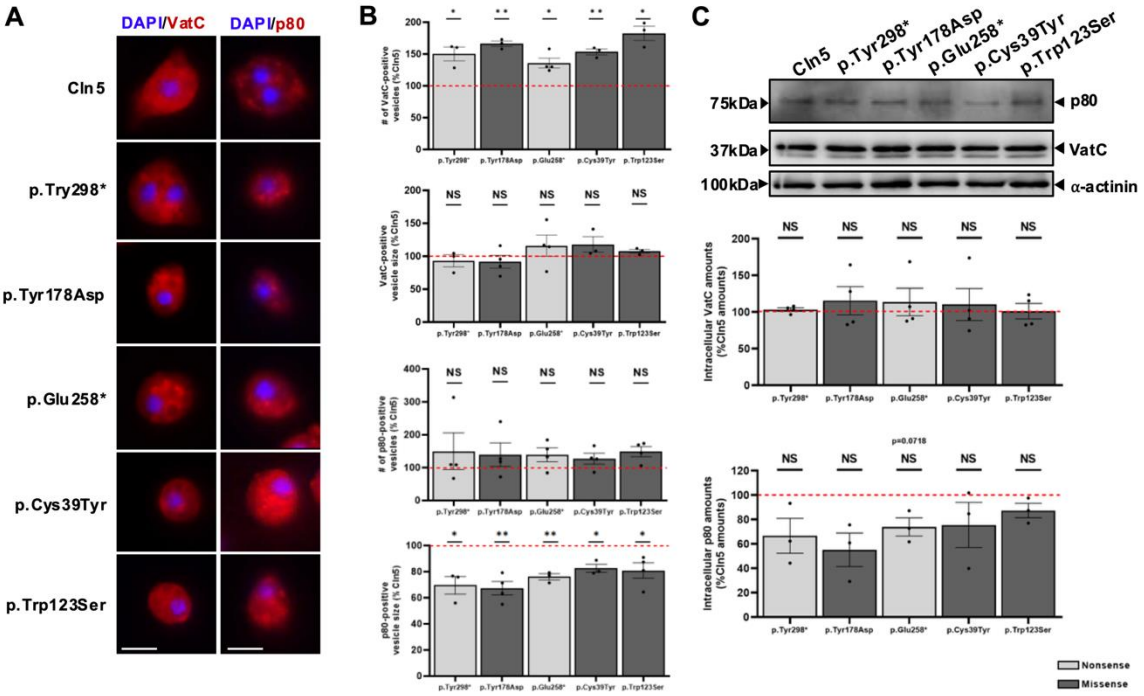

Figure 26. CLN5 disease-causing mutations affect compartments of the endo-lysosomal system. (A) Representative images of cells stained for p80, VatC, and DAPI. Scale bar: 20µm. **(B)** VatC- and p80-positive vesicle size were measured with Fiji/ImageJ. The number of vesicles stained by VatC and p80 was counted per cell. The number of vesicles and vesicular size obtained from Cln5 mutants were compared relative to cells expressing non-mutated Cln5. Data is presented as either mean # of vesicles or mean vesicle size (%Cln5) ± SEM (n≥3). **(C)** Western blot membrane probed for p80, VatC, and α-

actinin amounts within whole cell lysates of *cln5*$^{-}$ cells expressing either non-mutated or mutated forms of Cln5. Western blot data is presented as mean protein amount (%Cln5) ± SEM (n≥3). NS=not significant, *p<0.05, **p<0.01.

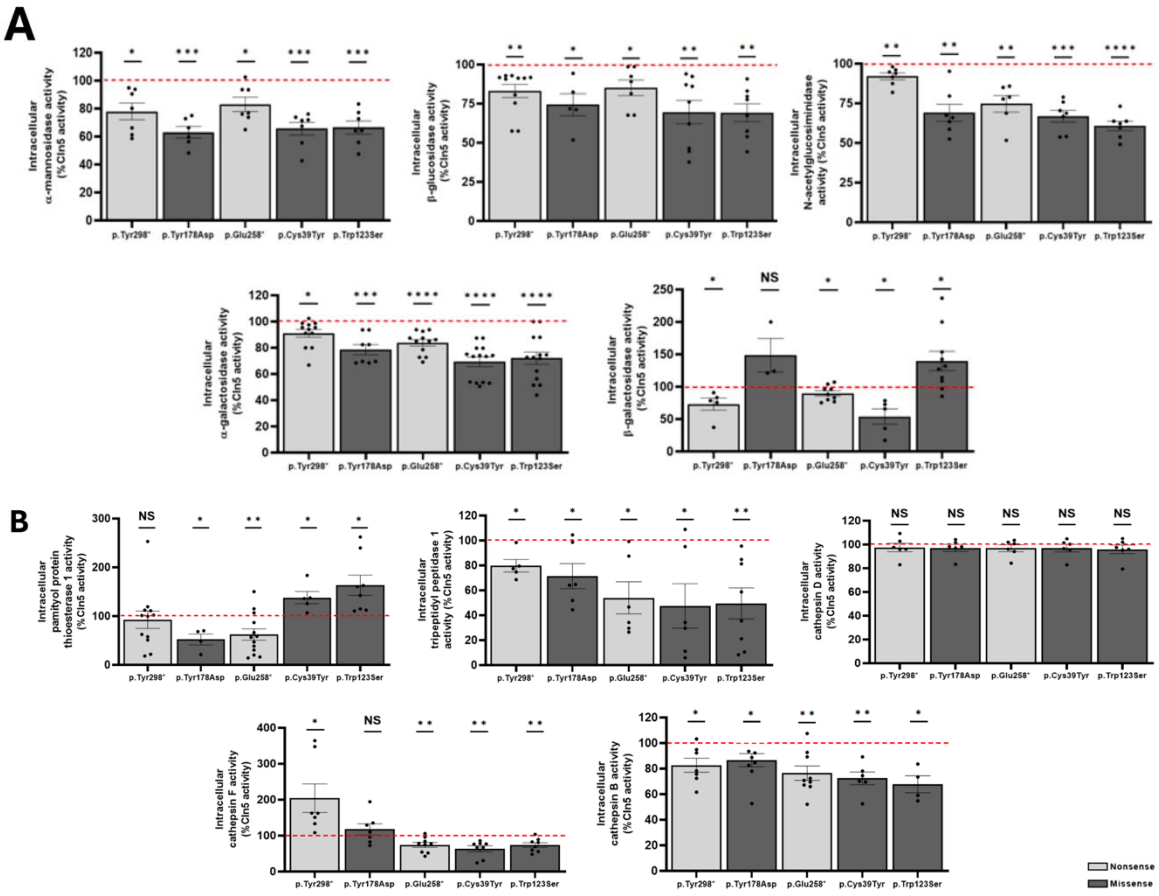

Figure 27. CLN5 disease-causing mutations affect intracellular lysosomal enzyme activity. (A) Intracellular α-mannosidase, β-glucosidase, N-acetylglucosiminidase, α-galactosidase, and β-galactosidase activity, as well as **(B)** palmitoyl protein thioesterase 1, tripeptidyl peptidase 1, cathepsin B, cathepsin D, and cathepsin F activity were assessed in *cln5*$^{-}$ cells expressing non-mutated or mutated Cln5. Activity values from cells expressing mutated Cln5 is compared to *cln5*$^{-}$ cells expressing non-mutated Cln5. Data is presented as mean activity (%Cln5) ± SEM (n≥3). NS=not significant, *p<0.05, **p<0.01, ***p<0.001, ****p<0.0001.

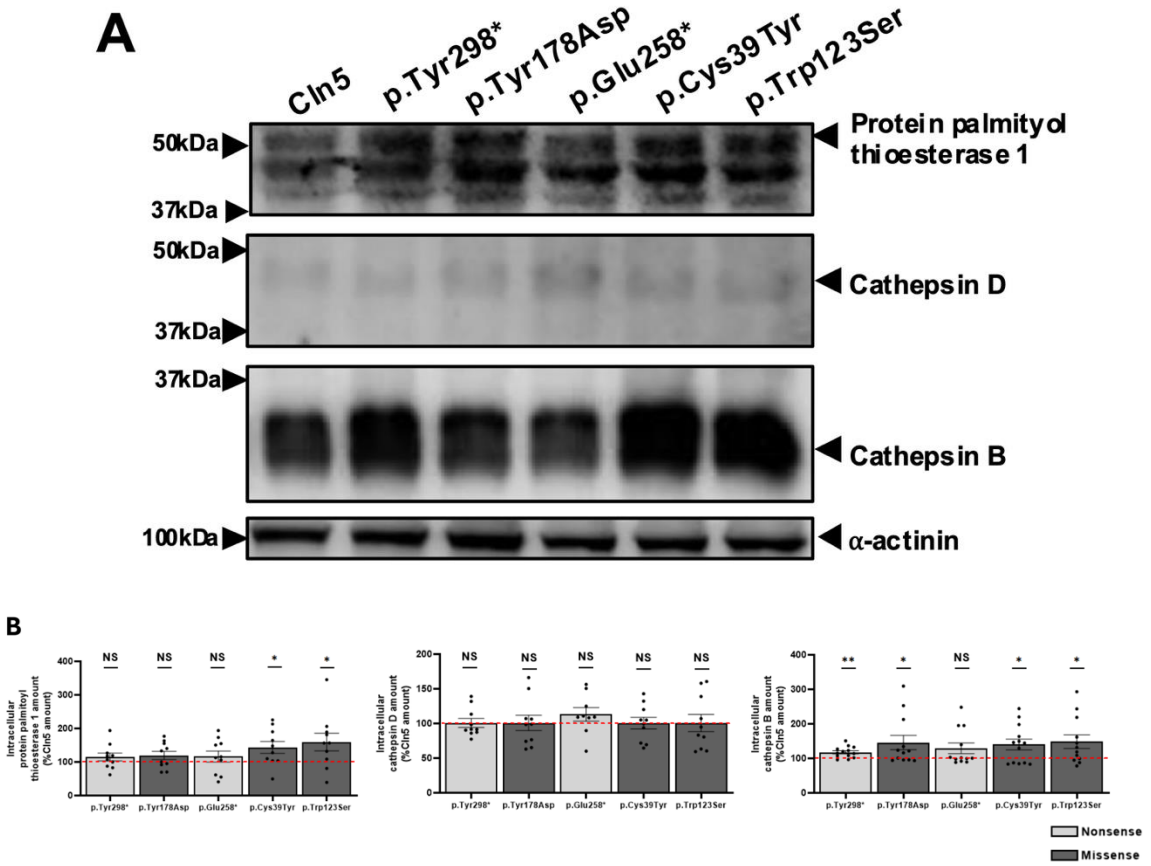

Figure 28. CLN5 disease-causing mutations alter the intracellular amount of cathepsin B and other lysosomal enzymes linked to NCL. (A) Western blot image containing whole cell lysates from *cln5*$^{-}$ cells expressing non-mutated Cln5 or Cln5 that encodes a CLN5 disease-causing mutation. Blots were probed for palmitoyl protein thioesterase 1, tripeptidyl peptidase 1A, tripeptidyl peptidase 1B, cathepsin B, cathepsin D, and α-actinin. **(B)** Protein bands were quantified via Fiji/ImageJ. Data is presented as mean protein amount (%Cln5) ± SEM (n≥9). NS=not significant, *p<0.05, **p<0.01.

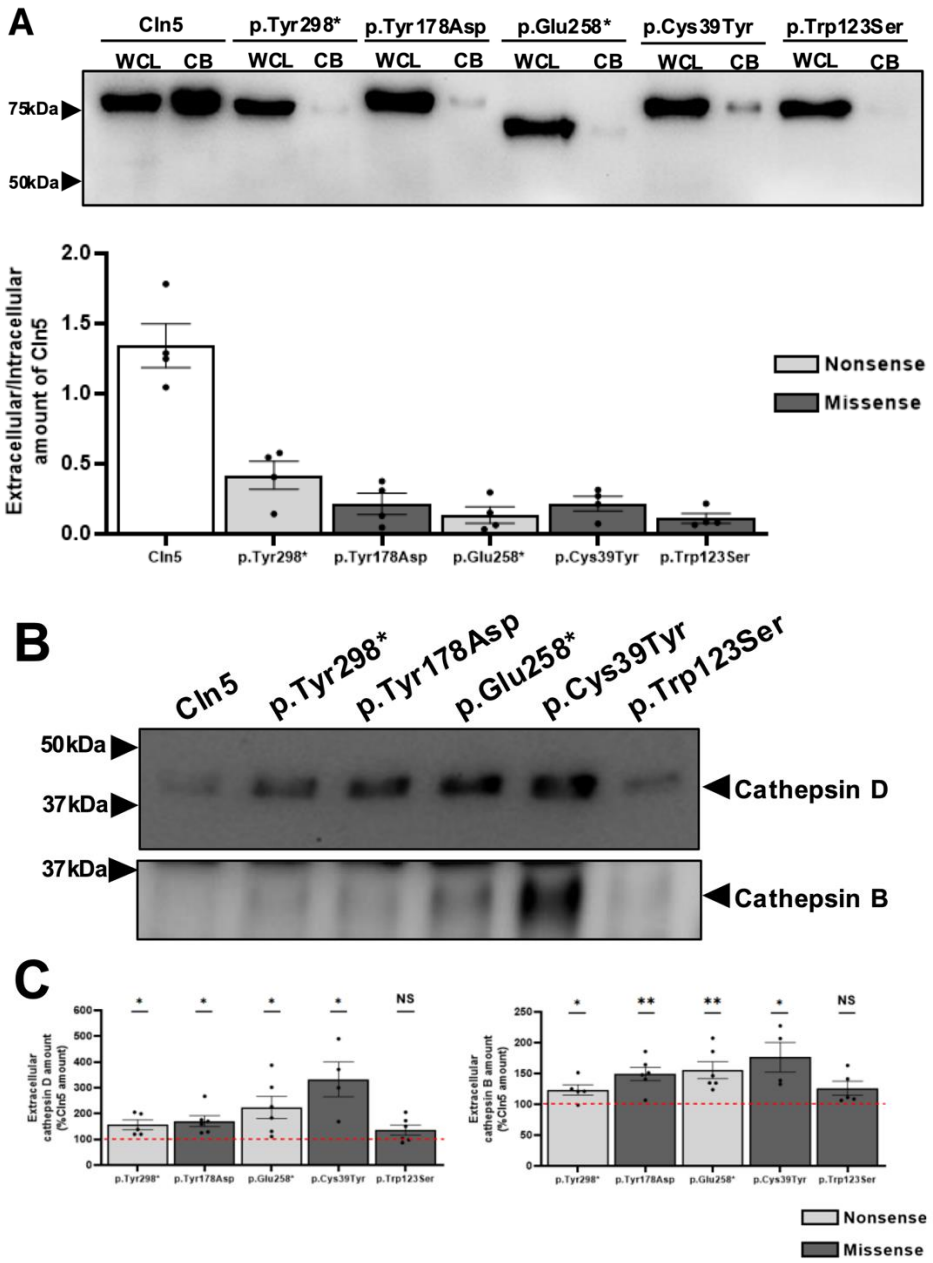

Figure 29. CLN5 disease-causing mutations reduce the secretion of Cln5 and other lysosomal enzymes. (A) Intracellular and extracellular Cln5 amounts were measured via western blotting from cells expressing non-mutated Cln5 or mutated Cln5. Data is presented as mean extracellular/intracellular Cln5 amount ± SEM (n=4). **(B)** Western blot image of extracellular amounts of tripeptidyl peptidase 1A, tripeptidyl peptidase 1B, cathepsin B, and cathepsin D in *cln5*$^{-}$ cells expressing non-mutated Cln5 or mutated Cln5. **(C)** Extracellular protein amounts were measured and is presented as mean protein amount (%Cln5) ± SEM (n≥3). NS=not significant, *p<0.05, **p<0.01. ***p<0.001, ****p<0.0001.

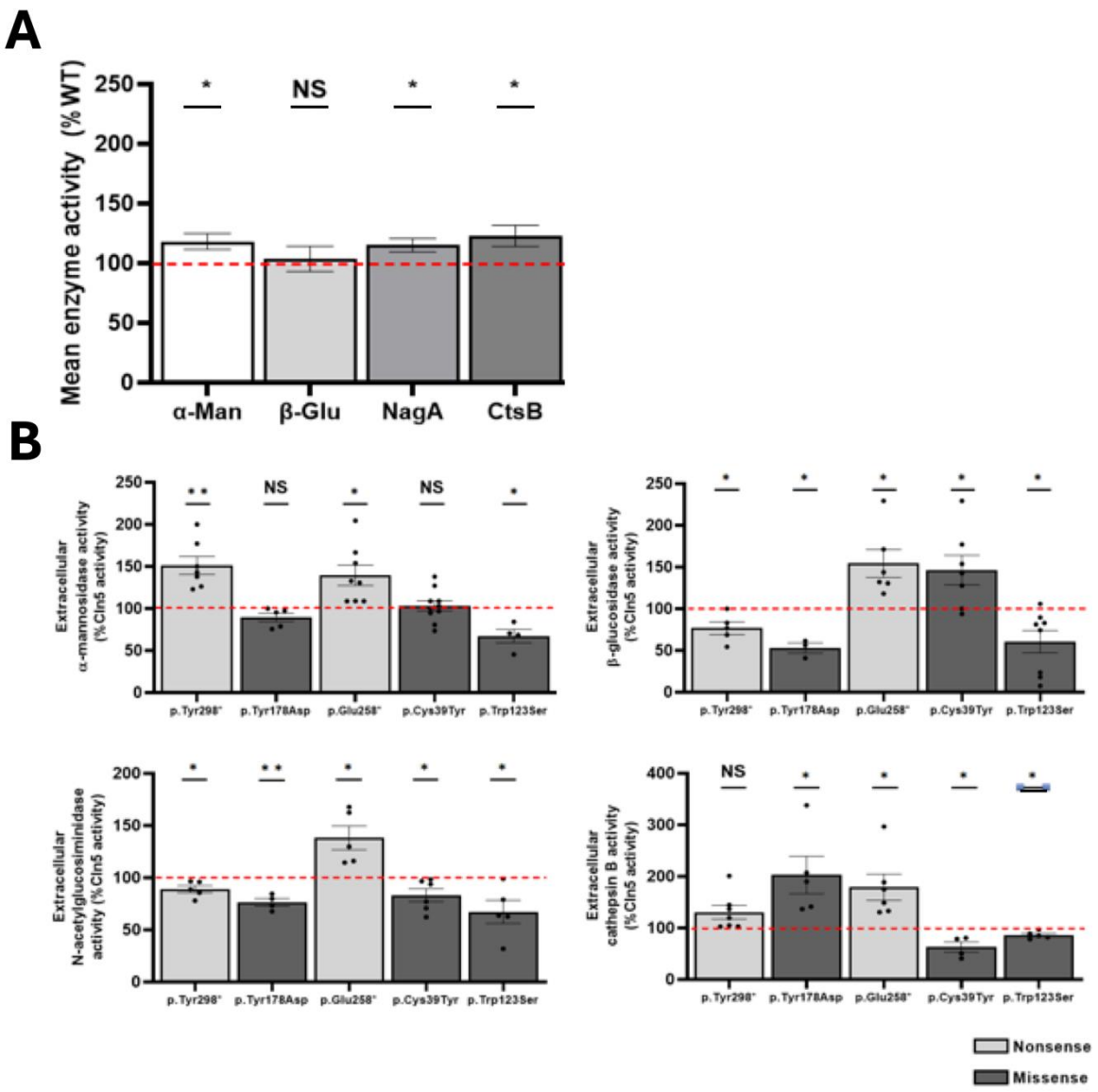

Figure 30. Loss of *cln5* and CLN5 disease-causing mutations alter the activity of cathepsin B and other lysosomal enzymes linked to NCL. Extracellular activity of α-mannosidase, β-glucosidase, N-acetylglucosiminidase, and cathepsin B were assessed in **(A)** AX3 and *cln5*$^{-}$ cells (n≥4), as well as in **(B)** *cln5*$^{-}$ cells expressing non-mutated Cln5 or Cln5 containing CLN5 disease-causing mutations (n≥3). Data is presented as either mean enzyme activity (%WT) or mean enzyme activity (%Cln5) ± SEM. NS=not significant, *p<0.05, **p<0.01.

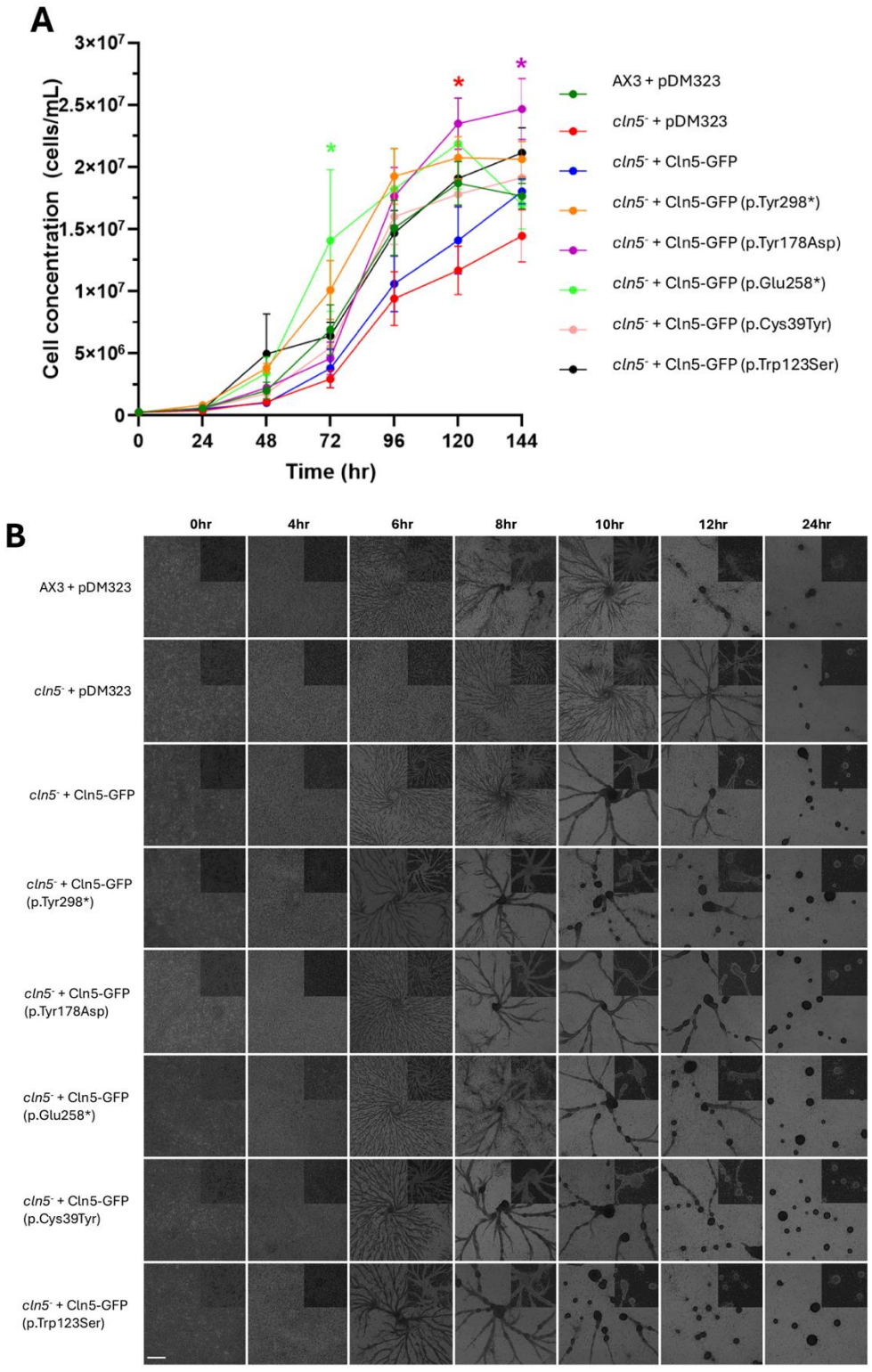

Figure 31. CLN5 disease-causing mutations do not affect cell proliferation or aggregation. (A) *cln5*$^{-}$ cells expressing non-mutated Cln5 or mutated Cln5 were set in HL5 within flasks (2 x 10^5 cells/ml), and the cell density was counted every 24 hours (n≥4). **(B)** Confluent cells on Petri dishes were submerged in KK2 buffer for 12 hours and images

were taken at time intervals within the figure. Images are representative of 6 independent experiments. Scale bar: 500µm.

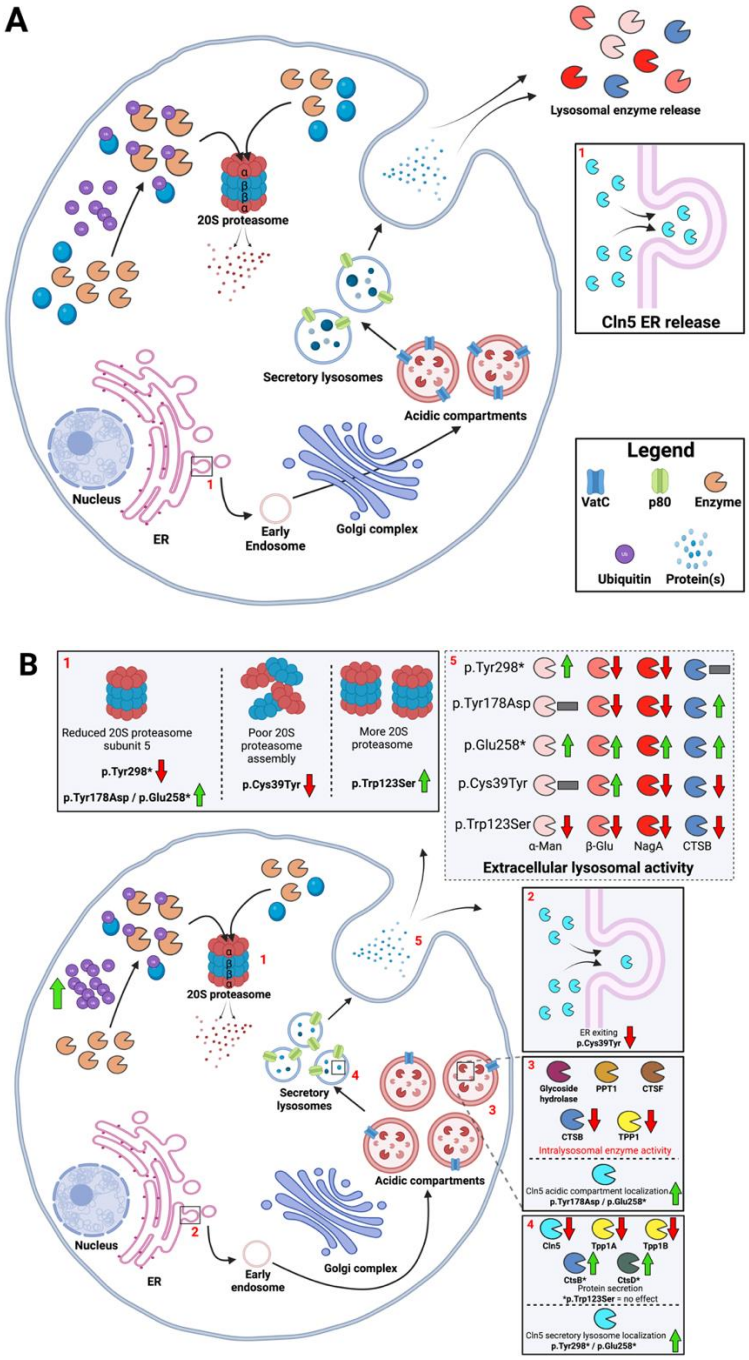

Figure 32. Visual models displaying processes affected by mutations in CLN5 disease. (A) In cells expressing unaffected Cln5, intracellular trafficking of Cln5 (starting from ER and eventually released into the extracellular space), specifically the intracellular acidic compartments (e.g., late endosomes, lysosomes) and secretory lysosomes remain unaffected. Furthermore, degradation of intracellular cargo via lysosomal enzymes and the 20S proteasome function optimally. **(B)** In cells with mutated Cln5, ***(1)*** the activity of the

20S proteasome is affected either by decreased amounts of the proteasomal subunit 5 (p.Tyr298*, p.Tyr178Asp, p.Glu258*), poor 20S proteasome assembly (p.Cys39Tyr), or more 20S proteasomes leading to increased activity (p.Trp123Ser). Mutations in CLN5 disease also perturb ubiquitin biology, leading to more free ubiquitin. ***(2)*** ER release of Cln5 is reduced in cells expressing the Cln5 p.Tyr298* mutation, while ***(3)*** the Cln5 p.Tyr178Asp and p.Glu258* mutations lead to more Cln5 in acidic compartment localization. Mutations in Cln5 disease also affect the activity of many enzymes within the lysosome including various glycoside hydrolases (α-mannosidase, β-glucosidase, N-acetylglucosiminidase, α-galactosidase, and β-galactosidase), protein palmitoyl thioesterase 1 (PPT1), cathepsin B (CTSB), cathepsin F (CTSF), and tripeptidyl peptidase 1 (TPP1). In addition to affecting lysosomal enzyme activity, CLN5 disease-causing mutations increase the number of acidic compartments but does not affect VatC amounts, indicating less VatC per acidic vesicle ultimately leading to less acidic vesicles. As more acidic vesicles are formed in cells expressing CLN5 disease-causing mutations, it is suggested that some early endosomes bypass the Golgi complex to prematurely form late endosomes. ***(4)*** CLN5 disease-causing mutations affect the size of secretory lysosomes, and the Cln5 p.Tyr298* and p.Glu258* nonsense mutations increase the localization of Cln5 to secretory lysosomes. Mutations in CLN5 disease reduce the secretion of Cln5 and, alter the secretion of various lysosomal enzymes including tripeptidyl peptidase 1A/B (Tpp1A/B), cathepsin B (CtsB), and cathepsin D (CtsD), except for the p.Trp123Ser not affecting the secretion of the cathepsins. ***(5)*** Finally, each mutation of CLN5 disease differentially affects the activity of lysosomal enzymes in the extracellular space. Figure was generated with BioRender.

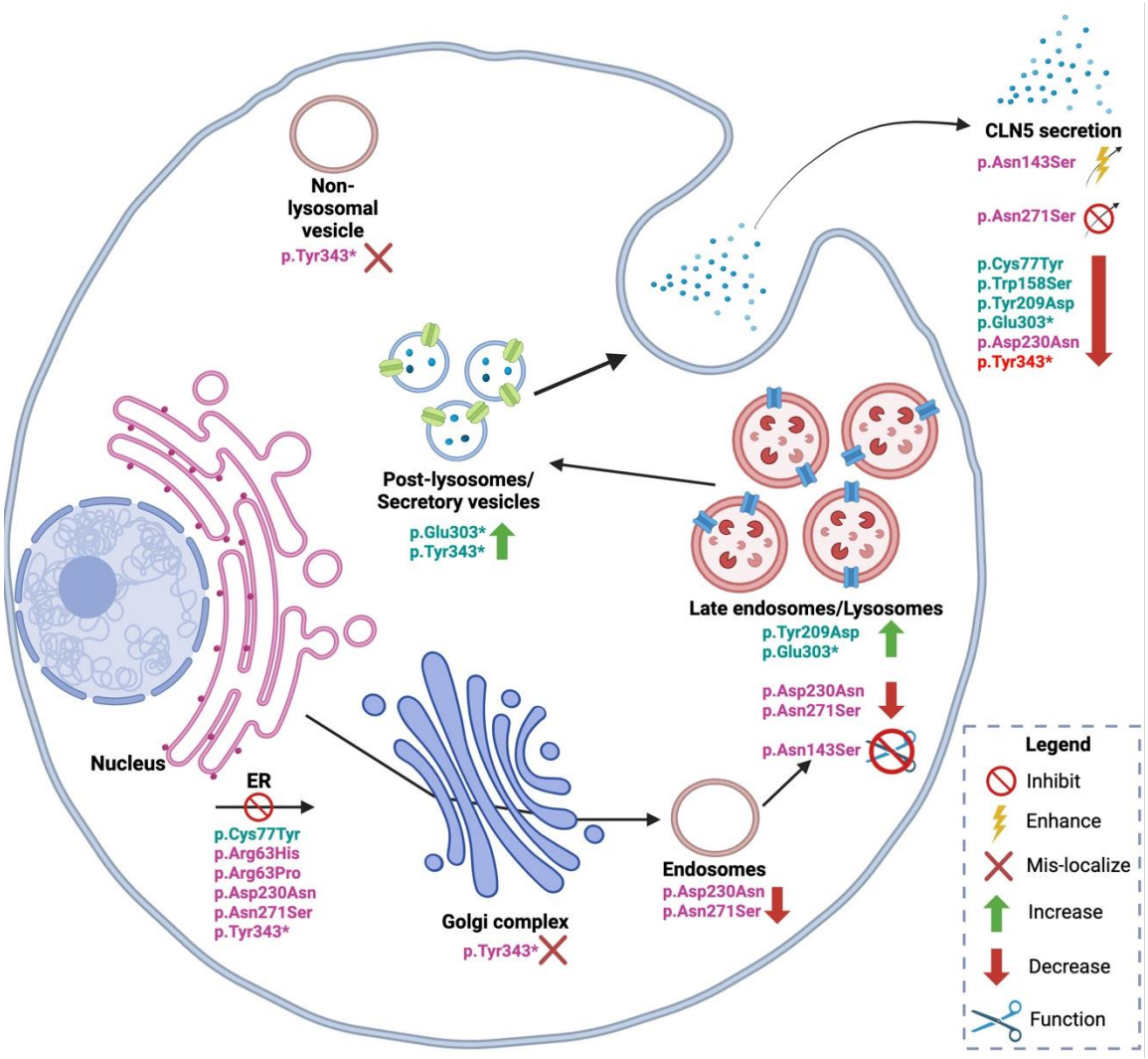

Figure 33. A visual model summarizing all literature on the effects of CLN5 disease-causing mutations on its protein trafficking. CLN5 disease-causing mutations are indicated underneath each organelle and during protein secretion. CLN5 disease-causing mutations studied in *Dictyostelium* in this report are in cyan text. Studies assessing the effect of mutations in CLN5 disease using mammalian cell models are indicated in purple text. Red text indicates CLN5 disease-causing mutations that have been studied in both *Dictyostelium* and mammalian cell models. A legend is provided to identify the symbols within the text. Figure was generated with BioRender.

Table 4. CLN5 disease-causing mutations created in this study. Primer sequences used in COE-PCR are provided. Information of the age of onset of each CLN5 disease subtype was acquired from the NCL mutation database.

cln5 Mutation	Age of onset (Human)	Type of mutation	cDNA gene mutation (*Dictyostelium*)	Protein nomenclature (*Dictyostelium*)	Reaction	Reason	Primer name	Primer sequence (5' - 3')
cln5.001	Late infantile	Deletion > Nonsense	Deletion of 'TA' nucleotides at position 892-893	p.Tyr298*	Reaction 1	Introducing the conserved *CLN5.001* mutation into *Dictyostelium cln5* to encode the p.Tyr298* mutation into *Dictyostelium* Cln5	Cln5GFP_Cterm-F	CCA AGA AAA ATG AAA AGG ACG AT
							D-cln5.001GFP-PS-R	ACT AGT TTT TGC ATT CAT AAA TGG ATA
cln5.011	Juvenile	Missense	Change from 'T' to 'G' nucleotide at nucleotide position 532	p.Tyr178Asp	Reaction 1	Creating the first half of the *Dictyostelium cln5* gene containing the conserved *CLN5.011* mutation. Reactions 1 and 2 are mixed in a single solution to form the single gene product (via COE-PCR) to encode the p.Tyr178Asp mutation	Cln5GFP_Cterm-F	CCA AGA AAA ATG AAA AGG ACG AT
							D-Cln5GFP-cln5.011-R	GTC CCA TGT TTG GTC TAC TGG ATT TG
					Reaction 2	Creating the second half of the *Dictyostelium cln5* gene containing the conserved *CLN5.011* mutation. Reactions 1 and 2 are mixed in a single solution to form the single gene product (via COE-PCR) to encode the p.Tyr178Asp mutation	D-Cln5GFP-cln5.011-F	CAA ATC CAG TAG ACC AAA CAT GGG AC
							Cln5GFP_Cterm-R	CCA ACT AGT ATT GAG ATG AAT AAA ATT
cln5.017	Juvenile-late infantile	Substitution > nonsense	'G' to 'T' nucleotide at nucleotide	p.Glu258*	Reaction 1	Introducing the conserved *CLN5.017* mutation into *Dictyostelium cln5* to encode the p.Glu258* mutation into *Dictyostelium* Cln5	Cln5GFP_Cterm-F	CCA AGA AAA ATG AAA AGG ACG AT
							D-cln5.017GFP-PS-R	ACT AGT TTT AAT TTC TAA TAC AGC TTC
cln5.021	Teenage	Missense	Change from 'G' to 'A' nucleotide at nucleotide position 116	p.Cys39Tyr	Reaction 1	Creating the first half of the *Dictyostelium cln5* gene containing the conserved *CLN5.021* mutation. Reactions 1 and 2 are mixed in a single solution to form the single gene product (via COE-PCR) to encode the p.Cys39Tyr mutation	Cln5GFP_Cterm-F	CCA AGA AAA ATG AAA AGG ACG AT
							D-Cln5GFP-cln5.021-R	GGT GTT TGT GGA TAA TCC TCT CTT TGA
					Reaction 2	Creating the second half of the *Dictyostelium cln5* gene containing the conserved *CLN5.021* mutation. Reactions 1 and 2 are mixed in a single solution to form the single gene product (via COE-PCR) to encode the p.Cys39Tyr mutation	D-Cln5GFP-cln5.021-F	GAA TTC AAA GAG AGG ATT ATC CAC AA
							Cln5GFP_Cterm-R	CCA ACT AGT ATT GAG ATG AAT AAA ATT
cln5.030	Juvenile	Missense	Change from 'G' to 'C' nucleotide at nucleotide position 368	p.Trp123Ser	Reaction 1	Creating the first half of the *Dictyostelium cln5* gene containing the conserved *CLN5.030* mutation. Reactions 1 and 2 are mixed in a single solution to form the single gene product (via COE-PCR) to encode the p.Trp123Ser mutation	Cln5GFP_Cterm-F	CCA AGA AAA ATG AAA AGG ACG AT
							D-Cln5GFP-cln5.030-R	CAG CAT TAC ACG ATA AAA GTT CAT CTT
					Reaction 2	Creating the second half of the *Dictyostelium cln5* gene containing the conserved *CLN5.030* mutation. Reactions 1 and 2 are mixed in a single solution to form the single gene product (via COE-PCR) to encode the p.Trp123Ser mutation	D-Cln5GFP-cln5.030-F	GGT AAA GAT GAA CTT TTA TCG TGT AAT
							Cln5GFP_Cterm-R	CCA ACT AGT ATT GAG ATG AAT AAA ATT

Table 5. Summarized table of the effect of CLN5 disease-causing mutations on the cellular distribution of Cln5. Grey indicates no effect, while green indicates increased co-localization of Cln5 to an intracellular compartment.

Co-localization analysis			
Cln5 Mutation	Endoplasmic reticulum	Lysosomes	Secretory lysosomes
p.Tyr298*			
p.Tyr178Asp			
p.Glu258*			
p.Cys39Tyr			
p.Trp123Ser			

Table 6. Summarized table of impaired ubiquitin and 20S proteasome biology affected by mutations in CLN5 disease. Grey indicates no effect. Red indicates lowered activity or protein amounts. Green indicates increased activity or protein amounts.

Proteasomal-mediated protein degradation										
	Growth	Starved	Growth	Starved	Growth	Starved	Growth	Starved	Growth	Starved
Cln5 Mutation	20S proteasome activity		Ubiquitin-positive protein amount		Free ubiquitin amount		Proteasomal subunit amount		Proteasomal subunit 5 amount	
p.Tyr298*										
p.Tyr178Asp										
p.Glu258*										
p.Cys39Tyr										
p.Trp123Ser										

Table 7. Summarized table of the endo-lysosomal compartments affected by mutated Cln5. Grey indicates no effect. Red indicates lowered # of vesicles, protein amounts, or reduced vesicle size. Green indicates increased # of vesicles, protein amounts, or vesicle size.

Endo-lysosomal pathway												
	Immunofluorescence assay								Western blot			
	Growth	Starved	Growth	Starved	Growth	Starved	Growth	Starved	Growth	Starved	Growth	Starved
Cln5 Mutation	# of VatC-positive vesicles		VatC-positive vesicle size		# of p80-positive vesicles		p80-positive vesicle size		VatC amounts		p80 amounts	
p.Tyr298*												
p.Tyr178Asp												
p.Glu258*												
p.Cys39Tyr												
p.Trp123Ser												

Table 8. Summarized table of CLN5 disease-causing mutations affecting intracellular lysosomal enzyme activity. Grey indicates no effect. Red indicates reduced enzyme activity. Green indicates elevated activity.

Intracellular lysosomal enzyme activity																				
	Growth	Starved	Growth	Starved	Growth	Starved	Growth	Starved	Growth	Starved	Growth	Starved	Growth	Starved	Growth	Starved	Growth	Starved	Growth	Starved
Cln5 Mutation	Alpha galactosidase		Beta galactosidase		Beta glucosidase		Alpha mannosidase		N-acetylglucosiminidase		PPT1		TPP1		CTSD		CTSF		CTSB	
p.Tyr298*																				
p.Tyr178Asp																				
p.Glu258*																				
p.Cys39Tyr																				
p.Trp123Ser																				

Table 9. Summarized table of CLN5 disease-causing mutations affecting the amounts of intracellular cathepsin B and other lysosomal enzymes linked to NCL. Grey indicates no effect. Red and green indicate reduced and elevated protein amounts respectively.

Intracellular lysosomal protein amount										
	Growth	Starved	Growth	Starved	Growth	Starved	Growth	Starved	Growth	Starved
Cln5 Mutation	Ppt1		Tpp1A		Tpp1B		CtsD		CtsB	
p.Tyr298*										
p.Tyr178Asp										
p.Glu258*										
p.Cys39Tyr										
p.Trp123Ser										

Table 10. Summarized table of the impact of mutations in CLN5 disease on the secretion of Cln5, cathepsin B, and cathepsin D. Grey indicates no effect on protein secretion. Red indicates reduced protein secretion. Green indicates elevated protein secretion.

Lysosomal enzyme secretion			
Cln5 Mutation	Cln5	CtsD	CtsB
p.Tyr298*			
p.Tyr178Asp			
p.Glu258*			
p.Cys39Tyr			
p.Trp123Ser			

Table 11. Summarized table of affected extracellular lysosomal enzyme activity caused by CLN5 disease-causing mutations. Grey indicates no effect. Red indicates reduced enzyme activity. Green indicates elevated activity.

Extracellular lysosomal enzyme activity								
	Growth	Starved	Growth	Starved	Growth	Starved	Growth	Starved
Cln5 Mutation	Alpha mannosidase		Beta glucosidase		N-acetylglucosiminidase		Cathepsin B	
p.Tyr298*								
p.Tyr178Asp								
p.Glu258*								
p.Cys39Tyr								
p.Trp123Ser								

4.9. REFERENCES

Abi Habib, J., Lesenfants, J., Vigneron, N., & Van den Eynde, B. J. (2022). Functional Differences between Proteasome Subtypes. Cells, 11(3), Article 3. https://doi.org/10.3390/cells11030421

Adams, J., Feuerborn, M., Molina, J. A., Wilden, A. R., Adhikari, B., Budden, T., & Lee, S. Y. (2019). Autophagy–lysosome pathway alterations and alpha-synuclein up-regulation in the subtype of neuronal ceroid lipofuscinosis, CLN5 disease. Scientific Reports, 9(1), 151. https://doi.org/10.1038/s41598-018-36379-z

Bakthavatsalam, D., & Gomer, R. H. (2010). The secreted proteome profile of developing Dictyostelium discoideum cells. Proteomics, 10(13), 2556–2559. https://doi.org/10.1002/pmic.200900516

Basak, I., Hansen, R. A., Ward, M. E., & Hughes, S. M. (2021). Deficiency of the Lysosomal Protein CLN5 Alters Lysosomal Function and Movement. Biomolecules, 11(10), 1412. https://doi.org/10.3390/biom11101412

Ben-Nissan, G., & Sharon, M. (2014). Regulating the 20S Proteasome Ubiquitin-Independent Degradation Pathway. Biomolecules, 4(3), 862–884. https://doi.org/10.3390/biom4030862

Best, H. L., Clare, A. J., McDonald, K. O., Wicky, H. E., & Hughes, S. M. (2021). An altered secretome is an early marker of the pathogenesis of CLN6 Batten disease. Journal of Neurochemistry, 157(3), 764–780. https://doi.org/10.1111/jnc.15285

Best, H. L., Neverman, N. J., Wicky, H. E., Mitchell, N. L., Leitch, B., & Hughes, S. M. (2017). Characterisation of early changes in ovine CLN5 and CLN6 Batten disease neural cultures for the rapid screening of therapeutics. Neurobiology of Disease, 100, 62–74. https://doi.org/10.1016/j.nbd.2017.01.001

Buratta, S., Tancini, B., Sagini, K., Delo, F., Chiaradia, E., Urbanelli, L., & Emiliani, C. (2020). Lysosomal Exocytosis, Exosome Release and Secretory Autophagy: The Autophagic- and Endo-Lysosomal Systems Go Extracellular. International Journal of Molecular Sciences, 21(7), 2576. https://doi.org/10.3390/ijms21072576

Butz, E. S., Chandrachud, U., Mole, S. E., & Cotman, S. L. (2020). Moving towards a new era of genomics in the neuronal ceroid lipofuscinoses. Biochimica et Biophysica Acta (BBA) - Molecular Basis of Disease, 1866(9), 165571. https://doi.org/10.1016/j.bbadis.2019.165571

Cárcel-Trullols, J., Kovács, A. D., & Pearce, D. A. (2015). Cell biology of the NCL proteins: What they do and don't do. Biochimica et Biophysica Acta (BBA) - Molecular Basis of Disease, 1852(10), 2242–2255. https://doi.org/10.1016/j.bbadis.2015.04.027

Charette, S. J., & Cosson, P. (2006). Exocytosis of late endosomes does not directly contribute membrane to the formation of phagocytic cups or pseudopods in *Dictyostelium*. FEBS Letters, 580(20), 4923–4928. https://doi.org/10.1016/j.febslet.2006.08.009

Charette, S. J., & Cosson, P. (2008). Altered Composition and Secretion of Lysosome-Derived Compartments in *Dictyostelium* AP-3 Mutant Cells. Traffic, 9(4), 588–596. https://doi.org/10.1111/j.1600-0854.2008.00706.x

Dangat, Y., Freindorf, M., & Kraka, E. (2024). Mechanistic Insights into S-Depalmitolyse Activity of Cln5 Protein Linked to Neurodegeneration and Batten Disease: A QM/MM Study. Journal of the American Chemical Society, 146(1), 145–158. https://doi.org/10.1021/jacs.3c06397

Dimond, R. L., Burns, R. A., & Jordan, K. B. (1981). Secretion of Lysosomal enzymes in the cellular slime mold, *Dictyostelium discoideum*. Journal of Biological Chemistry, 256(13), 6565–6572. https://doi.org/10.1016/S0021-9258(19)69026-5

Fey, P., Dodson, R. J., Basu, S., Hartline, E. C., & Chisholm, R. L. (2019). dictyBase and the Dicty Stock Center (version 2.0)—A progress report. The International Journal of Developmental Biology, 63(8-9–10), Article 8-9–10. https://doi.org/10.1387/ijdb.190226pf

Fey, P., Kowal, A. S., Gaudet, P., Pilcher, K. E., & Chisholm, R. L. (2007). Protocols for growth and development of *Dictyostelium discoideum*. Nature Protocols, 2(6), 1307–1316. https://doi.org/10.1038/nprot.2007.178

Fok, A. K., Clarke, M., Ma, L., & Allen, R. D. (1993). Vacuolar H+-ATPase of *Dictyostelium discoideum* A monoclonal antibody study. Journal of Cell Science, 106(4), 1103–1113. https://doi.org/10.1242/jcs.106.4.1103

Gammaldi, N., Pezzini, F., Michelucci, E., Di Giorgi, N., Simonati, A., Rocchiccioli, S., Santorelli, F. M., & Doccini, S. (2023). Integrative human and murine multi-omics: Highlighting shared biomarkers in the neuronal ceroid lipofuscinoses. Neurobiology of Disease, 189, 106349. https://doi.org/10.1016/j.nbd.2023.106349

Gaudet, P., Pilcher, K. E., Fey, P., & Chisholm, R. L. (2007). Transformation of *Dictyostelium discoideum* with plasmid DNA. Nature Protocols, 2(6), 1317–1324. https://doi.org/10.1038/nprot.2007.179

Haddad, S. E., Khoury, M., Daoud, M., Kantar, R., Harati, H., Mousallem, T., Alzate, O., Meyer, B., & Boustany, R.-M. (2012). CLN5 and CLN8 protein association with ceramide synthase: Biochemical and proteomic approaches. ELECTROPHORESIS, 33(24), 3798–3809. https://doi.org/10.1002/elps.201200472

Hagedorn, M., Neuhaus, E. M., & Soldati, T. (2006). Optimized fixation and immunofluorescence staining methods for *Dictyostelium* cells. Methods in Molecular Biology (Clifton, N.J.), 346, 327–338. https://doi.org/10.1385/1-59745-144-4:327

Haltia, M., & Goebel, H. H. (2013). The neuronal ceroid-lipofuscinoses: A historical introduction. Biochimica et Biophysica Acta (BBA) - Molecular Basis of Disease, 1832(11), 1795–1800. https://doi.org/10.1016/j.bbadis.2012.08.012

Haver, H. N., & Scaglione, K. M. (2021). *Dictyostelium discoideum* as a Model for Investigating Neurodegenerative Diseases. Frontiers in Cellular Neuroscience, 15. https://doi.org/10.3389/fncel.2021.759532

Huber, R. J. (2016). Using the social amoeba *Dictyostelium* to study the functions of proteins linked to neuronal ceroid lipofuscinosis. Journal of Biomedical Science, 23(1), 83. https://doi.org/10.1186/s12929-016-0301-0

Huber, R. J. (2017). Loss of Cln3 impacts protein secretion in the social amoeba *Dictyostelium*. Cellular Signalling, 35, 61–72. https://doi.org/10.1016/j.cellsig.2017.03.022

Huber, R. J. (2021). Altered protein secretion in Batten disease. Disease Models & Mechanisms, 14(12), dmm049152. https://doi.org/10.1242/dmm.049152

Huber, R. J. (2023). Recent insights into the networking of CLN genes and proteins in mammalian cells. Journal of Neurochemistry, 165(5), 643–659. https://doi.org/10.1111/jnc.15822

Huber, R. J., Gray, J., & Kim, W. D. (2023). Loss of mfsd8 alters the secretome during *Dictyostelium* aggregation. European Journal of Cell Biology, 102(4), 151361. https://doi.org/10.1016/j.ejcb.2023.151361

Huber, R. J., Hughes, S. M., Liu, W., Morgan, A., Tuxworth, R. I., & Russell, C. (2020). The contribution of multicellular model organisms to neuronal ceroid lipofuscinosis research. Biochimica et Biophysica Acta (BBA) - Molecular Basis of Disease, 1866(9), 165614. https://doi.org/10.1016/j.bbadis.2019.165614

Huber, R. J., Kim, W. D., & Wilson-Smillie, M. L. D. M. (2024). Mechanisms regulating the intracellular trafficking and release of CLN5 and CTSD. Traffic, 25(1), e12925. https://doi.org/10.1111/tra.12925

Huber, R. J., & Mathavarajah, S. (2018a). Cln5 is secreted and functions as a glycoside hydrolase in *Dictyostelium*. Cellular Signalling, 42, 236–248. https://doi.org/10.1016/j.cellsig.2017.11.001

Huber, R. J., & Mathavarajah, S. (2018b). Secretion and function of Cln5 during the early stages of *Dictyostelium* development. Biochimica et Biophysica Acta (BBA) -

Molecular Cell Research, 1865(10), 1437–1450. https://doi.org/10.1016/j.bbamcr.2018.07.017

Huber, R. J., Mathavarajah, S., & Yap, S. Q. (2020). Mfsd8 localizes to endocytic compartments and influences the secretion of Cln5 and cathepsin D in *Dictyostelium*. Cellular Signalling, 70, 109572. https://doi.org/10.1016/j.cellsig.2020.109572

Huber, R. J., Williams, R. S., & Müller-Taubenberger, A. (2022). Editorial: *Dictyostelium*: A Tractable Cell and Developmental Model in Biomedical Research. Frontiers in Cell and Developmental Biology, 10. https://doi.org/10.3389/fcell.2022.909619

Hughes, S. M., Hope, K. M., Xu, J. B., Mitchell, N. L., & Palmer, D. N. (2014). Inhibition of storage pathology in prenatal CLN5-deficient sheep neural cultures by lentiviral gene therapy. Neurobiology of Disease, 62, 543–550. https://doi.org/10.1016/j.nbd.2013.11.011

Husom, A. D., Peters, E. A., Kolling, E. A., Fugere, N. A., Thompson, L. V., & Ferrington, D. A. (2004). Altered proteasome function and subunit composition in aged muscle. Archives of Biochemistry and Biophysics, 421(1), 67–76. https://doi.org/10.1016/j.abb.2003.10.010

Hussain, H., & Chong, N. F.-M. (2016). Combined Overlap Extension PCR Method for Improved Site Directed Mutagenesis. BioMed Research International, 2016, 8041532. https://doi.org/10.1155/2016/8041532

Isosomppi, J., Vesa, J., Jalanko, A., & Peltonen, L. (2002). Lysosomal localization of the neuronal ceroid lipofuscinosis CLN5 protein. Human Molecular Genetics, 11(8), 885–891. https://doi.org/10.1093/hmg/11.8.885

Iwan, K., Clayton, R., Mills, P., Csanyi, B., Gissen, P., Mole, S. E., Palmer, D. N., Mills, K., & Heywood, W. E. (2021). Urine proteomics analysis of patients with neuronal ceroid lipofuscinoses. iScience, 24(2), 102020. https://doi.org/10.1016/j.isci.2020.102020

Journet, A., Chapel, A., Jehan, S., Adessi, C., Freeze, H., Klein, G., & Garin, J. (1999). Characterization of *Dictyostelium discoideum* cathepsin D Molecular cloning, gene disruption, endo-lysosomal localization and sugar modifications. Journal of Cell Science, 112(21), 3833–3843. https://doi.org/10.1242/jcs.112.21.3833

Kim, W. D., DiGiacinto, A. F., & Huber, R. J. (2024). Assaying Lysosomal Enzyme Activity in *Dictyostelium discoideum*. In A. R. Kimmel (Ed.), Dictyostelium discoideum: Methods and Protocols (pp. 55–79). Springer US. https://doi.org/10.1007/978-1-0716-3894-1_4

Kim, W. D., & Huber, R. J. (2022). An altered transcriptome underlies *cln5*-deficiency phenotypes in *Dictyostelium discoideum*. Frontiers in Genetics, 13. https://doi.org/10.3389/fgene.2022.1045738

Kim, W. D., Wilson-Smillie, M. L. D. M., Thanabalasingam, A., Lefrancois, S., Cotman, S. L., & Huber, R. J. (2022). Autophagy in the Neuronal Ceroid Lipofuscinoses (Batten Disease). Frontiers in Cell and Developmental Biology, 10. https://doi.org/10.3389/fcell.2022.812728

Kocaturk, N. M., & Gozuacik, D. (2018). Crosstalk Between Mammalian Autophagy and the Ubiquitin-Proteasome System. Frontiers in Cell and Developmental Biology, 6. https://doi.org/10.3389/fcell.2018.00128

Kohan, R., Halac, I. N. de, Anzolini, V. T., Cismondi, A., Ramírez, A. M. O., Capra, A. P., & Kremer, R. D. de. (2005). Palmitoyl Protein Thioesterase1 (PPT1) and Tripeptidyl Peptidase-I (TPP-I) are expressed in the human saliva. A reliable and non-invasive source for the diagnosis of infantile (CLN1) and late infantile (CLN2) neuronal ceroid lipofuscinoses. Clinical Biochemistry, 38(5), 492–494. https://doi.org/10.1016/j.clinbiochem.2004.12.007

Kumar Deshmukh, F., Yaffe, D., Olshina, M. A., Ben-Nissan, G., & Sharon, M. (2019). The Contribution of the 20S Proteasome to Proteostasis. Biomolecules, 9(5), 190. https://doi.org/10.3390/biom9050190

Kunjappu, M. J., & Hochstrasser, M. (2014). Assembly of the 20S Proteasome. Biochimica et Biophysica Acta, 1843(1), 10.1016/j.bbamcr.2013.03.008. https://doi.org/10.1016/j.bbamcr.2013.03.008

Leinonen, H., Keksa-Goldsteine, V., Ragauskas, S., Kohlmann, P., Singh, Y., Savchenko, E., Puranen, J., Malm, T., Kalesnykas, G., Koistinaho, J., Tanila, H., & Kanninen, K. M. (2017). Retinal Degeneration In A Mouse Model Of CLN5 Disease Is Associated With Compromised Autophagy. Scientific Reports, 7(1), 1597. https://doi.org/10.1038/s41598-017-01716-1

Luebben, A. V., Bender, D., Becker, S., Crowther, L. M., Erven, I., Hofmann, K., Söding, J., Klemp, H., Bellotti, C., Stäuble, A., Qiu, T., Kathayat, R. S., Dickinson, B. C., Gärtner, J., Sheldrick, G. M., Krätzner, R., & Steinfeld, R. (2022). Cln5 represents a new type of cysteine-based S-depalmitoylase linked to neurodegeneration. Science Advances, 8(15), eabj8633. https://doi.org/10.1126/sciadv.abj8633

Luo, S., Bi, B., Zhu, B., Tan, L., Zhao, P., Huang, Y., Wu, G., Zhou, A., & He, X. (2020). Functional Analysis of a Novel CLN5 Mutation Identified in a Patient With Neuronal Ceroid Lipofuscinosis. Frontiers in Genetics, 11. https://doi.org/10.3389/fgene.2020.536221

Lyly, A., von Schantz, C., Heine, C., Schmiedt, M.-L., Sipilä, T., Jalanko, A., & Kyttälä, A. (2009). Novel interactions of CLN5 support molecular networking between Neuronal Ceroid Lipofuscinosis proteins. BMC Cell Biology, 10(1), 83. https://doi.org/10.1186/1471-2121-10-83

Mamo, A., Jules, F., Dumaresq-Doiron, K., Costantino, S., & Lefrancois, S. (2012). The Role of Ceroid Lipofuscinosis Neuronal Protein 5 (CLN5) in Endosomal Sorting. Molecular and Cellular Biology, 32(10), 1855–1866. https://doi.org/10.1128/MCB.06726-11

Marchese, M., Bernardi, S., Vivarelli, R., Doccini, S., Santucci, L., Ogi, A., Licitra, R., Zang, J., Soliymani, R., Mero, S., Neuhauss, S. C., Ciarmoli, L., Signore, G., Lalowski, M. M., & Santorelli, F. M. (2025). CLN5 deficiency impairs glucose uptake and uncovers PHGDH as a potential biomarker in Batten disease. Molecular Psychiatry, 1–14. https://doi.org/10.1038/s41380-025-03043-8Mathavarajah, S., Flores, A., & Huber, R. J. (2017). *Dictyostelium discoideum*: A Model System for Cell and Developmental Biology. Current Protocols Essential Laboratory Techniques, 15(1), 14.1.1-14.1.19. https://doi.org/10.1002/cpet.15

McLaren, M. D., Mathavarajah, S., Kim, W. D., Yap, S. Q., & Huber, R. J. (2021). Aberrant Autophagy Impacts Growth and Multicellular Development in a *Dictyostelium* Knockout Model of CLN5 Disease. Frontiers in Cell and Developmental Biology, 9. https://doi.org/10.3389/fcell.2021.657406

Medoh, U. N., Hims, A., Chen, J. Y., Ghoochani, A., Nyame, K., Dong, W., & Abu-Remaileh, M. (2023). The Batten disease gene product CLN5 is the lysosomal bis(monoacylglycero)phosphate synthase. Science, 381(6663), 1182–1189. https://doi.org/10.1126/science.adg9288

Minnis, C. J., Thornton, C. D., FitzPatrick, L. M., & McKay, T. R. (2020). Cellular models of Batten disease. Biochimica et Biophysica Acta (BBA) - Molecular Basis of Disease, 1866(9), 165559. https://doi.org/10.1016/j.bbadis.2019.165559

Mirdita, M., Schütze, K., Moriwaki, Y., Heo, L., Ovchinnikov, S., & Steinegger, M. (2022). ColabFold: Making protein folding accessible to all. Nature Methods, 19(6), 679–682. https://doi.org/10.1038/s41592-022-01488-1

Moharir, A., Peck, S. H., Budden, T., & Lee, S. Y. (2013). The Role of N-Glycosylation in Folding, Trafficking, and Functionality of Lysosomal Protein CLN5. PLOS ONE, 8(9), e74299. https://doi.org/10.1371/journal.pone.0074299

Müller-Taubenberger, A., Lupas, A. N., Li, H., Ecke, M., Simmeth, E., & Gerisch, G. (2001). Calreticulin and calnexin in the endoplasmic reticulum are important for phagocytosis. The EMBO Journal, 20(23), 6772–6782. https://doi.org/10.1093/emboj/20.23.6772

Néel, E., Chiritoiu-Butnaru, M., Fargues, W., Denus, M., Colladant, M., Filaquier, A., Stewart, S. E., Lehmann, S., Zurzolo, C., Rubinsztein, D. C., Marin, P., Parmentier, M.-L., & Villeneuve, J. (2024). The endolysosomal system in conventional and unconventional protein secretion. Journal of Cell Biology, 223(9), e202404152. https://doi.org/10.1083/jcb.202404152

Nittari, G., Tomassoni, D., Roy, P., Martinelli, I., Tayebati, S. K., & Amenta, F. (2023). Batten disease through different in vivo and in vitro models: A review. Journal of Neuroscience Research, 101(3), 298–315. https://doi.org/10.1002/jnr.25147

Otto, G. P., Wu, M. Y., Kazgan, N., Anderson, O. R., & Kessin, R. H. (2003). Macroautophagy Is Required for Multicellular Development of the Social Amoeba *Dictyostelium discoideum**. Journal of Biological Chemistry, 278(20), 17636–17645. https://doi.org/10.1074/jbc.M212467200

Palmer, D. N., Barns, G., Husbands, D. R., & Jolly, R. D. (1986). Ceroid lipofuscinosis in sheep. II. The major component of the lipopigment in liver, kidney, pancreas, and brain is low molecular weight protein. Journal of Biological Chemistry, 261(4), 1773–1777. https://doi.org/10.1016/S0021-9258(17)36006-4

Palmer, D. N., Fearnley, I. M., Walker, J. E., Hall, N. A., Lake, B. D., Wolfe, L. S., Haltia, M., Martinus, R. D., & Jolly, R. D. (1992). Mitochondrial ATP synthase subunit c storage in the ceroid-lipofuscinoses (Batten disease). American Journal of Medical Genetics, 42(4), 561–567. https://doi.org/10.1002/ajmg.1320420428

Poole, A. R., Hembry, R. M., & Dingle, J. T. (1973). Extracellular localization of cathepsin D in ossifying cartilage. Calcified Tissue Research, 12(1), 313–321. https://doi.org/10.1007/BF02013744

Qureshi, Y. H., Patel, V. M., Berman, D. E., Kothiya, M. J., Neufeld, J. L., Vardarajan, B., Tang, M., Reyes-Dumeyer, D., Lantigua, R., Medrano, M., Jiménez-Velázquez, I. J., Small, S. A., & Reitz, C. (2018). An Alzheimer's Disease-Linked Loss-of-Function CLN5 Variant Impairs Cathepsin D Maturation, Consistent with a Retromer Trafficking Defect. *Molecular and Cellular Biology*, *38*(20), e00011-18. https://doi.org/10.1128/MCB.00011-18

Remtulla, A. A. N., & Huber, R. J. (2023). The conserved cellular roles of CLN proteins: Novel insights from *Dictyostelium discoideum.* European Journal of Cell Biology, 102(2), 151305. https://doi.org/10.1016/j.ejcb.2023.151305

Rossomando, E. F., Maldonado, B., Crean, E. V., & Kollar, E. J. (1978). Protease secretion during onset of development in Dictyostelium discoideum. Journal of Cell Science, 30(1), 305–318. https://doi.org/10.1242/jcs.30.1.305

Sahu, I., Mali, S. M., Sulkshane, P., Xu, C., Rozenberg, A., Morag, R., Sahoo, M. P., Singh, S. K., Ding, Z., Wang, Y., Day, S., Cong, Y., Kleifeld, O., Brik, A., & Glickman, M. H. (2021). The 20S as a stand-alone proteasome in cells can degrade the ubiquitin tag. Nature Communications, 12(1), 6173. https://doi.org/10.1038/s41467-021-26427-0

Savchenko, E., Singh, Y., Konttinen, H., Lejavova, K., Mediavilla Santos, L., Grubman, A., Kärkkäinen, V., Keksa-Goldsteine, V., Naumenko, N., Tavi, P., White, A. R., Malm, T., Koistinaho, J., & Kanninen, K. M. (2017). Loss of Cln5 causes altered

neurogenesis in a mouse model of a childhood neurodegenerative disorder. Disease Models & Mechanisms, 10(9), 1089–1100. https://doi.org/10.1242/dmm.029165

Schauer, T. M., Nesper, M., Kehl, M., Lottspeich, F., Müller-Taubenberger, A., Gerisch, G., & Baumeister, W. (1993). Proteasomes from *Dictyostelium discoideum*: Characterization of Structure and Function. Journal of Structural Biology, 111(2), 135–147. https://doi.org/10.1006/jsbi.1993.1044

Schindelin, J., Arganda-Carreras, I., Frise, E., Kaynig, V., Longair, M., Pietzsch, T., Preibisch, S., Rueden, C., Saalfeld, S., Schmid, B., Tinevez, J.-Y., White, D. J., Hartenstein, V., Eliceiri, K., Tomancak, P., & Cardona, A. (2012). Fiji: An open-source platform for biological-image analysis. Nature Methods, 9(7), 676–682. https://doi.org/10.1038/nmeth.2019

Schleicher, M., Noegel, A., Schwarz, T., Raff, E. W., Brink, M., Faix, J., Geriscii, G., & Isenberg, G. (1988). A *Dictyostelium* mutant with severe defects in α-actinin: Its characterization using cDNA probes and monoclonal antibodies. Journal of Cell Science, 90(1), 59–71. https://doi.org/10.1242/jcs.90.1.59

Schmiedt, M.-L., Bessa, C., Heine, C., Ribeiro, M. G., Jalanko, A., & Kyttälä, A. (2010). The neuronal ceroid lipofuscinosis protein CLN5: New insights into cellular maturation, transport, and consequences of mutations. Human Mutation, 31(3), 356–365. https://doi.org/10.1002/humu.21195

Seehafer, S. S., & Pearce, D. A. (2006). You say lipofuscin, we say ceroid: Defining autofluorescent storage material. Neurobiology of Aging, 27(4), 576–588. https://doi.org/10.1016/j.neurobiolaging.2005.12.006

Simonati, A., & Williams, R. E. (2022). Neuronal Ceroid Lipofuscinosis: The Multifaceted Approach to the Clinical Issues, an Overview. Frontiers in Neurology, 13. https://doi.org/10.3389/fneur.2022.811686

St. P. McNaught, K., Belizaire, R., Isacson, O., Jenner, P., & Olanow, C. W. (2003). Altered Proteasomal Function in Sporadic Parkinson's Disease. Experimental Neurology, 179(1), 38–46. https://doi.org/10.1006/exnr.2002.8050

Stajdohar, M., Rosengarten, R. D., Kokosar, J., Jeran, L., Blenkus, D., Shaulsky, G., & Zupan, B. (2017). dictyExpress: A web-based platform for sequence data management and analytics in *Dictyostelium* and beyond. BMC Bioinformatics, 18(1), 291. https://doi.org/10.1186/s12859-017-1706-9

Tancini, B., Buratta, S., Delo, F., Sagini, K., Chiaradia, E., Pellegrino, R. M., Emiliani, C., & Urbanelli, L. (2020). Lysosomal Exocytosis: The Extracellular Role of an Intracellular Organelle. Membranes, 10(12), Article 12. https://doi.org/10.3390/membranes10120406

Tyynelä, J., Palmer, D. N., Baumann, M., & Haltia, M. (1993). Storage of saposins A and D in infantile neuronal ceroid-lipofuscinosis. FEBS Letters, 330(1), 8–12. https://doi.org/10.1016/0014-5793(93)80908-D

Vesa, J., Chin, M. H., Oelgeschläger, K., Isosomppi, J., DellAngelica, E. C., Jalanko, A., & Peltonen, L. (2002). Neuronal Ceroid Lipofuscinoses Are Connected at Molecular Level: Interaction of CLN5 Protein with CLN2 and CLN3. Molecular Biology of the Cell, 13(7), 2410–2420. https://doi.org/10.1091/mbc.e02-01-0031

Yap, S. Q., Kim, W. D., & Huber, R. J. (2022). Mfsd8 Modulates Growth and the Early Stages of Multicellular Development in *Dictyostelium discoideum*. Frontiers in Cell and Developmental Biology, 10. https://doi.org/10.3389/fcell.2022.930235

Yasa, S., Sauvageau, E., Modica, G., & Lefrancois, S. (2021). CLN5 and CLN3 function as a complex to regulate endolysosome function. Biochemical Journal, 478(12), 2339–2357. https://doi.org/10.1042/BCJ20210171

5.0. CHAPTER 5

5.1. GENERAL DISCUSSION

The early goal in CLN5 disease research was to determine the basic science of CLN5, including its location on the human genome, gene elements that regulate *CLN5* expression, and its localization (Savouski et al., 1998; Isosomppi et al., 2002; Basak et al., 2021). Subsequently, as time progressed, the research started to focus on revealing the molecular function of CLN5, the pathways in which CLN5 plays a role in, and the intracellular impact of mutations linked to CLN5 disease (Isosomppi et al., 2002; Vesa et al., 2002; Schmiedt et al., 2010; Moharir et al., 2013; Adams et al., 2019; Luo et al., 2020; Yasa et al., 2021). Fortunately, research efforts have narrowed down to four putative molecular functions, including a ceramide synthase, a glycoside hydrolase, a depalmitoylase, and a BMP synthase, and the biological pathways that CLN5 is involved in, such as lipid metabolism, autophagy, and biometal homeostasis (Haddad et al., 2012; Grubman et al., 2014; Huber & Mathavarajah, 2018a; Leinonen et al., 2017; Adams et al., 2019; McLaren et al., 2021; Luebben et al., 2022; Medoh et al., 2023). Furthermore, research showed that CLN5 is secreted (Isosomppi et al., 2002; Moharir et al., 2013; Hughes et al., 2014; Huber & Mathavarajah, 2018ab). There are regions in the CLN5 peptide sequence, such as N-glycosylation residues, that affect its secretion, as well as its protein folding and intracellular trafficking (Moharir et al., 2013). In this thesis, we expanded the current literature on the biological processes that the loss of *CLN5* affects and explored different regions of the CLN5 peptide sequence using *Dictyostelium*. This thesis comprises of two major themes:(1) the genetics behind *cln5*-deficiency (Chapter 3), and (2) the biochemistry and molecular biology of the N-terminal region of CLN5 and

mutations in CLN5 disease. Each data chapter will be highlighted in this general discussion. Finally, this general discussion will include directions for future experiments.

5.2. THE GENETICS BEHIND *cln5*-DEFICIENCY

This component of the thesis was an extension of previous work in our lab, such as the aberrant phenotypes associated with *cln5*-deficiency, and previous RNA sequencing analysis in *Cln5*$^{-/-}$ mice revealing some biological processes including but not limited to cell adhesion and regulation of various metabolic processes (von Schantz et al., 2008; McLaren et al., 2021). In this study, we revealed a variety of biological processes affected by the loss of *cln5* in *Dictyostelium*. Specifically, we found the following:

1) A list of DEGs that underpinned each phenotype affected by *cln5*-deficiency during growth, including cellular proliferation and cytokinesis, and during early development in the *Dictyostelium* lifecycle, such as aggregation and adhesion (Huber & Mathavarajah, 2018a).
2) A list of DEGs supporting previously affected biological processes with loss of *CLN5* including protein ubiquitination/deubiquitination and autophagy, as shown in various CLN5 disease models including *Dictyostelium*, mice, rodents, sheep, and human cells (Best et al., 2017; Leinonen et al., 2017; Adams et al., 2019; McLaren et al., 2021).
3) A list of DEGs revealed new cellular components, including the ubiquitin ligase complex, and biological processes like carbohydrate metabolism and protein phosphorylation affected by *cln5*-deficiency.

4) A list of genes that encoded lysosomal enzymes and proteins associated with proteasomal-mediated protein degradation were differentially expressed with the loss of *cln5* .
5) A list of DEGs altered by the loss of *cln5* which transcribes the Cln proteins in *Dictyostelium.*
6) A list of DEGs that showed that the process of secretion is affected by the loss of *cln5*. Around the time of this publication, various CLN5 disease models, including *Dictyostelium*, baby hamster kidney-21 cells, and HEK 293T cells, showed that CLN5 is secreted (Isosomppi et al., 2002; Hughes et al., 2014; Huber & Mathavarajah, 2018a). Similarly, the excreted material (e.g., urine) in CLN5 disease patients showed a different protein profile relative to normal individuals (Iwan et al., 2021).

Although a comparative RNA sequencing approach was conducted in *Cln5*$^{-/-}$ mice (von Schantz et al., 2008), our research established a detailed comparative RNA sequencing analysis of *cln5*-deficiency at the cellular level. During this research, we hypothesized that Cln5 plays a role in various processes in *Dictyostelium* and predicted that there would be DEGs associated with many biological processes. These findings in Chapter 2 aided our understanding of biological processes in that Cln5 plays a role such as altering gene expression of proteins involved in autophagy, including the *atg* genes (Leinonen et al., 2017; Adams et al., 2019; McLaren et al., 2021). Researchers focused on revealing the affected mechanism of autophagy with loss of *CLN5* (Leinonen et al., 2017; Adams et al., 2019; McLaren et al., 2021). Where autophagy relies on lysosomal enzymes to degrade intracellular cargo (Yim & Mizushima, 2020), work in this thesis showed that loss of *cln5* dysregulates lysosomal function via impaired activity in glycosidase hydrolases, proteases,

and a protein palmitoyl thioesterase (Kim & Huber, 2022). This research was also the first to reveal affected protein degradation via the proteasome in CLN5 disease. As ubiquitination interplays with the two intracellular protein degradative processes, autophagy and the proteasome, this research, along with our previous research, laid the initial foundation of a crosstalk mechanism between these processes affected by *cln5*-deficiency (Kocaturk & Gozuacik, 2020; McLaren et al., 2021; Kim & Huber, 2022). Finally, this thesis chapter provides novel insights into the role of Cln5 in secretion, one of the findings that shaped the next few chapters in my thesis.

5.3. THE BIOCHEMISTRY AND MOLECULAR BIOLOGY OF THE N-TERMINAL REGION OF CLN5 AND MUTATIONS IN CLN5 DISEASE

The CLN5 disease research community established the localization of CLN5, including being present extracellularly (Isosomppi et al., 2002; Hughes et al., 2014; Huber & Mathavarajah, 2018ab). Past research also revealed via bioinformatics tools that CLN5 contains an N-terminal SP, an amino acid segment that directs proteins through the conventional secretory pathway to be secreted into the extracellular space (Isosomppi et al., 2002; Schmeidt et al., 2010; Larkin et al., 2013; Jules et al., 2017; Huber & Mathatvarajah, 2018a). In addition, blocking the N-terminus of Cln5 via GFP tagging affected its secretion and showed ER retention in *Dictyostelium* (Huber & Mathavarajah, 2018a). From this, we hypothesized in Chapter 3 that the SP in *Dictyostelium* Cln5 plays an essential role in its secretion. We predicted that loss of the SP would prevent Cln5 from being released into the extracellular space, which in turn would display aberrant phenotypes observed in *cln5*-deficient cells, including reduced cellular proliferation and aggregation. We generated *cln5*$^{-}$ cell lines expressing Cln5-GFP without the SP (e.g., ΔSP-Cln5-GFP),

as well as used both AX3 and *cln5*-deficient cells expressing GFP-Cln5 that were validated in a previous study (Huber & Mathavarajah, 2018a). We also extended our SP analysis in the secretion of CtsD, another CLN protein that is secreted and contains a SP (as reviewed in Huber, 2021). In this thesis chapter, we showed that:

1) *Dictyostelium* Cln5 and CtsD contained a functional SP that was crucial for their release into the extracellular space (Huber et al., 2024).
2) Loss of the SP altered the localization of Cln5 and induced protein instability in CtsD.
3) Preventing CtsD secretion via SP deletion elevated Cln5 secretion, while the reverse did not apply (Huber et al., 2024).
4) Expressing ΔSP-Cln5-GFP in WT cells phenocopied *cln5*-deficient phenotypes, including cell proliferation and aggregation, along with the rate of late multicellular development being reduced.
5) An overabundance of Cln5 in the ER (e.g., GFP-Cln5) caused an ER stress response.

As deleting the SP or blocking the function of the N-terminus of Cln5 resulted in these findings presented in Chapter 3, we explored the molecular effects caused by mutations in CLN5 disease (Chapter 4). Most CLN5 disease-causing mutation research has primarily focused on the affected intracellular trafficking of CLN5 and less on the molecular mechanisms that these mutations impact (Isosomppi et al., 2002; Vesa et al., 2002; Schmiedt et al., 2010; Moharir et al., 2013; Adams et al., 2019; Luo et al., 2020; Yasa et al., 2021). Consequently, the aim of Chapter 4 was to expand our understanding biochemical and molecular impacts of mutations in CLN5 disease. We hypothesized that

mutations in CLN5 disease impact the function of Cln5 and predicted that each CLN5 disease-causing mutation would result in dysfunction in the biological processes of the lysosome. To assess the impact of each CLN5 disease-causing mutation, we generated mutant forms of Cln5 and studied the cellular and molecular biology of these mutations. In this data chapter, we revealed the following:

1) Mutations in CLN5 disease altered the protein structure of *Dictyostelium* Cln5 and human CLN5.
2) CLN5 disease-causing mutations affected protein degradation mediated by the proteasome and dysregulated lysosomal function via defective lysosomal enzymes.
3) Some mutated Cln5 altered the localization of Cln5, but all mutated forms of Cln5 studied in this chapter dysregulated the endo-lysosomal system.
4) Mutations in CLN5 disease reduced its secretion and other lysosomal enzymes.
5) Mutant Cln5 did not impact cell proliferation and aggregation, while delayed aggregation was observed in cells expressing Cln5 lacking its SP.

Altogether, these results from Chapter 4 indicated that all CLN5 disease-causing mutations studied in this chapter affect the intracellular trafficking within the endomembrane system. This, in turn, affected downstream events, altering the function and secretion of lysosomal enzymes. These findings of affected lysosomal biology were further supported by many studies suggesting autophagy as a central pathway affected in CLN5 disease (Leinonen et al., 2017; Adams et al., 2019; McLaren et al., 2021; Yasa et al., 2021; Kim et al., 2022). Since there is a crosstalk mechanism between the ubiquitin-proteasome system and the autophagy pathway, we showed that the proteasome activity and amounts were affected, suggesting that both processes are affected in CLN5 disease. Overall, this research provided insights into the molecular and biochemical impact of mutations in

CLN5 disease and demonstrated the heterogeneity behind this disease. In addition, this thesis further supports using *Dictyostelium* as a model in CLN5 disease research.

5.4. FUTURE DIRECTIONS

In Chapter 2, we generated a list of DEGs that are associated with cellular components and biological pathways affected by *cln5*-deficiency. There were some biological pathways present in the comparative transcriptomics that were not explored at all in the CLN5 disease research community, including but not limited to signal transduction and protein phosphorylation (Kim & Huber, 2022). Furthermore, there were cellular components within our RNA sequencing analysis that have not been explored yet, such as the cullin-RING ubiquitin ligase complex and lamellar bodies. Currently, there is limited research on how CLN5 plays a role in these novel biological processes or how CLN5 regulates these cellular components within the cell. There has been research on how mutations in potassium channel tetramerization domain containing 7, a gene linked to CLN14 disease when mutated, affect intracellular CLN5 degradation via the cullin-RING ubiquitin ligase function (Wang et al., 2022). In summary, since this RNA sequencing dataset has revealed unexplored pathways and components within the cell, research should be conducted in this area to potentially reveal new mechanisms affected by the loss of *cln5*.

In Chapter 3, we created a *cln5*$^{-}$ cell line expressing Cln5 without its SP, along with WT cells expressing ΔSP-CtsD-GFP. From this, we showed that loss of the SP resulted in Cln5 and CtsD not being secreted. In addition, loss of the SP altered the intracellular trafficking of Cln5, including diffused cytoplasmic distribution, and protein instability of CtsD. We also revealed that the release of Cln5 is increased when CtsD lacks its SP, suggesting a role for CtsD in modulating Cln5 secretion. Since Cln5 and CtsD are

interactors in *Dictyostelium,* and there is a regulatory mechanism of CtsD affecting Cln5 secretion, further studying this protein interaction would shed light on one of the many regulatory mechanisms that modulate the secretion of Cln5. Furthermore, a study exploring the extracellular function of CLN5 would be essential, as there is limited research on this. In this PhD thesis, we attempted to pull down extracellular Cln5, but unfortunately had no success. Thus, alternative techniques to isolate extracellular Cln5 need to be explored.

As Chapters 3 and 4 share a similar theme (e.g., loss of an amino acid segment or a change in the amino acid of Cln5 to study its impact) and there is limited knowledge on many of the CLN5 disease-causing mutations, we focused Chapter 4 on studying the molecular impacts of CLN5 disease-causing mutations using *Dictyostelium*. In this study, we generated mutant forms of Cln5, including p.Tyr298*, p.Tyr178Asp, p.Glu258*, p.Cys39Tyr, and p.Trp158Ser, and focused our analysis on lysosomal biology and secretion. We showed that vesicles within the endo-lysosomal pathway are affected by mutations in Cln5, as well as impairing intracellular degradative processes mediated by the proteasome and lysosomal proteins. As many of the glycoside hydrolases revealed lower activity in cells expressing mutated Cln5, a future study on the glycomics of each Cln5 mutant is suggested since there is no research on this topic aside from N-glycosylation in CLN5 (Moharir et al., 2013; Huber & Mathavarajah, 2018a; Huber et al., 2024). Moreover, in this thesis, mutations in Cln5 significantly reduced the secretion of Cln5 and lysosomal enzymes. To follow up with this study, a drug screening approach, particularly towards remedying autophagic defects observed in CLN5 disease, in these Cln5 mutants would give insights into which pathways each CLN5 disease-causing mutation affects. Furthermore, it would be informative to conduct a study that either 1) treats cells containing mutated Cln5 with chemicals to restore the secretory amounts of these proteins, or 2) reveals how

lysosomal proteins are trafficked within cells expressing these mutations of Cln5. As our study only focused on 5 mutations in CLN5 disease, four of which have not been previously studied, researchers should also focus on other CLN5 disease-causing mutations. Finally, since there are 70 distinct CLN5 disease-causing mutations to date, the development of affordable kits that perform rapid tests for autophagic defect would also be another research field in Batten disease to explore in disease prognosis.

5.5. FINAL CONCLUSIONS

Findings in this thesis have further solidified *Dictyostelium* as a model for studying Batten disease. A comparative list of genes affected by *cln5*-deficiency at the cellular level has been developed to further our understanding of the pathways that Cln5 regulates. Where secretion was one of the processes affected by the loss of *cln5* in our RNA sequencing analysis, the SP in Cln5 and CtsD is involved in their secretion. Trapping Cln5 has been implicated in reducing cell proliferation (N-terminal GFP) and aggregation (N-terminal GFP, ΔSPS-Cln5-GFP). We also showed that mutations in Cln5 alter the structure of human CLN5 and *Dictyostelium* Cln5. Mutations in CLN5 disease impaired the endo-lysosomal pathway and the activity of lysosomal enzymes within and outside the cell. In addition, CLN5 disease-causing mutations significantly reduced the release of Cln5 and other lysosomal proteins. Finally, within this thesis, we developed methods for assessing the activity of various lysosomal enzymes in *Dictyostelium*. These methods brought the focus of lysosomal enzymes within *Dictyostelium* back into the spotlight and can be used to inform other researchers in their research endeavours.

5.6. REFERENCES

Adams, J., Feuerborn, M., Molina, J. A., Wilden, A. R., Adhikari, B., Budden, T., & Lee, S. Y. (2019). Autophagy–lysosome pathway alterations and alpha-synuclein up-regulation in the subtype of neuronal ceroid lipofuscinosis, CLN5 disease. *Scientific Reports*, *9*(1), 151. https://doi.org/10.1038/s41598-018-36379-z

Basak, I., Wicky, H. E., McDonald, K. O., Xu, J. B., Palmer, J. E., Best, H. L., Lefrancois, S., Lee, S. Y., Schoderboeck, L., & Hughes, S. M. (2021). A lysosomal enigma CLN5 and its significance in understanding neuronal ceroid lipofuscinosis. *Cellular and Molecular Life Sciences: CMLS*, *78*(10), 4735–4763. https://doi.org/10.1007/s00018-021-03813-x

Best, H. L., Neverman, N. J., Wicky, H. E., Mitchell, N. L., Leitch, B., & Hughes, S. M. (2017). Characterisation of early changes in ovine CLN5 and CLN6 Batten disease neural cultures for the rapid screening of therapeutics. *Neurobiology of Disease*, *100*, 62–74. https://doi.org/10.1016/j.nbd.2017.01.001

Grubman, A., Pollari, E., Duncan, C., Caragounis, A., Blom, T., Volitakis, I., Wong, A., Cooper, J., Crouch, P. J., Koistinaho, J., Jalanko, A., White, A. R., & Kanninen, K. M. (2014). Deregulation of biometal homeostasis: The missing link for neuronal ceroid lipofuscinoses?†. *Metallomics*, *6*(4), 932–943. https://doi.org/10.1039/c4mt00032c

Haddad, S. E., Khoury, M., Daoud, M., Kantar, R., Harati, H., Mousallem, T., Alzate, O., Meyer, B., & Boustany, R.-M. (2012). CLN5 and CLN8 protein association with ceramide synthase: Biochemical and proteomic approaches. *ELECTROPHORESIS*, *33*(24), 3798–3809. https://doi.org/10.1002/elps.201200472

Huber, R. J. (2021). Altered protein secretion in Batten disease. *Disease Models & Mechanisms*, *14*(12), dmm049152. https://doi.org/10.1242/dmm.049152

Huber, R. J., Kim, W. D., & Wilson-Smillie, M. L. D. M. (2024). Mechanisms regulating the intracellular trafficking and release of CLN5 and CTSD. *Traffic*, *25*(1), e12925. https://doi.org/10.1111/tra.12925

Huber, R. J., & Mathavarajah, S. (2018a). Cln5 is secreted and functions as a glycoside hydrolase in *Dictyostelium*. *Cellular Signalling*, *42*, 236–248. https://doi.org/10.1016/j.cellsig.2017.11.001

Huber, R. J., & Mathavarajah, S. (2018b). Secretion and function of Cln5 during the early stages of *Dictyostelium* development. *Biochimica et Biophysica Acta (BBA) - Molecular Cell Research*, *1865*(10), 1437–1450. https://doi.org/10.1016/j.bbamcr.2018.07.017

Hughes, S. M., Hope, K. M., Xu, J. B., Mitchell, N. L., & Palmer, D. N. (2014). Inhibition of storage pathology in prenatal *CLN5*-deficient sheep neural cultures by lentiviral

gene therapy. *Neurobiology of Disease*, *62*, 543–550. https://doi.org/10.1016/j.nbd.2013.11.011

Isosomppi, J., Vesa, J., Jalanko, A., & Peltonen, L. (2002). Lysosomal localization of the neuronal ceroid lipofuscinosis CLN5 protein. *Human Molecular Genetics*, *11*(8), 885–891. https://doi.org/10.1093/hmg/11.8.885

Iwan, K., Clayton, R., Mills, P., Csanyi, B., Gissen, P., Mole, S. E., Palmer, D. N., Mills, K., & Heywood, W. E. (2021). Urine proteomics analysis of patients with neuronal ceroid lipofuscinoses. *iScience*, *24*(2), 102020. https://doi.org/10.1016/j.isci.2020.102020

Jules, F., Sauvageau, E., Dumaresq-Doiron, K., Mazzaferri, J., Haug-Kröper, M., Fluhrer, R., Costantino, S., & Lefrancois, S. (2017). CLN5 is cleaved by members of the SPP/SPPL family to produce a mature soluble protein. *Experimental Cell Research*, *357*(1), 40–50. https://doi.org/10.1016/j.yexcr.2017.04.024

Kim, W. D., & Huber, R. J. (2022). An altered transcriptome underlies cln5-deficiency phenotypes in Dictyostelium discoideum. *Frontiers in Genetics*, *13*. https://doi.org/10.3389/fgene.2022.1045738

Kocaturk, N. M., & Gozuacik, D. (2018). Crosstalk Between Mammalian Autophagy and the Ubiquitin-Proteasome System. *Frontiers in Cell and Developmental Biology*, *6*. https://doi.org/10.3389/fcell.2018.00128

Larkin, H., Ribeiro, M. G., & Lavoie, C. (2013). Topology and Membrane Anchoring of the Lysosomal Storage Disease-Related Protein CLN5. *Human Mutation*, *34*(12), 1688–1697. https://doi.org/10.1002/humu.22443

Leinonen, H., Keksa-Goldsteine, V., Ragauskas, S., Kohlmann, P., Singh, Y., Savchenko, E., Puranen, J., Malm, T., Kalesnykas, G., Koistinaho, J., Tanila, H., & Kanninen, K. M. (2017). Retinal Degeneration In A Mouse Model Of CLN5 Disease Is Associated With Compromised Autophagy. *Scientific Reports*, *7*(1), 1597. https://doi.org/10.1038/s41598-017-01716-1

Luebben, A. V., Bender, D., Becker, S., Crowther, L. M., Erven, I., Hofmann, K., Söding, J., Klemp, H., Bellotti, C., Stäuble, A., Qiu, T., Kathayat, R. S., Dickinson, B. C., Gärtner, J., Sheldrick, G. M., Krätzner, R., & Steinfeld, R. (n.d.). Cln5 represents a new type of cysteine-based S-depalmitoylase linked to neurodegeneration. *Science Advances*, *8*(15), eabj8633. https://doi.org/10.1126/sciadv.abj8633

Luo, S., Bi, B., Zhu, B., Tan, L., Zhao, P., Huang, Y., Wu, G., Zhou, A., & He, X. (2020). Functional Analysis of a Novel CLN5 Mutation Identified in a Patient With Neuronal Ceroid Lipofuscinosis. *Frontiers in Genetics*, *11*. https://doi.org/10.3389/fgene.2020.536221

McLaren, M. D., Mathavarajah, S., Kim, W. D., Yap, S. Q., & Huber, R. J. (2021). Aberrant Autophagy Impacts Growth and Multicellular Development in a Dictyostelium

Knockout Model of CLN5 Disease. *Frontiers in Cell and Developmental Biology*, *9*. https://doi.org/10.3389/fcell.2021.657406

Medoh, U. N., Hims, A., Chen, J. Y., Ghoochani, A., Nyame, K., Dong, W., & Abu-Remaileh, M. (2023). The Batten disease gene product CLN5 is the lysosomal bis(monoacylglycero)phosphate synthase. *Science*, *381*(6663), 1182–1189. https://doi.org/10.1126/science.adg9288

Moharir, A., Peck, S. H., Budden, T., & Lee, S. Y. (2013). The Role of N-Glycosylation in Folding, Trafficking, and Functionality of Lysosomal Protein CLN5. *PLOS ONE*, *8*(9), e74299. https://doi.org/10.1371/journal.pone.0074299

Savukoski, M., Klockars, T., Holmberg, V., Santavuori, P., Lander, E. S., & Peltonen, L. (1998). CLN5, a novel gene encoding a putative transmembrane protein mutated in Finnish variant late infantile neuronal ceroid lipofuscinosis. *Nature Genetics*, *19*(3), 286–288. https://doi.org/10.1038/975

Schmiedt, M.-L., Bessa, C., Heine, C., Ribeiro, M. G., Jalanko, A., & Kyttälä, A. (2010). The neuronal ceroid lipofuscinosis protein CLN5: New insights into cellular maturation, transport, and consequences of mutations. *Human Mutation*, *31*(3), 356–365. https://doi.org/10.1002/humu.21195

Vesa, J., Chin, M. H., Oelgeschläger, K., Isosomppi, J., DellAngelica, E. C., Jalanko, A., & Peltonen, L. (2002). Neuronal Ceroid Lipofuscinoses Are Connected at Molecular Level: Interaction of CLN5 Protein with CLN2 and CLN3. *Molecular Biology of the Cell*, *13*(7), 2410–2420. https://doi.org/10.1091/mbc.E02-01-0031

von Schantz, C., Saharinen, J., Kopra, O., Cooper, J. D., Gentile, M., Hovatta, I., Peltonen, L., & Jalanko, A. (2008). Brain gene expression profiles of Cln1 and Cln5 deficient mice unravels common molecular pathways underlying neuronal degeneration in NCL diseases. *BMC Genomics*, *9*(1), 146. https://doi.org/10.1186/1471-2164-9-146

Wang, Y., Cao, X., Liu, P., Zeng, W., Peng, R., Shi, Q., Feng, K., Zhang, P., Sun, H., Wang, C., & Wang, H. (n.d.). KCTD7 mutations impair the trafficking of lysosomal enzymes through CLN5 accumulation to cause neuronal ceroid lipofuscinoses. *Science Advances*, *8*(31), eabm5578. https://doi.org/10.1126/sciadv.abm5578

Yasa, S., Sauvageau, E., Modica, G., & Lefrancois, S. (2021). CLN5 and CLN3 function as a complex to regulate endolysosome function. *Biochemical Journal*, *478*(12), 2339–2357. https://doi.org/10.1042/BCJ20210171

Yim, W. W.-Y., & Mizushima, N. (2020). Lysosome biology in autophagy. *Cell Discovery*, *6*(1), 6. https://doi.org/10.1038/s41421-020-0141-7